Identification and characterisation of novel virulence factors from Dothideomycete pathogens

A thesis presented in partial fulfilment of the requirements for the degree of

Doctor of Philosophy (PhD)

In

Genetics

at Massey University, Manawatū, New Zealand

Hannah Margaret McCarthy

2023

MASSEY UNIVERSITY
TE KUNENGA KI PŪREHUROA
UNIVERSITY OF NEW ZEALAND

GRADUATE RESEARCH SCHOOL

Note for Examiners of Doctoral Theses
Explanation of COVID-19 Impacts

The Doctoral Research Committee recognises the impacts of Covid-19 on research, particularly for doctoral candidates, and we appreciate the efforts made by supervisors and candidates to ensure timely completion of the doctoral thesis. We know that in some cases this has meant the project has needed to be changed in some way, including its final presentation. For students whose work has been impacted, we invite supervisors to provide a note for examiners explaining the circumstances.

Instructions for Supervisors:

The note is designed to enable you to communicate to examiners your desire for them to take account of certain factors in their assessment of a thesis to address delays and disruptions experienced by a thesis student as a result of the Covid-19 pandemic.

The attached form should be used to provide **an explanation** to the examiners on what to consider in their evaluation. It should detail how the project was altered or how the final product of the thesis has been affected as a result of the disruption. Statements should be clear and succinct for the benefit of the examiners and in fairness to the student and others in the student cohort.

The form should be signed by the student, the supervisor and the Head of Academic Unit, or nominee, and included in the information that is sent out with the thesis.

For doctoral candidates, the completed form should be inserted into the front of the thesis before the abstract by the candidate when submitting their digital thesis for examination in the Student Portal. At the completion of the examination, the amended form which excludes any confidential comments to the examiners, should be included in the appendices.

Please be sure to indicate whether a student has received a suspension of studies due to Covid-19 and/or an extension, as it is important to note if students have already had some special consideration.

September 2021

MASSEY UNIVERSITY
TE KUNENGA KI PŪREHUROA
UNIVERSITY OF NEW ZEALAND

GRADUATE RESEARCH SCHOOL

Note for Examiners
Explanation of COVID-19 Impacts

Thank you for taking the time to examine this thesis, which has been undertaken during the Covid-19 pandemic. The New Zealand Government's response to Covid-19 includes a system of Alert Levels which have impacted upon researchers. Our University's pandemic plan applied the Government's expectations to our research environment to ensure the health and safety of our researchers, however, research was impacted by restrictions and disruptions, as outlined below.

For a six-week period from March 26 to April 27 2020, New Zealand was placed under very strict lockdown conditions (Level 4 – Lockdown), with students and staff unable to physically access University facilities, unless they were involved in essential research related to Covid-19. All field work ceased and data collection with humans was restricted to online methods, if appropriate. The restrictions were partially lifted on April 27, but students and staff were not generally allowed back into University facilities until May 13.

Ongoing disruptions have also been encountered for some students due to uncertainties over the potential for future Covid-19-related restrictions on activities, and a Covid-19 cluster outbreak based in Auckland in New Zealand on 12 August 2020 led to the imposition of rolling Level 2 (Reduce) and Level 3 (Restrict) conditions until 23 September 2020. Auckland campus based students remained on Level 2 until 7 October 2020.

This Alert Level system continues to be utilised throughout 2021, and in particular from 17 August 2021 when the whole of New Zealand again moved to Level 4 lockdown for an extended period. The Auckland region remained in alert level 3 or 4 for a number of months. Please see the NZ Government website for more information on lockdown dates.

These changing Alert Levels have meant that some research students had experimental, clinical, laboratory, field work, and/or data collection or analysis interrupted, and consequently may have had to adjust their research plans. For some students, the impacts of Covid-19 have been substantial as they may have had to significantly revise their research plans.

Overseas travel is not permitted by the University and restrictions have been placed on the New Zealand borders which are closed to non-New Zealand citizens and permanent residents. This meant that international students who were based offshore at the time of lockdown, were unable to return to New Zealand. A small number of offshore students were provided permission to return to New Zealand in early 2021. Many students have also suffered from anxiety and stress-related issues, and have had financial impacts, meaning their research progress has been significantly delayed.

This form, as completed by the supervisor and student, outlines the extent that the research has been affected by Covid-19 conditions.

Approved by DRC 10/Feb/2021
DRC 21/02/03
Updated September 2021

Please consider the factors listed below in your assessment of the work.

This statement has been prepared by the candidate's supervisor in consultation with the student and has been endorsed by the relevant Head of Academic Unit.

Student Name:	Hannah Margaret McCarthy	ID Number:	14013350
Supervisor Name:	Prof. Rosie E. Bradshaw	Date:	19-Feb-23
Thesis title:	Identification and characterisation of novel virulence factors from Dothideomycete pathogens		

Considerations to be taken into account. Note: This statement will remain in the final copy of the thesis which will be available from the Massey University Library following the examination process.
[*Enter key considerations here for the examiners. This can include but is not limited to change of scope, scale, topic, focus; limitations in relation to data collection, access to necessary literature or archival materials, laboratories, field sites; disruptions as a result of lockdown and various alert levels, medical or health considerations etc*]

As a consequence of the first and second nationwide COVID-19 lockdowns, D. septosporum cultures that were being grown for spore harvesting before the lockdown became non viable. Due to the slow growth and poor sporulation rate of D. septosporum, it took another four weeks to grow the cultures to the same stage again.

Another consequence of the second nationwide COVID-19 lockdown was delayed ordering. In particular, the virulence assessment of D. septosporum mutants was not able to start until September 2022, due to the plant growth room failing an inspection, and requiring a new AC unit from overseas which was substantially delayed in arrival and set-up.

As a consequence of the first and second nation-wide COVID-19 lockdowns, a 6 month COVID-19 extension was given.

Approved by DRC 10/Feb/2021
DRC 21/02/03
Updated September 2021

Confidential for Examiners Only: [*Please enter any other considerations which are confidential for examiners only and should not be placed in the final thesis version submitted to Library following the examination process]*

Signed, confirming this is a fair reflection of the impact of Covid-19 on this research.

Student	Hannah McCarthy	Digitally signed by Hannah McCarthy Date: 2023.02.24 09:20:45 +13'00'
Supervisor	Bradshaw, Rosie	Digitally signed by Bradshaw, Rosie Date: 2023.02.24 09:10:10 +13'00'
Head of Academic Unit (or nominee)	Maria Minor	Digitally signed by Maria Minor Date: 2023.02.24 09:38:15 +13'00'

Approved by DRC 10/Feb/2021
DRC 21/02/03
Updated September 2021

Abstract

The Dothideomycetes class of fungi contains some of the most important plant pathogens, including *Dothistroma septosporum* and *Fulvia fulva*. Dothistroma needle blight, caused by *D. septosporum*, is a devasting disease of pines that has been increasing in severity and incidence worldwide. Tomato leaf mould, caused by *F. fulva*, has recently risen in importance after overcoming resistance breeding efforts. There is now an urgent need to identify novel genes from these pathogens that encode virulence factors, such as effector proteins. These proteins contribute to pathogen virulence, so the study of virulence factors not only enables a deeper understanding of how pathogens and their hosts interact at the molecular level, but also provides information that may lead to the development of new methods for disease control. As such, the aim of this thesis was to identify and characterise new candidate virulence factors from *D. septosporum* and *F. fulva*. Candidate virulence factor CfEcp11-1 from *F. fulva*, previously identified to trigger plant defences in wild tomato cultivars, was a particular focus in Chapter 2. Two new homologues of CfEcp11-1 were identified from *Fusarium oxysporum* and suggested to be part of the same Leptosphaeria AviRulence and Suppressing (LARS) effector family. Recognition of CfEcp11-1 by the tomato receptor was also examined through the design of chimeric and mutant protein sequences. CRISPR/Cas9 was used for the first time in *F. fulva* to disrupt *CfEcp11-1* and generate single- and double-copy mutants; to the best of our knowledge this was the first report of multiple gene copy disruption by CRISPR/Cas9 in a fungal pathogen. In Chapter 3, candidate virulence factors from *D. septosporum* and *F. fulva* were identified through a prediction pipeline, which selected proteins with predicted roles as effectors that manipulate plant defences, or as transcription factors which regulate the expression of other genes. Because *D. septosporum* and *F. fulva* are hemibiotrophic pathogens, they transition from colonising living plant tissue to killing and feeding on dead tissue, a transition termed the necrotrophic switch. It is currently unknown what mechanisms govern this important disease process, so a key focus was on candidate virulence factors with a possible role in the necrotrophic switch. In Chapter 4, some of these candidates were further characterised, and new candidates identified, from proteomic analysis of the culture filtrates of *D. septosporum* and *F. fulva* grown in different conditions. Existing transcriptomic data were used to assess which of these proteins were likely to be functional *in planta*. Among those identified were several characterised effectors, such as Cf/DsEcp2-1, Cf/DsEcp20-1, Cf/DsEcp20-3, and CfAvr4E, which were secreted in culture despite having known functions *in planta*. Novel candidate virulence factors from *D. septosporum* and *F. fulva* were also identified in this analysis, including a Nis1 domain-containing protein from *D. septosporum* with a possible role in the necrotrophic

switch. This analysis illustrates that in culture proteomic analysis can be a useful tool for the identification of candidate effector proteins. In Chapter 5, two candidate virulence factor genes of *D. septosporum* with predicted roles in the necrotrophic switch were disrupted through CRISPR/Cas9 gene editing; this was the first use of this method for gene disruption in *D. septosporum*. The disruption mutants were tested for virulence on the *P. radiata* host. One of the mutants was disrupted in *DsCE3*, which was suggested to be a virulence factor, with a possible role in the necrotrophic switch. Overall, the results presented in this thesis have provided new research methodologies as well as valuable knowledge about the molecular tools these two pathogens use to invade their hosts. Whilst further work is required, these developments will ultimately aid future disease control strategies in pine and tomato.

Acknowledgements

Firstly, I want to thank my supervisors Prof Rosie Bradshaw and Dr Carl Mesarich. Rosie, it has been such a delight to work with you over the last four years. Your passion for plant pathology is truly inspiring. You're always ready with a laugh and a smile and have so much compassion for your students. Thank you for being such a fantastic supervisor, I would not be where I am today without your guidance and support. Carl, I am so grateful to have you as a supervisor for both my MSc and my PhD. It's been a pleasure getting to know you over the years, and I really appreciate how you're always ready with a laugh to lighten everyone's mood. Thank you for your eagerness to work through problems together, your bright ideas, and your guidance and support.

I would also like to thank Dr Preeti Panda for your support during my first year, and guidance during my Internship at Scion. I am grateful to Trevor Loo for your patience and guidance with the proteomic work. Thank you to Pranav Chettri for your help and advice about *D. septosporum* transformation. I would also like to thank Scion for providing the pine seedlings and tissue culture-generate shoots for virulence assays. I am also grateful to Massey University for funding my PhD through a Doctoral Scholarship.

I was lucky to be part of a fantastic lab group. Thank you to Mel, Silvia, Ellie, Mariana, Merce, Berit, and Ashleigh for being such great friends and colleagues. I enjoyed our laughs and good times both inside and outside of work. You have all supported me through this PhD and made this journey unforgettable.

I would not be where I am today without the support and love of my friends and family. Eilish, Jess, Steph, Nicole, and Emma, you have always been there for me, whether it be for a laugh or a cry. Thank you for all the good times, I love you all. Matt and Tanya, I love our games nights and am so thankful for your friendship and support. To the Te Punga family, you have all showed me so much love and support over the years. I want to thank Jude, John, and Rachel for welcoming me into your family with open arms, and always being there to support me. To my family, thank you for always being there for me and believing in me. To my parents, thank you for the guidance, love, and support you have shown me over the years. I love you both dearly. To Sam, you have been my rock through these crazy times and have always made me feel loved and valued. I cannot express how thankful I am to have you in my life, I love you.

Table of contents

List of figures

List of tables

List of appendices

List of abbreviations

%	percentage
°C	degree Celsius
µE/m2/s	microeinstein per second and square meter
µg	microgram
µL	microlitre
µM	micromole
µmol/m2/s	micromole per second and square meter
aa	amino acid
AmpR	ampicillin resistance
AOX	alternative oxidase
ATMT	*Agrobacterium tumefaciens*-mediated transformation
Avr	avirulence
BAK1	BRI1-associated receptor kinase 1
bp	base pair
bZIP	basic-leucine zipper
CAD	cinnamyl alcohol dehydrogenase
CAP	cysteine-rich secretory proteins, antigen 5, and pathogenesis-related 1 proteins
Cas9	CRISPR-associated
CAZyme	carbohydrate-active enzyme
CBM14	carbohydrate-binding module family 14
CDS	coding sequence
CE	candidate effector
CRC	cytochrome-dependent respiratory chain
CRISPR	clustered regularly interspaced short palindromic repeats
crRNA	CRISPR RNA
Ct	cycle-threshold
CTAB	hexadecyltrimethylammonium bromide
d	day
DAMP	damage-associated molecular pattern
dDNA	donor DNA
DIG	digoxigenin
DM	Dothistroma medium
DNA	deoxyribonucleic acid
DNB	Dothistroma needle blight
dpi	days post-inoculation
DSB	double-strand break
DSM	Dothistroma sporulation medium
dsRNA	double-stranded RNA
DW	dry weight
E	efficiency
EDTA	ethylenediaminetetraacetic acid
eGFP	enhanced green fluorescent protein
ETI	effector-triggered immunity

EtOH	ethanol
ETS	effector-triggered susceptibility
EV	empty vector
ExIPs	extracellular immunogenic pattern
ExTI	extracellularly-triggered immunity
FDR	false discovery rate
FPKM	fragments per kilobase of exon per million fragments mapped
g	gravity
g/L	grams per litre
GABA	γ-aminobutyric acid
gDNA	genomic DNA
GFP	green fluorescent protein
GH	glycoside hydrolase
GPI	glycosylphosphatidylinositol
h	hour
HA	hemagglutinin
HIGS	host-induced gene silencing
HPLC	high-performance liquid chromatography
HR	hypersensitive response
ID	identity
IM	induction medium
InIPs	intracellular immunogenic pattern
InTI	intracellularly-triggered immunity
IP	invasion pattern
IPR	invasion pattern receptor
IPTR	IP-triggered responses
Iv	*in vitro*
JGI	Joint Genome Institute
kb	kilobase
kDa	kilodaltons
LAMP	loop-mediated isothermal amplification
LARS	*Leptosphaeria* avirulence and suppressing
LB	lysogeny broth
LC-MS	liquid chromatography-mass spectrometry
LDM	low Dothistroma medium
LPch	Quoirin and Lepoivre medium with charcoal
LRR	leucine-rich repeat
LysM	lysin motif
M	molar
MAMP	microbial-associated molecular pattern
MES	2-(N-morpholino)ethanesulfonic acid
mg	milligram
min	minute
mL	millilitre
mM	millimolar
MM	minimal media

MS	Murashige and Skoog basal salt mixture
NB-LRR/NLR	nucleotide-binding leucine-rich repeat
NCBI	National Center for Biotechnology Information
ng	nanogram
NHEJ	non-homologous end-joining
NPS	non-ribosomal peptide synthase
nt	nucleotide
OD	optical density
OSCAR	one step construction of *Agrobacterium*-recombination
PAM	protospacer adjacent motif
PAMP	pathogen-associated molecular pattern
PC1	principal component 1
PC2	principal component 2
PCA	principle component analysis
PCR	polymerase chain reaction
PDA	potato dextrose agar
PDB	potato dextrose broth
PEG	polyethylene glycol
PHI-base	pathogen–host interaction database
PKS	polyketide synthase
PMMG	pine minimal salts medium
PRR	pattern recognition receptor
Pry	pathogen-related in yeast
PTI	PAMP-triggered immunity
PVX	Potato Virus X
qPCR	quantitative PCR
R	resistance
RG	regeneration medium
RLK	receptor-like kinase
RLP	receptor-like protein
RNA	ribonucleic acid
RNAi	RNA interference
ROS	reactive oxygen specie
RPBC	Radiata Pine Breeding Company
rpm	revolutions per minute
RPMK	reads per million per kilobase
SDS	sodium dodecyl sulfate
SDS-PAGE	SDS-polyacrylamide gel electrophoresis
sec	second
SERK	somatic embryogenesis receptor kinase
sgRNA	single guide RNA
SIGS	spray-induced gene silencing
SIX	secreted in xylem
SM	secondary metabolite
SOBIR1	suppressor of BAK1
SSP	small secreted protein

TAE	tris-acetate-EDTA
TF	transcription factor
TLC	thin layer chromatography
UV	ultraviolet
WBD	witches' broom disease
WT	wild type

Chapter 1 – Introduction

Plants are one of humanity's most important resources. From the crops that provide the food on our tables, or nourish our livestock, to the plants and trees that are essential to make our clothes or build our homes, plants are the backbone of human civilization. One of the most significant threats to plant life are fungal phytopathogens and the diseases they cause. Many fungal species have evolved to utilize nutrients from plant matter, and the manner in which these nutrients are acquired is used to categorize the lifestyle of a fungal pathogen. Fungi which feed on living plant material are considered biotrophs, those that kill plant cells to feed on the dead plant material are considered necrotrophs, and those which feed on living plant cells at the start of infection and then later kill the cells for nutrients are considered hemibiotrophs. What governs the switch from biotrophic to necrotrophic feeding in hemibiotrophic fungi, known as the 'necrotrophic switch', is currently unknown and understudied.

Two hemibiotrophic fungi *Dothistroma septosporum* and *Fulvia fulva* (previously called *Cladosporium fulvum*) are closely related Dothideomycete species that infect two very different host plants; pine (a gymnosperm) and tomato (an angiosperm), respectively. What genetic aspects of these fungi enable them to infect such different hosts? Are the genes governing the necrotrophic switch in each fungus specific, or is this switch a conserved mechanism they have inherited from a common ancestor? In this chapter, the current knowledge of these two phytopathogens will be examined in detail. Firstly, the molecular components of fungal plant disease will be reviewed and the significance of the Dothideomycete fungal class will be described. *D. septosporum* and *F. fulva* will be then examined by the disease threat they pose, their life cycle on the host, and what molecular components of disease from each fungus have been identified to date. The current knowledge gaps will be identified throughout this chapter, and those which will be examined in this thesis will be outlined in the aims and objectives.

1.1 Molecular components of plant disease and immunity

The molecular interactions that take place when a microbe attempts to enter a plant and cause disease are highly complex. The first layer of plant defence is constitutive physical or chemical barriers at the plant surface. These barriers, such as a waxy cuticle, tough plant cell wall, or antimicrobial secondary metabolites, can halt disease before the microbe establishes infection structures. Usually, when constitutive defences prevent infection of all isolates of a plant pathogen, the plant is considered a non-host and exhibits non-host resistance. Non-host resistance is a powerful defence mechanism that prevents infection by the majority of microbial

invaders. However, for every plant species there are a small number of microbes that have evolved to overcome its constitutive defences, and instead are faced with the induced plant immune system. Several models have been proposed over the years to explain the plant immune system, and these are detailed below.

The first model, proposed by Flor (1942) was the 'gene-for-gene' model. It is suggested in this model that plant resistance occurs when a plant R factor (encoded by an R gene) recognizes a matching pathogen avirulence (Avr) protein (encoded by an Avr gene) and triggers the plant immune system. When there is no plant R factor to recognize the pathogen Avr protein, or no corresponding Avr protein to be recognized, host immunity is not triggered, and disease ensues. This model is limited because plant R factors can recognize more than one pathogen Avr factor, and Avr factors can be recognized by more than one plant R factor (Petit-Houdenot & Fudal, 2017). Furthermore, while this model provides an explanation for specific plant immunity, it does not explain non-specific plant immunity.

Another model that was proposed was the 'zigzag' model by Jones and Dangl (2006) (**Figure 1.1**). This model suggests that the plant immune system has two branches of non-specific and specific plant immunity. During non-specific immunity, microbial- or pathogen-associated molecular patterns (MAMPs or PAMPs) are recognized by transmembrane pattern recognition receptors (PRRs) to active PAMP-triggered immunity (PTI). PAMPs are considered to be slowly evolving (Jones & Dangl, 2006) and include the flg22-domain of bacterial flagellin (Felix, Duran, Volko, & Boller, 1999) and the bacterial cold shock protein (Felix & Boller, 2003). However, some pathogens can use effector proteins to interfere with PTI, enabling disease to occur through effector-triggered susceptibility (ETS). Effectors are considered pathogen-derived molecules that manipulate host cell structure and function to facilitate infection (Kamoun, 2006). In turn, these effectors can be recognized, directly or indirectly, by plant nucleotide-binding leucine-rich repeat (NB-LRR/NLR) proteins, causing a specific form of plant immunity, termed effector-triggered immunity (ETI). ETI is considered a stronger form of immunity than PTI and results in plant resistance. ETI usually involves a hypersensitive response (HR), which is a localized cell death reaction at the infection site that halts disease. Furthermore, with the continued evolutionary arms race between plants and pathogens, recognised effectors can be modified through mutation (or the genes encoding these recognised effectors, deleted) to avoid recognition and ETI, or new effectors can be acquired to suppress ETI. In turn, plant NB-LRR proteins can then evolve to recognize these new or modified effectors. Therefore, in some plant-pathogen systems, ETI and ETS can fluctuate as each organism adapts to outcompete the other.

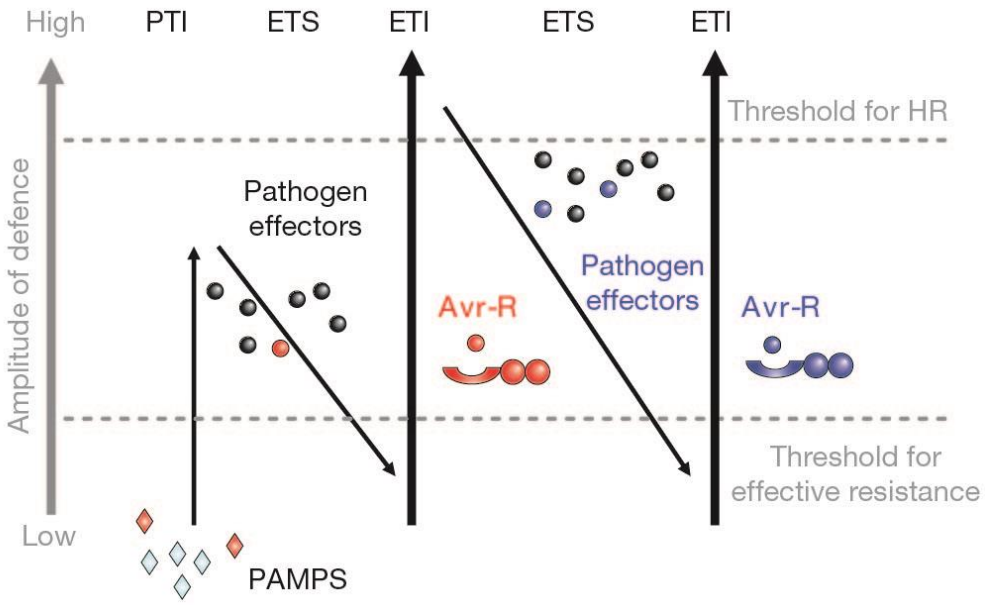

Figure 1.1. Schematic of the 'zigzag' model. In phase one, the plant detects microbial/pathogen-associated molecular patterns (MAMPs/PAMPs, red diamonds) through pattern recognition receptors (PRRs) to activate PAMP-triggered immunity (PTI). In phase two, successful pathogens use effectors to interfere with PTI, resulting in effector-triggered susceptibility (ETS). In phase three, an effector is recognized by a plant nucleotide-binding leucine-rich repeat (NB-LRR/NLR) protein, activating effector-triggered immunity (ETI), a stronger version of PTI that often induces the hypersensitive response (HR). In phase four, successful pathogen isolates have lost or modified the red effector to prevent ETI, or perhaps gained new effectors (in blue) to suppress ETI. Plants can then evolve new NB-LRR/NLR alleles to recognize these modified or new effectors, resulting in ETI again. Figure taken with permission from Jones and Dangl (2006).

One of the limitations of the 'zigzag' model is that it does not include damage-associated molecular patterns (DAMPs) which are endogenous molecules from the plant that are released as a consequence of pathogen infection and can trigger PTI (Boller & Felix, 2009; Matzinger, 2002); for example, plant cutin monomers released by the activity of pathogen cutinases (Boller & Felix, 2009). Another limitation is that the 'zigzag' model does not consider the recognition of extracellular effectors by PRRs (Zipfel & Oldroyd, 2017) or the plant immune response to necrotrophic pathogens. HR triggered by ETI is not effective against necrotrophic pathogens because they can survive in dead host tissue (Jones & Dangl, 2006) and therefore this model does not explain how plants can be resistant to such pathogens. The 'zigzag' model encountered the same problem shared by many detailed and specific models, in that as more research is performed, more exceptions to the rules are found.

Many of the exceptions to the 'zigzag' model were discussed by Cook, Mesarich, and Thomma (2015) and concern the distinctions between PAMPs and effectors, and PTI and ETI. These authors suggested that the plant immune system should be viewed more broadly as a surveillance system that evolves to detect invasion, termed the 'invasion model' (Cook et al., 2015) (**Figure 1.2**). In this model, host receptors, whether extracellular PRRs or intracellular NB-LRRs, are thought of as invasion pattern receptors (IPRs) that can detect either invader-encoded ligands, or self-encoded ligands which have been modified through invasion, called invasion patterns (IPs). Recognition of an IP by an IPR results in IP-triggered responses (IPTRs). Whether IPTRs result in the cessation or continuation of infection, depends on the actions and lifestyle of the invader. Infection will continue if the IPTRs can be suppressed by an effector (eg., by a biotroph) or utilized by the pathogen (eg., by a necrotroph), while infection will be halted if the IPTRs cannot be manipulated by the invader. Because of its simplicity, this model can be applied to a large range of different plant-pathogen interactions.

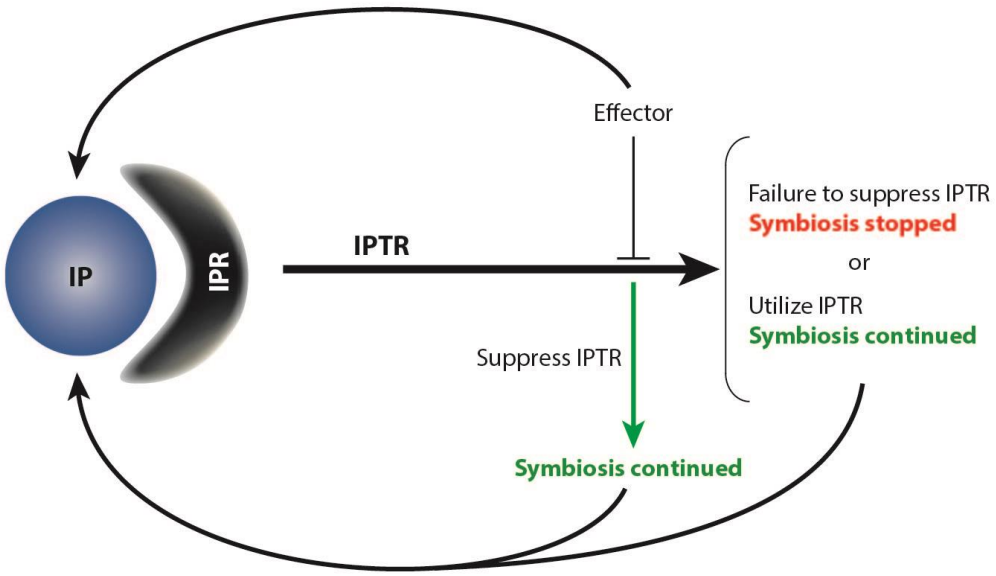

Figure 1.2. Schematic of the 'invasion model'. When a pathogen attempts to invade a plant, invasion patterns (IPs) are perceived by plant IP receptors (IPRs), activating an IP-triggered response (IPTR). The invading pathogen can use effectors to influence the interaction by suppressing (e.g., by biotrophs) or utilizing the IPTR (e.g., by necrotrophs) to continue symbiosis. However, if the pathogen fails to suppress or utilize IPTR, then symbiosis is halted. Continued symbiosis and effector use may generate host-perceivable IPs, leading to a continued IPTR. In summary, multiple recognition events and pathogen

strategies influence IPTR and will eventually result in either the continuation or termination of symbiosis. Figure taken with permission from Cook et al. (2015).

Several other models have been proposed since the 'invasion model'. The 'danger model' proposed by Gust, Pruitt, and Nürnberger (2017) was the first to account for sterile inflammation, where immunity is triggered when no infection has occurred. In this model, immunogenic patterns are called 'danger signals' and are divided into exogenous (non-self) and endogenous (self) groups. This model was recently improved upon by also defining the plant immune response by the site of microbe recognition (van der Burgh & Joosten, 2019). In this 'spatial immunity model', danger signals can be extracellular or intracellular immunogenic patterns (ExIPs or InIPs), and their recognition can occur through cell-surface receptors or cytoplasmic receptors to result in extracellularly- or intracellularly-triggered immunity (ExTI or InTI). InIPs are usually recognized by cytoplasmic NBS-LRR/NLR proteins (Zhang, Dodds, & Bernoux, 2017), while ExIPs are recognized by cell-surface PRRs (Zipfel & Oldroyd, 2017). Recognition specificity of PRRs is determined through different motifs in the ectodomains (Zipfel & Oldroyd, 2017). Some PRRs with a leucine-rich repeat (LRR)-based ectodomain contain an intrinsic kinase domain (receptor-like kinases, RLKs), while some lack a kinase domain (receptor-like proteins, RLPs). RLPs interact with the RLK SOBIR1 (suppressor of BRI1-associated receptor kinase 1 (BAK1)), to enable signalling in the absence of an intrinsic kinase domain (Liebrand et al., 2013). Upon ExIP recognition, RLKs recruit the co-receptor BAK1, or other SERK (somatic embryogenesis receptor kinase) family members (Heese et al., 2007), to enable downstream signalling and the eventual ExTI (van der Burgh & Joosten, 2019).

A similar 'spatial invasion model' was proposed by Kanyuka and Rudd (2019), but as an improvement on the 'invasion model', rather than the 'danger model'. This model was designed to cover only the interactions between the plant and the adapted pathogen, therefore removing the sterile inflammation interactions. In this 'spatial invasion model', apoplastic or cytoplasmic invasion molecules are recognized by cell surface immune receptors or intracellular immune receptors, triggering two distinct immune responses that cycle through activation, signal transduction, and downstream responses.

Most recently, the 'iceberg model' was proposed by Thordal-Christensen (2020) to explain why plants and pathogens have such high numbers of NBS-LRR/NLR receptor and effector genes, respectively, despite so few appearing to function as *R* genes and *Avr* effector genes. The 'iceberg model' suggests that many 'interaction units' are silent. This is because the 'interaction

unit' consists of an immunity component monitored by an NBS-LRR/NLR, an ETS effector targeting the immunity component, and a second ETS effector which prevents activation of host defence by the NBS-LRR/NLR. This model proposes that these silent units are not identified from genetic studies because host resistance is not activated and are therefore in the bottom of the iceberg. While the 'interaction units' that are visible from genetic studies are those that result in host immunity, where a second ETS effector is not present to suppress defence responses. These 'interaction units' are shown in the top of the iceberg and illustrates how current genetic studies only observes the 'tip of the iceberg', while as the evolutionary arms race continues, more silent 'interaction units' fall to the bottom of the iceberg.

Many different models have been proposed over the years to explain the plant immune system and the interaction between plants and pathogens. While each new model offers new insight into the plant-pathogen interaction, there is debate among researchers as to which one should be used. For simplicity in this thesis, proteins which contribute to virulence will be referred to as virulence factors, and those which prevent infection as avirulence factors.

1.2 Introduction to Dothideomycetes

Dothideomycete fungi belong to a class that contains some of the most important biotrophic, necrotrophic, and hemibiotrophic fungal phytopathogens today. This class diverged from a common ancestor around 280 million years ago (Ohm et al., 2012) and the first ancestral Dothideomycete was proposed to have been a saprophyte (Haridas et al., 2020; Pandaranayaka, Frenkel, Elad, Prusky, & Harel, 2019). Fungi of this class are vast in their diversity; some can inhibit and degrade rocks (Ruibal et al., 2009), others acquire nutrients from dead plant material as saprophytes (Hudson, Buchholz, Doyle, & Sundue, 2019), while some parasitize other fungi (Trakunyingcharoen et al., 2014) or other organisms, such as insects (Haridas et al., 2020). The majority of Dothideomycete species are phytopathogens. The strategy of infecting plants was hypothesised to have evolved 6–8 separate times throughout the lineage (Haridas et al., 2020) so that today, most major crops are threatened by a disease caused by a Dothideomycete fungus (Haridas et al., 2020; Ohm et al., 2012).

The Dothideomycete class contains a vast diversity of phytopathogenic species with different hosts and infection strategies, and this diversity can be observed even between closely related species. Fungi of the Sigatoka disease complex; *Pseudocercospora musae*, *P. eumusae* and *P. fijiensis* likely evolved from a common ancestor but have different sized genomes, thought to be mainly due to retrotransposon proliferation. Despite their close phylogenetic relationship, these three fungi are thought to have evolved different hemibiotrophic strategies for infecting the

banana host. Indeed, each retain rather unique effector repertoires, as ~50% of the effector genes are considered species-specific (Chang, Salvucci, Crous, & Stergiopoulos, 2016).

Another example is the two hemibiotrophic fungi *D. septosporum* and *F. fulva* which infect vastly different hosts; pine (a gymnosperm) and tomato (an angiosperm), respectively, yet are highly similar in other aspects. These two fungi share similar hemibiotrophic infection strategies (Mesarich 2023). They are phylogenetically closely related (**Figure 1.3**) and thought to share a recent common ancestor (de Wit et al., 2012). Furthermore, 70% of their gene content is homologous and they share several functional effector orthologues, including Avr4 (de Wit et al., 2012). *F. fulva* also contains a mostly intact biosynthesis pathway for the *D. septosporum* secondary metabolite dothistromin (de Wit et al., 2012), but production is blocked by the pseudogenization of a few early pathway genes (Chettri et al., 2013). The current knowledge of these two pathogens, such as their infection strategies, current control methods, and known virulence factors, will be examined in the following sections.

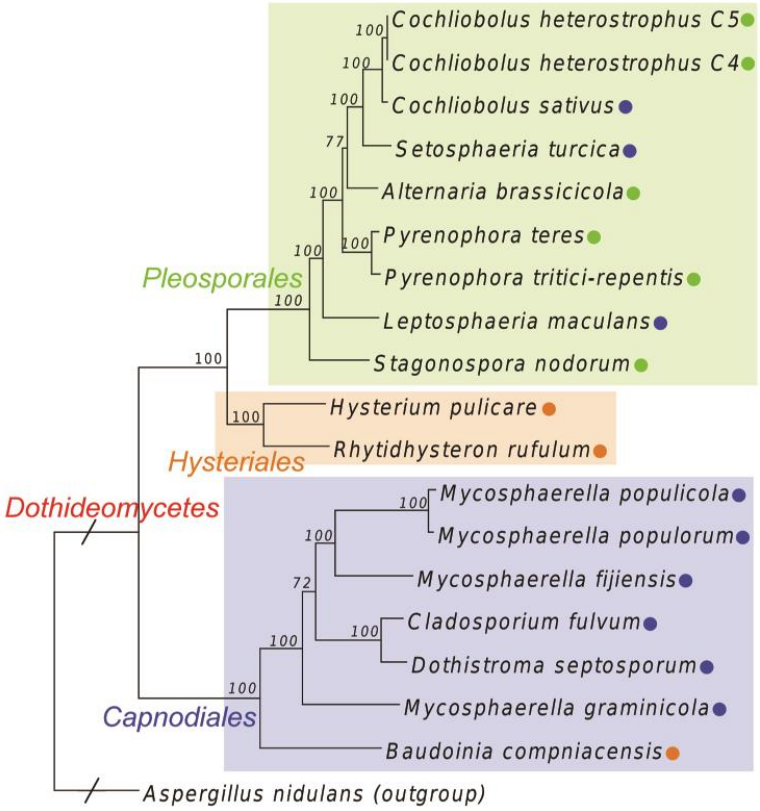

Figure 1.3. Phylogenetic tree of 18 Dothideomycete species. Genome-based phylogenetic tree computed using 51 conserved protein families. Bootstrap values are labelled on the branches. Fungal lifestyle is

indicated by a coloured circle; green, necrotroph; orange, saprotroph; and blue, hemibiotroph. *Aspergillus nidulans* was used as an outgroup and its branch is not to scale. Taken from Ohm et al. (2012).

1.3 *Dothistroma septosporum*

1.3.1 Life cycle

D. septosporum causes Dothistroma needle blight (DNB), one of the most devastating fungal diseases threatening pine health worldwide. As a hemibiotrophic pathogen, the lifecycle of *D. septosporum* has an early biotrophic-like stage (**Figure 1.4a**), a mid stage (**Figure 1.4b**) when the necrotrophic switch occurs through an unknown mechanism, and a late stage (**Figure 1.4c**) where growth is necrotrophic (Kabir, Ganley, & Bradshaw, 2015b). During the early stage (**Figure 1.4a**), a *D. septosporum* spore that has landed on a pine needle will germinate, grow epiphytically and randomly on the surface, before encountering an open stoma and entering the epistomatal chamber. The fungus then colonizes the intercellular spaces between mesophyll cells, growing asymptomatically. It is currently unknown whether *D. septosporum* feeds biotrophically during this period. In the mid stage (**Figure 1.4b**), growth then switches to become necrotrophic, where cell death occurs and the first early lesions are observed. In the late stage (**Figure 1.4c**), cell death continues until mature lesions are formed with fruiting bodies that erupt through the epidermal layer to release spores, and complete the lifecycle (Brown & Webber, 2008; Kabir et al., 2015b). In a laboratory setting, the lifecycle is quite variable and is reported to take 6–12 weeks to complete (Kabir et al., 2015b). Although the fruiting bodies produced in spring or summer are asexual (Brown & Webber, 2008), the fungus is also able to reproduce sexually with ascospores. The two mating types of *D. septosporum* and their mating genes were characterised by Groenewald et al. (2007), but it was found that only one mating type is present in New Zealand, Australia, and Chile.

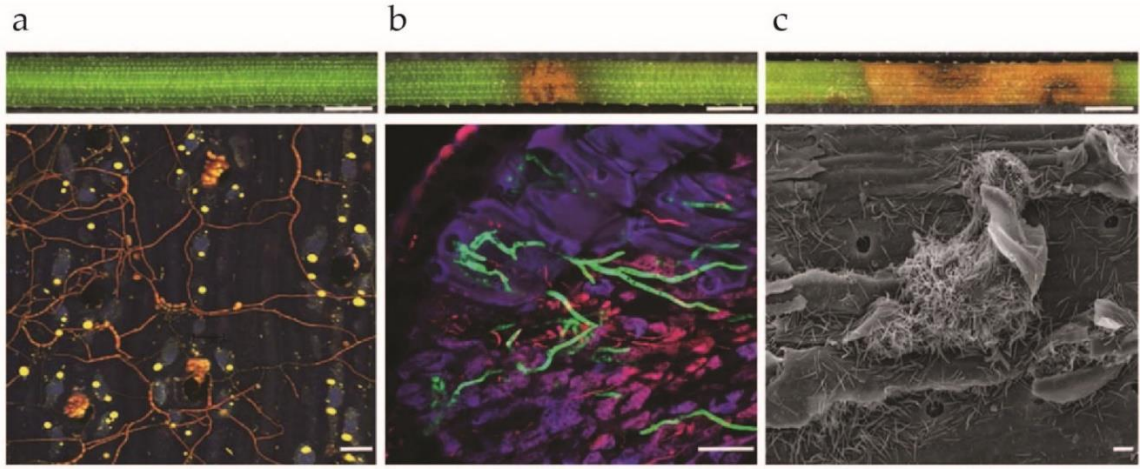

Figure 1.4. Lifecycle of *Dothistroma septosporum* illustrating the three growth stages. Early is the penetration and biotrophic colonisation stage, mid is the early necrotrophic stage when lesions first appear, and late is the necrotrophic sporulating lesion stage. The top row are infected needles from an infection assay, and the bottom row are microscopic images from needles at the same stage. (**a**) Fungi were stained with trypan blue and imaged by confocal microscopy. (**b**) A green fluorescent protein-labelled strain was used and imaged with confocal microscopy. (**c**) Scanning electron microscopy was used to examine the needle surface. Scale bars of the top macroscopic images are 1 mm and of the bottom microscopic images are 20 µm. Taken from Bradshaw et al. (2016).

1.3.2 Incidence

DNB is predominantly caused by *D. septosporum*, and to a lesser extent its sister species *D. pini*. DNB is characterised by lesions observed in the mid- and late-stages of infection. These lesions appear as yellow dots on the pine needles which later develop into red-brown necrotic lesions, with black fruiting bodies. Lesions can initially appear water-soaked and eventually extend to girdle the needle (Kabir et al., 2015b). The characteristic red-brown pigmentation is due to production of the mycotoxin dothistromin (Brown & Webber, 2008). Usually, the needle then dies back from the lesion, leaving the base green and healthy (Jones & Dangl, 2006). DNB can result in a decrease in wood volume proportional to the disease severity (Gibson, 1974; Woods, 2003), and successive years of heavy infection can even result in tree death (Brown & Webber, 2008).

DNB disease has increased dramatically in incidence and severity over the last two decades. Since the first symptoms of DNB were observed in *Pinus radiata* in Tanzania (Gibson, 1972), ensuing outbreaks were reported in East Africa, Chile and New Zealand (Gibson, 1974), the latter of which appears to contain an almost clonal population (Bradshaw et al., 2019; Hirst,

Richardson, Carson, & Bradshaw, 1999). Since then, epidemics have occurred throughout the world and in many different pine species. DNB has been reported in at least 76 countries and while *Pinus* is still the most severely affected genus, other genera including *Abies*, *Cedrus*, *Larix*, *Picea*, and *Pseudotsuga* can also be infected (Drenkhan et al., 2016). The recent increased incidence of DNB is attributed partly to climate change, where regions that did not previously have an environment suitable for infection now have crossed an "environmental threshold" for DNB (Woods, Coates, & Hamann, 2005; Woods et al., 2016). The health of our forests and their value as carbon sinks have become increasingly important to mitigate the effects of climate change. Therefore, considerable effort is being made to understand the diseases that threaten our forests and to find ways to effectively control their impact and incidence.

1.3.3 Control

Currently, the main methods of DNB control are silviculture (increasing air movement and reducing needle wetness through pruning), copper-based fungicide application, and planting trees with increased levels of resistance (Carnegie & Kathuria, 2023). In New Zealand, the Dothistroma Control Committee coordinates the aerial application of cuprous oxide (Bulman, Gadgil, Kershaw, & Ray, 2004), and the planting of tree stocks with increased levels of DNB resistance (Hammond & Bulman, 2022). Copper-based fungicides are not as effective in areas with severe infection and high inoculum loads (Brown & Webber, 2008; Hirst et al., 1999), therefore requiring an additional fungicide application in some areas (Bulman et al., 2004; Carnegie & Kathuria, 2023). The expense of such high levels of fungicide application has become unsustainable for some areas, requiring the planting of alternative pine species (Barnes, van der Nest, Granados, & Wingfield, 2022).

It has been suggested that preventing the transport of infected seedlings would be an effective control measure (Möykkynen, Fraser, Woodward, Brown, & Pukkala, 2017). Recently, loop-mediated isothermal amplification (LAMP) was established for *D. septosporum* and *D. pini*, which will enable rapid and on-site screening of imported seedlings (Aglietti et al., 2021). Developing new pine resistance varieties is an important avenue of research, and recent comparative gene expression analysis of DNB-infected tolerant and susceptible lodgepole pines (*Pinus contorta*) identified candidate *R* genes with signatures of selection, likely from adaption to *D. septosporum*. The next step for this research is to identify the corresponding *D. septosporum* effector proteins and confirm the function of the pine *R* genes (Lu et al., 2021). Indeed, identification of pine *R* genes can also be performed from the pathogen perspective, by identifying *Avr* effectors genes of *D. septosporum* first, then screening for the corresponding *R*

gene. The current virulence and *Avr* factors identified from *D. septosporum* are detailed in the following sections.

1.3.4 Virulence factors

The first virulence factor identified from *D. septosporum* was the mycotoxin dothistromin (Kabir, Ganley, & Bradshaw, 2015a), responsible for causing the characteristic red banding symptom of DNB (Brown & Webber, 2008). As well as its phytotoxic properties, a knock-out of key dothistromin genes indicated it is important for mesophyll colonization, lesion expansion and sporulation (Kabir et al., 2015a). The role of dothistromin as a secondary metabolite will be discussed in more detail in **section 1.3.5**. The secondary metabolite produced by DsNps3 is also suggested to be a virulence factor of *D. septosporum* (Ozturk et al., 2019). While the metabolite itself could not be analysed due to low quantities, knock-out of the *DsNps3* gene significantly reduced virulence. The expression profile and orthology to other functionally characterised genes suggested that the *DsNps3* metabolite may have antifungal and insecticidal properties to provide a competitive edge during early infection against other fungi and plant-feeding insects (Ozturk et al., 2019).

Candidate virulence factors have also been identified from effector prediction pipelines. Hunziker (2018) identified 55 candidates (several of which were orthologous to characterised effectors of *F. fulva*), while Tarallo (2022) identified 29 (not all unique from the previous pipeline), two of which were conserved in the other *P. radiata* pathogens *Cyclaneusma minus* and *Phytophthora pluvialis* (DsEcp57-1 and DsCE15). A number of these candidates were screened for a cell death response in non-host *Nicotiana* species through agro-infiltration, as well as in susceptible and tolerant *P. radiata* genotypes through *Pichia pastoris*-mediated heterologous expression and secretion. Candidates of particular interest were DsEcp2-1, DsCE3, DsCE15, DsEcp20-3, DsEcp32-3, and Ds74283 that triggered cell death in one or more *Nicotiana species* and all *P. radiata* genotypes to some extent (Hunziker, 2018; Hunziker et al., 2021; Tarallo, 2022; Tarallo et al., 2022). Targeted gene disruption and virulence assessment also tentatively suggested that Ds74283 and DsEcp57-1 may have an effect on virulence, but further work is required to confirm this result (Tarallo, 2022).

1.3.5 Avirulence factors

Currently, only one likely *Avr* factor has been identified from *D. septosporum*, *DsEcp2-1*. This gene is highly upregulated at the mid stage of infection (Bradshaw et al., 2016) and, as discussed above, encodes a protein that triggers cell death in both non-host *Nicotiana* species and susceptible and tolerant *P. radiata* genotypes (Hunziker, 2018; Hunziker et al., 2021; Tarallo,

2022). Gene knock-out and virulence assessment on *P. radiata* showed that mutants had increased fungal biomass, suggesting that DsEcp2-1 acts as an *Avr* factor (Guo, Hunziker, et al., 2020). The next step for this research would be to identify the cognate *P. radiata R* gene, which would be invaluable for future resistance Breeding programs.

1.3.6 Secondary metabolites

The *D. septosporum* genome contains nine secondary metabolite backbone genes, however only four were expressed in culture or in planta (Ozturk et al., 2019). One of these was *DsPksA*, the polyketide synthase (PKS) involved in dothistromin production. Another was *DsNps3*, a non-ribosomal peptide synthase (NPS) gene which, as described previously, is suggested to be involved in the biosynthesis of a metabolite that contributes to virulence through antifungal and insecticidal properties. The other two genes *DsPks1* and *DsPks2*, were suggested to be involved in the biosynthesis of melanin (de Wit et al., 2012; Ozturk et al., 2017) and squalestatin (Bonsch et al., 2016), respectively. However, melanin was shown to be produced mainly through a PKS-independent pathway (Ozturk et al., 2017), and no evidence was found to support the production of squalestatin in culture (Ozturk et al., 2019). Gene knock-outs (Ozturk et al., 2017) and virulence assessments on the *P. radiata* host further suggested that neither *DsPks1* or *DsPks2* play a role in virulence (Ozturk et al., 2019). Therefore, it is still unknown what function *DsPks1* and *DsPks2* perform in *D. septosporum*.

As a virulence factor, dothistromin is the most important secondary metabolite produced by *D. septosporum*. Dothistromin is a difuroanthraquinone with a similar structure to sterigmatocystin and versicolorin B (Brown et al., 1996), a precursor of aflatoxin produced by *Aspergillus flavus* and some other *Aspergillus* species (Shaw, Chick, & Hodges, 1978). Dothistromin is unusual among secondary metabolites because it is expressed and synthesized early during infection, rather than in the late exponential and stationary phase of growth (Schwelm, Barron, Zhang, & Bradshaw, 2008); furthermore, the biosynthesis genes are spread over six loci rather than being clustered (Chettri et al., 2013; Zhang, Schwelm, Jin, Collins, & Bradshaw, 2007). The early timing of dothistromin production is controlled through chromatin modification, and this was hypothesized to be important for the adaption of dothistromin as a virulence factor (Chettri, Dupont, & Bradshaw, 2018).

1.3.7 Available genomic, transcriptomic, and proteomic resources

Over the years that *D. septosporum* has been studied, several genomic and transcriptomic resources have been made available. The genome of the *D. septosporum* NZE10 strain, which has been well studied as a representative of the clonal population present in New Zealand, was

sequenced, and studied comparatively with the *F. fulva* 0WU genome (de Wit et al., 2012). A global population study of *D. septosporum* strains isolated from different pine hosts in 15 different countries, made another 18 genomes available for research (Bradshaw et al., 2019). Transcriptome analysis of the *D. septosporum* NZE10 strain over the course of infection on the *P. radiata* host has been performed (Bradshaw et al., 2016). Illumina sequencing of RNA from NZE10 and *ΔDsLaeA* (global regulator mutant) strains grown in different *in vitro* conditions is also available for further analysis (Ozturk et al., 2019). The resources available for both *D. septosporum* and *F. fulva* have been recently reviewed in more detail by Mesarich et al. (2023). Despite the considerable number of genomic and transcriptomic resources available, proteomic analysis of *D. septosporum* has yet to be performed, presenting a gap in our current knowledge of this important pathogen.

1.4 *Fulvia fulva*

1.4.1 Life cycle

Fulvia fulva causes tomato leaf mould, a devastating disease often prevalent in glasshouse environments. *F. fulva* is a hemibiotrophic pathogen with a lifecycle similar to *D. septosporum*, although some key differences are apparent. Conidia of *F. fulva* are spread by wind, like *D. septosporum*, as well as by water and must land on the abaxial side of the leaf. Both species require high humidity for the spores to germinate (**Figure 1.5a & b**). Similar to *D. septosporum*, hyphae from germinated spores grow randomly until encountering an open stoma (**Figure 1.5c**). Once inside the substomatal cavity, the hyphae grow in diameter by at least two-fold and move inwards to colonize the apoplast of the spongy mesophyll cells with long, branched hyphal structures (Thomma, van Esse, Crous, & de Wit, 2005). Hyphal growth appears to be directional towards the vascular tissues, likely due to the sucrose gradient (Van den Ackerveken et al., 1994; Wubben, Joosten, & De Wit, 1994). The fungus does not produce feeding structures but appears to require close contact with the host cells (Thomma et al., 2005). *F. fulva* obtains nutrients from host apoplastic sucrose, which it can convert and store mainly as mannitol (Joosten, Hendrickx, & De Wit, 1990), a polyol that tomato cannot metabolize (Lewis & Smith, 1967). It is also hypothesized that *F. fulva* can utilize the abundant tomato amino acid γ-aminobutyric acid (GABA) as a nutrient source and may even manipulate host GABA production for its own benefit (Oliver & Solomon, 2004; Solomon & Oliver, 2002). After ~10 days, hyphal aggregations (stromatic bodies) form in the substomatal cavities and aerial mycelium extend through the stomata to release the conidia (Thomma et al., 2005) (**Figure 1.5d**), thereby completing the lifecycle. The conidia produced from infection of tomato are asexual (Thomma et al., 2005) and,

despite the discovery of two mating type genes and tentative evidence for recombination occurring in some strains (Stergiopoulos, De Kock, Lindhout, & De Wit, 2007), it is still uncertain whether *F. fulva* can reproduce sexually (Mesarich et al., 2023).

In contrast to *D. septosporum*, *F. fulva* does not need to kill host cells to produce spores and complete its lifecycle. For this reason, *F. fulva* was considered a biotrophic pathogen for many years. However, studies have observed that in the late stages of infection the aerial mycelium and spores clog the stomata, resulting in wilting, defoliation, necrosis and, in severe cases, plant death (Jones, Jones, Stall, & Zitter, 1997; Thomma et al., 2005). It was also observed that *F. fulva* has a larger number of carbohydrate-active enzyme (CAZyme)-encoding genes and genes encoding enzymes for the production of secondary metabolites (Collemare et al., 2014; de Wit, 2016) than most biotrophs, being more comparable with hemibiotrophs and necrotrophs (de Wit et al., 2012; Hane, Paxman, Jones, Oliver, & de Wit, 2019). This evidence supported the recent reclassification of *F. fulva* to that of a hemibiotrophic pathogen (Mesarich et al., 2023).

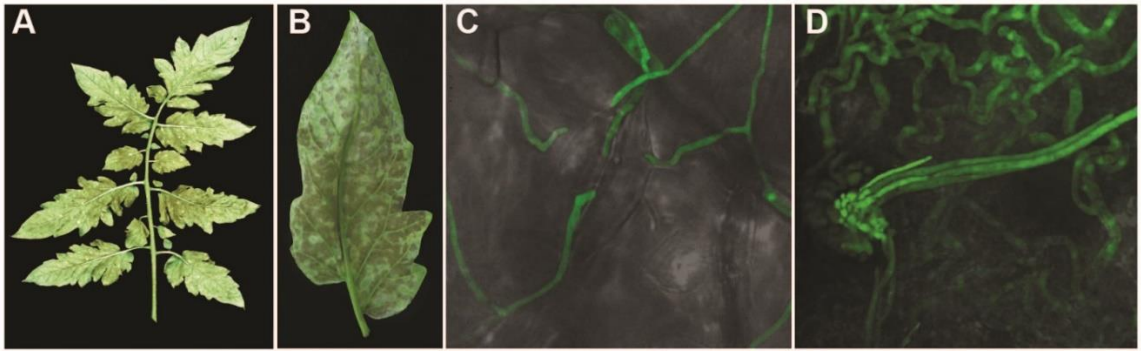

Figure 1.5. Tomato leaf mould symptoms caused by *Fulvia fulva*. (**a–b**) – *F. fulva* sporulating on the abaxial side of a tomato leaf two weeks post inoculation. (**c**) – *F. fulva* (green fluorescent protein (GFP)-transgenic strain) runner hyphae on the surface of a tomato leaf and entering a stoma four days post-inoculation. (**d**) – *F. fulva* (GFP-transgenic strain) conidiophores emerging from a tomato stoma 10 days post-inoculation. Figure adapted from de Wit et al. (2012).

1.4.2 Incidence

F. fulva generally infects the leaves of the tomato host, but has occasionally been observed to attack stems, flowers and fruits (Thomma et al., 2005). Initial mould symptoms occur as pale green or yellow spots on the leaves, and, as disease progresses, the underside of the leaf becomes covered in olive-brown fungal growth. Late disease symptoms can include dark leaf

spots, leaf curling, premature leaf drop, reduced fruit yield and, as discussed previously, plant death in severe cases (Hammond-Kosack, Harrison, & Jones, 1994; Iida et al., 2015).

The first outbreak of tomato leaf mould was reported in the late 1800s, in the USA state of South Carolina (Cooke, 1883). However, this disease is thought to originate in the same place as the tomato host: South America (Jenkins, 1948). Tomato leaf mould caused significant global economic impact during the first half of the 20th century, mainly in moderate temperature zones with high relative humidity (de Wit, 1992; de Wit et al., 2012), and in glasshouse settings (Butler & Jones, 1949). The identification of tomato *R* genes (termed *Cf* genes for resistance to *C. fulvum*) and introgression of these genes into commercial varieties during the late 1970s effectively controlled this disease for many years (Joosten et al., 1990). Since the first fungal *Avr* effector gene, *CfAvr9*, was cloned from this pathogen in 1991 (van Kan, van den Ackerveken, & de Wit, 1991), *F. fulva* has become a well-established model species for studying plant-pathogen interactions (Mesarich et al., 2023). However, control of tomato leaf mould through tomato *Cf R* genes has been breaking down (the details of which are in **section 1.4.3**) and, as a consequence, tomato leaf mould is becoming a significant economic threat again today (Mesarich et al., 2023).

1.4.3 Control

Control of tomato leaf mould was originally performed by application of fungicides. However, this was not sustainable as the sole control method because as well as the damage fungicides can cause to the environment and human health, fungicide-resistant *F. fulva* strains began emerging. It was discovered that for some fungicides, a single point mutation was sufficient for *F. fulva* to become resistant (Watanabe, Horinouchi, Muramoto, & Ishii, 2017; Yan, Chen, Zhang, & Ma, 2008), and the development of rapid multiplex allele-specific polymerase chain reaction (PCR) assays to detect certain fungicide-resistant genotypes may help growers make informed decisions about fungicide control measures (Yan et al., 2008).

As mentioned previously, introgression of tomato *Cf R* genes from related wild species into cultivated tomato cultivars was a measure which successfully controlled this disease for many years (Thomma et al., 2005). The first *Cf R* gene isolated was *Cf-9* (*Cf-9C*) (Jones, Thomas, Hammond-Kosack, Balint-Kurti, & Jones, 1994), after the characterisation of the corresponding *F. fulva Avr* gene *Avr9* (van Kan et al., 1991). To date, six major *Cf R* genes have been cloned (*Cf-2*, *Cf-4*, *Cf-4E*, *Cf-5*, *Cf-9*, and *Cf-9B*) (Dixon, Hatzixanthis, Jones, Harrison, & Jones, 1998; Dixon et al., 1996; Jones et al., 1994; Joosten, Cozijnsen, & De Wit, 1994; Takken et al., 1999), with these genes having been introgressed into various commercial tomato cultivars (Iida et al.,

2015). However, as this introgression often involved single *Cf R* genes, or *Cf R* genes with non-overlapping temporal resistance profiles, there was strong selection pressure on the pathogen to overcome the resistance(s). Consequently, as of today, *F. fulva* strains have been identified that can overcome one or more of all six major cloned *Cf R* genes, through modification or deletion of their corresponding *Avr* genes (Iida et al., 2015; Mesarich et al., 2023). As such, there is now an urgent need to identify new *Cf R* genes for the development of new *F. fulva*-resistant tomato cultivars. Identification of *F. fulva Avr* genes can aid this process by acting as markers for resistance identification (Mesarich et al., 2023), and the current research about *F. fulva* virulence and *Avr* factors will be detailed in the following sections.

1.4.4 Virulence factors

To date, eight effectors of *F. fulva* with confirmed roles in virulence have been identified: CfAvr4, CfEcp6, CfEcp1, CfEcp2-1, CfAvr2, CfTom1, CfAvr5, and CfEcp20-2. For several of these virulence factors, the exact function of the protein and how it contributes to virulence, is currently unknown. Effectors CfEcp1 and CfEcp2-1 were identified as virulence factors after gene deletion analysis was performed (Laugé, Joosten, Van den Ackerveken, Van den Broek, & De Wit, 1997). When the mutant strains were tested on the tomato host, colonization was reduced, fewer *in planta*-produced proteins were secreted, and a more severe plant defence response was observed compared with the wild type (WT) (Laugé et al., 1997). CfEcp2-1 is conserved in the other fungal species *P. fijiensis* (Stergiopoulos et al., 2010) and, as discussed previously in **section 1.3.5**, *D. septosporum*, suggesting this protein plays an important role in virulence across multiple types of plant pathogens (Stergiopoulos et al., 2010). Avr5 functions as an *Avr* factor when recognised by the corresponding tomato Cf-5 R protein (Dixon et al., 1998) and is not essential for virulence because Race 5 *F. fulva* strains, which lack a functional *Avr5* gene, can still infect tomato (Mesarich et al., 2014). However, it was found that complementation of a Race 5 strain with *Avr5* lead to increased fungal biomass during infection of susceptible tomato (lacking Cf-5), showing Avr5 contributes to virulence (Mesarich et al., 2014). *CfEcp20-2* is another effector gene, where gene deletion mutants had significantly reduced fungal biomass during infection of susceptible tomato. CfEcp20-2 has homologues in other Dothideomycete fungi and has the best predicted structural similarity with the characterised effector PevD1 of *Verticillium dahliae*, suggesting a conserved role in virulence (Karimi-Jashni, Maeda, Yazdanpanah, de Wit, & Iida, 2022; Tarallo et al., 2022).

The remaining virulence factors have been well-studied, where their function and contribution to virulence has been characterised. CfAvr4 is an effector that binds to chitin in the fungal cell

wall, via a carbohydrate-binding module family 14 (CBM14) domain (van den Burg, Harrison, Joosten, Vervoort, & de Wit, 2006). This interaction occurs through two CfAvr4 molecules dimerizing and forming a sandwich-like structure, which envelopes two molecules of the chitin-derived oligosaccharide chitohexaose $(GlcNAc)_6$ (Hurlburt, Chen, Stergiopoulos, & Fisher, 2018). This chitin-binding function protects against the activity of plant chitinases, which release chitin fragments to be recognised as PAMPs and activate PTI in the host (van den Burg et al., 2006). However, resistant tomato varieties carry *Cf-4*, which encodes an R proteins that can recognise CfAvr4 as an Avr factor (de Wit, 1977). Interestingly, the solved crystal structure of CfAvr4 in complex with chitohexaose showed that chitin-binding activity and Cf-4 recognition occur through separate residues (Hurlburt et al., 2018). Similar to CfAvr5, CfAvr4 also functions as a virulence factor. Heterologous expression of *CfAvr4* in *Arabidopsis* and tomato increased the virulence of several fungal pathogens with exposed chitin in their fungal cell walls. Furthermore, silencing of *CfAvr4* resulted in reduced virulence of *F. fulva* when infecting susceptible tomato lacking Cf-4 (van Esse, Bolton, Stergiopoulos, de Wit, & Thomma, 2007). CfAvr4 homologues have been identified in other Dothideomycete species, as well as functional orthologues in *P. fijiensis* (Stergiopoulos et al., 2010) and *D. septosporum* (de Wit et al., 2012), suggesting a conserved virulence and/or avirulence function. Additional functions such as interacting with pectin in the plant cell wall to increase the effectiveness of enzymatic degradation (Chen et al., 2021), and influencing expression of the *Cercospora* cf. *flagellaris* toxin cercosporin (Rezende, Zivanovic, Costa de Novaes, & Chen, 2020), have also been identified from CfAvr4 homologues and paralogs.

CfAvr2 is an effector protein that can inhibit diverse tomato cysteine proteases such as Rcr3 and Pip1 (Dixon, Golstein, Thomas, Van Der Biezen, & Jones, 2000; Krüger et al., 2002; Rooney et al., 2005). CfAvr2 physically interacts with and inhibits the tomato protein Rcr3, an extracellular papain-like cysteine protease required for disease resistance (Krüger et al., 2002). However, CfAvr2 binding of Rcr3 causes a conformational change which is recognised by the Cf-2 R protein, resulting in plant resistance (Rooney et al., 2005). This interaction can be explained by the guard hypothesis model, where plant components targeted by invaders, such as Rcr3, can be monitored or guarded by the products of plant resistance genes, such as *Cf-2* (Rooney et al., 2005; Van Der Biezen & Jones, 1998). Recently it was shown that ancient Rcr3 homologues are present in tomato, potato, eggplant, pepper, and petunia, and can be inhibited by Avr2 (Kourelis et al., 2020). This study also suggested that unlike other indirect pathogen recognition mechanisms, *Cf-2* evolved relatively recently by co-opting the pre-existing *Rcr3* in the *Solanum* genus (Kourelis et al., 2020). Therefore, when infecting tomato varieties carrying *Cf-2*, CfAvr2

functions as an Avr factor. However, it has also been shown that heterologous expression of CfAvr2 in *A. thaliana* enhances susceptibility towards specific extracellular fungal pathogens such as *Botrytis cinerea* and *V. dahliae*. Furthermore, heterologous expression of *CfAvr2* in tomato enhanced susceptibility to both *B. cinerea* and *V. dahliae*, as well as *F. fulva* strains with defective CfAvr2 (van Esse et al., 2008), suggesting CfAvr2 can also function as a virulence factor in susceptible tomato.

CfEcp6 is an effector protein with three LysM carbohydrate-binding domains (Bolton et al., 2008; Sánchez-Vallet et al., 2013) which can bind chitin (de Jonge et al., 2010). Sequestering chitin fragments released from the fungal cell wall through the activity of plant chitinases, prevented these molecules from being recognised as PAMPs to activate host immunity (de Jonge et al., 2010). This interaction occurs through the dimerization of the LysM1 and LysM3 domains, which form a groove that outcompetes host PRRs to bind chitin (de Jonge et al., 2010; Sánchez-Vallet et al., 2013). It was shown that heterologous expression of *CfEcp6* in *Fusarium oxysporum* significantly increases virulence on tomato (Bolton et al., 2008). Furthermore, RNA interference (RNAi)-mediated gene silencing of *CfEcp6* in *F. fulva* reduced virulence on susceptible tomato (Bolton et al., 2008). Orthologues of CfEcp6 have been found in several Dothideomycete and Sordariomycete phytopathogens, including *D. septosporum*, suggesting that Ecp6 is an important conserved virulence factor.

CfTom1 is a secreted glycosyl hydrolase (GH10) enzyme. A basal defence response in tomato is the production of α-tomatine, an antifungal glycoalkaloid. It was shown that *F. fulva* CfTom1 can hydrolyse α-tomatine into the less harmful compound, tomatidine. Gene disruption analysis showed that mutants were more sensitive to α-tomatine, and had reduced fungal biomass when infecting susceptible tomato, suggesting that CfTom1 functions as a virulence factor (Ökmen et al., 2013).

1.4.5 Avirulence factors

As discussed previously (**section 1.4.3**) several Avr factors have been identified from *F. fulva*. The Avr factors CfAvr2, CfAvr4, and CfAvr5 were discussed above (**section 1.4.4**), because they also function as virulence factors in susceptible tomato. The remaining avirulence factors to discuss are CfAvr4E, CfAvr9, CfAvr9B, and CfAvr9E. CfAvr4E is a cysteine-rich protein secreted during colonisation of the tomato apoplast (Westerink, Brandwagt, De Wit, & Joosten, 2004). The existence of CfAvr4E was first suggested by Takken et al. (1999), after the discovery of the Cf-4 homologue, Cf-4E. CfAvr4E functions as an Avr factor in resistant tomato and is likely not essential for virulence as some *F. fulva* strains have adapted through deletion of *CfAvr4E*.

However, it was also found that Cf-4E recognition could be evaded through a single amino acid substitution (Westerink et al., 2004). There are two other Avr factors (CfAvr9B and CfAvr9E) hypothesised to exist, due to the existence of two *Cf-9* homologues, *Cf-9B* and *Cf-9E* (Jones et al., 1994; Parniske et al., 1997). CfAvr9B was recently identified (de la Rosa, 2022), while CfAvr9E is yet to be identified.

CfAvr9 is an Avr protein that, after secretion, is processed by fungal and plant proteases into a stable peptide elicitor (Van den Ackerveken, Vossen, & De Wit, 1993). CfAvr9 is recognised by the Cf-9 receptor protein in resistant tomato (van Kan et al., 1991). It has been shown through iodine-125 labelling at the N-terminal tyrosine residue, that CfAvr9 can bind to the plasma membrane of tomato cells, independent of the presence of Cf-9 (Kooman-Gersmann, Honee, Bonnema, & De Wit, 1996). It is possible that another host target is involved in the CfAvr9-Cf-9 interaction because no direct interaction between the two proteins has been shown (Luderer et al., 2001). It is likely that CfAvr9 is not essential for virulence because *F. fulva* strains that lack CfAvr9 can still infect tomato (Stergiopoulos et al., 2007), and deletion of *CfAvr9* does not affect virulence (Marmeisse, Van Den Ackerveken, Goosen, De Wit, & Van Den Broek, 1993).

Recently, another 10 candidate Avr factors were identified from apoplastic washing fluid of a compatible interaction between *F. fulva* and tomato (Mesarich et al., 2018). In this study, 61 novel small secreted protein (SSP) effectors were identified, and 41 were tested for their ability to trigger an HR on wild tomato accessions. The 10 candidate Avr factors that triggered HR were; CfEcp8, CfEcp9-1, CfEcp10-1, CfEcp11-1, CfEcp12, CfEcp13, CfEcp14-1, CfEcp15, CfEcp16 and CfEcp17. The next step for this research is to identify corresponding tomato *R* genes, which would be invaluable for future resistance breeding strategies.

1.4.6 Secondary metabolites

F. fulva contains six secondary metabolite (SM)-encoding gene clusters that have undergone rearrangements and gene loss due to the presence of transposable elements, and are conserved in other fungi (Collemare et al., 2014). This fungus is thought to have the genes necessary to produce elsinochrome and cercosporin toxins, but the corresponding core genes are not expressed *in planta*. The only core SM genes expressed during infection of tomato are *CfPks6* and the nonribosomal peptide synthetase *CfNps9*, however their expression is significantly down-regulated during mesophyll colonisation. *In vitro* SM profiling could only identify the SM produced by CfPks6, cladofulvin (Collemare et al., 2014; Griffiths et al., 2016). Cladofulvin does not have phytotoxic properties on Solanaceae plants or any antimicrobial activity (Collemare et al., 2014), therefore suggesting it does not appear to contribute to virulence on the tomato host.

However, cladofulvin may protect *F. fulva* conidia against abiotic stresses such as UV light and cold (Griffiths et al., 2016).

The *F. fulva* 0WU and Race 5 genomes also contain a complete set of predicted dothistromin genes (de Wit et al., 2012; Mesarich et al., 2023). Analysis of the new chromosome-level *F. fulva* Race 5 genome identified that these dothistromin genes are fragmented in a similar way to those in the *D. septosporum* genome, in subclusters throughout chromosome 13, although some rearrangements are present (Mesarich et al., 2023). However, key biosynthetic genes have been pseudogenized in the *F. fulva* genome such that functional proteins cannot be made (Chettri et al., 2013). Consequently, dothistromin cannot be produced, at least from these *F. fulva* isolates, and indeed dothistromin could not be detected by high-performance liquid chromatography (HPLC) analysis of *in vitro F. fulva* extracts (de Wit et al., 2012). At the time of this research, *F. fulva* was considered a biotrophic pathogen. It would be interesting to re-evaluate dothistromin production in *F. fulva* during the late stages of infection, when this fungus is thought to exhibit necrotrophic growth.

1.4.7 Available genomic, transcriptomic, and proteomic resources

As an important fungal pathogen, and model system for studying plant-pathogen interactions for many years, there are many genomic, transcriptomic, and proteomic resources available for *F. fulva*. As discussed above in **section 1.3.7**, the genome of the *F. fulva* 0WU strain was sequenced in a comparative study with *D. septosporum* (de Wit et al., 2012). Because *F. fulva* has a repeat-rich genome, a chromosome-level genome assembly was not possible at that time (de Wit et al., 2012). Recently, third generation sequencing technology and the Hi-C chromatin conformation capture technique were utilized to produce a 98.9% complete genome sequence of the *F. fulva* Race 5 strain which was assembled to chromosome level (Zaccaron, Chen, Samaras, & Stergiopoulos, 2022). Transcriptome analyses are available for the 0WU and Race 5 strains both *in vitro* (Mesarich et al., 2014; Zaccaron et al., 2022) and *in planta* (Mesarich et al., 2014), although for the Race 5 strain only one time point was analysed in planta. Proteomic analysis has also been performed with the apoplastic washing fluid of tomato infected with four global isolates, including 0WU and Race 5, at different time points (Mesarich et al., 2018). However, proteomic analysis has not been performed with *F. fulva* extracts grown in vitro, presenting an avenue for future research. As mentioned previously in **section 1.3.7**, the current resources available for *F. fulva* were recently reviewed in detail by Mesarich et al. (2023).

1.4.8 The necrotrophic switch in hemibiotrophic plant pathogens

As discussed previously, hemibiotrophic pathogens such as *D. septosporum* and *F. fulva* transition from biotrophic to necrotrophic growth through an unknown mechanism. Several genes have been identified that may play a role in the necrotrophic switch, and these are listed in **Table 1.1**. Several of these genes encode transcription factors (TFs); sequence-specific DNA-binding proteins that can modulate gene expression (John, Singh, Oliver, & Tan, 2021). These TFs have been analysed through gene deletion studies and tentatively suggested to play a role in the transition to necrotrophy. Deletion of the homeobox TF *CoHox1* from *Colletotrichum orbiculare* results in mutants that are non-pathogenic and cannot produce lesions even on wounded leaves (Yokoyama, Izumitsu, Irie, & Suzuki, 2019). Deletion of *PacCL* of *Colletotrichum lindemuthianum*, a pH-responsive TF, results in mutants blocked at the switch to necrotrophy, that are unable to produce secondary hyphae, and trigger an HR in the host (Dufresne, Perfect, Pellier, Bailey, & Langin, 2000). Deletion of *CLNR1* from *C. lindemuthianum*, a major nitrogen regulator, results in non-pathogenic mutants blocked at the necrotrophic switch (Pellier, Laugé, Veneault-Fourrey, & Langin, 2003). Finally, deletion of *Pf2*, a Zn_2Cys_6-type TF from *Parastagonospora nodorum*, and transcriptome analysis of the mutant compared to the WT, showed that Pf2 positively regulates the expression of 12 effector-like genes, including necrotrophic effectors *SnToxA* and *SnTox3* (Jones et al., 2019; Rybak et al., 2017).

Several other genes have been suggested to play a role in the necrotrophic switch. The effector *CtNUDIX* of *Colletotrichum truncatum* elicits strong cell death when transiently expressed in *Nicotiana benthamiana*, is expressed specifically at the necrotrophic switch stage, and is essential for disease progression. Over-expression of *CtNUDIX* in *C. truncatum* and rice blast pathogen *Magnaporthe oryzae* resulted in incompatibility with their respective hosts, lentil and barley, due to an HR-like response at the biotrophic stage (Bhadauria, Banniza, Vandenberg, Selvaraj, & Wei, 2013). It was hypothesised that premature secretion of *CtNUDIX* during the early biotrophic stage blocks the transition to necrotrophic growth in these two pathogens, and that CtNUDIX-triggered cell death may normally trigger the switch to necrotrophy (Bhadauria et al., 2013; Shao, Smith, Kabbage, & Roth, 2021).

Table 1.1. Genes that may be required for the switch to necrotrophy in different hemibiotrophic fungi.

Fungal organism	Gene	Gene prediction[1]	Source
Colletotrichum orbiculare	*CoHox1*	Homeobox TF	Yokoyama et al. (2019)
Colletotrichum lindemuthianum	*PacCL*	pH-responsive TF	Dufresne et al. (2000)
C. lindemuthianum	*CLNR1*	Major nitrogen regulator TF	Pellier et al. (2003)
Parastagonospora nodorum	*PnPf2*	Zinc finger TF	Jones et al. (2019)
Colletotrichum truncatum	*CtNUDIX*	Nudix hydrolase domain	Bhadauria et al. (2013)

1 – TF, transcription factor.

The necrotrophic switch has been well-studied in *Moniliophthora perniciosa*, the causal agent of witches' broom disease (WBD) in cacao. In this pathosystem, it has been suggested that nutrient depletion may act as a cue for the transition to necrotrophic growth. Several findings support this hypothesis, such as that high levels of glycerol can maintain biotrophic-like growth of *M. perniciosa in vitro* (Meinhardt et al., 2006). Also, the expression of several necrotrophic effectors, such as cell death inducer *MpNEP2*, are induced upon carbon starvation in this fungus, and delayed when apoplastic sugar is artificially increased (Barau et al., 2015). However, it has also been hypothesised that a change in the respiratory pathway may trigger the switch to necrotrophic growth in *M. perniciosa*. It was suggested that during biotrophic growth this fungus uses an alternative respiratory pathway requiring a mitochondrial alternative oxidase (*AOX*) gene, because it can detoxify reactive oxygen species (ROS) from the host and is not inhibited by the plant defence compound nitric oxide. Then, during necrotrophic growth, the fungus switches to the conventional pathway, CRC (Cytochrome-dependent Respiratory Chain), because ROS and nitric oxide are not being produced by the dead plant cells, and this pathway generates more energy (Thomazella et al., 2012). These hypotheses present two processes that may regulate the switch to necrotrophy, however further work is required to determine what specifically triggers the transition to necrotrophy in this fungus. It would be of interest to test whether either of these hypotheses are supported in other hemibiotrophic fungi. Despite this work performed in *M. perniciosa* and the genes listed in **Table 1.1** with possible roles in the necrotrophic switch, it is still uncertain what regulates this transition in hemibiotrophic fungi.

1.5 Aims and objectives

The Dothideomycetes fungal class is the most diverse class and is overrepresented in plant-pathogenic species. The aim of this research was to identify and characterise virulence factors of Dothideomycete pathogens, specifically of the closely related fungi *D. septosporum* and *F. fulva*. As part of an ongoing collaboration, *CfEcp11-1*, which is an orthologue of a known virulence/*Avr* gene from an important Dothideomycete pathogen, was a key focus for *F. fulva*. As a fungal phytopathogen with a hemibiotrophic lifestyle, a key focus with *D. septosporum* was to identify virulence factors with a role in the necrotrophic switch. Virulence factors identified and characterised in this study will aid future research in other Dothideomycete species and help to inform resistance breeding strategies for Dothistroma needle blight and tomato leaf mould.

Aim 1. Characterise candidate effector *CfEcp11-1* of *F. fulva* and identify and characterise homologues in other species.

Candidate effector CfEcp11-1 was identified in *F. fulva* by Mesarich et al. (2018) and found to be a homologue of the Avr effector AvrLm3 from *Leptosphaeria maculans*, as well as of two proteins from *Zymoseptoria ardabiliae*. A collaboration with international research groups working on *L. maculans* and *F. fulva* was formed, and it was hypothesised that more homologues of CfEcp11-1 and AvrLm3 may be present in other fungal species. The specific objectives for this aim were to:

- Use bioinformatic analyses to identify and compare CfEcp11-1 homologues present in other fungal species.
- Identify which amino acids of CfEcp11-1 and AvrLm3 are involved in R protein recognition in tomato. C. Mesarich (per comm) showed that CfEcp11-1 is recognized by the hypothetical R protein Cf-Ecp11-1, but AvrLm3 is not, so chimeric proteins will be designed with region swaps and amino acid substitutions between the two proteins.
- Test the chimeric proteins for a hypersensitive response (HR) in tomato (Cf-Ecp11-1), using Potato Virus X (PVX)-based transient expression.
- Test CfEcp11-1 homologues for a HR in tomato (Cf-Ecp11-1) using PVX-based transient expression, based on the finding that CfEcp11-1 was recognized in the *L. maculans* host *Brassica napus* (Lazar et al., 2022).

- Determine whether *CfEcp11-1* contributes to virulence in *F. fulva* by developing a gene deletion or disruption mutant and testing it for virulence on tomato.

Aim 2. Identify candidate virulence factors from *D. septosporum*, with a key focus on those with a role in the necrotrophic switch. The specific objectives for this aim were to:

- Use available genomic and transcriptomic resources and bioinformatic analyses to develop a candidate virulence factor prediction pipeline for *D. septosporum*.
- Use the prediction pipeline to identify candidate virulence factors and then use literature searches, homology to other virulence factors, and gene expression to generate a shortlist of candidates for further study.
- Analyse the shortlisted candidate virulence factors by comparing with the literature and examining gene phylogenies.
- Use the generated analysis to select candidate virulence factors for gene deletion analysis.

Aim 3. Investigate the *D. septosporum* and *F. fulva* culture filtrate proteomes to identify new candidate virulence factors. The specific objectives for this aim were to:

- Grow *D. septosporum* and *F. fulva* under different conditions and harvest the culture filtrate.
- Prepare proteins from harvested culture filtrate for LC-MS analysis.
- Perform LC-MS analysis (to be carried out by a third party).
- Use the LC-MS data and previously predicted secreted protein lists of *D. septosporum* and *F. fulva* to identify proteins present in the culture filtrate samples.
- Use available bioinformatic prediction tools to identify classically secreted proteins and to predict protein domains and possible functions.
- Use the generated data to characterise the effect of different growth conditions on the presence or absence of classically secreted proteins from both fungi.
- Identify homologues between *D. septosporum* and *F. fulva* classically secreted proteins and use available transcriptomic data to compare the expression of the genes that encode them.
- Analyse the culture filtrate proteomes of *D. septosporum* and *F. fulva* and available transcriptomic data to identify candidate virulence factors.

Aim 4. Generate gene disruption mutants of *D. septosporum* candidate virulence factors and test virulence in the *P. radiata* host. The specific objectives for this aim were to:

- Develop a CRISPR/Cas9 gene disruption method in *D. septosporum* targeting the characterised gene *DsAflR* for which there is a known phenotype.
- Analyse the *DsAflR* disrupted transformants through PCR, sequencing and Southern hybridization.
- Use CRISPR/Cas9 with donor DNA to disrupt several candidate virulence factors shortlisted in Aim 2.
- Analyse the disrupted candidate virulence factor mutants through PCR, sequencing and Southern hybridization to identify candidates for virulence assessment.
- Complement the disrupted mutants and perform qPCR analysis to determine the gene complement copy number.
- Examine radial growth and sporulation of *D. septosporum* WT, CRISPR/Cas9 mutants, and complemented strains to identify if any mutants are phenotypically different to WT.
- Inoculate *P. radiata* seedlings with the D. septosporum WT, CRISPR/Cas9 mutant, and complemented strains to assess virulence.
- Assess virulence of the *D. septosporum* WT, CRISPR/Cas9 mutants and complemented strains, by assessment of disease symptoms and estimating fungal biomass by qPCR, to determine if the candidate virulence factors play a role in virulence.

Chapter 2 - Candidate effector CfEcp11-1 of *Fulvia fulva*

2.1 Introduction

The candidate effector CfEcp11-1 was first discovered from apoplastic washing fluid of a compatible interaction between *Fulvia fulva* (formerly *Cladosporium fulvum*) and its tomato host (*Solanum lycopersicum* cv. Heinz [H]-Cf-0) (Mesarich et al., 2018). CfEcp11-1 was shown to trigger a hypersensitive response (HR) on eight different wild tomato cultivars thought to carry a corresponding *Cf* (for resistance to *C. fulvum*) resistance (*R*) gene, tentatively named *Cf-Ecp11-1* (Mesarich et al., 2018). The *CfEcp11-1* gene was induced during infection and the protein found to be homologous to the avirulence (Avr) effector AvrLm3 from *Leptosphaeria maculans*, as well as to two uncharacterised proteins from *Zymoseptoria ardabiliae*, the causal agent of Septoria tritici blotch disease of wheat (Mesarich et al., 2018).

Like *Dothistroma septosporum* and *F. fulva*, *L. maculans* is a Dothideomycete, and it is the causal agent of oilseed rape stem canker or blackleg disease. So far, 14 effectors encoded by *Avr* genes have been identified from *L. maculans* (Borhan, Van De Wouw, & Larkan, 2022), including the homologue of CfEcp11-1, AvrLm3. In *L. maculans*, an interesting relationship was found between AvrLm3 and another effector AvrLm4-7. When a functional allele of *AvrLm4-7* is present, Rlm3-mediated recognition of AvrLm3 is masked (Plissonneau et al., 2016). It was later found that recognition of another avirulence effector, AvrLm5-9, could also be masked by AvrLm4-7 (Ghanbarnia et al., 2018). The mechanism by which AvrLm4-7 masks recognition of AvrLm3 and AvrLm5-9 does not appear to occur through direct protein interaction or gene regulation (Ghanbarnia et al., 2018; Plissonneau et al., 2016), and is still unknown.

The crystal structures of CfEcp11-1 and AvrLm5-9 were recently solved by Lazar et al. (2022) while the crystal structure of AvrLm4-7 was solved previously by Blondeau et al. (2015). Although sufficient AvrLm3 protein could not be obtained for crystallography, a 3D model of AvrLm3 was made based on the solved structure of CfEcp11-1 (Lazar et al., 2022). This revealed that CfEcp11-1, AvrLm3, and AvrLm5-9 are all structural analogues of AvrLm4-7, containing a four-stranded β-sheet and helical connections, as well as six conserved cysteines involved in disulphide bridges (Lazar et al., 2022). The tertiary structures of CfEcp11-1 and AvrLm3 are shown in **Figure 2.1**, illustrating their similarities.

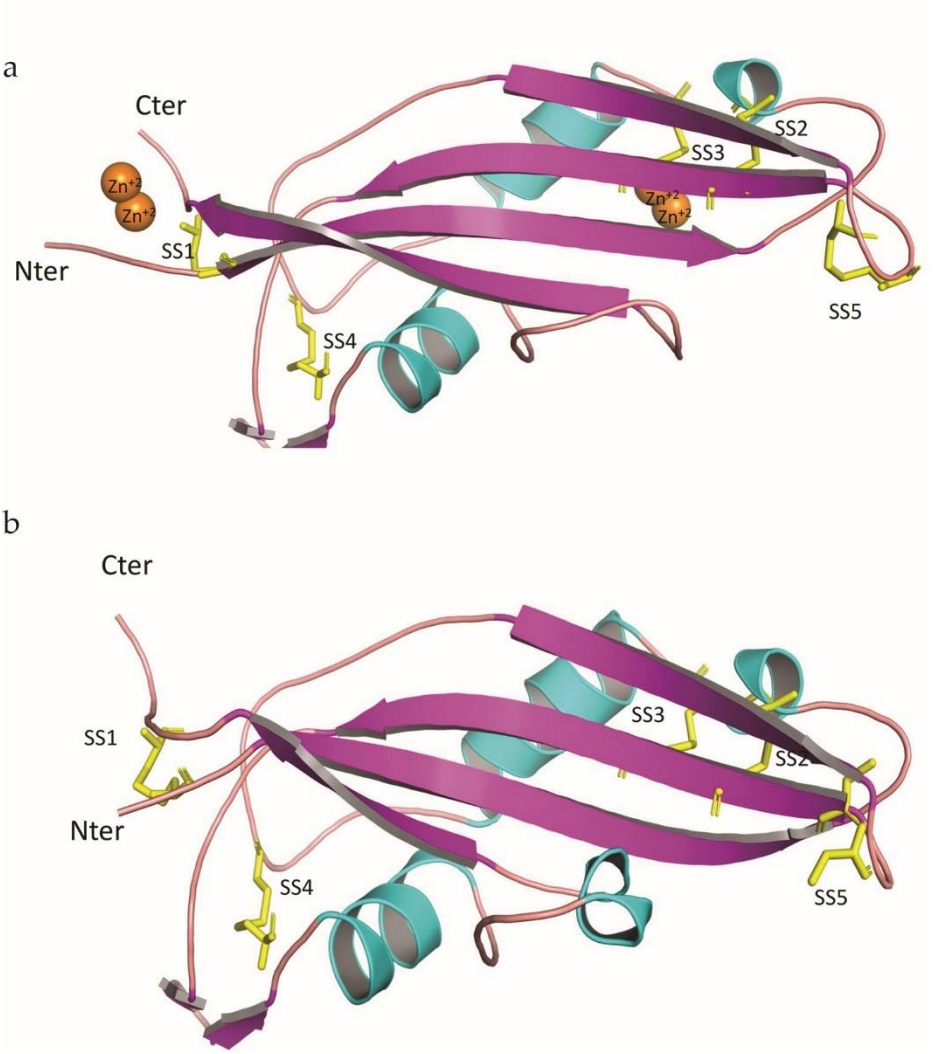

Figure 2.1. Tertiary structures of CfEcp11-1 from *Fulvia fulva* and AvrLm3 from *Leptosphaeria maculans*. Proteins are shown as cartoons and coloured according to secondary structure (α-helix in cyan, and β-strand in magenta). The amino (N)- and carboxyl (C)-termini are labelled. The disulphide bonds are shown by yellow sticks and labelled and numbered according to the sequence alignment in Lazar et al. (2022). (**a**) Structure of CfEcp11-1, based on X-ray crystallography data, with the Zn^{2+} ions required for crystallisation shown as orange spheres. (**b**) Swiss-Model structure of AvrLm3, determined by comparison with the CfEcp11-1 X-ray structure. Figure was taken from Lazar et al. (2022), with permission.

Putative structural analogues from *L. maculans* and other fungal species were identified by Lazar et al. (2022), and these proteins, including CfEcp11-1, were named LARS (Leptosphaeria AviRulence and Suppressing) effectors. The relationship between CfEcp11-1, AvrLm3, and AvrLm4-7 was further investigated in the study by Lazar et al. (2022), and it was found that CfEcp11-1 could be recognised by Rlm3, and that this recognition could be masked by AvrLm4-7. In contrast, Potato virus X (PVX)-based transient expression of AvrLm3 in *Cf-Ecp11-1* tomato

did not trigger a response (**Figure 2.2**), suggesting that AvrLm3 was not recognised by the CfEcp11-1 receptor (C. Mesarich, L. Deurhof and M. Joosten, unpublished results). From these analyses, it was hypothesised that either CfEcp11-1 performs the same activity as AvrLm3 in *B. napus* and therefore enables recognition by Rlm3, or that this recognition is due to structural conservation between CfEcp11-1 and AvrLm3 (Lazar et al., 2022).

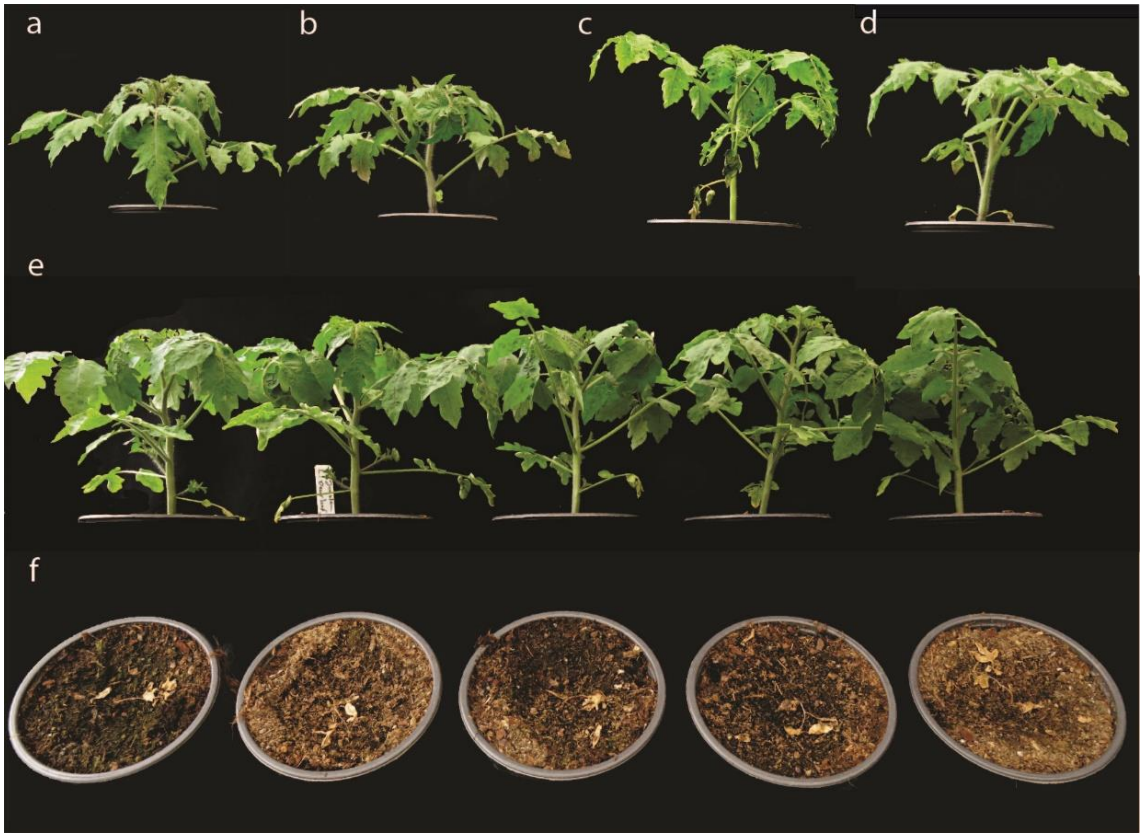

Figure 2.2. Potato virus X (PVX)-based transient expression of *CfEcp11-1* from *Fulvia fulva* and *AvrLm3* from *Leptosphaeria maculans* in tomato. Tomato cultivars were infiltrated with *Agrobacterium tumefaciens* strains carrying the following: (**a**) Tomato (MoneyMaker [MM]-Cf-0) with pSfinx::AvrLm3 Potato virus X (PVX) expression vector. (**b**) Tomato (MM-Cf-0) with pSfinx::CfEcp11-1 PVX expression vector. (**c**) Tomato (CGN 15484) with pSfinx empty expression vector. (**d**) Tomato (MM-CF-0) with pSfinx empty expression vector. (**e**) Tomato (CGN 15484) with pSfinx::AvrLm3 expression vector. (**f**) Tomato (CGN 15484) with pSfinx::CfEcp11-1 expression vector (plants died). The tomato cultivar MM-Cf-0 does not carry any *Cf* resistance (*R*) genes, while CGN 15484 carries the putative *Cf-Ecp11-1 R* gene. Photos were taken three weeks post-infiltration. Experiment performed by C. Mesarich, L. Deurhof and M. Joosten (unpublished results).

This chapter outlines an investigation into the role of CfEcp11-1 in the *F. fulva*-tomato interaction. Additional homologues of CfEcp11-1 from other plant-pathogenic fungi were identified to broaden our understanding of this effector family. The aim was then to investigate the interaction between the tomato *Cf-Ecp11-1* receptor and the effectors CfEcp11-1 and AvrLm3 through region swap analysis and PVX-based transient expression, to determine what regions of Ecp11-1 are required for recognition by Cf-Ecp11-1. Finally, this chapter aimed to determine whether CfEcp11-1 functions as a virulence factor of *F. fulva* through gene disruption analysis, using clustered regularly interspaced short palindromic repeats (CRISPR)/Cas9 technology for the first time in this fungus.

2.2 Materials and methods

2.2.1 Biological materials

The *F. fulva* strains 0WU (de Wit et al., 2012) and Race 5 were used in this study (Stergiopoulos et al., 2007). Strain 0WU was originally used due to it being the only strain with a sequenced genome at the time. However, 0WU had a low sporulation rate so later work was performed with the Race 5 strain. The bacterial strains used in this study were *Escherichia coli* DH5α (Taylor, Walker, & McInnes, 1993), *Agrobacterium tumefaciens* AGL1 (Lazo, Stein, & Ludwig, 1991), GV3101::pMP90 (Hellens, Mullineaux, & Klee, 2000; Koncz & Schell, 1986) and 1D1249 (C. Kado, UC Davis). The tomato plant *Solanum pimpinellifolium* CGN 15484, carrying the putative *Cf-Ecp11-1 R* gene, was used in this study.

2.2.1.1 Cultivation of *F. fulva*

F. fulva was routinely cultured on half-strength potato dextrose agar (PDA: 19.5 g/L potato dextrose agar (Merck, New York, USA) and 7.5 g/L Agar, Bacteriological (Pure Science, Wellington, NZ)), and incubated in the dark at 22°C. Sub-culturing was performed by flooding the plates with ~3 mL sterile MilliQ water and, after 10 min, suspending the spores with a plate spreader, then spreading the spores onto a new PDA plate. Spore harvesting was performed in the same way, except after collection of spores the spore concentration was determined with a haemocytometer. For short-term storage, plates were wrapped in parafilm and kept at 4°C. For long-term storage, spores were mixed with glycerol to a final concentration of 25%, snap-frozen in liquid nitrogen, and stored at -80°C.

For genomic DNA (gDNA) extraction, *F. fulva* spores were inoculated into 125 mL conical flasks with 25 mL potato dextrose broth (PDB; Scharlau, Barcelona, Spain), and incubated in the dark at 22°C, with shaking at 160 rpm (classic series C10 platform shaker (New Brunswick Scientific, New Jersey, USA)). Mycelium was filtered through a sterile nappy liner or Miracloth (EMD Millipore Corp., Darmstadt, Germany), washed with sterile MilliQ water, snap-frozen in liquid nitrogen, and stored at -80°C. Prior to gDNA extraction, frozen mycelium was freeze-dried overnight or until all moisture was removed.

To obtain pure cultures, all *F. fulva* transformants were single spore-purified. To achieve this, spores were harvested from a PDA plate and 50 µL of spore suspension streaked onto a new PDA plate using an inoculation loop. The spores from a single colony were then transferred onto a new PDA plate using a wet inoculation loop, to repeat the spore streak a second time.

2.2.1.2 Bacterial culturing

Bacteria were routinely cultured on low-salt lysogeny broth (LB) agar plates (20 g/L LB low salt (Duchefa Biochemie, Haarlem, Netherlands) and 15 g/L Agar, Bacteriological (Pure Science) with antibiotics as required, and incubated at 37°C for *E. coli*, and 28°C for *A. tumefaciens*. Bacteria were also routinely cultured in low-salt LB broth (20 g/L LB low salt (Duchefa Biochemie) with antibiotics as required, at the same temperature but with shaking at 180 rpm (classic series C10 platform shaker (New Brunswick Scientific)). For short-term storage, plates were wrapped in parafilm and kept at 4°C. For long-term storage, spores were mixed with glycerol to a final concentration of 25% and stored at -80°C.

2.2.1.3 Growth and maintenance of tomato plants

Tomato plants were grown for PVX-based transient expression experiments. All plants were germinated from seed in soil (Daltons premium seed mix, Fruitfed, New Zealand) that had been semi-sterilized at 60°C for at least 72 h and transferred to individual pots for sowing. Two different plant growth rooms were used for these experiments: a light- and temperature-controlled room (22°C temperature, 12 h:12 h light:dark cycle, 80–85 µmol/m^2/s light intensity) that did not have regulatory approval for PVX work, and a plant growth room with PVX approval but not temperature-, light-, or humidity-regulation. Thus, for PVX transient expression assays, plants to be agroinfiltrated at the cotyledon stage were germinated in the light- and temperature-controlled room and then moved to the other room for PVX infection. Plants to be agroinfiltrated by toothpick inoculation were germinated and grown for 4 weeks in the first room before being moved for the PVX transient expression assay.

2.2.2 General molecular techniques

2.2.2.1 *F. fulva* gDNA extraction

Extraction of *F. fulva* gDNA was performed using two different methods. For methods that did not require high-quality DNA, such as PCR screening of transformants, the simple salts/ethanol precipitation method by Liu, Coloe, Baird, and Pederson (2000) was performed. When high quality gDNA was required, a modified version of the extraction method described by van Kan et al. (1991) was performed. Freeze-dried fungal material was ground in liquid nitrogen, then 1 mL of extraction buffer (0.5 M NaCl, 10 mM Tris-HCl, 10 mM EDTA, 1% SDS, pH 7.5) added while stirring. Once thawed, the solution was pipetted into a new tube, mixed well by vortexing, then incubated at 65°C for 30 min. The tube was then left at room temperature for 2 min, before centrifuging at 13,000 rpm (Heraeus™ Pico 17 microcentrifuge (Thermo Fisher Scientific,

Massachusetts, USA)) for 5 min. The supernatant was transferred to a new tube, 4 µL RNAse (20 mg/mL) added, vortexed and incubated at 37°C for 15 min. Phenol (0.5 volumes) was added and mixed gently by inversion, then 0.5 volumes $CHCl_3$:IAA (24:1) were added and mixed gently. The tube was centrifuged as before, and the aqueous layer transferred to a new tube. Then, 1 volume of phenol/$CHCl_3$ (1:1) was added, mixed gently, and then centrifuged again as before. The aqueous layer was transferred to a new tube, 1 volume of $CHCl_3$:IAA (24:1) added and mixed gently, then centrifuged again at the same speed. The aqueous layer was transferred to a new tube, 0.1 volume of 3 M NaOAc and 2 volumes of 95% EtOH were added, the solutions were mixed gently and then incubated overnight at 4°C. The tube was then centrifuged at 13,000 rpm for 30 min at 4°C. The supernatant was decanted, the DNA pellet washed with 70% EtOH, and then centrifuged again at the same speed for 5 min at 4°C. The supernatant was decanted, and the DNA pellet air-dried for 15 min. The DNA was then dissolved in MilliQ water and stored at -20°C.

2.2.2.2 Plasmid extraction

For extraction of plasmids from bacteria, cultures were grown in LB and extraction performed with an E.N.Z.A. Plasmid DNA Mini Kit I (Omega Bio-Tek, Norcross, Georgia) as per the manufacturer's instructions. All plasmids used in this chapter are listed in **Appendix 1**.

2.2.2.3 Gel and column purification

For purification of PCR and restriction digestion products from agarose gels, an E.N.Z.A. Gel Extraction Kit (Omega Bio-Tek) was used as per the manufacturer's instructions. For purification of DNA from PCRs, an E.N.Z.A. Cycle Pure Kit (Omega Bio-Tek) was used as per the manufacturer's instructions.

2.2.2.4 Genomic and plasmid DNA quantification

Quantification of DNA was performed using a Nanodrop® ND-1000 UV-Vis spectrophotometer and Nanodrop® software version 3.1.0 (Nanodrop Technologies Inc., North Carolina, USA).

2.2.2.5 Polymerase chain reaction (PCR)

All PCRs were performed in a Mastercycler® nexus (Eppendorf, Hamburg, Germany) machine. Standard PCRs were performed with Taq DNA polymerase with ThermoPol Buffer (New England Biolabs, Massachusetts, USA) following the manufacturer's protocols. For high-fidelity amplification (such as for cloning or sequencing), PCR was performed with Phusion High-Fidelity DNA polymerase (New England Biolabs) as per the manufacturer's instructions. PCR primers

were designed using Geneious (v9.1.8 software) as ~15 bases long, melting temperature of ~55°C, GC content of ~50% and, if possible, no predictions of hairpin or primer-dimer formation.

2.2.2.6 Quantitative PCR

Quantitative PCRs (qPCRs) were performed using a LightCycler®2.0 instrument (Roche, Basel, Switzerland), and the data analysed using LightCycler®480 v1.5.1 software (Roche). All reactions were made with a SensiFAST™ SYBR® No-ROX kit (Meridian Bioscience, Ohio, USA) in a 10 µL volume according to the manufacturer's protocol. The qPCR conditions used were: one cycle at 95°C for 3 min, 45 cycles of 95°C for 5 sec, 60°C for 10 sec, and 72°C for 20 sec, then one cycle at 40°C for 10 sec. All samples were analysed with three technical replicates.

To calculate primer efficiency, standard curves were produced by performing qPCR with seven 5-fold dilutions, each with three replicates, starting with 1000 ng *F. fulva* wild type (WT) gDNA. The cycle-threshold (Ct) values were plotted against log gDNA concentration, and the primer efficiency calculated as $10^{(-1/\text{slope})}$. Primers were used if they had a primer efficiency of greater than 75%, and a single peak in the melt curve. When using the primers in a PCR plate different to the one used to construct the standard curve, one reaction with WT gDNA diluted to one of the standard curve dilutions was run in the same plate to confirm the primer efficiency was accurate across plates.

2.2.2.7 Copy number determination by quantitative PCR

To determine the *CfEcp11-1* gene copy number of mutant #25, qPCR analysis (**Materials and methods section 2.2.2.6**) was performed with 50 ng WT and mutant #25 gDNA using primers that amplified the target gene (*CfEcp11-1*) and the single-copy reference gene *actin* (JGI ID: 189818) (Mesarich et al., 2014; Zaccaron et al., 2022). From the standard curves (**Materials and methods section 2.2.2.6**), the primer efficiencies (E) were determined to be: *CfEcp11-1* (E=1.75), and *actin* (E=1.78). Primer sequences are listed in **Appendix 2**. The Ct ratio between the target and reference gene of the WT and the mutant #25 gDNA was calculated using the following formula:

$$\text{Ratio} = \frac{(E\text{target})^{\Delta\text{Ct target }(control\ -\ sample)}}{(E\text{ref})^{\Delta\text{Ct ref }(control\ -\ sample)}}$$

In this formula, E_{target} is the primer efficiency of the target gene (*CfEcp11-1*), and E_{ref} is the primer efficiency of the reference gene (*actin*). The ΔCt target (control-sample) is the Ct of the target gene in WT minus the Ct of the target gene in the mutant gDNA. While the ΔCt ref (control-sample) is the Ct of the reference gene in WT minus the Ct of the reference gene in the mutant gDNA. The calculated ratio is the copy number of the target gene.

2.2.2.8 Sequencing

Sequencing of PCR products or plasmid DNA was performed by the Massey Genome Service (Massey University, Palmerston North, New Zealand), and the data analysed using Geneious (v9.1.8 software).

2.2.2.9 Gene synthesis

The *CfEcp11-1* and *AvrLm3* WT, chimeric, and homologous genes were synthesised in a pTwist Amp High Copy plasmid by Twist Bioscience (California, USA).

2.2.2.10 DNA ligation

DNA ligations were performed using T4 DNA ligase (New England Biolabs) according to the manufacturer's instructions, in a 20 µL volume with a 3:1 molar insert:vector ratio, and incubating overnight at 4°C.

2.2.2.11 Restriction enzyme digestion

Digestion of DNA was performed with specific restriction enzymes as required, and the appropriate buffer solution, according to the manufacturer's instructions. Reactions were incubated at the appropriate temperature in a heat block (or Mastercycler® Nexus for smaller reaction volumes) from 1 h to overnight. When the digestion products were required for downstream purposes, the reaction was heat-inactivated at 65°C for 10 min. Digested DNA was then examined by gel electrophoresis (**Materials and methods section 2.2.2.12**).

2.2.2.12 Agarose gel electrophoresis

DNA was routinely examined following electrophoresis on a 0.8–2% agarose gel (HyAgarose™, HydraGene, Piscataway, New Jersey, USA) run at 80–110 volts in 1x Tris-acetate-EDTA (TAE) buffer (190 mM Tris, 342 mM acetic acid (Emsure®, Merck), 2.5 mM EDTA). DNA was loaded with 0.2 volumes of SDS loading dye (0.2% bromophenol blue (Avantor Sciences Inc., Pennsylvania, USA), 20% sucrose, 1% SDS, 5 mM EDTA, pH 6.8). When DNA fragment size estimation was required, a 1 kb plus DNA ladder (Invitrogen, California, USA) was also loaded in the gel. After electrophoresis, the DNA in the gel was stained with ethidium bromide (1 µg/mL,

BDH, Poole, England) for 15 min, then imaged with a UV Transilluminator Gel Documentation system (Bio-Rad, California, USA).

2.2.3 Bacterial transformation

2.2.3.1 Preparation and transformation of chemically competent cells

Chemically competent cells of *E. coli* were prepared by culturing as described previously (**Materials and methods section 2.2.1.2**). A 2.5 mL starter culture was grown overnight in LB medium and used to inoculate 250 mL of LB medium in a 1 L conical flask. The culture was incubated and the OD_{600} measured every hour, then every 20 min after OD_{600} of 0.2 until it reached an OD_{600} of 0.4. The flask was immediately placed on ice for 30 min, swirling occasionally. The culture was poured into pre-chilled centrifuge bottles and centrifuged at 3,000 x g (Heraeus Megafuge 16R Centrifuge (ThermoFisher Scientific, Massachusetts, USA)) for 15 min at 4°C. The supernatant was carefully decanted, the pellet gently resuspended in 100 mL ice-cold 100 mM $MgCl_2$, and the cells centrifuged at 2,000 x g for 15 min at 4°C. The supernatant was decanted, the pellet resuspended in 50 mL ice-cold 100 mM $CaCl_2$, then the cells chilled on ice for 20 min. The cells were then centrifuged again at the same speed, the supernatant decanted and the pellet resuspended in 12.5 mL ice-cold 85 mM $CaCl_2$, 15% glycerol. The cells were transferred to a pre-chilled 50 mL Corning™ Falcon™ Conical Centrifuge tube (ThermoFisher Scientific) and centrifuged at 1,000 x g for 15 min at 4°C. The supernatant was decanted, and the pellet resuspended in ~2 mL ice-cold 85 mM $CaCl_2$, 15% glycerol to reach a final OD_{600} of 200–250. The cells were then aliquoted into pre-chilled 0.6 µL tubes, snap-frozen in liquid nitrogen, and stored at -80°C.

Transformation of chemically competent cells was performed by thawing 40 µL of cells on ice, adding ~5 ng DNA and mixing well. After 20 min, the cells were placed into a 42°C water bath for 1 min, then on ice for 2 min. Then 900 µL of SOC (2% tryptone, 0.5% yeast extract (Merck), 10 mM NaCl, 2.5 mM KCl, 10 mM $MgCl_2$, 10 mM $MgSO_4.7H_2O$, and 20 mM glucose) was added, mixed well, and the cells incubated at 37°C for 1 h, with shaking at 180 rpm (classic series C10 platform shaker (New Brunswick Scientific)). The cells were then diluted or concentrated, depending on the transformation, then spread onto LB plates with the appropriate antibiotic for selection, and incubated at 37°C overnight.

2.2.3.2 Preparation and transformation of electrocompetent cells

Electrocompetent cells of *E. coli* and *A. tumefaciens* were prepared by culturing as described previously (**Materials and methods section 2.2.1.2**). A 2.5 mL starter culture was grown

overnight in LB medium and used to inoculate 250 mL of LB medium in a 1 L conical flask. The culture was incubated and the OD_{600} measured every hour, until it reached an OD_{600} of 0.5–0.7. The flask was immediately placed on ice for 20 min, swirling occasionally. The culture was poured into pre-chilled centrifuge bottles and centrifuged at 4,000 x g (Heraeus Megafuge 16R Centrifuge (ThermoFisher Scientific)) for 15 min at 4°C. The supernatant was carefully decanted, the pellet gently resuspended in 250 mL ice-cold 10% glycerol, and the cells centrifuged again. The supernatant was carefully decanted, the pellet gently resuspended in 125 mL ice-cold 10% glycerol and the cells centrifuged again. The supernatant was carefully decanted, the pellet gently resuspended in 10 mL ice-cold 10% glycerol, the cells transferred to pre-chilled 50 mL Corning™ Falcon™ Conical Centrifuge tubes (ThermoFisher Scientific) and centrifuged again. Finally, the pellet was resuspended in 1–2 mL 10% glycerol, aliquoted into pre-chilled 0.6 µL tubes, snap-frozen in liquid nitrogen, and stored at -80°C.

Transformation of electrocompetent cells was performed by thawing the cells on ice, adding the DNA and mixing well. After 10 min, the cells were transferred to a pre-chilled 0.2 mm electroporation cuvette, and electroporated with a MicroPulser™ (BioRad, California, USA) using pre-set *E. coli* or *A. tumefaciens* settings. Then, 1 mL LB medium was added, mixed well, and the cells were incubated at 28°C (for *A. tumefaciens*) or 37°C (for *E. coli*), for 1 h, with shaking at 180 rpm (classic series C10 platform shaker (New Brunswick Scientific)). The cells were then diluted or concentrated as required, spread onto LB plates with the appropriate antibiotic selection, and incubated appropriately (**Materials and methods section 2.2.1.2**).

2.2.4 Homologous recombination with *A. tumefaciens*-mediated transformation

2.2.4.1 Construction of an *CfEcp11-1* knock-out plasmid for homologous recombination

The *CfEcp11-1* knock-out construct was developed by PCR amplification of the backbone of plasmid pFBTS1, a modified version of pFBT004 (Bolton et al., 2008), the hygromycin resistance gene *hph* from plasmid pFBTS1, and 1 kb flanking sequences either side of *CfEcp11-1*, using primers listed in **Appendix 2**. The sequences were then joined together using Gibson Assembly (Gibson et al., 2009). A schematic of the *CfEcp11-1* knock-out plasmid is shown in **Appendix 3**. The ligation mixture was then transformed into *E. coli* DH5α by chemical transformation (**Materials and methods section 2.2.3.1**) with 50 µg/mL kanamycin (ACTgene, New Jersey, USA) as selection. The plasmid was extracted (**Materials and methods section 2.2.2.2**) and sequenced (**Materials and methods section 2.2.2.8**) using primers listed in **Appendix 2**, then transformed

into *A. tumefaciens* AGL1 by electroporation (**Materials and methods section 2.2.3.2**), with 50 µg/mL kanamycin and 25 µg/mL rifampicin (Duchefa Biochemie) as selection.

2.2.4.2 *A. tumefaciens*-mediated transformation of *F. fulva*

Homologous recombination of *F. fulva* was performed by *A. tumefaciens*-mediated transformation (ATMT). The *A. tumefaciens* AGL1 strain containing the *CfEcp11-1* knock-out plasmid was inoculated into 3 mL LB with appropriate antibiotics in a 50 mL Corning™ Falcon™ Conical Centrifuge tube (ThermoFisher Scientific) and incubated at 28°C, 200 rpm (Ecotron, INFORS-HT, Bottmingen, Switzerland). After 48 h incubation, 400 µL of the culture was centrifuged at 6,500 rpm for 30 sec. The supernatant was discarded, and the pellet resuspended in 400 µL minimal media (MM). This culture was then added to 20 mL of MM with antibiotics in a 50 mL Falcon tube and incubated overnight with the same conditions. The culture was then centrifuged at 4,500 rpm for 10 min and the supernatant discarded. The pellet was resuspended in 1 mL induction medium (IM) with antibiotics and 200 µM acetosyringone, then a 10-fold dilution was made to check the OD_{600}. The 1 mL culture was then diluted to an OD_{600} of 0.15 in ~5 mL total volume of IM, in a 50 mL conical flask. The culture was incubated for 6 h with the same conditions.

ATMT was then performed by mixing an equal volume of 10^6 *F. fulva* spores/mL (harvested as detailed in **Materials and methods section 2.2.1.1**, but also washed twice with sterile MilliQ water) with *A. tumefaciens* AGL1 (carrying the *CfEcp11-1* knock-out construct, after the 6 h incubation). Then 100 µL of the spore/*A. tumefaciens* solution was plated onto each IM agar plate, covered with a sterile Hybond™-N+ filter (Amersham, Buckinghamshire, United Kingdom). The transformation plates were then incubated for 48 h in the dark at 22°C. The filters were then transferred to selection media (SM) agar plates with 50 µg/mL hygromycin B (Roche) and 200 µM cefotaxime (Sigma-Aldrich, Missouri, USA), using sterile forceps and the plates were incubated in the dark at 22°C for at least three weeks. The media used for ATMT are detailed in **Appendix 4**.

2.2.4.3 Screening homologous recombination transformants

Transformants that grew on *CfEcp11-1* homologous recombination transformation plates were transferred to 12-well PDA plates, sub-cultured to standard PDA plates, and then single spore-purified (**Materials and methods section 2.2.1.1**) on PDA plates (all media contained 50 µg/mL hygromycin B (Roche) and 200 µM cefotaxime (Sigma-Aldrich)). Transformants were screened by PCR (**Materials and methods section 2.2.2.5**), and PCR products sequenced (**Materials and methods section 2.2.2.8**). All primers used are listed in **Appendix 2**.

2.2.5 CRISPR/Cas9 transformation with *A. tumefaciens*-mediated transformation

2.2.5.1 Construction of CRISPR/Cas9 plasmid with sgRNA and transformation

Selection of the CRISPR single guide RNA (sgRNA) is important for the efficiency of gene editing. The sgRNA was designed to target a protospacer adjacent motif (PAM) site near the start of the coding region of *CfEcp11-1* (**Table 2.1**), to maximize the effect of any frameshift mutations produced during double-strand break (DSB) repair (Doench et al., 2014). The sgRNA was identified using the "find CRISPR sites" tool in Geneious (v9.1.8 software) and selected for a high on-target activity score and an off-target score of 100% (**Table 2.1**). The sgRNA was designed as part of an oligonucleotide, as described by Chambers, Van de Wouw, Gardiner, Elliott, and Idnurm (2021), and produced by Integrated DNA Technologies (Iowa, USA). The sequence of the oligonucleotide is shown in **Appendix 2**. The oligonucleotide containing the sgRNA was then inserted into the pMAI105 plasmid (Chambers et al., 2021) by Gibson Assembly (Gibson et al., 2009), as described by Chambers et al. (2021). The pMAI105 plasmid containing the sgRNA was transformed into *E. coli* DH5α chemically competent cells (**Materials and methods section 2.2.3.1**), the transformants screened by PCR (**Materials and methods section 2.2.2.5**) and the PCR products sequenced (**Materials and methods section 2.2.2.8**), using primers listed in **Appendix 2**. The plasmid was then extracted (**Materials and methods section 2.2.2.2**), transformed into *A. tumefaciens* AGL1 by ATMT (**Materials and methods section 2.2.4.2**) and plated on transformation plates with 50 µg/mL hygromycin B (Roche) and 200 µM cefotaxime (Sigma-Aldrich).

Table 2.1. CRISPR/Cas9 sgRNA protospacer used to target the *CfEcp11-1* gene of *Fulvia fulva*.

Sequence (5'–3') [1]	Binding site (bp)	Direction	Off-target sites [2]	Off-target score [3]	On-target activity score [4]
CACCAGTTCAGAATACCTGGGGG	109–131	Forward	0	100%	0.593

1 – Underlined bases are the protospacer adjacent motif (PAM) site.

2 – Off-targets found in the coding sequence (CDS) of the *F. fulva* genome using Geneious (v9.1.8).

3 - Off-target score calculated using Geneious (v9.1.8) by scoring against the *F. fulva* genome, based on Hsu et al. (2013), where scores are between 1 and 100 and a high score indicates less off-target activity.

4 - On-target activity score based on sequence features of the sgRNA, calculated using Geneious (v9.1.8). The score is from 0–1, with a score closer to 1 indicating higher activity, based on Doench et al. (2016).

2.2.5.2 Screening CRISPR/Cas9 transformants

Transformants that grew on *CfEcp11-1* CRISPR/Cas9 transformation plates were transferred to 12-well PDA plates with 50 µg/mL hygromycin B (Roche) and 200 µM cefotaxime (Sigma-Aldrich). Rapid gDNA extraction (**Materials and methods section 2.2.2.1**), and PCR screening (**Materials and methods section 2.2.2.5**) was performed, using primers listed in **Appendix 2**. High-quality gDNA of several transformants was then extracted (**Materials and methods section 2.2.2.1**), PCR performed, and then the PCR products were sequenced (**Materials and methods section 2.2.2.8**), using primers listed in **Appendix 2**. These transformants were then single spore purified (**Materials and methods section 2.2.1.1**), and another round of sequencing performed to confirm that purification did not change the sequencing results.

2.2.6 Identification of CfEcp11-1 homologues

Potential homologues of CfEcp11-1 were searched for by performing BlastP analysis with the protein query sequences of CfEcp11-1, AvrLm3, AvrLm5-9, AvrLm4-7, and the two predicted proteins from *Zymoseptoria ardabiliae* (Scaffold_667:56424-56906 and Scaffold_1237:24046-24549). BlastP analysis was performed with the non-redundant protein sequences database, using a BLOSUM62 matrix and standard parameters. The top five BlastP hits were then used as a new query in BlastP analysis to identify any new proteins. This process was continued two or three times. Any new protein sequences identified were analysed for conserved cysteine residues by performing a Geneious alignment with CfEcp11-1, as a global alignment with free end gaps using a BLOSUM62 cost matrix in Geneious software (v9.1.8).

2.2.7 Chimeric *CfEcp11-1* and *AvrLm3* gene development and characterisation

2.2.7.1 Generation of CfEcp11-*1* and *AvrLm3* chimeric protein sequences

To determine what regions of CfEcp11-1 are required for recognition by the Cf-Ecp11-1 receptor, chimeric genes containing a mixture of the *CfEcp11-1* and *AvrLm3* gene sequences were developed. Chimeric protein sequences were designed in collaboration with a research group in France led by Dr Isabelle Fudal. The sequences were synthesised by Twist Bioscience in the pTwist Amp High-Copy cloning vector. The vectors containing the chimeric gene sequences were transformed into *E. coli* DH5α by electroporation (**Materials and methods section 2.2.3.2**) with 50 µg/mL kanamycin (ACTgene) for selection, then the plasmids extracted (**Materials and methods section 2.2.2.2**).

Due to the collaborative effort, some of the sequences were designed with the PR1α signal peptide from *Nicotiana tabacum* (Hammond-Kosack et al., 1994) and some with the native signal

peptide. Those with the PR1α signal peptide were also designed with *Asc*I and *Not*I restriction sites at each end of the gene sequence, including the signal peptide-encoding sequence. For these constructs, PCR amplification of the genes was performed with Phusion High-Fidelity DNA polymerase (New England Biolabs). The PCR products were digested with *Asc*I and *Not*I-High-Fidelity® (**Materials and methods section 2.2.2.11**), gel-extracted (**Materials and methods section 2.2.2.3**), and then ligated (**Materials and methods section 2.2.2.10**) into the PVX-compatible pSfinx plasmid (Takken et al., 1999).

For the constructs that were designed with the native SP, this had to be replaced with the PR1α signal peptide. This was done by overlap PCR, where the nucleotide sequence encoding the PR1α signal peptide and each gene were amplified separately with overlapping primers (listed in **Appendix 2**), then combined in the same reaction with the primers that bind at the 5' end of the *PR1α* signal peptide sequence and the 3' end of the gene. The primers were also designed with *Asc*I and *Not*I restriction sites, so after amplification of the chimeric gene carrying the *PR1α* signal peptide, the products could be cloned as described above and inserted into pSfinx. Two positive cell death controls were used with these chimeric sequences; PaINF1 (Guo, Dupont, et al., 2020) and CfAbn1 (known cell death elicitor from *F. fulva*; Mesarich lab, unpublished).

2.2.7.2 Potato virus X (PVX)-based transient expression analysis in tomato

To test the chimeric CfEcp11-1/AvrLm3 sequences designed above for a response in tomato, the PVX-based transient expression system (Hammond-Kosack, Staskawicz, Jones, & Baulcombe, 1995; Takken et al., 2000) was used. First, the chimeric sequences in the pSfinx plasmids were transformed into *A. tumefaciens* GV3101 by electroporation (**Materials and methods section 2.2.3.2**). *A. tumefaciens* colonies were inoculated into 3 mL LB medium containing 50 µg/mL kanamycin (ACTgene) and 25 µg/mL rifampicin (Duchefa Biochemie) and incubated for 1.5–2 days at 28°C and 200 rpm (Ecotron, INFORS-HT). Next, 250 µL of each culture was inoculated into 15 mL Yeast Extract Beef (YEB) liquid medium (5 g/L beef extract, 5 g/L bacteriological peptone, 5 g/L sucrose, 1 g/L yeast extract, 2 mL of 1 M $MgSO_4$) containing 1 mM acetosyringone, 10 mM 2-(N-morpholino)ethanesulfonic acid (MES), and appropriate antibiotics, then incubated overnight at 28°C and 200 rpm (Heraeus Megafuge 16R, Thermo Scientific). Cultures were collected by centrifugation for 8 min at 4,000 rpm, and the pellets re-suspended in 10 mL MMA liquid medium (20 g/L sucrose, 5 g/L Murashige and Skoog basal salt mixture (MS) without vitamins, 1.95 g/L MES, pH 5.6) containing 200 mM acetosyringone, to a final OD_{600} of 1.0. Cultures were then incubated at room temperature for 3 h with no shaking, collected by centrifugation as above, and resuspended in a final volume of 0.5 mL of MMA liquid medium

and tested into tomato plants by infiltration with a needless 1 mL syringe (Terumo Corporation, Laguna, Philippines), or by inoculation with a toothpick. The age of the tomato plants was variable and is described in **section 2.3.3**.

2.3 Results

2.3.1 CfEcp11-1 of *Fulvia fulva* has homologues in both Dothideomycetes and Sordariomycetes fungi

It was shown that CfEcp11-1 is a homologue of AvrLm3 from *L. maculans*, and of two predicted proteins from *Z. ardabiliae* (Mesarich et al., 2018). To determine if CfEcp11-1 homologues are present in other fungal species, reciprocal BlastP analysis was performed, and cysteine residues analysed as an indication of conserved protein structure. This work was performed prior to the study by Lazar et al. (2022), which used a more sensitive HMM-based search method on an in-house database of the annotated proteomes from 116 fungal species. Therefore, only two new CfEcp11-1 homologues were identified in this study, whilst Lazar et al. (2022) found 49 more.

Six CfEcp11-1 homologues were investigated, four were identified previously, and two were identified in this study (**Table 2.2**). As mentioned previously, AvrLm3, and the two *Z. ardabiliae* proteins (named 667 and 1237) were identified as CfEcp11-1 homologues by Mesarich et al. (2018), while AvrLm5-9 was identified by Ghanbarnia et al. (2018). The two new CfEcp11-1 homologues identified in this study were from *Fusarium oxysporum*, proteins BFJ63 and BFJ70. Protein BFJ63 was identified from *F. oxysporum* f. sp. *narcissi* N139, a strain isolated from the daffodil host on which the pathogenicity was not tested (Taylor et al., 2019). Protein BFJ70 was identified from *F. oxysporum* PG, an isolate non-pathogenic on onion (Armitage et al., 2018).

The similarity between CfEcp11-1 and the six CfEcp11-1 homologues was examined (**Table 2.3**). The amino acid identity was quite low (15–47%) between all seven proteins, and AvrLm5-9 appeared to be the most dissimilar. Interestingly, protein BFJ63 from *F. oxysporum* had a slightly higher amino acid identity to CfEcp11-1 than AvrLm3 had to CfEcp11-1 in this analysis. The highest percentage of identity (47%) was between the two *Z. ardabiliae* proteins and, of particular interest, between *F. oxysporum* protein BFJ63 and AvrLm3.

Amino acid sequences of CfEcp11-1 and the CfEcp11-1 homologues were aligned, and conservation of cysteine residues was examined (**Figure 2.3a**). As evident from the amino acid identities, the protein sequences do not appear to be well conserved. However, the conservation of cysteine residues suggested structural similarity between the proteins. AvrLm3, *Z. ardabiliae* protein 1237, and both *F. oxysporum* proteins each contain ten cysteine residues, like CfEcp11-1, although in this alignment some of the cysteines did not align in the same position (such as the fifth and sixth cysteines). In contrast, the *Z. ardabiliae* protein 667 and AvrLm5-9 have nine and eight cysteines, respectively, while AvrLm5-9 had six.

Phylogenetic analysis of CfEcp11-1 and the CfEcp11-1 homologues was performed (**Figure 2.3b**). Homologues AvrLm3 and *F. oxysporum* protein BFJ63 clustered closely to each other and to CfEcp11-1. The two *Z. ardabiliae* proteins also clustered together, while AvrLm5-9 and *F. oxysporum* protein BFJ70 appeared to be the most phylogenetically distant to CfEcp11-1. In summary, these results showed that two new homologues of CfEcp11-1 were identified from *F. oxysporum*, one of which is closely related to CfEcp11-1 and AvrLm3.

Table 2.2. Homologues of CfEcp11-1 identified from other fungal species.

Protein name	Accession[1]	Species	Source
CfEcp11-1	AQA29221.1	*Fulvia fulva* 0WU	Mesarich et al. (2018)
AvrLm3	ALS92799.1	*Leptosphaeria maculans*	Plissonneau et al. (2016)
AvrLm5-9	AHB63016	*L. maculans*	Ghanbarnia et al. (2018)
hypothetical protein BFJ63_vAg18418	RYC78709.1	*Fusarium oxysporum* f. sp. *narcissi*, N139	Taylor et al. (2019)
hypothetical protein BFJ70_g16777	RKL08708.1	*F. oxysporum*, PG	Armitage et al. (2018)
Scaffold_667: 56424-56906	GCA_000223765.2[2]	*Zymoseptoria ardabiliae*, STIR04_1.1.2	Stukenbrock et al. (2011)
Scaffold_1237: 24046-24549	GCA_000223765.2[2]	*Z. ardabiliae*, STIR04_1.1.2	Stukenbrock et al. (2011)

1 – GenBank protein accession number from the NCBI website (https://www.ncbi.nlm.nih.gov/).

2 – No protein accession number is available for these sequences, so the GenBank assembly accession number is shown.

Table 2.3. Matrix of percentage amino acid identities between CfEcp11-1 and homologous proteins from other fungal species.

Protein	*Ff* CfEcp11-1	*Lm* AvrLm3	*Za* 667	*Za* 1237	*Fo* BFJ63	*Fo* BFJ70	*Lm* AvrLm5-9
***Ff* CfEcp11-1**	-	33	26	30	35	22	17
***Lm* AvrLm3**	33	-	33	34	**47**	21	18
***Za* 667**	26	33	-	**47**	33	26	19
***Za* 1237**	30	34	**47**	-	37	20	18
***Fo* BFJ63**	35	**47**	33	37	-	21	15
***Fo* BFJ70**	21	21	26	20	21	-	21
***Lm* AvrLm5-9**	17	18	19	18	15	21	-

Species names are abbreviated; *Ff* (*Fulvia fulva*), *Lm* (*Leptosphaeria maculans*), *Za* (*Zymoseptoria ardabiliae*), *Fo* (*Fusarium oxysporum*). Some protein names are abbreviated; 667 (Scaffold_667:56424-56906), 1237 (Scaffold_1237:24046-24549), BFJ63 (BFJ63_vAg184180), and BFJ70 (BFJ70_g16777). Amino acid identity was determined by performing a ClustalW alignment, with a BLOSUM cost matrix, of all seven sequences, and examining the percentage amino acid identity between sequences using Geneious (software v9.1.8). The highest amino acid identity is in bold.

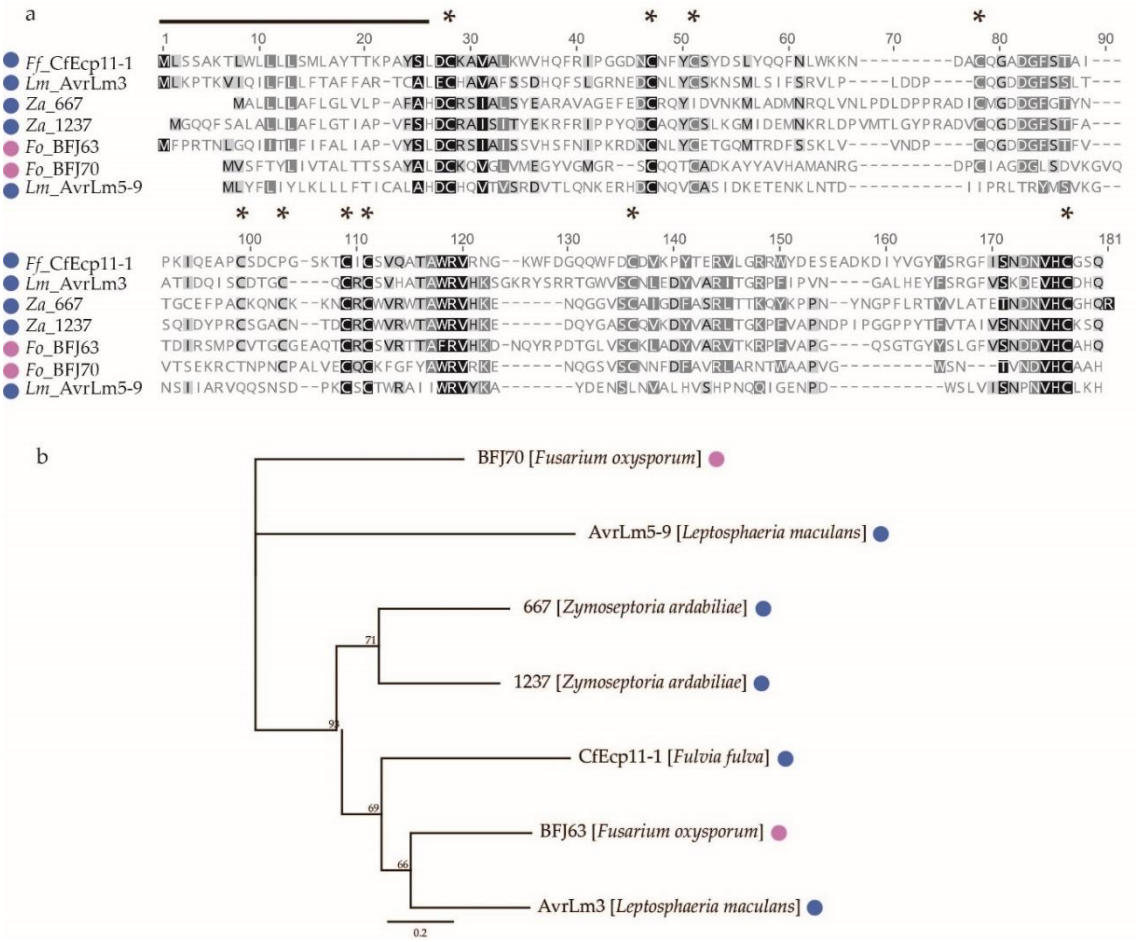

Figure 2.3. Protein sequence alignment and phylogenetic tree of *Fulvia fulva* CfEcp11-1 and homologues from other fungal species. (**a**) Amino acid sequence alignment of CfEcp11-1 and homologues. Asterisks above the alignment indicate positions of cysteine residues. The position of signal peptides is shown above the alignment by a black line and was determined by SignalP v4.1. The ClustalW alignment was performed with a BLOSUM cost matrix, using Geneious (v9.1.8). Amino acids are shaded to illustrate similarity; black with white font (100% similar), grey with white font (80–100% similar), light grey with black font (60–80% similar), and unshaded with grey font (less than 60% similar). Species names are abbreviated; *Ff* (*Fulvia fulva*), *Lm* (*Leptosphaeria maculans*), *Za* (*Zymoseptoria ardabiliae*), *Fo* (*Fusarium oxysporum*). Some protein names are abbreviated; 667 (Scaffold_667:56424-56906), 1237 (Scaffold_1237:24046-24549), BFJ63 (BFJ63_vAg184180), and BFJ70 (BFJ70_g16777). (**b**) Phylogenetic tree of CfEcp11-1 and homologues where coloured circles next to the species names indicate what fungal class they belong to: purple for Sordariomycetes and blue for Dothideomycetes. The tree was made with Geneious (v9.1.8.) using the Neighbour-Joining method and the Jukes-Cantor genetic distance model, with 100 bootstrap replicates. Consensus support is illustrated at each node as a percentage.

2.3.2 Chimeric protein sequence design to examine CfEcp11-1, AvrLm3, and CfEcp11-1 homologue recognition by the tomato Cf-Ecp11-1 receptor

Previous work suggested that CfEcp11-1 is recognised by both the tomato Cf-Ecp11-1 receptor (Mesarich et al., 2018), and the *B. napus* Rlm3 receptor (Lazar et al., 2022), while AvrLm3 is only recognised in the *B. napus* host (Plissonneau et al., 2016) and not tomato (C. Mesarich, L. Deurhof and M. Joosten, unpublished results). To examine what region(s) of these two proteins are involved in receptor recognition, and why their recognition is different in tomato, genes encoding chimeric protein sequences with a mix of CfEcp11-1 and AvrLm3 were developed to be screened for an HR on *Cf-Ecp11-1* tomato by PVX-based transient expression assays (Hammond-Kosack et al., 1995; Takken et al., 2000). Furthermore, CfEcp11-1 homologues were to be screened in the same way to determine if, like CfEcp11-1, these proteins are recognised by a receptor in a non-host plant, tomato. This research was performed in collaboration with a group in France lead by Dr Isabelle Fudal, where chimeric proteins were designed by me with suggestions and advice from the collaborators, with testing in tomato performed in New Zealand, and testing in *B. napus* in France.

A total of 20 chimeric protein sequences were designed, including four with region swaps, four with amino acid substitutions, four with CfEcp11-1 homologues, and eight with tags (**Figure 2.4**), for reasons explained below. The region-swapped and amino acid-substituted sequences were designed to examine what regions of CfEcp11-1 are required for receptor recognition. The region-swapped proteins (**Figure 2.4b**) involve two regions that were swapped between CfEcp11-1 and AvrLm3 that were selected based on the recently solved crystal structure of CfEcp11-1 and 3D model of AvrLm3 (Lazar et al., 2022). Region 1 covers a loop structure, while region 2 covers a β-sheet structure (**Figure 2.5**) and the conserved WR(F/L/V)(R/K) motif.

The four amino acid-substituted protein sequences (**Figure 2.4c**) contained either two or three amino acid substitutions in CfEcp11-1 and AvrLm3. These amino acids were previously identified as variants in AvrLm3 protein sequences of *L. maculans* isolates that are virulent on *B. napus* varieties carrying *Rlm3*, therefore suggesting that they might be involved in Rlm3 recognition (Plissonneau et al., 2017). The locations of the substituted amino acids in the 3D protein structures of CfEcp11-1 and AvrLm3 are shown in **Figure 2.5**.

The homologous sequences were designed to examine whether CfEcp11-1 homologues can be recognised, in a non-host, by the tomato Cf-Ecp11-1 receptor. The four homologous sequences (**Figure 2.4d**) contain the WT amino acid sequences from BFJ63 and BFJ70 from *F. oxysporum* and 667 and 1237 from *Z. ardabiliae*, discussed in **section 2.3.1**.

Tagged sequences were also designed as these chimeric proteins will be screened for an HR on tomato with the Cf-Ecp11-1 receptor, and tagging is required to confirm successful production of protein in the plant. Previous work suggested that addition of a hemagglutinin (HA) tag to the C-terminus of AvrLm3 disrupted recognition by Rlm3 in *B. napus* (I. Fudal, personal comm.). Therefore, to investigate whether a tag could be added to CfEcp11-1 that would not disrupt recognition by the Cf-Ecp11-1 receptor, eight sequences were designed with 6xHIS or 3xFLAG tags in four different locations in the protein (**Figure 2.4e**). If a tagged sequence was identified that did not disrupt receptor recognition, chimeric proteins of interest could be redesigned with that specific tag.

In summary, 20 chimeric protein sequences were designed, with the aim of screening them in tomato carrying Cf-Ecp11-1 and determining what regions or amino acids of CfEcp11-1 are required for receptor recognition. Sequences were also designed to determine if CfEcp11-1 can be tagged in a way that receptor recognition is not disrupted.

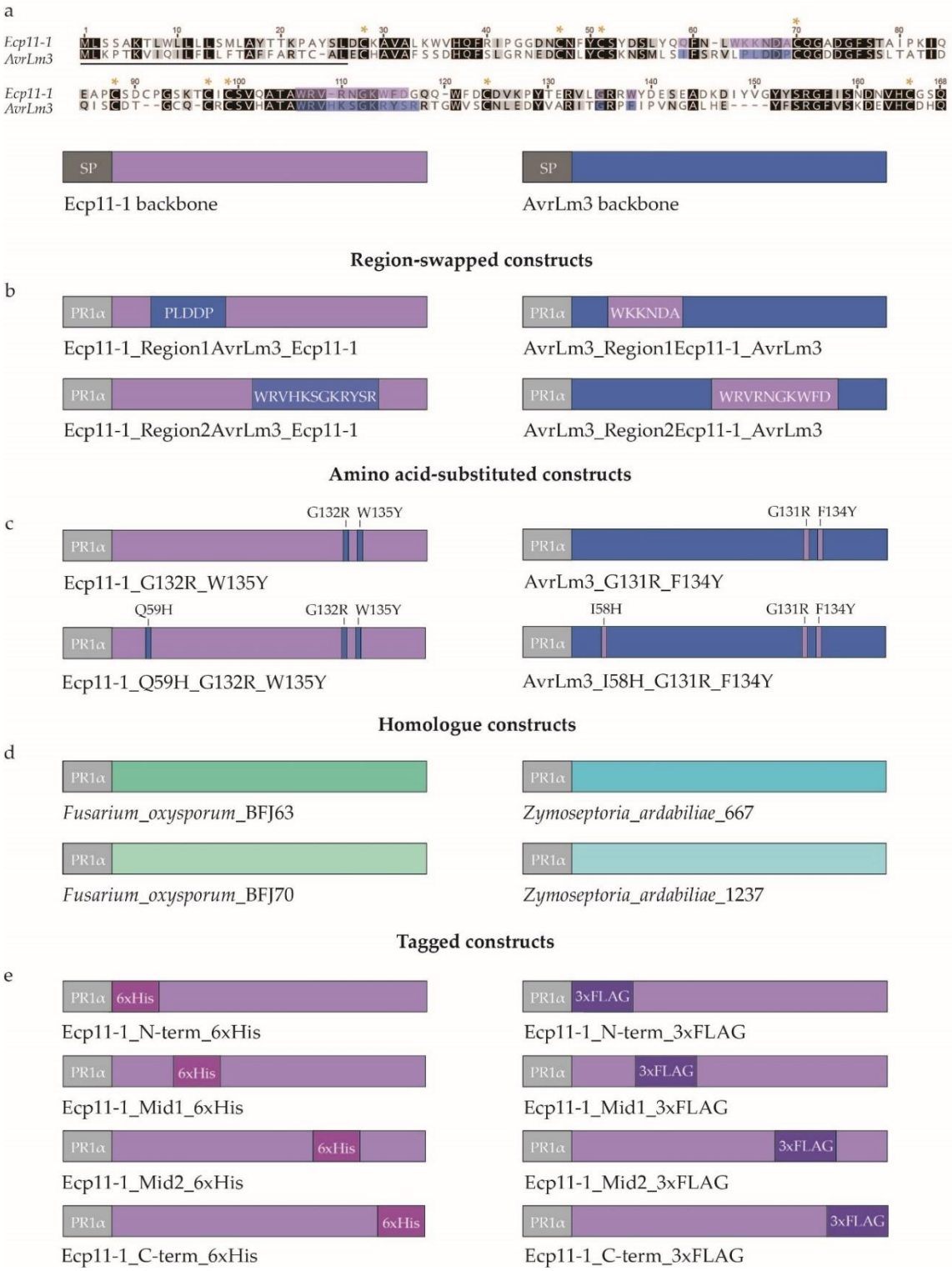

Figure 2.4. Schematic of chimeric protein sequence designs between CfEcp11-1 of *Fulvia fulva* and AvrLm3 of *Leptosphaeria maculans*. (**a**) Alignment of CfEcp11-1 and AvrLm3 protein sequences showing positions of regions swaps and amino acid substitutions. The signal peptide is shown by a black line below the alignment. All regions to be swapped and amino acids to be substituted in CfEcp11-1 are shaded blue and in AvrLm3 are shaded purple. An asterisk above the sequence alignment shows the position of a conserved cysteine residue. The CfEcp11-1 (purple bar) and AvrLm3 (blue bar) backbones are shown underneath the

alignment, with the native signal peptide (SP). (**b–e**) Chimeric protein design. Each protein has the PR1α signal peptide from *Nicotiana tabacum* to direct secretion of the protein into the apoplastic environment, and the name of the protein sequence design in shown underneath the schematic. (**b**) Design of region-swapped sequences. Swapped regions are coloured blue if from AvrLm3 or purple from CfEcp11-1, and the amino acid sequence swapped is shown in the region. (**c**) Design of amino acid-substituted sequences. The amino acids substituted are shown by a blue or purple bar (from AvrLm3 or CfEcp11-1 respectively), and the substitution is labelled above the bar. (**d**) Design of homologue sequences. These proteins are the wild type sequences of four homologues of CfEcp11-1, the names of which have been abbreviated; *Fusarium oxysporum* BFJ63 (BFJ63_vAg184180) and BFJ70 (BFJ70_g16777), and *Zymoseptoria ardabiliae* 667 (Scaffold_667:56424-56906) and 1237 (Scaffold_1237:24046-24549). (**e**) Design of tagged protein sequences. All tagged proteins were designed in CfEcp11-1 and contained either a 6xHis tag (pink/purple) or 3xFLAG (dark purple) for detection by Western blotting.

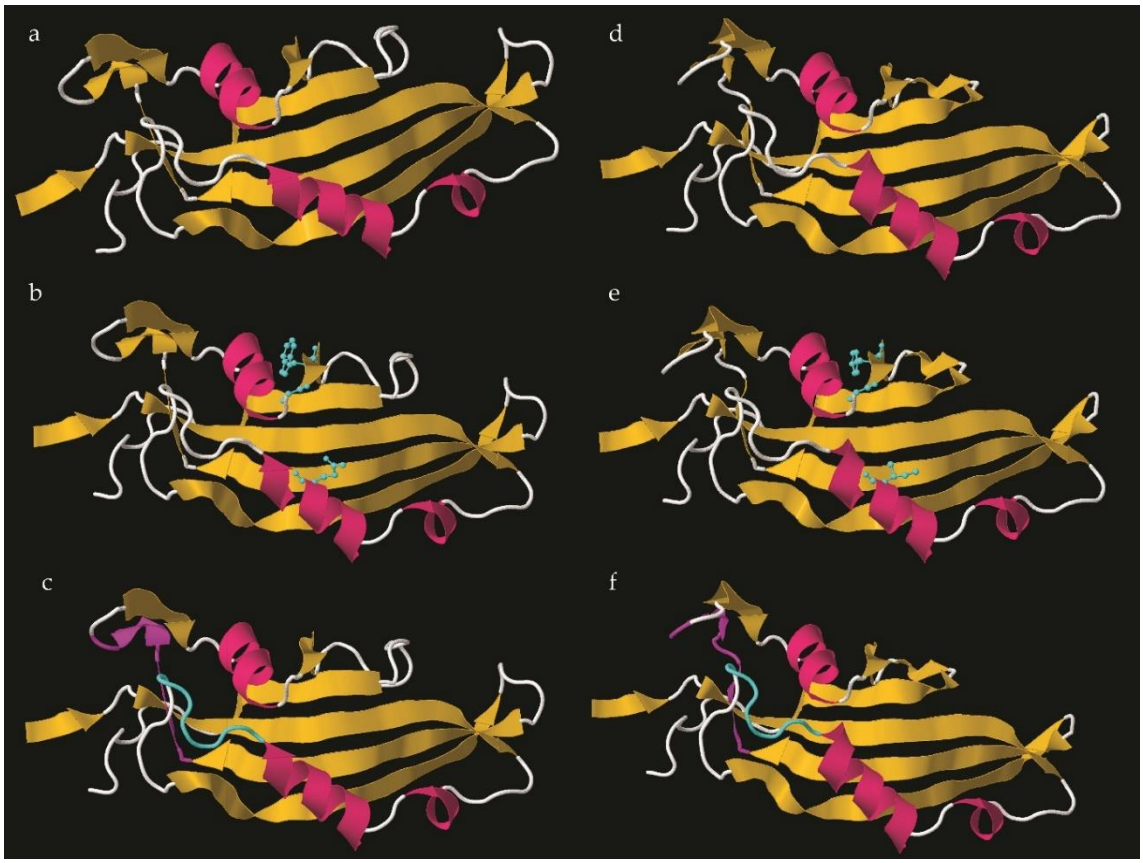

Figure 2.5. 3D protein structures of *Fulvia fulva* CfEcp11-1, *Leptosphaeria maculans* AvrLm3, and chimeric proteins. (**a**—**c**) 3D structures of CfEcp11-1. (**d**—**f**) 3D structures of AvrLm3. (**a**) 3D structure of CfEcp11-1. (**d**) 3D structure of AvrLm3. (**b**) & (**e**) 3D structures showing the three amino acids that will be substituted in the amino acid-substituted chimeric proteins. The amino acids are shown in the ball and stick style and in cyan. (**c**) & (**f**) 3D structures showing the two regions to be swapped in the region-swapped chimeric proteins. Regions are coloured cyan and magenta for regions 1 and 2, respectively. The

3D structures are shown in cartoon style and coloured by structure, where α-helixes are pink, β-strands are yellow, and loop structures are white. The 3D structures were manipulated using Geneious software (v9.1.8). The 3D structure coordinate files were provided by Dr Isabelle Fudal (Université Paris-Saclay).

2.3.3 Screening chimeric proteins for an HR in tomato carrying *Cf-Ecp11-1*

Chimeric protein sequences designed to examine CfEcp11-1, AvrLm3, and CfEcp11-1 homologue recognition by the tomato Cf-Ecp11-1 receptor were to be screened in tomato using the PVX-based transient expression system (Hammond-Kosack et al., 1995; Takken et al., 2000). Before all 20 chimeric proteins were examined by PVX infiltration, a preliminary trial was performed with the WT CfEcp11-1 protein. In this preliminary trial, seven-day old tomato seedlings (*S. pimpinellifolium* CGN 15484) carrying the corresponding *Cf-Ecp11-1* receptor (tentatively named *Cf-Ecp11-1*, (Lazar et al., 2022)) were infiltrated with *A. tumefaciens* strains carrying the empty vector pSfinx and WT CfEcp11-1 protein sequence. After 27 days, the plants infiltrated with the *A. tumefaciens* strain expressing CfEcp11-1 had no visible necrosis to suggest that CfEcp11-1 recognition by Cf-Ecp11-1 had not occurred (**Figure 2.6**). These results were unexpected as the same *CfEcp11-1* vector had been used previously, with the CfEcp11-1 protein shown to trigger HR on the same tomato cultivar (Mesarich et al., 2018). Furthermore, plants infiltrated with *A. tumefaciens* strains expressing empty vector or CfEcp11-1 did not present any typical PVX symptoms (mosaic chlorosis, **Figure 2.6**) suggesting that the virus had not accumulated enough to infect the plant systemically, or that viral infection had not occurred at all.

PVX-based transient expression experiments have been performed successfully in tomato in many studies, and were always performed in temperature-, light- and humidity-controlled conditions (Laugé, Goodwin, De Wit, & Joosten, 2000; Mesarich et al., 2014; Mesarich et al., 2018; Takken et al., 2000; Wulff, Thomas, Smoker, Grant, & Jones, 2001). Unfortunately, due to regulatory restrictions, PVX experiments could only be performed in a plant growth room that was not controlled for any of these environmental parameters.

Other trials were performed where tomato seeds were germinated in a different plant growth room (temperature-, light- and humidity-regulated), then moved for PVX infiltration, however these gave the same negative results as before. To test whether localised PVX-based transient expression would work, the leaves of 4-week-old plants were toothpick-inoculated with the empty vector, three positive controls, CfEcp11-1, PaINF1, and CfabN, and the 20 chimeric proteins designed in **section 2.3.2**. Two weeks after inoculation, no chlorosis or necrosis symptoms were visible, although leaves exhibited evidence of heat stress. This trial was also

repeated with tomato plants that were first grown in the temperature-, light- and humidity-regulated plant growth room for four weeks, then moved for PVX inoculation, but the same results were observed. Several trials were also performed with the empty vector and *CfEcp11-1* sequences transformed into a different *A. tumefaciens* strain (1D1249, **Materials and methods section 2.2.1**) but the same results were found. Unsuccessful PVX-based transient expression performed at the same time and in the same plant growth room was also observed by Ellie Bradley (Massey University), who also trialled infiltrating *A. tumefaciens* at different OD levels but found no difference in the results.

These results suggested that PVX-based transient expression was not possible at Massey University due to the lack of a suitable temperature-, light- and humidity-controlled PC2 plant growth room with the appropriate regulatory approvals. Therefore, the 20 chimeric protein sequences designed in **section 2.3.2** were sent to collaborators at Wageningen University in the Netherlands (team led by Assoc. Prof. Matthieu Joosten at the Laboratory of Phytopathology). This laboratory has state-of-the-art plant growth facilities and is expected to have success performing PVX-based transient expression and screening these proteins in Cf-Ecp11-1 tomato. At the time of writing, this work had not yet been completed.

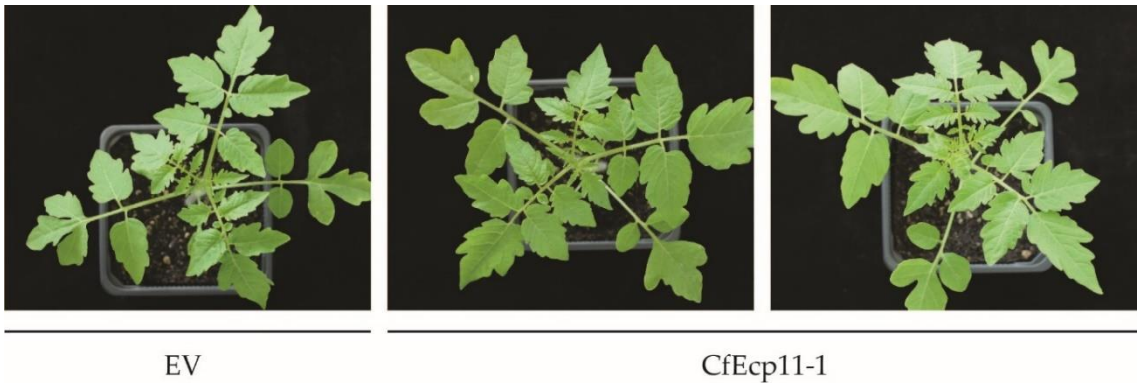

Figure 2.6. Potato virus X (PVX)-based transient expression of pSfinx empty vector (EV) and wild type *CfEcp11-1* in *Solanum lycopersicum* (CGN 15484). Seven-day old seedlings were infiltrated with *Agrobacterium tumefaciens* GV3101 containing the two constructs, and photos were taken 14 days post-inoculation. Three plants were tested; one with empty vector (expected to produce chlorotic mosaic symptoms from PVX viral infection, but no necrosis), and two with CfEcp11-1, expected to cause systemic cell death upon recognition by the Cf-Ecp11-1 receptor (as well as general PVX symptoms like the EV).

2.3.4 *CfEcp11-1* gene knock-out attempts by homologous recombination

Due to the homology CfEcp11-1 shares with other effector proteins, and the fact that *CfEcp11-1* has been found to be upregulated during infection, it is possible that CfEcp11-1 functions as a virulence factor in *F. fulva*. To investigate this, the next objective was to generate a *CfEcp11-1* knock-out mutant and test it for virulence on the tomato host. Several different *F. fulva* homologous recombination transformation methods were attempted before an *CfEcp11-1* mutant was successfully obtained.

Development of homologous recombination constructs was first attempted using the One Step Construction of *Agrobacterium*-Recombination-ready-plasmids (OSCAR) system (Gold, Paz, Garcia-Pedrajas, & Glenn, 2017; Paz et al., 2011). This cloning process uses one BP clonase reaction to combine the two plasmids pOSCAR and pA-Hyg-OSCAR, and the flanking regions of the gene. However, after PCR screening of many *E. coli* transformants, none were found to contain the correct construct. Troubleshooting identified that the *ccdB* gene in the pOSCAR plasmid was no longer functional (possibly due to a random mutation), and selection was not being applied to the transformants. Therefore, a new method to develop an *CfEcp11-1* homologous recombination construct was attempted.

The next method involved Gibson Assembly (Gibson et al., 2009) to develop the homologous recombination constructs. The backbone of plasmid pFBTS1 (Bolton et al., 2008), the hygromycin resistance gene *hph* cassette from plasmid pFBTS1, and flanks from either side of *CfEcp11-1*, were amplified by PCR and then successfully ligated together using Gibson Assembly (**Materials and methods section 2.2.4.1**). Two knock-out constructs were designed because *CfEcp11-1* is located between two long stretches of repeat regions. One of the constructs was designed with flanks that stopped before the repeat regions, while the other was designed with 1 kb flanks which contained repeat regions. However, during cloning, only the construct with the 1 kb flanks was obtained and, due to time constraints, the transformation was continued with this construct alone. The *CfEcp11-1* knock-out construct was then transformed into *A. tumefaciens* AGL1 and used in *A. tumefaciens*-mediated transformation (ATMT) of *F. fulva* (**Materials and methods section 2.2.4.2**). While preparing the AGL1 *A. tumefaciens* strain (with the *CfEcp11-1* knock-out construct) for ATMT, bacterial growth was slow, and the cultures had to be grown for longer than the protocol suggested (**Materials and methods section 2.2.4.2**). After three weeks, no transformants had grown on the transformation plates. This was believed to be due to the slow growth of the *A. tumefaciens* AGL1 strain, and thus insufficient inoculum to enable successful transformation.

Further attempts using the same *CfEcp11-1* knock out construct with 1 kb flanks were performed with the *F. fulva* 0WU strain, and the well-sporulating and faster-growing Race 5 strain. A greater inoculum of *A. tumefaciens* AGL1 was used, and the plates were monitored for transformants for a longer period (4–5 weeks). Many transformants grew on the 0WU strain transformant plates, however after several rounds of sub-culturing on selective media, only one of 120 transformants grew. Fewer transformants grew on the Race 5 strain transformation plates, but after several rounds of sub-culturing 15 out of 73 grew. These results suggested that the transformation efficiency was very low.

An initial PCR screen of crude gDNA from the transformants was performed using primers that amplified *actin* (as a control for gDNA amplification), the hygromycin *hph* gene, and *CfEcp11-1*. A subset of seven transformants were selected that amplified actin and hygromycin but not *CfEcp11-1*, then good quality gDNA was extracted from these. A PCR was then performed with primers (HM105/HM106) that amplify the *F. fulva actin* gene (as a control for gDNA amplification). Then another PCR was performed with two sets of primers that were expected to amplify the junction between *CfEcp11-1* and *hph* in transformants where homologous recombination had occurred (**Figure 2.7a**). In this PCR screen, gDNA from WT and all transformants amplified *actin* but no transformants amplified with the *CfEcp11-1* knock-out primers, suggesting that homologous recombination had not occurred as expected (**Figure 2.7b**). Another transformation attempt was performed with the same conditions and the Race 5 strain but was also unsuccessful. Because knock-out of *CfEcp11-1* by homologous recombination was not successful despite many attempts, it was decided to trial another gene editing method to obtain a mutant disrupted for *CfEcp11-1*.

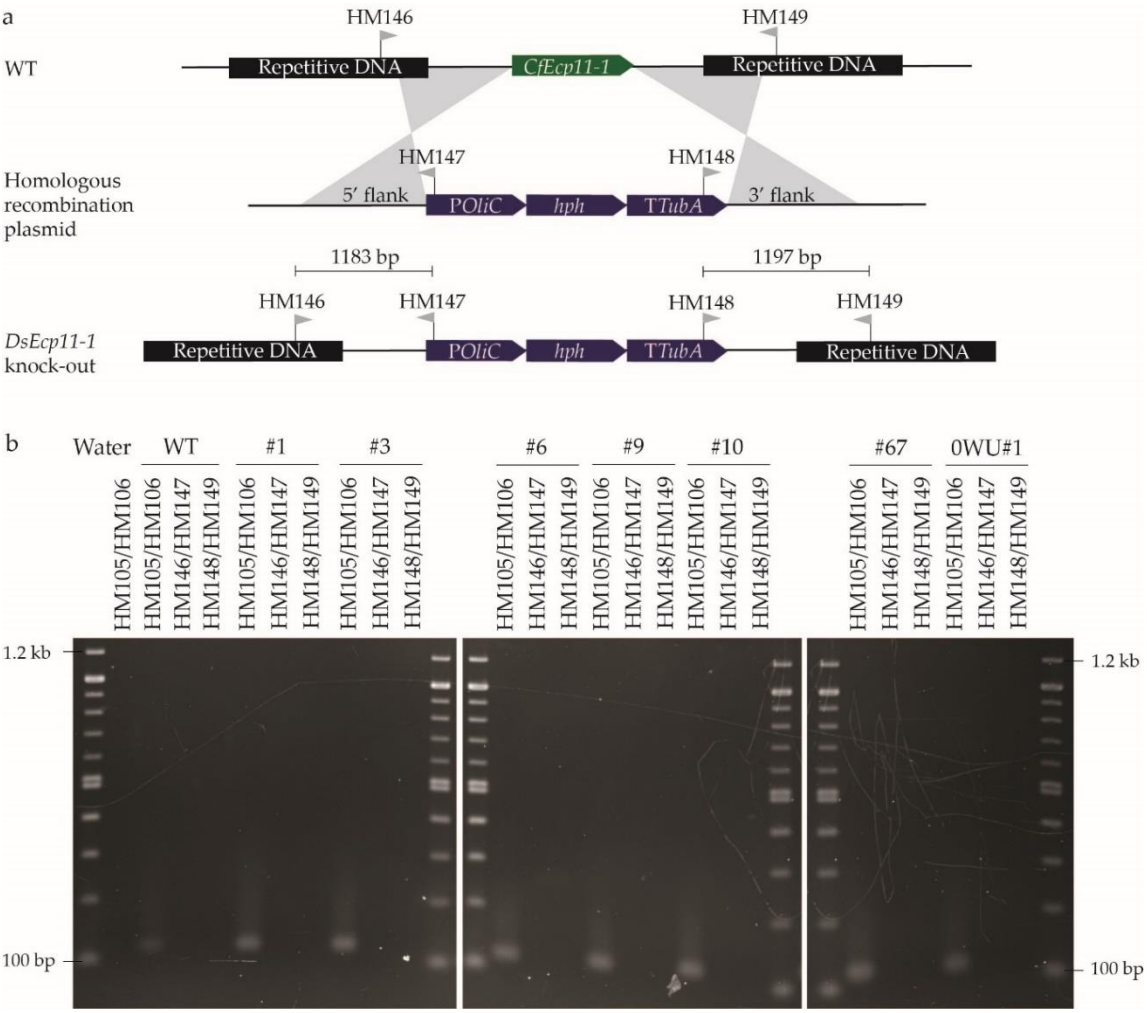

Figure 2.7. PCR analysis of *Fulvia fulva* wild type (WT) and *CfEcp11-1* homologous recombination transformants. (**a**) Schematic of the *CfEcp11-1* locus. The *CfEcp11-1* gene is shown by a green bar, the black bars represent repetitive DNA regions, and blue bars show the plasmid DNA replacing *CfEcp11-1* after homologous recombination including the hygromycin gene (*hph*), the promoter (P*OliC*), and terminator (T*tubA*). The 1 kb *CfEcp11-1* flanks are shown by grey triangles. Primer positions are shown by grey flags with the primer name and PCR product sizes above. (**b**) PCR screen of *F. fulva* WT and *CfEcp11-1* transformants. PCR was performed with water as a negative control, WT gDNA as a positive control, and transformant gDNA (labelled with the transformant number). The transformant labelled 0WU#1 is from the *F. fulva* 0WU transformation, while all others are from the Race 5 transformation. Primers used are labelled above the gel pictures, HM105/HM106 amplified a 122 bp fragment from *actin* (JGI ID: 189818), as a control for gDNA amplification. The other primer pairs were expected to amplify the junction between *CfEcp11-1* and *hph* in transformants if homologous recombination had occurred. Relevant DNA ladder sizes are shown on either side of the gel pictures.

2.3.5 Protoplast generation trials in *F. fulva*

The success of CRISPR/Cas9 gene editing in other filamentous fungi (Schuster & Kahmann, 2019) suggested this method might be a viable option to obtain a *CfEcp11-1*-disrupted transformant. It is preferred to use an autonomously replicating plasmid for CRISPR/Cas9 transformation so that Cas9 will eventually be lost (therefore reducing the chance of off-target effects); another benefit of losing this plasmid is that the antibiotic resistance it confers will also be lost, enabling further transformations to be performed using the same selection. The objective was to use the autonomously replicating plasmid designed by Rocafort, Arshed, et al. (2022) in a PEG-mediated protoplast transformation. However, whilst a method was established for protoplast generation in *F. fulva* by Harling et al. (1988), the lysing enzyme used was Novozym 234, which is no longer available. An attempt to generate protoplasts from 0WU *F. fulva* using the Harling et al. (1988) method, but with Glucanex as the lysing enzyme, produced very few protoplasts. A second attempt, using a different method based on Yelton, Hamer, and Timberlake (1984), and used successfully for *D. septosporum* (Chettri et al., 2018), was performed with *F. fulva* 0WU ground mycelium and the Glucanex enzyme. This method was successful, with 1.7 x 10^6 protoplasts/mL obtained.

The protoplast generation trials were performed with the 0WU strain of *F. fulva*, as this was the only strain for which a genome had been sequenced at that time. However, in the previous transformation attempt using this strain (**section 2.3.4**), only one transformant was obtained, and the low sporulation and slow growth rate of 0WU lengthened the incubation times. Therefore, the Race 5 strain was used for protoplast transformation instead as it is faster growing and high-sporulating. However, when the same protoplast generation method used successfully with 0WU was repeated with Race 5, no protoplasts were obtained. Further protoplast generation trials testing different inoculation methods, growth times, and $MgSO_4$ molarity in the OM buffer were all unsuccessful in producing *F. fulva* protoplasts. Therefore, it was decided to change the transformation method for CRISPR/Cas9 gene editing from protoplast transformation to ATMT.

2.3.6 Successful disruption of *CfEcp11-1* using CRISPR/Cas9 with *Agrobacterium tumefaciens*-mediated transformation

Because of difficulties obtaining protoplasts from Race 5 *F. fulva*, an autonomously replicating plasmid could not be used for CRISPR/Cas9 gene editing. Instead, the *A. tumefaciens*-compatible plasmid pMAI105, developed by Chambers et al. (2021), was used for CRISPR/Cas9 with ATMT. This plasmid contains a bidirectional promoter from the histone gene cluster to drive expression

of Cas9 and produce the single guide RNA (sgRNA), which is then cleaved by a double ribozyme (Chambers et al., 2021). During transformation, the plasmid is inserted into the genome, then the Cas9 and the sgRNA are expressed and can edit the target gene. The only selection used in this study was hygromycin resistance, to screen for integration of the pMAI105 plasmid into the genome. Therefore, if the CRISPR/Cas9 mutation efficiency was low, many transformants would need to be screened and sequenced to identify a mutation in *CfEcp11-1*. A sgRNA was selected to target *CfEcp11-1* and inserted into the pMAI105 plasmid by Gibson Assembly (**Materials and methods section 2.2.5.1**, (Gibson et al., 2009)). The pMAI105/CfEcp11-1 plasmid was transformed into *A. tumefaciens* AGL1 and an ATMT performed using *F. fulva* Race 5 spores (**Materials and methods section 2.2.4.2**). Transformation plates were spread with spore solutions of various concentrations, and after two weeks of incubation, ~300 colonies grew from the plates spread with 10^5 spores.

Approximately 200 colonies were sub-cultured to selective media and, after incubation, all but two grew. Genomic DNA was extracted from a sub-set of 15 transformants and screened by PCR with primers that amplified *CfEcp11-1* from ~50 bp either side. These PCR results showed that gDNA from all transformants screened amplified WT-sized *CfEcp11-1*, with no evidence of large indels (**Appendix 5**). To examine whether CRISPR/Cas9 transformation caused point mutations, the PCR products were sequenced. The sequencing results showed that, for most transformants, a mixed chromatogram with more than one sequence trace was visible after the PAM site, suggesting that the transformants were not pure. However, after two rounds of single spore purification, the same sequencing results were found (**Appendix 6**). Fortunately, shortly after this analysis, the *F. fulva* Race 5 genome sequence was published by Zaccaron et al. (2022), where two identical, tandem copies of *CfEcp11-1* were identified. With this new information, the trace files were examined again, and it was found that the trace files could be teased apart to reveal the two copies of *CfEcp11-1* (**Appendix 7**).

Analysis of the two *CfEcp11-1* copies using the trace files (**Appendix 7**) suggested that, of the 15 transformants analysed, one had two WT copies of *CfEcp11-1*, ten were disrupted in a single copy, and four were disrupted in both copies (**Table 2.4**, **Figure 2.8**). Transformant #113 had only one sequencing trace visible, of the WT *CfEcp11-1* sequence. Therefore, it appeared that this transformant was not disrupted in *CfEcp11-1* or one copy was deleted. Of the ten transformants suggested to have a single disrupted copy of *CfEcp11-1*, eight had the same single nucleotide deletion at the double-strand break (DSB) site (nucleotide position 125, **Table 2.4**), which resulted in a frameshift mutation. The other two transformants (#128, and #167) each

had a nucleotide substitution at the DSB site, and a (different) nucleotide deletion elsewhere which caused a frameshift mutation.

Table 2.4. Summary of *CfEcp11-1* CRISPR/Cas9 transformants of *Fulvia fulva* strain Race 5.

Transformant	Plate[1]	Copy/copies mutated[2]	Copy mutated[3]	Mutation[4]	Frameshift[5]
113	4	WT	-	-	-
63	3	Single	Copy A	Nt del (125)	Yes
91	1	Single	Copy A	Nt del (125)	Yes
93	1	Single	Copy A	Nt del (125)	Yes
120	5	Single	Copy A	Nt del (125)	Yes
125	1	Single	Copy A	Nt del (125)	Yes
173	-	Single	Copy A	Nt del (125)	Yes
180	-	Single	Copy A	Nt del (125)	Yes
186	-	Single	Copy A	Nt del (125)	Yes
128	1	Single	Copy A	Nt del (124), sub (125)	Yes
167	-	Single	Copy A	Nt sub (125), del (131)	Yes
25	2	Double	Copy A	Nt del (125)	Yes
			Copy B	Nt del (125)	Yes
55	3	Double	Copy A	Nt del (125)	Yes
			Copy B	Nt sub (127)	No
92	1	Double	Copy A	Nt del (125)	Yes
			Copy B	Nt ins (126)	Yes
127	1	Double	Copy A	Nt del (125)	Yes
			Copy B	Nt ins (126)	Yes

1 - Transformant plate number, a dash means unknown.

2 -Whether one (single) or both (double) copies of *CfEcp11-1* appeared to be mutated. This was assessed from the sequencing trace data in **Appendix 7**. WT, wild type.

3 - It is unknown which copy is which as both are identical, but labelled A and B to show differences.

4 - Mutation type as nucleotide (Nt) deletion (del), substitution (sub), or insertion (ins), followed by nucleotide position in brackets.

5 – If a frameshift occurred due to the mutation, suggested from analysis of the sequencing trace data in **Appendix 7**.

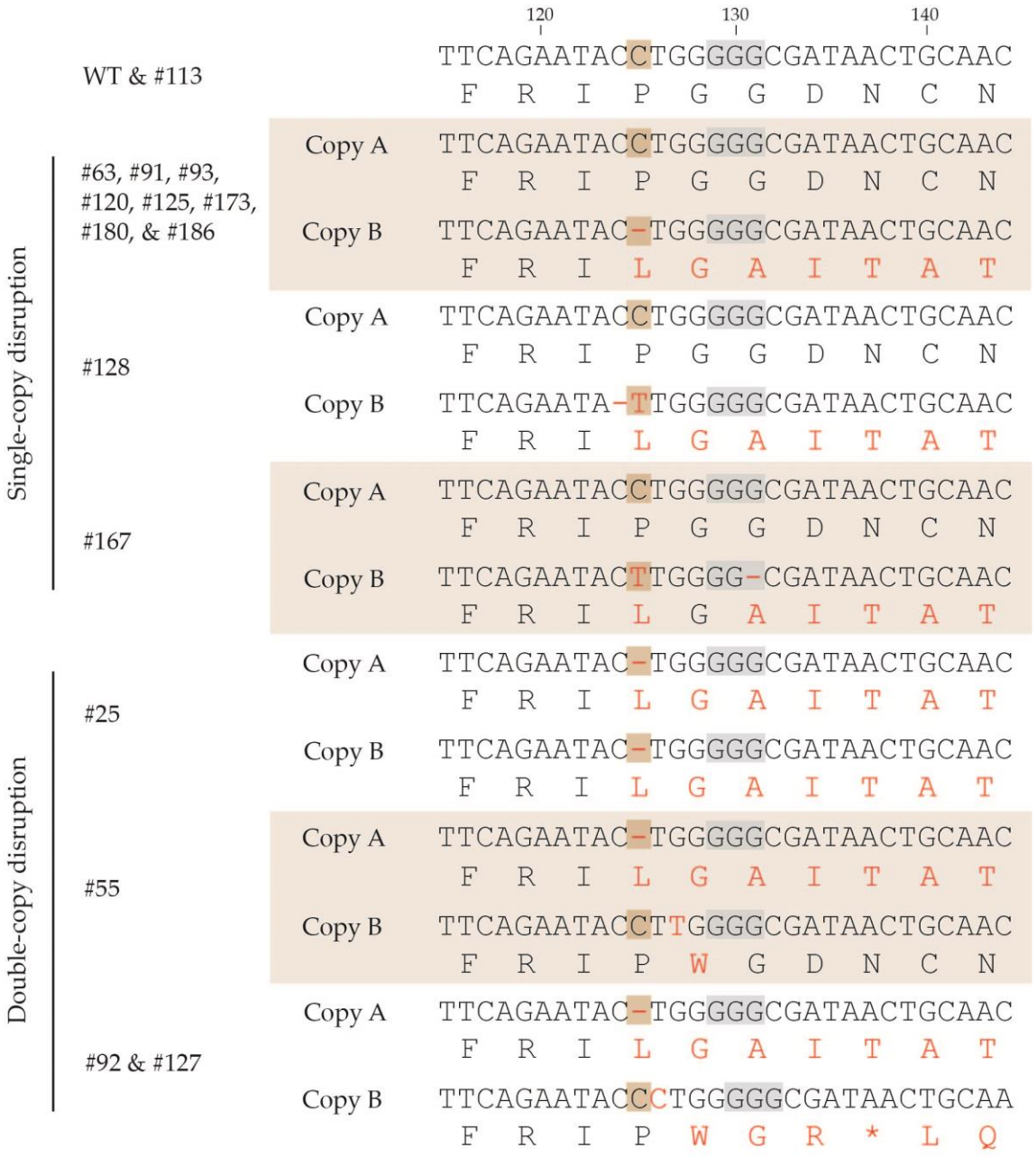

Figure 2.8. Schematic of mutations observed in both copies of *CfEcp11-1* from *Fulvia fulva* CRISPR/Cas9 transformants. A segment of *CfEcp11-1* nucleotide sequence containing the double-strand break (DSB) site (shaded in brown), and the protospacer adjacent motif (PAM) site (shaded in grey) is shown with the amino acid translation underneath. Nucleotide sequence numbers are shown above the wild type (WT) sequence. Mutations in the nucleotide and amino acid sequences are shown in red, and nucleotide deletions are indicated by a dash. The WT *CfEcp11-1* sequence is shown at the top of the figure, and transformant #113 was also suggested to have a WT sequence for both *CfEcp11-1* copies (but only one is shown). For the other transformants, the sequences of the two identical copies of *CfEcp11-1* (copy A and copy B) are shown (although as both WT copies are identical it is not known which is which). Some transformants had a mutation in only one *CfEcp11-1* gene copy (labelled single-copy disruption), while others had mutations in both copies (labelled double-copy disruption). Nucleotide sequences of both

CfEcp11-1 copies were obtained from sequencing PCR products, and the trace files were examined to determine what mutations occurred (**Appendix 7**).

Of the four transformants suggested to have both copies of *CfEcp11-1* disrupted, two (transformant #92 and #127) had the same mutations - a single nucleotide deletion in one *CfEcp11-1* copy and insertion in the other, resulting in frameshift mutations in both (**Table 2.4**, **Figure 2.8**). As they were both from the same transformation plate, these are possibly clones from the same transformation event. Another transformant (#55) had a single nucleotide deletion at the DSB (G127T) in one copy, resulting in a frameshift, and a single nucleotide substitution in the other copy, causing a single amino acid change. The last transformant (#25) had only one sequencing trace visible, where a nucleotide deletion was present at the DSB. As it is unlikely that both copies obtained the exact same mutation, one copy may have been completely deleted (across where the primers bind). To test this hypothesis, qPCR was performed to determine the *CfEcp11-1* gene copy number in this transformant. The ratio of Ct values suggested that only one copy was present (**Appendix 8**), supporting the hypothesis that one copy had been deleted.

In summary, these results show that CRISPR/Cas9 can target both copies of *CfEcp11-1*, and that the DSB site is the most likely nucleotide position for mutation. The aim of this research was to test these *CfEcp11-1*-disrupted mutants in the tomato (Cf-0, no *Cf R* genes) host and assess virulence, to determine whether CfEcp11-1 is a virulence factor. However, due to plant growth facilities being unavailable, these mutants could not be tested *in planta* at Massey University. Instead, the mutant strains were sent to our collaborators at Wageningen University in the Netherlands (laboratory of Assoc. Prof. Matthieu Joosten), to be tested in their state-of-the-art plant growth facilities. At the time of writing, this work had not yet been completed.

2.4 Discussion

In the work described in this chapter, a candidate effector of *F. fulva*, CfEcp11-1, was analysed through homology to other characterised effectors, as well as through a gene deletion study. Two new homologues of CfEcp11-1 were identified from *Fusarium oxysporum*, chimeric protein sequences were designed to analyse Cf-Ecp11-1-mediated recognition of CfEcp11-1, and *CfEcp11-1* was successfully disrupted through CRISPR/Cas9 gene editing. This discussion will focus on the key findings presented in this chapter, outline the limitations in this work, and also present future avenues of research.

The effector CfEcp11-1 was identified by Mesarich et al. (2018) to have homology to AvrLm3 and two proteins from *Z. ardabiliae*. In this study, analysis of these four proteins identified low amino acid similarity, but high conservation of cysteine residues, suggesting a conserved structure (**section 2.3.1**). In the current study, two new homologues of CfEcp11-1 were identified from *F. oxysporum* with all 10 conserved cysteine residues and amino acid identity of 20–35% to CfEcp11-1 (**Table 2.3**, **Figure 2.3a**). It would be of interest in the future to examine amino acid similarity as well as identity, as it is possible that these proteins share functionally redundant amino acids and may be more similar at the protein level than previously thought. After the analysis in this chapter was performed, our collaborators identified 49 structural analogues of AvrLm3, AvrLm4-7, AvrLm5-9, and CfEcp11-1, using structure-informed sequence database searches and using their in-house database of annotated proteomes from 116 fungal species (Lazar et al., 2022). The authors suggested that these proteins are part of a homologous family, which they named the LARS (Leptosphaeria AviRulence and Suppressing) effector family (Lazar et al., 2022).

CfEcp11-1 is thus a member of the LARS family; this is supported not only by structural analogy, but also by conserved functionality. Differences in plant receptor recognition between CfEcp11-1 and AvrLm3 prompted the design of chimeric proteins to identify protein regions and amino acids required for receptor recognition in tomato and *B. napus*. A total of 20 chimeric proteins were designed (**Figure 2.4**) in collaboration with Dr Isabelle Fudal's group. The chimeric regions were chosen based on analysis of the solved crystal structure of CfEcp11-1 and 3D model of AvrLm3 (Lazar et al., 2022). Region 1 covered a loop structure (**Figure 2.4** & **2.5**); these structures are often involved in protein interactions and have been shown to contain active site residues (Dhar & Chakrabarti, 2015; Hu, Wang, Ke, & Kuhlman, 2007). The recent study by Lazar et al. (2022) also found that the majority of polymorphic residues of CfEcp11-1, AvrLm3, and AvrLm5-9 in *F. fulva* and *L. maculans* populations were located in loop structures. Region 2 contained

the conserved WR(F/L/V)(R/K) motif (**Figure 2.4**), which was recently shown to be conserved in members of the LARS family (Lazar et al., 2022). Site-directed mutagenesis experiments also suggested that this motif was important for the ability of AvrLm4-7 to suppress recognition of AvrLm3 by Rlm3 (Lazar et al., 2022). The amino acid residues chosen for substitution were identified through analysis of population studies of *L. maculans* and *F. fulva* (Lazar et al., 2022; Mesarich et al., 2018), the details of which are described by Lazar et al. (2022). After design and construction of these chimeras, testing these proteins in tomato was to be performed in New Zealand as part of this chapter, and testing in *B. napus* in France by Dr Isabelle Fudal's group.

The chimeric proteins were tested in tomato using PVX-based transient expression (Hammond-Kosack et al., 1995; Takken et al., 2000) and ATMT, a method that has been used successfully in tomato in many other studies (Laugé et al., 2000; Mesarich et al., 2014; Mesarich et al., 2018; Takken et al., 2000; Wulff et al., 2001). Light, temperature and humidity have a huge impact on the HR, and it was shown that when humidity and/or temperatures are too high (>30°C/>90%) HR can be delayed, or even blocked (Negeri et al., 2013; Wang, Cai, & Zheng, 2005). Therefore, it is hypothesised that the PVX-based transient expression system could not be optimised in this study to test the chimeric proteins due to the available plant growth room not being light-, temperature-, or humidity-controlled. The plasmids were thus sent to our collaborators in the Netherlands (laboratory of Assoc. Prof. Matthieu Joosten) to test by PVX-based transient expression, and unfortunately these experiments were not completed in time for the results to be included in this thesis.

The work performed in other studies (Lazar et al., 2022; Mesarich et al., 2018) and this chapter suggest that *CfEcp11-1* is upregulated *in planta*, is recognised by a receptor in tomato and *B. napus*, and is part of the structurally conserved LARS effector family. This accumulated evidence suggests that CfEcp11-1 may function as a virulence factor in *F. fulva*. Therefore, I sought to develop a *ΔCfEcp11-1* mutant strain to test for virulence on Cf-0 tomato. The *CfEcp11-1* homologous recombination construct was designed with long 1kb flanks to increase transformation efficiency (Xu et al., 2014). However, in the repeat-rich *F. fulva* genome (de Wit et al., 2012; Mesarich et al., 2023), *CfEcp11-1* is located between two repeat regions, meaning a proportion of the 1 kb flanks contain these repeat sequences (**Figure 2.7**). Therefore, it is possible that in these transformants, the flanks matched closely enough to other repeat regions in the genome and the hygromycin cassette was inserted elsewhere, rather than at the *CfEcp11-1* loci. Due to the highly repetitive nature of the *F. fulva* genome, a more specific gene disruption method was therefore attempted.

CRISPR (Clustered Regularly Interspaced Short Palindromic Repeats)/Cas9 is a highly specific gene editing technology that was modified from an adaptive immune system in prokaryotes (Barrangou et al., 2007; Mojica, Díez-Villaseñor, García-Martínez, & Soria, 2005). A sgRNA is designed to match a short (~20 bp) target sequence and PAM (Protospacer Adjacent Motif) site and will direct the Cas9 nuclease to the site to produce a double-strand break (DSB) (Shi et al., 2017). In this study, no repair template was added, so DSB repair was expected to occur through non-homologous end-joining (NHEJ). Unfortunately, an autonomously replicating plasmid could not be used as there were difficulties obtaining protoplasts from *F. fulva* (**section 2.3.5**). Instead, an *A. tumefaciens*-compatible plasmid was utilised which, after transformation, will directly insert into the *F. fulva* genome (Chambers et al., 2021). A limitation of this method is that because the CRISPR/Cas9 plasmid will remain in the genome, Cas9 will be constitutively active and may cause off target effects. Therefore, when testing the mutants for virulence it will be important to include a complementation strain, to determine if an off-target effect occurred that might have disrupted virulence. Another limitation of this method is that when complementing the mutant, the PAM site in the *CfEcp11-1* sequence must be modified, or else the still functional Cas9 may target it (Chambers et al., 2021). Despite these limitations, this method is still valuable for testing gene function in combination with a complemented strain.

CRISPR/Cas9 gene editing through ATMT was successfully performed with the Race 5 strain. A sub-set of transformants were screened by PCR and PCR amplicon sequencing, and it appeared that disruption of *CfEcp11-1* had occurred with 99.3% efficiency of screened transformants. This transformation efficiency is quite high compared to CRISPR/Cas9 disruption in other fungi (Rocafort, Arshed, et al., 2022; Wenderoth, Pinecker, Voß, & Fischer, 2017), and may suggest that *CfEcp11-1* is in a part of the *F. fulva* genome that is more accessible for the Cas9 protein (Yarrington, Verma, Schwartz, Trautman, & Carroll, 2018). Sequencing the *CfEcp11-1*-disrupted transformants identified two traces which, after publication of the 98.9% complete *F. fulva* Race 5 genome (Zaccaron et al., 2022), were suggested to be two identical copies of *CfEcp11-1*. Third generation sequencing technology and Hi-C chromatin conformation capture techniques enabled the identification of two identical copies of *CfEcp11-1* (named copy A and B, (Zaccaron et al., 2022)), which due to the highly repetitive DNA content of the *F. fulva* genome, were not identified previously (de Wit et al., 2012). With this new information, the sequencing trace files were examined again, and it was found that the two traces could be teased apart and two distinct sequences, *CfEcp11-1* copy A and B, identified (**Figure 2.8**). These results showed that some of the transformants were disrupted in one copy of *CfEcp11-1*, while others were disrupted in both copies (**Table 2.4**), giving efficiencies of 66.7% and 26.7% respectively.

Most of the transformants contained a single nucleotide indel, which was expected from NHEJ (Zhang, Meng, Wei, & Lu, 2016), while a smaller number contained two nucleotide indels, or a single nucleotide substitution (**Table 2.4**). The majority of these single nucleotide mutations occurred at the DSB site. All transformants appeared to have different mutations in each *CfEcp11-1* gene copy (**Table 2.4**), except transformant #25 where only one copy was present (**Table 2.4**), suggesting that a large deletion, covering the region where the primers bind, had occurred in the other copy. This is not the first study to report CRISPR/Cas9 disruption of multiple gene copies, as it has been shown in the allotetraploid plant *B. napus* (Yang et al., 2018; Zhai et al., 2020), as well as in diploid and octoploid strawberry plants (Wilson, Harrison, Armitage, Simkin, & Harrison, 2019). Nevertheless, to the best of my knowledge, this study is the first to report CRISPR/Cas9 disruption of multiple gene copies in a fungus.

The work described in this chapter led to the identification of two new members of the LARS effector family and contributed to the design of chimeric proteins which will be used to further analyse the functions of these proteins and how they are recognised in both host and non-host species. This chapter also presents the first CRISPR/Cas9 gene editing in *F. fulva*, which occurred with very high efficiency, and the first report in a fungus of CRISPR/Cas9 disruption of multiple copies of the same gene. These results have contributed to understanding the role of CfEcp11-1 in *F. fulva* and provided a foundation for future work. The development of *CfEcp11-1* mutants, in particular, will enable experiments that will reveal if CfEcp11-1 is a virulence factor.

Chapter 3 - Identification of candidate virulence factors in *Dothistroma septosporum*

3.1 Introduction

The increased availability of genetic resources, such as genome sequences and transcriptome data, has been invaluable in the search for virulence factors. The identification of genes used by plant pathogens to cause disease is an important step in developing control strategies and informing resistance breeding. Many candidate virulence factors have been identified from *F. fulva* in recent years (Mesarich et al., 2023), including CfEcp11-1 which was examined in **Chapter 1**. However, only a handful of candidates have been identified from *D. septosporum* and there is an urgent need to identify more. In some plant pathogen systems, virulence-related genes can be identified through forward genetics approaches such as large-scale mutagenesis studies (Dufresne et al., 2000; King et al., 2017). However, as a slow-growing fungus that requires 10–12 weeks to complete its lifecycle on the pine host (Kabir et al., 2015b), such forward genetic approaches are not feasible with *D. septosporum*. Instead, to identify virulence factors of *D. septosporum*, a reverse genetics approach must be used where candidate genes are selected, mutant strains developed, and those strains tested on the host for reduced infection. This method was recently used to identify and characterise effector *DsEcp2-1* as an avirulence factor of *D. septosporum* (Guo, Hunziker, et al., 2020).

There are several resources already available to assist selection of candidate virulence factors in *D. septosporum*. Firstly, the genome has been fully sequenced, and a comparative genomics study was performed between *D. septosporum* and its close relative *Fulvia fulva*, highlighting genes with possible roles in virulence (de Wit et al., 2012). Secondly, a transcriptomic study was performed on *D. septosporum* both *in vitro* and on the host *Pinus radiata*, providing expression data over the course of infection (Bradshaw et al., 2016). Thirdly, an effector prediction pipeline was recently developed to identify candidate effector genes, which were then recombinantly expressed and tested for cell death-inducing activity in the non-host species *Nicotiana* (Hunziker, 2018), and the host species *P. radiata* (Hunziker et al., 2021; Tarallo et al., 2022).

In this study, I used these available resources to inform my search for candidate virulence factors. I also made use of the close phylogenetic relationships between *D. septosporum* and other plant-pathogenic fungal species with characterised virulence factors. Combining these resources, I searched for virulence factors that are transcription factors as well as effectors. Traditionally, in searches for a molecular component of disease, secreted effector proteins are

sought after because they are easy to screen for a hypersensitive response (HR) on the host (Vleeshouwers & Oliver, 2014). Furthermore, identification of the host receptor that recognizes the effector can inform breeding efforts and result in the generation of new resistant host cultivars (Joosten & De Wit, 1999). However, transcription factors are also important for disease, and with the increased availability of gene manipulation methods such as CRISPR/Cas9 and RNA interference, functional characterization of transcription factors is becoming far more common (John et al., 2021). As more transcription factors are identified as essential for pathogenicity, it has become apparent that these genes would be ideal targets for disease control strategies (Cho, 2015; John et al., 2021).

Transcription factors are sequence-specific DNA-binding proteins that modulate gene expression by binding to gene promoter elements (John et al., 2021). Transcription factors that regulate virulence factors and are essential for virulence, are ideal targets for disease control by either spray-induced gene silencing (SIGS) involving double-stranded RNA (dsRNA) or host-induced gene silencing (HIGS) (John et al., 2021). Several transcription factor genes have already been identified as ideal candidates (John et al., 2021); these include *VdFft1* from *Verticillium dahlia* (Zhang et al., 2018), *Ftf1* from *Fusarium oxysporum* (Niño-Sánchez et al., 2016)*, Pf2* from *Parastagonospora nodorum* (Jones et al., 2019) and *Tri6* from *Fusarium graminearum* (Scherm et al., 2011; Shostak et al., 2020), which have all been shown to regulate expression of virulence factors. While the first three transcription factors regulate expression of virulence factors such as proteinaceous effectors, *Tri6* regulates the production of secondary metabolites involved in virulence (Shostak et al., 2020), as well around 200 other genes (Nasmith et al., 2011; Seong et al., 2009). HIGS of fungal transcription factors important for disease has been performed previously (Song & Thomma, 2018) and found to successfully reduce virulence of *Puccinia striiformis* f. sp. *tritici* and *Magnaporthe oryzae* (Guo et al., 2019; Zhu et al., 2018).

Several transcription factors have been characterised as playing a role in the necrotrophic switch, where fungi transition from biotrophic to necrotrophic growth. The necrotrophic switch occurs in all hemibiotrophic fungal phytopathogens, including *D. septosporum*, however little is known about this important transition stage and there are many unanswered questions. For example, is the necrotrophic switch regulated by a single gene or multiple genes and are these genes conserved among all hemibiotrophic fungi? Several transcription factors suggested to be involved in the necrotrophic switch include *Zt107320* of *Zymoseptoria tritici* (Habig, Bahena-Garrido, Barkmann, Haueisen, & Stukenbrock, 2020), *PacCL* of *Colletotrichum lindemuthianum* (Soares et al., 2014) and *CoHox1* of *Colletotrichum orbiculane* (Yokoyama et al., 2019), as outlined in **Chapter 1**. However, deletion of these transcription factor genes also impacts

vegetative growth and other core functions, suggesting these genes may have functional orthologs in other fungal species. This would make these genes undesirable targets for gene silencing as a disease control strategy due to the potential for off-target effects in other fungi such as those that form a beneficial part of the host's microbiota. In contrast, *CLTA1* and *CLNR1* of *C. lindemuthianum* have been identified with possible roles in the necrotrophic switch, where gene deletion mutations show a reduction in virulence but no alteration in vegetative growth. Mutants of *CLTA1* induce an HR-like response early in infection but no secondary hyphae are produced to enable the transition to necrotrophic growth (Dufresne et al., 2000). Mutants of the nitrogen regulator *CLNR1* are disrupted specifically at the transition to necrotrophy (Pellier et al., 2003). Therefore, transcription factor genes *CLTA1* and *CLNR1* could make ideal targets for SIGS or HIGS as a disease control strategy.

As a Dothideomycete species, *D. septosporum* is related to many well-studied plant pathogenic fungi. These relationships can be utilized to identify candidate virulence factors of *D. septosporum.* In this study, I will compare *D. septosporum* candidate virulence factor genes with those characterised from other phylogenetically-related fungal plant pathogens, to suggest possible functions. A particular focus will be on comparing *D. septosporum* genes with those from its close relative, *F. fulva*. *D. septosporum* and *F. fulva* infect vastly different host plants (the gymnosperm pine and the angiosperm tomato, respectively) and, while both are considered hemibiotrophs, they differ in that plant cell death is required for sporulation by *D. septosporum*, but not by *F. fulva* (Kabir et al., 2015b; Mesarich et al., 2023). Despite the significant differences in their hosts, these two fungi have many genes in common, and share several functional effectors such as Ecp2-1 and Avr4 (de Wit et al., 2012; Mesarich et al., 2016). Identification and analysis of candidate virulence factors that are either common to both *D. septosporum* and *F. fulva* or are unique to one of those species could provide insights into gene function and their roles in the fungal lifestyle.

This chapter presents the identification of *D. septosporum* candidate virulence factors using a prediction pipeline based on available genomic and transcriptomic analyses, homology to virulence factors from other species as well as *F. fulva*, and gene expression. The shortlisted candidates will be further analysed through bioinformatic prediction tools and literature searches to identify those with a possible role in virulence. Finally, several candidates will be selected to take through gene disruption analysis and virulence assessment in **Chapter 5**, to determine whether these genes are essential for virulence of *D. septosporum*.

3.2 Materials and methods

3.2.1 Identification of candidate virulence factors of *Dothistroma septosporum* based on homology to characterised genes

Candidate virulence factors of *D. septosporum* were identified using a prediction pipeline (**Figure 3.1**). The pipeline employed used two strategies; searching the literature for characterised virulence factors, or analysing the previous research performed in *D. septosporum*. In the strategy where literature searches were performed, virulence factors characterised in other fungal plant pathogens as playing a role in virulence, specifically in the necrotrophic switch, were examined. Then, the likely *D. septosporum* homologue of the virulence factor was identified by performing BlastP analysis with the protein sequence of the virulence factor identified from the literature as the query, against the *D. septosporum* NZE10 v1.0 database (filtered gene models, BLOSUM62 scoring matrix, expect 1.0E-5, filtering low complexity regions), using the Joint Genome Institute (JGI) website (https://mycocosm.jgi.doe.gov/Dotse1/Dotse1.home.html). Finally, gene expression of the *D. septosporum* homologue was examined and, if the gene was upregulated *in planta* relative to *in vitro*, it was selected as a candidate virulence factor. The other strategy utilised in this pipeline involved examination of the research already performed on *D. septosporum*. This included comparative genome analysis with *F. fulva* (de Wit et al., 2012), transcriptome analysis over the course of *D. septosporum* infection of the host *P. radiata* (Bradshaw et al., 2016), and an effector prediction pipeline used to select candidate effectors and test their response in both the non-host species *Nicotiana spp.* (Hunziker, 2018), and the host species *P. radiata* (Hunziker et al., 2021). Genes identified from this search which were also upregulated in gene expression from *in vitro* to *in planta* were selected as candidate virulence factors.

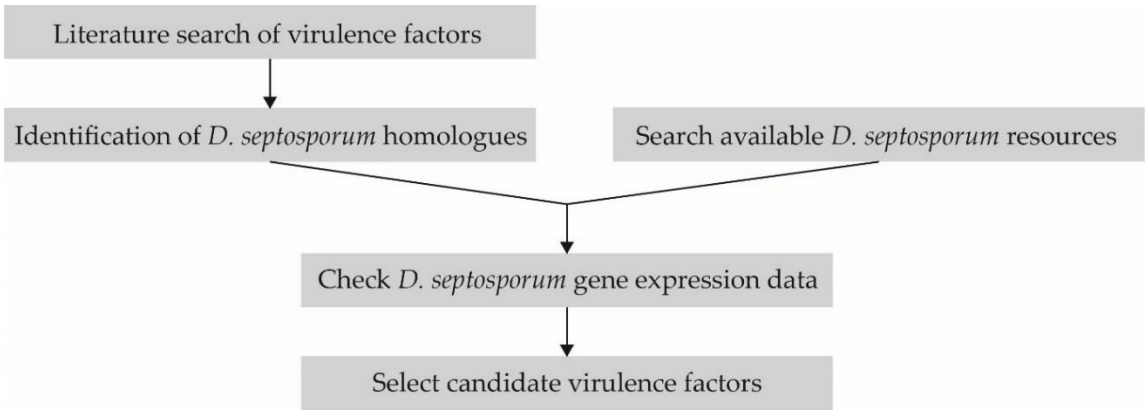

Figure 3.1. Pipeline used to identify *Dothistroma septosporum* candidate virulence factors.

3.2.2 Identification of *Fulvia fulva* homologues of *Dothistroma septosporum* candidate virulence factors

F. fulva homologues of *D. septosporum* candidate virulence factors were identified, and their gene expression analysed, to determine if the activity of this *F. fulva* homologue could provide insight into possible roles of this candidate virulence factor in *D. septosporum*. The *F. fulva* genome (taxid:5499, non-redundant protein sequences database) was analysed by BlastP using the National Center for Biotechnology Information (NCBI) website (https://blast.ncbi.nlm.nih.gov/Blast.cgi) with a BLOSUM62 matrix and standard parameters, queried with *D. septosporum* candidate virulence factor protein sequences. The BlastP hit with the highest percentage identity and subject coverage was selected as the *F. fulva* homologue and expression of the gene it encodes was analysed using existing transcriptome data of *F. fulva* strain 0WU *in vitro* and *in planta* on H-Cf-0 tomato plants (Mesarich et al., 2014).

3.2.3 Reciprocal BlastP analysis to determine orthology

Reciprocal BlastP analysis was performed to determine whether genes encoding homologous proteins (inherited through a common ancestor) were also orthologues (retained a similar function when inherited). Reciprocal BlastP analysis was performed by identifying the top hit in proteins predicted from the proteome of one organism, then performing BlastP analysis with that top hit back against those of the organism of the original search. If the two proteins being analysed were the top hits from each reciprocal search, the proteins were considered possible orthologues.

Reciprocal BlastP analysis was performed between three groups of proteins (**Figure 3.2**): the *D. septosporum* candidate virulence factors, virulence factors from other fungal species found to

be homologous to *D. septosporum* candidates, and the *F. fulva* homologue of the *D. septosporum* candidate. BlastP analysis was performed using the NCBI website and conditions described above. However, the proteome database used was specific to the organism whose gene was being analysed. For BlastP analysis of the *D. septosporum* candidate virulence factor protein, the search was specific to the *Dothistroma septosporum* (taxid:64363) proteome database, for the *F. fulva* homologue the *Fulvia fulva* (taxid:5499) database was used, and for the homologous virulence factor from another fungal species, the database was specific to that species.

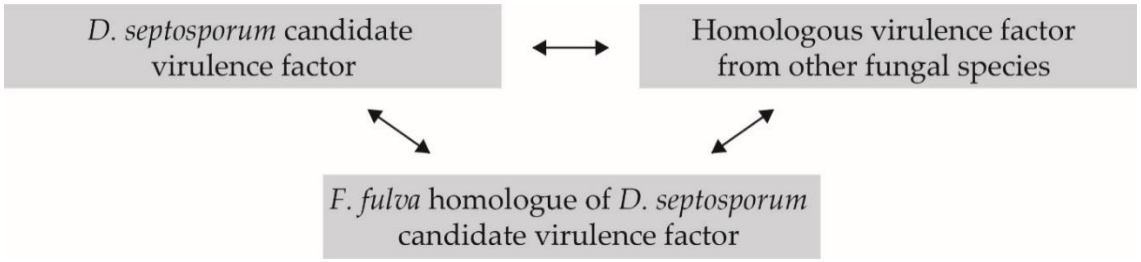

Figure 3.2. Schematic showing reciprocal BlastP analyses performed between proteins from different fungal species.

3.2.4 Construction of phylogenetic trees of *Dothistroma septosporum* candidate virulence factors and top 30 BlastP hits in Dothideomycetes

To provide further information about the transcription factor genes selected as *D. septosporum* candidate virulence factors, phylogenetic trees were constructed. The top 30 BlastP hits of the virulence factor protein sequence were first identified by performing BlastP analysis using the NCBI website against the non-redundant protein sequences database in Dothideomycetes (taxid: 147541) with a BLOSUM62 matrix and standard parameters. The protein sequences were compiled using Geneious software (v9.1.8) and a Geneious alignment constructed as a global alignment with free end gaps, with a BLOSUM62 cost matrix. From the protein alignment, Geneious Tree Builder was used to construct a phylogenetic tree using the Jukes-Cantor genetic distance model, built using the Neighbor-Joining method with 100 Bootstrap replicates, to construct a consensus tree. The lifestyle of each fungal species was then identified from the literature and each phylogenetic tree annotated with this information.

3.2.5 Alignment of protein sequences of the top BlastP hits of DsPf2

To further investigate any relationship between the Pf2 transcription factor protein sequence and fungal lifestyle, an alignment of DsPf2 and the top three BlastP hits to DsPf2 from Dothideomycete species, was performed. The protein sequences were previously identified from the top 30 BlastP hits of *D. septosporum* Pf2 used to construct the phylogenetic tree (**section 3.2.4**). These sequences were then analysed using InterPro (http://www.ebi.ac.uk/interpro/) to identify the Zn_2Cys_6 binuclear cluster domain (Pfam domain: PF00172) and fungal-specific transcription factor domain (Pfam domain: PF04082). An alignment of the protein sequences was performed using Geneious (v9.1.8) as described in **section 3.2.4**.

3.3 Results and discussion

3.3.1 Identification of *Dothistroma septosporum* candidate virulence factors

The final shortlist of ten *D. septosporum* candidate virulence factors was identified (**Table 3.1**) using the pipeline shown in materials and methods **section 3.2.1**. The original list of candidates contained 20 genes. Among those not shortlisted were genes with low expression levels, those that lacked enough evidence to support a role in virulence in other fungi, and those shown through gene deletion studies in other fungi to have an additional essential role in fungal growth, such as the *D. septosporum PacCL* homologue (Soares et al., 2014).

The table of shortlisted candidate virulence factors (**Table 3.1**) shows the gene expression *in vitro* and *in planta* across the course of infection on the *P. radiata* host (Bradshaw et al., 2016), as well as Pfam domains, and BlastP analysis of closely related proteins of interest. This table is separated into three sections: reference genes, effector genes and transcription factor genes. The reference genes *DsPksA* and *DsAflR* were included to show what are likely functional gene expression levels in *D. septosporum*. Both *DsPksA* and *DsAflR* are involved in production of dothistromin, a toxin shown to be a virulence factor of *D. septosporum* (Kabir et al., 2015a). *DsPksA* is a gene involved in the early stage of biosynthesis of dothistromin (Bradshaw & Zhang, 2006), while *DsAflR* is a regulator of dothistromin biosynthesis gene expression (Chettri et al., 2013).

Proteins in the effector section were suggested to be effectors because they contained a signal peptide, were predicted to be secreted, and all except DsGH11 were previously selected as candidate effectors by Hunziker (2018). Two candidates in the effector section had no suggested protein domain or class, while the other three contained a cerato-platanin, 'Cysteine-rich secretory proteins, Antigen 5, and Pathogenesis-related 1 proteins' (CAP), or glycosyl hydrolase domain. The proteins in the transcription factor section were suggested to be transcription factors based on the presence of protein domains or homology to other characterised transcription factors. Of the five proteins selected, one was a basic-leucine zipper (bZIP) transcription factor, another was a GATA zinc finger transcription factor, and the other three were Zn_2Cys_6 fungal transcription factors. The candidate virulence factors in **Table 3.1** were also examined by BlastP analysis in *F. fulva* (**Table 3.2**), to determine if this pathogen contains homologues or orthologues and if there are any differences in protein sequence or gene expression that could be related to fungal lifestyle. The results in **Table 3.2** showed that all *D. septosporum* candidate virulence factor proteins except Ds74812 had a homologue in *F. fulva*.

Of the predicted proteins of these *F. fulvia* homologues, all except DsGH11 were also identified as orthologues through reciprocal BlastP analysis (**Table 3.2**).

Table 3.1. Candidate virulence factors of *Dothistroma septosporum*.

Name & JGI ID[1]	Pfam domain[2]	Normalised expression[3]				Characterised proteins with similarity[4]						Details[6]
		Iv	Early	Mid	Late	Protein name and description	Organism	GenBank Accession	Query cover	E value	aa ID[5]	
Reference[7]												
DsPksA	-	27	10	94	63	-		-			-	-
DsAflR	-	230	46	89	157	-		-			-	-
Effectors[8]												
DsCE3 (Ds71487)	-	27	239	145	982	Cell Death-Inducing 1 (RcCDI1)	*Rhynchosporium commune*	ARB51385.1	88%	1E-37	44%	Cell death-eliciting activity in *Nicotiana* species (Hunziker et al., 2021). Orthologue of PAMP RcCDI1 (Franco-Orozco et al., 2017)
DsCE15 (Ds131885)	-	1	9	369	203	hypothetical protein (VmE02)	*Valsa mali*	KUI69068.1	100%	7E-53	60%	Cell death-eliciting activity in *Nicotiana* species (Hunziker et al., 2021). Orthologue of cross-kingdom PAMP VmE02 (Nie, Yin, Li, Wu, & Huang, 2019)
DsCPL1 (Ds70155)	Cerato-platanin	257	71	507	1303	cerato-platanin-like protein 2 (HaCPL2)	*Heterobasidion annosum*	AKA43766.1	82%	2E-46	56%	No cell death-eliciting activity in *Nicotiana* species (Hunziker, 2018). Orthologue of cell death elicitor HaCPL2 (Chen, Quintana, Kovalchuk, Ubhayasekera, & Asiegbu, 2015)
DsEcp57-*1* (Ds69335)	CAP	426	1448	1012	554	candidate effector 14 (ViCE14)	*Venturia inaequalis*	ACM90103.1	59%	3E-65	63%	No cell death-eliciting activity in *Nicotiana* species (Hunziker, 2018). Orthologue of ViCE14 (Prokchorchik, 2017)
DsGH11 (Ds137959)	Glyco_hydro_11	4	88	391	203	*endo-1,4-beta-xylanase (SNOG_15270)	*Parastagonospora nodorum*	QRC97940.1	99%	1E-72	58%	Similarity to putative effector SNOR_15270, regulated by PnPf2 (Jones et al., 2019). Similarity to Xyn11A (Brito, Espino, & González, 2006)
Transcription factors												
DsPf2 (Ds68376)	Zn_clus, Fungal_trans	33	18	42	26	*Zn_2Cys_6 binuclear cluster transcription factor PnPf2	*P. nodorum*	QRC91151.1	79%	0	54%	Orthologue of PnPf2 of *P. nodorum*, regulator of necrotrophic effectors (Rybak et al., 2017)
Ds74812	-	66	5	101	80	hypothetical protein	*Pyrenophora teres f. teres*	EFQ85926.1	99%	2E-92	44%	Possible necrotrophic switch regulator based on gene expression profile (Bradshaw et al., 2016)
Ds69328	Zn_clus, Fungal_trans	9	6	122	19	Uncharacterised protein	*Fulvia fulva*	XP_047758835.1	71%	0	84%	Possible necrotrophic switch regulator based on gene expression profile (Bradshaw et al., 2016)
Ds41021	GATA zinc finger	80	109	35	70	*major nitrogen regulatory protein	*Colletotrichum lindemuthianum*	AAN65464.1	76%	5E-127	42%	Orthologue of CLNR1 from *C. lindemuthianum*, required for the transition to necrotrophic growth (Pellier et al., 2003)
Ds68895	Zn_clus, Fungal_trans	32	24	23	76	*putative GAL4-like transcriptional activator	*C. lindemuthianum*	AAG25917.1	77%	1E-123	40%	Orthologue of CLTA1 of *C. lindemuthianum*, required for the transition to necrotrophic growth (Dufresne 2000)

1 – Joint Genome Institute (JGI) protein ID from the *D. septosporum* genome page (https://mycocosm.jgi.doe.gov/Dotse1/Dotse1.home.html).

2 –Pfam domains (Mistry et al., 2021) were identified from the JGI protein pages. Pfam accession numbers are: Cerato-platanin (PF07249), CAP (PF00188), Glyco_hydro_11 (PF00457), Zn_clus (PF00172), Fungal_trans (PF04082), GATA zinc finger (PF00320).
3 – Gene expression is shown as Reads Per Million per Kilobase (RPMK) and was sourced from a transcriptome analysis performed on *D. septosporum*-infected *Pinus radiata* seedlings. Three *in planta* stages were sampled: early, mid, and late, as well as an *in vitro* (Iv) control of fungal mycelium (Bradshaw et al., 2016). Expression values are highlighted based on fold change compared to *in vitro* gene expression (orange is fold change >2, red is fold change >10).
4 – BlastP analysis of the top hit to the *D. septosporum* protein or of the homologous protein used to identify the protein (marked with an asterisk). Query cover, E-value, and amino acid identity (aa ID) are shown.
5 – Amino acid identity (aa ID).
6 – Evidence from a variety of sources why each protein was selected as a candidate virulence factor of *D. septosporum*. Proteins were confirmed as orthologues by reciprocal BlastP analysis. PAMP; pathogen-associated molecular patterns.
7 – The expression levels of two well-studied *D. septosporum* genes; *DsAflR* (JGI ID: Ds75566) a regulator of dothistromin synthesis, and *DsPksA* (JGI ID: Ds192192) an early-stage dothistromin biosynthesis gene, are provided to illustrate expression levels of fully functional virulence-associated genes in this *D. septosporum* dataset.
8 – All proteins in the effector category are annotated on the JGI website as having a signal peptide and predicted to be secreted.

Table 3.2. Top BlastP hits of *Dothistroma septosporum* candidate virulence factors in *Fulvia fulva*.

D. septosporum candidate gene	Protein description	Top BlastP hit in *F. fulva*[1] GenBank accession	Query cover	E value	aa ID[2]	Gene expression[3] Iv	4 dpi	8 dpi	12 dpi
Effectors									
DsCE3 (*Ds71487*)	Uncharacterised protein	XP_047762506.1	89%	3E-84	70%	3	0	8	10
DsCE15 (*Ds131885*)	Uncharacterised protein	XP_047763808.1	99%	1E-73	83%	150	0	3	108
DsCPL1 (*Ds70155*)	Extracellular protein (Ecp45)	XP_047767036.1	87%	4E-82	91%	15	142	447	240
DsEcp57-1 (*Ds69335*)	Extracellular protein (Ecp57-1)	XP_047758105.1	100%	8E-117	76%	1491	1531	771	1179
DsGH11 (*Ds137959*)	Endo-1,4-beta-xylanase B	XP_047764621.1	90%	6E-68	55%	0	0	0	0
Transcription factors									
DsPf2 (*Ds68376*)	Putative sucrose utilization protein SUC1	XP_047756992.1	100%	0	89%	90	0	3	5
Ds74812	No hits[4]								
Ds69328	Uncharacterised protein	XP_047758835.1	71%	0	84%	3	0	0	9
Ds41021	Nitrogen regulatory protein AreA	XP_047756925.1	99%	0	89%	27	0	9	16
Ds68895	Positive regulator of purine utilization	UJO11482.1	99%	0	87%	12	0	1	1

1 – The top BlastP hit of the *D. septosporum* candidate proteins in *F. fulva* was determined by BlastP analysis against the *F. fulva* proteome database (taxid:5499) using the National Center for Biotechnology Information (NCBI) website (https://blast.ncbi.nlm.nih.gov/Blast.cgi). Query cover, E-value, and amino acid identity (aa ID) are shown. All *F. fulva* proteins (except the top BlastP hit of DsGH11) were confirmed as orthologues of the *D. septosporum* candidate virulence factor by reciprocal BlastP analysis. These *F. fulva* proteins were also identified through reciprocal BlastP analysis to be orthologues of the characterised proteins from other species that were used as queries to identify the candidates in **Table 2.1**, except for SNOR_15270.

2 – Amino acid identity (aa ID).

3 – Gene expression in *F. fulva* is shown as Fragments Per Kilobase of exon per Million fragments mapped (FPKM) and was sourced from a transcriptome study of a compatible interaction of H-Cf-0 tomato plants inoculated with *F. fulva* 0WU strain and sampled 4, 8 and 12 days post-inoculation (dpi), as well as an *in vitro* (Iv) *F. fulva* sample grown in potato dextrose broth (Mesarich et al., 2014). Expression values are highlighted based on fold change compared to *in vitro* gene expression (orange is fold change >2, red is fold change >10).

4 – BlastP analysis with the default parameters did not produce any hits in *F. fulva* from Ds74812.

3.3.2 Analysis of candidate *D. septosporum* virulence factor effectors

All of the candidate virulence factors in the effector genes section in **Table 3.1**, except DsGH11, were previously identified as candidate effectors from a pipeline where selection relied on the protein having a signal peptide, no membrane or intracellular affiliation, and having adequate expression *in planta* (Hunziker, 2018). Some of these proteins were found to induce cell death in the non-host plants *N. benthamiana* and/or *N. tabacum* when delivered by *Agrobacterium tumefaciens*-mediated transient transformation (Hunziker, 2018). A cell death response could be due to phytotoxic properties of the protein, or recognition of the protein (directly or indirectly) by the plant in conjunction with the activation of a hypersensitive response (HR). In this section, available bioinformatic prediction tools, transcriptome data, literature, and homologues from *F. fulva* and other fungal species were analysed to suggest whether the protein might play a role in virulence, and specifically the necrotrophic switch.

3.3.2.1 DsCE3

DsCE3 was first identified by Hunziker (2018) as a candidate effector without any characterised homologues or Pfam domains. *DsCE3* is highly expressed across all *in planta* stages, with expression peaking at late stage (6.8-fold increase from mid stage and 36.1-fold increase from *in vitro*, **Table 3.1**). Functional analysis of DsCE3 found that this protein triggered cell death in *N. tabacum* in 58% of infiltration spots, and in *N. benthamiana* in 50% of infiltration spots but the cell death was restricted to the perimeter of the infiltration zone (Hunziker et al., 2021). The *F. fulva* orthologue of DsCE3 is also an uncharacterised protein with 70% predicted amino acid identity and 89% query coverage compared to DsCE3. The gene encoding this *F. fulva* protein is not highly expressed at any stage but is slightly upregulated at 8- and 12-days post-inoculation (dpi) from *in vitro* (**Table 3.2**).

In subsequent work, Hunziker et al. (2021) showed that DsCE3 has 44% amino acid identity (88% query coverage) with the proteinaceous pathogen-associated molecular pattern (PAMP) RcCDI1, of *Rhynchosporium commune*, the causal agent of scald disease on barley (Franco-Orozco et al., 2017) (**Table 2.1**). DsCE3 and the *F. fulva* orthologue of DsCE3 were identified as orthologues of RcCDI1 through reciprocal BlastP analysis (Hunziker et al., 2021) (**Table 2.2**). DsCE3 shares the same four cysteine residues conserved in RcCDI1 and other RcCDI1 homologues, which are suggested to form two intramolecular disulphide bonds (Franco-Orozco et al., 2017). Alignment of predicted secondary structures of DsCE3 and RcCDI1 suggested high similarity (Hunziker, 2018).

In *R. commune*, *RcCDI1* is expressed at 40-fold higher levels during early infection at 3 dpi than *in vitro*, which coincides with cuticle penetration and the start of apoplast colonization (Franco-Orozco et al., 2017). Numerous homologues of RcCDI1 were identified from Ascomycete species with a range of different lifestyles. RcCDI1, as well as RcCDI1 homologues from pathogenic fungi and a saprophytic fungus, were found to trigger strong cell death in *N. benthamiana* (Franco-Orozco et al., 2017). RcCDI1 was also shown to trigger strong cell death in the Solanaceae plants *Nicotiana sylvestris*, tomato, and potato, but not in *Arabidopsis thaliana*, bean, or several monocot species including the barley host (Franco-Orozco et al., 2017). Conservation of RcCDI1 across Ascomycete species and the discovery that recognition in *N. benthamiana* is dependent on the two leucine-rich repeat (LRR) receptor-like kinase (RLK) receptors, BAK1 and SOBIRI, lead to the suggestion that RcCDI1 is a PAMP (Franco-Orozco et al., 2017).

Despite *DsCE3* and the *F. fulva DsCE3* orthologue being orthologous to *RcCDI1*, these genes have different expression profiles. Moreover, the cell death induced in *N. benthamiana* by DsCE3 (Hunziker, 2018; Hunziker et al., 2021) is not as strong as that induced by RcCDI1 (Franco-Orozco et al., 2017). RcCDI1 was also shown to be recognized by tomato (Franco-Orozco et al., 2017), therefore it is likely that the *F. fulva* orthologue is also recognized as a PAMP by its tomato host. The expression profile of the *F. fulva* DsCE3 and RcCDI1 orthologue could be consistent with that of a PAMP, as this gene is lowly expressed during the biotrophic stage (**Table 2.2**), when recognition by the host could contribute to host resistance. Low expression at the biotrophic stage is also expected for *DsCE3* if this gene functions as a PAMP, but *DsCE3* is highly expressed across all *in planta* stages (**Table 2.1**). It is possible that DsCE3 is not recognized by *P. radiata* as a PAMP, or that DsCE3 recognition is masked by another effector during the biotrophic stage. In summary, *DsCE3* is a highly expressed gene in the late stage of infection by *D. septosporum*, the orthologue in *F. fulva* is not well expressed, but both are orthologous to well-characterised PAMPs in other fungal pathogens.

3.3.2.2 DsCE15

Like DsCE3, DsCE15 was first identified by Hunziker (2018) as a candidate effector with no characterised homologues or Pfam domains. Protein structure analysis of DsCE15 did not produce any hits to structures of characterised proteins, suggesting that DsCE15 may contain a novel structural fold (Hunziker, 2018). Expression of *DsCE15* is highly induced at the mid and late stages *in planta*, where the increase from *in vitro* to mid is the highest of all candidates at 256-fold (**Table 3.1**). Functional analysis showed that DsCE15 triggered strong and consistent cell death in at least 90% of infiltration zones in *N. tabacum*. However, in *N. benthamiana* leaves,

cell death was weak, restricted to the perimeter of the infiltration zone, and occurred in less than 50% of infiltrations (Hunziker et al., 2021). The *F. fulva* orthologue of DsCE15 is an uncharacterised protein with 83% amino acid identity (**Table 3.2**). The *F. fulva* gene encoding the DsCE15 orthologue is highly expressed *in vitro*, not expressed at 4 dpi *in planta* and peaks in expression at 12 dpi (**Table 3.2**).

Subsequent bioinformatic analysis revealed that *DsCE3* was similar to many hypothetical proteins with a total of 380 BlastP hits across Ascomycete and Basidiomycete fungal species (Hunziker et al., 2021). DsCE15 and its orthologue in *F. fulva* were both identified as orthologues of the cross-kingdom PAMP VmE02 of *Valsa mali*, the necrotrophic causal agent of apple *Valsa* canker (Hunziker et al., 2021; Nie et al., 2019). *VmE02* is upregulated at an early stage of infection (6 hours post-inoculation) on apple twigs (Nie et al., 2019). DsCE15 has 60% amino acid identity and ten conserved cysteine residues with VmE02 **(Table 2.1)** (Hunziker et al., 2021). Like DsCE15, VmE02 is well conserved across fungal species, and homologues of VmE02 are also found in some oomycetes. VmE02 and some homologues can trigger cell death in *N. benthamiana* (Nie et al., 2019). VmE02-triggered cell death is mediated by the receptor-like protein RE02 in complex with SOBIR1 and BAK1. RE02 is a target for future disease resistance strategies, as overexpression of *RE02* increases resistance in *N. benthamiana* to the phytopathogens *Phytophthora capsici* and *Sclerotinia sclerotiorum* (Nie et al., 2021). Interestingly, VmE02 was not suggested to be a virulence factor as deletion mutants were not affected in virulence. However, conidiation of these mutants was significantly reduced, suggesting that VmE02 acts as a positive regulator of conidiation (Nie et al., 2019).

Both *D. septosporum* and *F. fulva* have biotrophic stages of growth, where activation of host immunity would be detrimental to virulence. Interestingly, expression of *DsCE15* and the *F. fulva DsCE15* orthologue are low during these biotrophic periods of growth, which is consistent with what is expected from a PAMP, such as VmE02. However, the significant induction of *DsCE15* expression during the mid stage of pine infection, which coincides with early lesion development, is consistent with a possible function of DsCE15 during the necrotrophic stage. It has been shown that necrotrophic phytopathogens can manipulate the host immune response to their own advantage, and use host-triggered cell death to facilitate feeding and infection (Friesen & Faris, 2021; Wolpert & Lorang, 2016). Therefore, it is possible that DsCE15 could function as a PAMP during the mid stage to activate host-triggered cell death and facilitate lesion development, perhaps even facilitating the necrotrophic switch. In summary, *DsCE15* is a cell death elicitor highly expressed during the mid and late stages of infection of pine, with a possible role as a PAMP facilitating necrotrophic growth.

3.3.2.3 DsCPL1

DsCPL1 was also selected as a candidate effector from the prediction pipeline developed by Hunziker (2018). *DsCPL1* is suggested to encode a cerato-platanin protein (**Table 3.1**). *DsCPL1* is highly expressed *in vitro* and a decrease in gene expression of 3.6-fold is found in the early stage *in planta*. Expression increases at mid stage (7.2-fold increase from early stage), and also at late stage (2.6-fold increase from mid stage and 5.1-fold increase from *in vitro*, **Table 2.1**). Functional analysis showed that DsCPL1 does not elicit cell death in *N. benthamiana* or *N. tabacum* (Hunziker, 2018). The *F. fulva* orthologue of DsCPL1 was identified as FfEcp45, with 91% amino acid identity (87% query coverage) compared to DsCPL1. *FfEcp45* is upregulated *in planta* across all time points but expression peaks at 8 dpi where it is 30.5-fold higher than *in vitro* (**Table 3.2**).

DsCPL1 is the only gene in the *D. septosporum* genome (de Wit et al., 2012) that encodes a protein with the cerato-platanin Pfam domain (El-Gebali et al., 2018). Many cerato-platanins are thought to play a role in the interaction between fungus and plant host because they are both secreted and localized in the fungal cell wall (Pazzagli et al., 2014). Cerato-platanins have been found to act as elicitors or virulence factors (Pazzagli et al., 2014), with a cerato-platanin protein from *Fusarium oxysporum* (FocCP1) shown to be essential for virulence (S. Li et al., 2019).

DsCPL1 and Ecp45 of *F. fulva* are orthologues of HaCPL2 from the conifer pathogen *Heterobasidion annosum sensu stricto* (**Table 3.1**, **Table 3.2)** (Hunziker, 2018). DsCPL1 has 56% amino acid identity (82% query coverage) with HaCPL2 (**Table 3.1**). Recombinant expression of HaCPL2 in *Pichia pastoris*, followed by infiltration of the protein into both the host *Pinus sylvestris* (Scots pine) and the non-host *N. tabacum* was found to trigger a cell death response (Chen et al., 2015). *A. tumefaciens*-mediated transient transformation of HaCPL2 in *N. benthamiana* did not trigger cell death, but infiltration of the apoplastic washing fluid, containing HaCPL2, into susceptible genotypes of *P. radiata* induced a cell death response (Hunziker, 2018). It was hypothesised that HaCPL2 triggers cell death through recognition of a shared pattern recognition receptor (PRR) in *P. sylvestris* and *P. radiata* (Hunziker, 2018). As an orthologue of HaCPL2, it is possible that DsCPL1 is also recognised by the *P. radiata* host. Expression of *DsCPL1* is low in the early biotrophic stage compared to other stages, however whether this level of expression is low enough to avoid detection by the host is uncertain. It is possible that in *P. radiata*, recognition of DsCPL1 could be masked by another effector, as has been shown for AvrLm3 and AvrLm4-7 in *Leptosphaeria maculans* (Plissonneau et al., 2016). Expression of *DsCPL1* is upregulated from the mid stage onward (**Table 3.1**) when *D. septosporum* is growing necrotrophically. It is also possible that DsCPL1 could trigger cell death

to promote necrotrophy or even trigger the switch to necrotrophic growth. In summary, *DsCPL1* is a cerato-platanin gene that is highly expressed in the mid and late stages of infection that might trigger cell death in the *P. radiata* host, as suggested for the orthologue HaCPL2 of *H. annosum*, to facilitate necrotrophy.

3.3.2.4 DsEcp57-1

DsEcp57-1 was also first identified by Hunziker (2018) as a candidate effector. *DsEcp57-1* is highly expressed across all stages, with an expression peak at the early stage (3.4-fold increase from *in vitro*) and expression decreasing by the late stage (2.6-fold decrease from early stage, **Table 3.1**). Functional analysis found that DsEcp57-1 does not elicit cell death in *N. benthamiana* or *N. tabacum* (Hunziker, 2018). The *F. fulva* protein Ecp57-1, with 76% amino acid identity to DsEcp57-1, was identified as the orthologue of DsEcp57-1 (Hunziker, 2018). The gene encoding this *F. fulva* protein is highly expressed across all stages *in vitro* and *in planta*, with a small decrease at 8 dpi (**Table 3.2**). DsEcp57-1 contains a CAP domain (**Table 3.1**) and has predicted structural homology to many other CAP proteins, including 'Pathogen-related in yeast (Pry)-1' of *Saccharomyces cerevisiae* (Darwiche, Mene-Saffrane, Gfeller, Asojo, & Schneiter, 2017; Hunziker, 2018). Pry-1 is suggested to bind sterols as a defence strategy against other competing microbes (Gamir et al., 2017) and is a possible role DsEcp57-1 could play in *D. septosporum* against the various competing *Phytophthora* species and foliar pathogens or endophytes of pine (Brar et al., 2018; Scott & Williams, 2014).

DsEcp57-1 and Ecp57-1 of *F. fulva* are orthologues of candidate effector ViCE14 of *Venturia inaequalis*, the causal agent of apple scab disease (**Table 3.1**, **Table 3.2**) (Prokchorchik, 2017). DsEcp57-1 has 63% amino acid identity (59% query coverage) with ViCE14 (**Table 3.1**). ViCE14 was shown to suppress cell death responses in *N. benthamiana* leaves triggered by effector HopAS1 of *Pseudomonas syringae* (Prokchorchik, 2017). As *DsEcp57-1* is highly upregulated in the early stage *in planta*, when *D. septosporum* is in the biotrophic stage, cell death suppression to avoid triggering the host defence response could be a possible role for DsEcp57-1. *FfEcp57-1* of *F. fulva* may share this function as this gene is also highly expressed during the biotrophic stages of infection (**Table 3.2**). As well as high expression during the biotrophic stage, *FfEcp57-1* is also highly expressed *in vitro*, and in combination with the predicted CAP domain, this suggests the protein encoded by this gene may also have a sterol-binding function like DsEcp57-1 (**Table 3.2**) (Hunziker, 2018). In summary, *DsEcp57-1* is a gene highly expressed during the biotrophic stage of infection that may function as a cell death suppressor like *ViCE14* of *V. inaequalis*.

3.3.2.5 DsGH11

DsGH11 was the only shortlisted effector not selected from the pipeline developed by Hunziker (2018). Therefore, functional analysis to determine if DsGH11 triggers cell death in *Nicotiana* species has not been performed. DsGH11 was identified as a candidate virulence factor due to homology to SNOR_15270, a putative necrotrophic effector of *P. nodorum* regulated by PnPf2 (Jones et al., 2019). DsGH11 has 58% amino acid identity with SNOR_15270 (**Table 3.1**). *DsGH11* is highly expressed with significant upregulation at all *in planta* stages, with the largest increase being at the mid stage (111-fold increase from *in vitro*, **Table 3.1**). The top BlastP hit to DsGH11 from *F. fulva* was an endo-1,4-beta-xylanase B protein with 55% amino acid identity and 90% query coverage. The gene encoding this *F. fulva* protein is not expressed at any stage *in vitro* or *in planta* (**Table 3.2**).

DsGH11 is a glycosyl hydrolase of family 11 (GH11) (**Table 3.1**). GHs are the largest class of carbohydrate-active enzymes (CAZymes), and are involved in the biosynthesis, modification, or breakdown of glycosidic bonds found in glycoconjugates and carbohydrates. CAZymes are important for fungal phytopathogens, especially necrotrophs and hemibiotrophs, as shown by the greater numbers of CAZyme-encoding genes generally found in these pathogens compared to biotrophs (Bradley et al., 2022). GH proteins specifically hydrolyse and/or rearrange the glycosidic bonds in glycoconjugates, oligo- and polysaccharides. Many GHs are suggested to act as microbe-associated molecular patterns (MAMPs) as they can trigger cell death in the host, independent of their enzymatic activity (Bradley et al., 2022). One example is GH11 protein Xyn11A from *Botrytis cinerea* (Brito et al., 2006). Xyn11A induces cell death as well as other immune responses in host plants, including tomato, and gene deletion mutants have reduced virulence (Brito et al., 2006). Enzymatic activity is not required for Xyn11A-induced cell death responses, or virulence, as it has been shown that mutants complemented with a gene encoding an enzymatically inactive Xyn11A protein restore full virulence, suggesting Xyn11A contributes to virulence by inducing necrosis (Noda, Brito, & González, 2010).

SNOR_15270 and DsGH11 have similarity to Xyn11A (Jones et al., 2019) (**Table 3.1**), and the endo-1,4-beta-xylanase B protein from *F. fulva* is an orthologue (**Table 3.2**). Because tomato is one of the hosts of *B. cinerea* for grey mould disease (Brito et al., 2006), it seems likely that the *F. fulva* ortholog of Xyn11A would also trigger cell death in tomato. Therefore, expression of the gene encoding this protein might be significantly down-regulated during biotrophy to prevent activation of the host immune response. As a hemibiotroph, expression of DsGH11 in *D. septosporum* is expected to be low in the biotrophic stage, but high once cell death occurs in the

necrotrophic stage. However, *DsGH11* is highly expressed at all stages *in planta* (**Table 3.1**), suggesting that either DsGH11 is not recognised by the host to activate an immune response, or that other effectors function during the biotrophic stage to suppress cell death. In summary, DsGH11 has homology to known cell death-eliciting effector proteins, is highly expressed throughout infection and could potentially function in the necrotrophic switch.

3.3.3 Analysis of candidate transcription factors

Among the transcription factor candidates listed in **Table 3.1**, DsPf2, Ds41021, and Ds68895 were identified as potential homologues to characterised virulence factors from the literature, while Ds74812 and Ds69328 were previously described as potential necrotrophic switch factors from the transcriptional analysis of *D. septosporum* infection of *P. radiata* (Bradshaw et al., 2016). In this section, the candidate transcription factors in **Table 3.1** were analysed in the same way as the candidate effectors in **section 3.3.2**, with the addition of phylogenetic analysis of the top BlastP hits and comparison with fungal lifestyle. This analysis was performed to investigate whether these proteins could play a role in virulence, specifically in the necrotrophic switch.

3.3.3.1 DsPf2

DsPf2 was identified as a candidate virulence factor because of its orthology to PnPf2 of *P. nodorum*, sharing 54% amino acid identity (79% query coverage) (**Table 3.1**). DsPf2 is a Zn_2Cys_6 fungal transcription factor, as suggested by the presence of two Pfam domains of this type (**Table 3.1**). Gene expression of *DsPf2* is relatively consistent across all stages, with only a small increase from early to mid stage of 2.4-fold (**Table 3.1**). The *F. fulva* orthologue of DsPf2 and PnPf2 is the putative sucrose utilization protein SUC1, with 89% amino acid identity to DsPf2 and the same two domains as DsPf2, suggesting it is also a Zn_2Cys_6 fungal transcription factor. The *F. fulva* gene that encodes this protein is highly expressed *in vitro* but is barely expressed at any stage *in planta* (**Table 3.2**).

Analysis of the top 30 BlastP hits to DsPf2 from Dothideomycete species (**Appendix 10**) shows that DsPf2 is well conserved among Dothideomycetes. When compared to DsPf2, the top 30 hits all had amino acid identities higher than 68%, query coverage of greater than 78%, and an E value of 0 (**Appendix 10**). Phylogenetic analysis of these proteins (**Figure 3.3**) appears to show clustering due to phylogenetic relationships between species, rather than shared fungal lifestyle. About half of the proteins are from fungal species that are saprotrophic or non-pathogenic. DsPf2 clusters with a group of proteins from pathogenic fungi, the exception being the protein from saprophyte *Zasmidium cellare*. To compare the amino acid sequences from fungi with

different lifestyles, an alignment was performed between DsPf2, PnPf2 and the proteins from *Z. cellare* and *F. fulva* which clustered closest to DsPf2 (**Figure 3.4**). As expected from the phylogeny, the alignment showed that PnPf2 is the most different out of the four protein sequences, in sequence length and position of the fungal transcription factor domain. The fungal Zn_2Cys_6 binuclear cluster domain region is well conserved between the four sequences, with only four variable amino acids (marked with red asterisks, **Figure 3.4**). The amino acid at position 69 is variable between all four sequences; amino acids at positions 58 and 64 are different in the PnPf2 sequence only, and the amino acid at position 77 is different in the *Z. cellare* sequence only. The variable amino acids in the PnPf2 sequence reflect the fact that this protein is the most phylogenetically distant among those in the alignment.

The first Pf2 transcription factor identified was in *Alternaria brassiciola*, the causal agent of dark leaf spot of *Brassica* species (Cho, Ohm, Grigoriev, & Srivastava, 2013). Gene knock-out mutants were not affected in vegetative growth, when compared to the WT fungus, but unable to cause disease symptoms on the host. Expression of *AbPf2* was highly induced during the early stages of infection but decreased dramatically once colonization of the host tissues occurred. A total of 106 genes were found to be induced by AbPf2, eight of which encode putative effector proteins (Cho et al., 2013). The Pf2 orthologue in *P. nodorum*, causal agent of Septoria nodorum blotch of wheat, was subsequently investigated in a similar way (Jones et al., 2019; Rybak et al., 2017). Deletion of *PnPf2* caused necrotrophic effector genes *SnToxA* and *SnTox3* to be down-regulated and resulted in strongly reduced virulence on wheat cultivars with the corresponding receptors *Tsn1* and *Snn3*, respectively (Rybak et al., 2017). Similar results were found from deletion of the *Pf2* orthologue in *Pyrenophora tritici-repentis*, causal agent of tan spot of wheat (Rybak et al., 2017). Transcriptional analysis of the *P. nodorum PnPf2* deletion mutant compared with WT fungus showed that *PnPf2* up-regulates expression of genes associated with proteolysis and cell wall degradation, as well as 12 putative effector genes (Jones et al., 2019). These results suggest that through regulation of genes involved in breaking down the plant cell wall, and assimilating nutrients, *PnPf2* could be important for establishing the necrotrophic lifestyle of *P. nodorum* (Jones et al., 2019).

The *Pf2* genes from *A. brassiciola*, *P. nodorum* and *P. tritici-repentis* were all highly expressed during early infection and expression decreased once necrosis of the host tissue occurred (Cho et al., 2013; Rybak et al., 2017), while the *Pf2* gene from *D. septosporum* is not highly expressed at any stages *in vitro* or *in planta* (**Table 3.1**). However, during transcriptional analysis of *D. septosporum* (Bradshaw et al., 2016), *DsPf2* was mis-annotated, and a truncated version (~50% of full sequence) was analysed. Therefore, it is possible that the gene expression of *DsPf2*

recorded by Bradshaw et al. (2016) is not accurate. In summary, DsPf2 is a putative Zn_2Cys_6 transcription factor that may regulate the necrotrophic lifestyle in *D. septosporum* due to homology with PnPf2 of *P. nodorum*, although the available transcriptomic data suggest it has only low expression *in planta*.

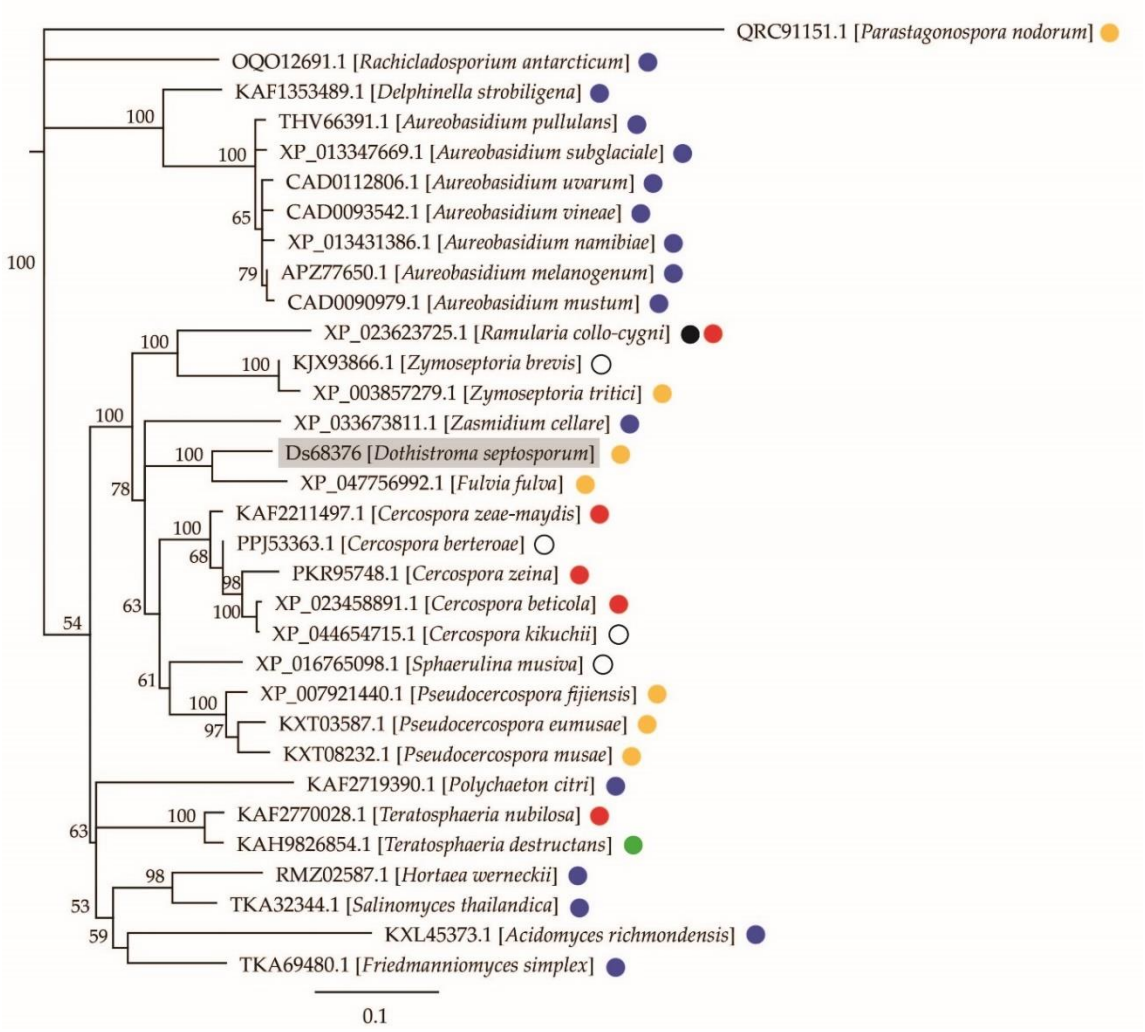

Figure 3.3. Phylogenetic tree of protein sequences of the top 30 BlastP hits from Dothideomycetes species (taxid: 147541) to *Dothistroma septosporum* DsPf2 (Ds68376), as well as homologue PnPf2 from *Parastagonospora nodorum* used to identify DsPf2. The lifestyles of the Dothideomycete fungi were determined from literature and illustrated by a coloured dot; blue, saprophytic or non-pathogenic; red, necrotrophic; green, biotrophic; yellow, hemibiotrophic; black, endophytic; white, pathogenic but lifestyle undetermined. One species has two dots, *Ramularia collo-cygni*, because in the literature this fungus has been shown to change from endophytic growth to necrotrophic. The tree was made using the Neighbour-Joining method and the Jukes-Cantor genetic distance model, with 100 bootstrap replicates. Consensus support is illustrated at each node as a percentage. The homologue of DsPf2, PnPf2, from *P. nodorum* was used as an outgroup.

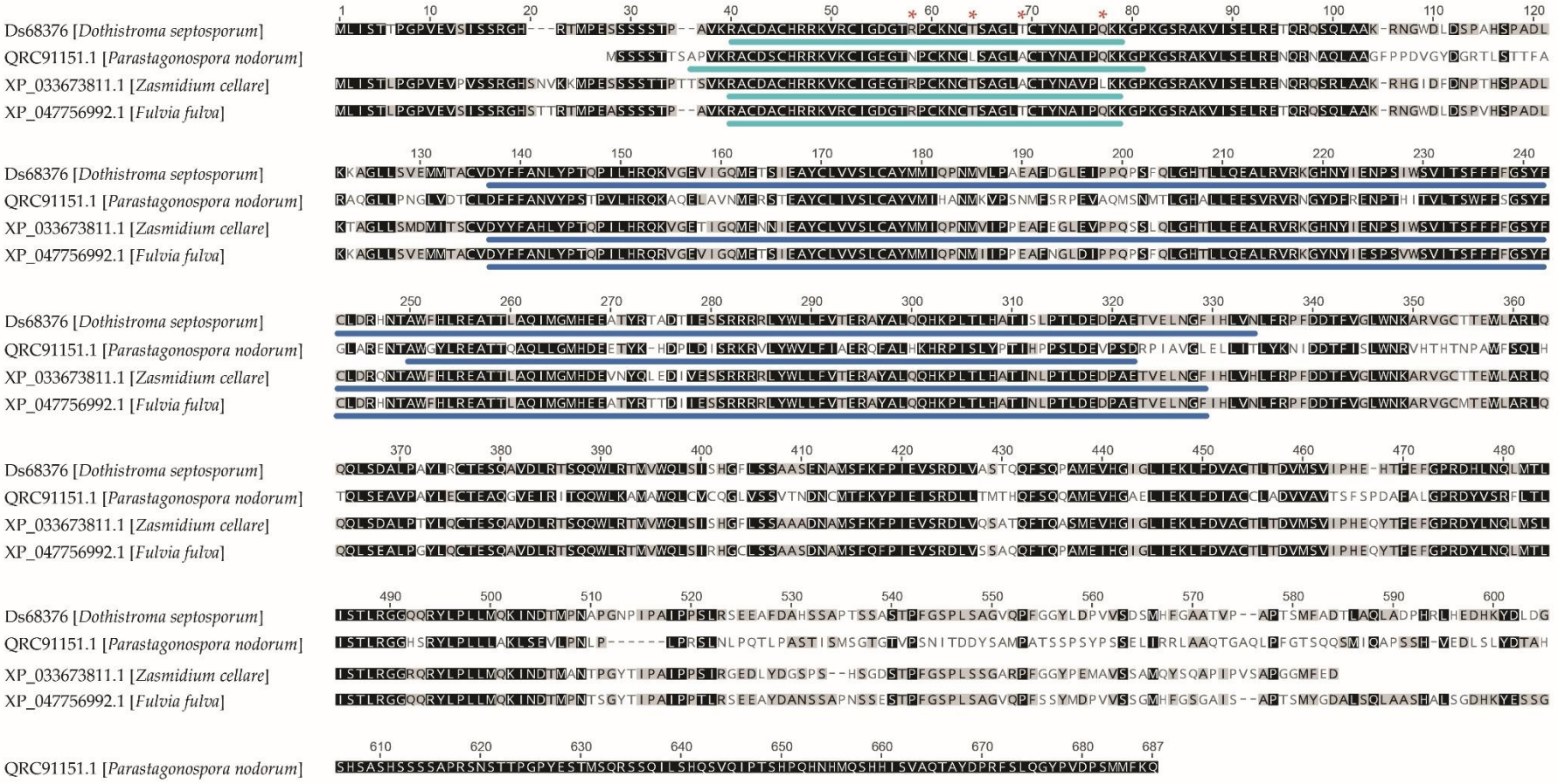
Ds68376 [Dothistroma septosporum]
QRC91151.1 [Parastagonospora nodorum]
XP_033673811.1 [Zasmidium cellare]
XP_047756992.1 [Fulvia fulva]

Figure 3.4. Amino acid alignment of DsPf2 and the BlastP hit sequences from *Parastagonospora nodorum* (PnPf2), *Zasmidium cellare*, and *Fulvia fulva*. Two domains predicted by InterPro (https://www.ebi.ac.uk/interpro/) are illustrated by a coloured line underneath the amino acid sequences; turquoise, Fungal Zn_2-Cys_6 binuclear cluster domain (PF00172); and dark blue, Transcription factor domain, fungi (IPR007219). Polymorphic amino acids of interest within the zinc cluster domain are marked with a red asterisk. Alignment was made using Geneious software (v9.1.8.) as a global alignment with free end gaps, using a Blosum62 cost matrix.

3.3.3.2 Ds74812

Ds74812 does not have any known Pfam domains (**Table 3.1**) but is predicted to encode a bZIP transcription factor protein (Bradshaw et al., 2016). Gene expression of *Ds74812* is high *in vitro* and decreases by 14.6-fold at the early stage. Expression increases dramatically from the early stage to be 22.4-fold higher in the mid stage and remains relatively high during the late stage (**Table 3.1**). This high induction of expression at the mid stage was not observed for any other *D. septosporum* bZIP transcription factor predicted from the genome, where the next highest difference from early to mid stage was 3.1-fold (**Appendix 11**). *Ds74812* was identified as a candidate virulence factor from the *D. septosporum* transcriptome study, where high expression at the mid stage suggested this gene could play a role in the necrotrophic switch (Bradshaw et al., 2016). Ds74812 does not have homology to any characterised proteins, and the top BlastP hit is to a hypothetical protein from *Pyrenophora teres f. teres* with 44% amino acid identity (**Table 3.1**). BlastP analysis of Ds74812 against the *F. fulva* proteome did not produce any hits (**Table 3.2**), suggesting that *F. fulva* lost or pseudogenized the gene encoding this protein, or Ds74812 evolved in *D. septosporum* after the two fungi split from their common ancestor. Therefore, it is possible that Ds74812 functions in a role specific to *D. septosporum*, such as eliciting cell death to enable lesion expansion and sporulation.

Analysis of the top 30 BlastP hits to Ds74812 (**Appendix 12**) showed that Ds74812 is not well conserved among Dothideomycete species. The top hits had less than 50% amino acid identity and, after the seventh top hit, query coverage dropped to less than 50% (**Appendix 12**). Phylogenetic analysis of the top 30 BlastP hits to Ds74812 from Dothideomycete species (**Figure 3.5**) showed that Ds74812 groups in a clade with proteins from pathogenic fungi. Proteins from fungi with different pathogenic lifestyles are spread throughout the tree, although the proportion of proteins from saprophytic or non-pathogenic species is low compared with the phylogenetic tree of DsPf2. The proteins which clustered closest with Ds74812 are from

Pseudocercospora eumusae and *Psedocercospora musae*, both of which are hemibiotrophic pathogens.

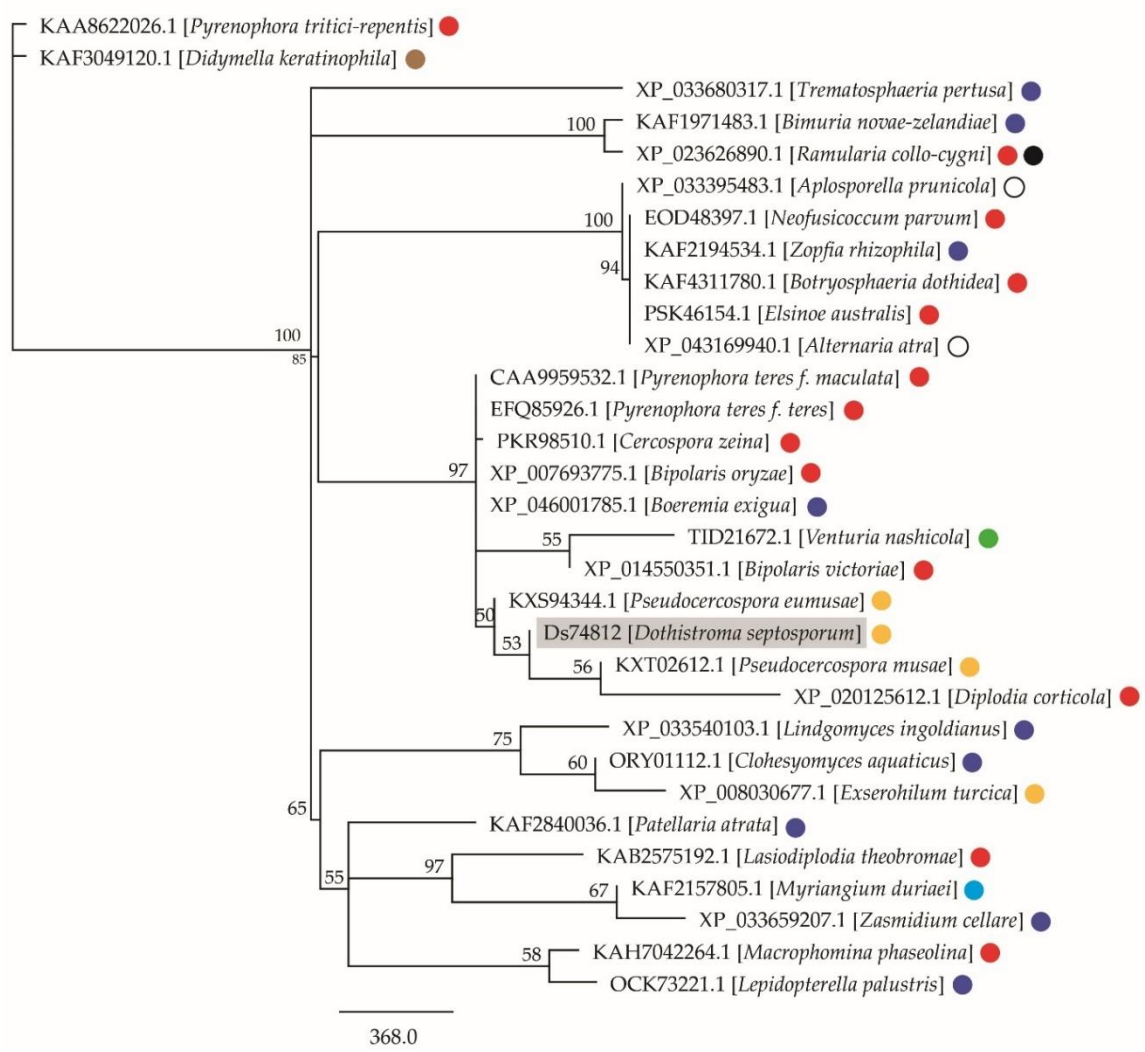

Figure 3.5. Phylogenetic tree of protein sequences of the top 30 BlastP hits from Dothideomycetes species (taxid: 147541) to *Dothistroma septosporum* protein Ds74812 (highlighted in grey). The lifestyle of the Dothideomycete fungi was determined from literature and illustrated by a coloured dot; dark blue, saprophytic or non-pathogenic; red, necrotrophic; green, biotrophic; yellow, hemibiotrophic; black, endophytic; white, pathogenic but lifestyle undetermined; brown, human pathogen; light blue, insect pathogen. One species has two dots, *Ramularia collo-cygni*, because in the literature this fungus has been shown to change from endophytic growth to necrotrophic. Phylogenetic tree was made using the Neighbour-Joining method and the Jukes-Cantor genetic distance model, with 100 bootstrap replicates. Consensus support is illustrated at each node as a percentage.

bZIPs are one of the major transcription factor families in fungi and are also found in abundance across other eukaryotes. These transcription factors regulate a wide range of cellular processes, partly due to their ability to form dimers with other bZIPs (John et al., 2021). Several bZIP transcription factors have been shown to be important for fungal virulence. The bZIP transcription factor *FpAda1* of *Fusarium pseudograminearum*, causal agent of *Fusarium* crown rot in wheat and barley, was shown to be important for virulence in a gene deletion study. Deletion of *FpAda1* led to defects in vegetative growth of the pathogen, while pathogenicity assays of the mutants showed successful penetration and proliferation in the host, but a reduction in virulence compared to the WT fungus (Chen et al., 2019). Similarly, the bZIP transcription factor *VdHapX* of *Verticillium dahliae*, which causes vascular wilt in over 200 plant species, was shown to be a key regulator of iron homeostasis, and was required for full virulence in smoke tree seedlings (Wang et al., 2018). These studies show that bZIP transcription factors can play important roles in virulence, as well as other cellular processes. In summary, Ds74812 is a predicted basic-leucine zipper transcription factor with a possible role in the necrotrophic switch due to induced gene expression at the mid stage, and absence of a homologous protein in *F. fulva*.

3.3.3.3 Ds69328

Ds69328 is suggested to encode a Zn_2Cys_6 fungal transcription factor based on the presence of two Pfam domains (**Table 3.1**). Expression of *Ds69328* is low *in vitro* and during the early stage. Similar to *Ds74812*, expression of *Ds69328* increases from early to mid stage by 21.8-fold, and at the mid stage gene expression is 14 times higher than *in vitro*. Gene expression then decreases at the late stage (**Table 3.1**). Like *Ds74812*, *Ds69328* was identified as a candidate virulence factor from the *D. septosporum* transcriptomic study, where induced expression at the mid stage suggested this gene could play a role in the necrotrophic switch (Bradshaw et al., 2016). Ds69328 does not have homology to any characterised proteins, and the *F. fulva* orthologue is an uncharacterised protein with 84% amino acid identity and 71% query coverage to Ds69328 (**Table 3.1**). Expression of the gene encoding this *F. fulva* protein is low *in vitro*, zero at 4 and 8 dpi, and low at 12 dpi (**Table 3.2**).

Analysis of the top 30 BlastP hits to Ds69328 from Dothideomycete species (**Appendix 13**) showed that Ds69328 is not well conserved outside of the top hit from *F. fulva*. The second hit had less than 50% amino acid identity and by the 30th hit amino acid identity was only 23%. Query coverage remained consistently around 70% for all hits (**Appendix 13**). Phylogenetic analysis of the top 30 BlastP hits to Ds69328 in Dothideomycete species (**Figure 3.6**) suggested

that clustering was due to phylogenetic relationships between the fungi rather than shared lifestyle. Ds69328 clustered with proteins from the two close relatives of *D. septosporum*: *F. fulva* and *Z. cellare*.

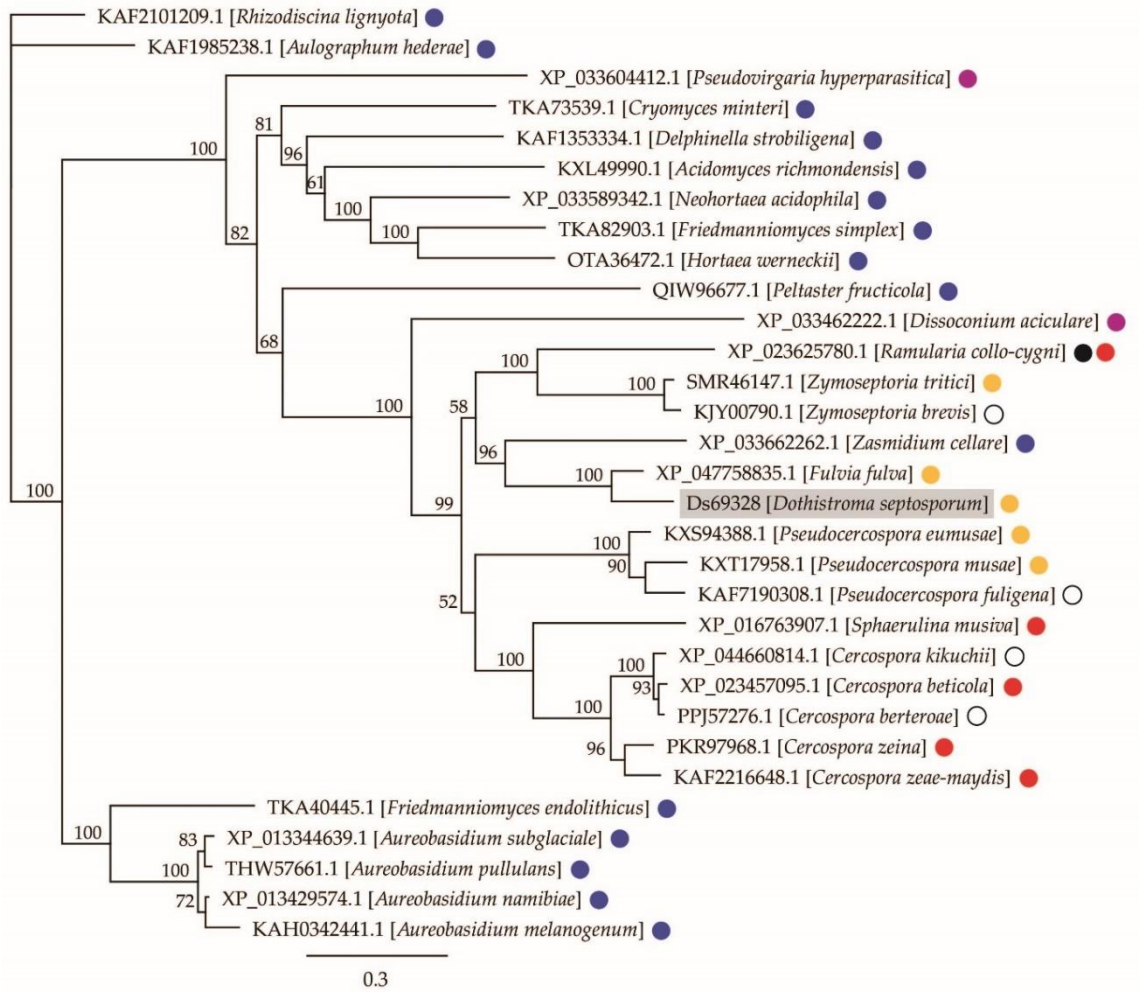

Figure 3.6. Phylogenetic tree of protein sequences of the top BlastP hits from Dothideomycetes species (taxid: 147541) to Dothistroma septosporum protein Ds69328 (highlighted in grey). The lifestyle of the Dothideomycete fungi was determined from literature and illustrated by a coloured dot; dark blue, saprophytic or non-pathogenic; red, necrotrophic; green, biotrophic; yellow, hemibiotrophic; black, endophytic; white, pathogenic but lifestyle undetermined.; purple, fungal parasite. One species has two dots, *Ramularia collo-cygni*, because in the literature this fungus has been shown to change from endophytic growth to necrotrophic. Phylogenetic tree was made using the Neighbour-Joining method and the Jukes-Cantor genetic distance model, with 100 bootstrap replicates. Consensus support is illustrated at each node as a percentage.

Ds69328 is a Zn_2Cys_6 transcription factor and this family is part of the largest transcription factor class in fungi, the zinc-coordinated "zinc fingers" (John et al., 2021). As well as PnPf2 (Cho et al., 2013) and Pf2 homologues, other Zn_2Cys_6 transcription factors have been found to play a role in virulence (John et al., 2021). One such example is *Ftf1* from the *Fusarium oxysporum* species complex, which was first identified as a 'sequence characterised amplified region' (SCAR) marker used for detection of highly virulent *F. oxysporum* f.sp. *phaseoli* strains (Alves-Santos, Ramos, García-Sánchez, Eslava, & Díaz-Mínguez, 2002). *Ftf1* was later found to be a multicopy gene (Ramos et al., 2007) thought to have evolved from the ancestral gene *Ftf2* by gene duplication (Niño-Sánchez et al., 2016). RNA-mediated gene silencing of the *Ftf1* gene copies showed a reduction in virulence and reduced expression of Secreted In Xylem (SIX) effector genes *SIX1* and *SIX6* (Niño-Sánchez et al., 2016). Another Zn_2Cys_6 transcription factor, *CoMTF4*, is from *Colletotrichum orbiculare*, the causal agent of cucumber anthracnose. This transcription factor was identified from a whole-genome transcript profile search for regulators of plant signal sensing and transduction. Gene deletion studies showed that *CoMTF4* plays an important role in regulating appressorium development after the delivery of plant-derived signals (Kodama, Nishiuchi, & Kubo, 2019). Other Zn_2Cys_6 transcription factors have been found to play roles in developmental processes such as sporulation, and hyphal development and branching (John et al., 2021). In summary, *Ds69328* is a putative Zn_2Cys_6 transcription factor that is not well conserved but has a possible role in the necrotrophic switch due to highly induced expression specifically at the mid stage.

3.3.3.4 Ds41021

Ds41021 is suggested to encode a GATA zinc finger transcription factor, based on Pfam domain analysis (**Table 3.1**). Ds41021 was first identified because of homology with protein CLNR1 of *C. lindemuthianum*, that was suggested to play a role in the necrotrophic switch (Pellier et al., 2003). Ds41021 has 42% amino acid identity and 76% query coverage to CLNR1 (**Table 3.1**). Gene expression of *Ds41021* is high *in vitro* and in the early stage *in planta* but decreases at the mid stage by 3.1-fold. A small increase of 2-fold then occurs from mid to late stage (**Table 3.1**). The *F. fulva* orthologue of Ds41021 is a predicted nitrogen regulatory protein AreA with 89% amino acid identity and 99% query coverage to Ds41021. The gene encoding this *F. fulva* protein is expressed most highly *in vitro*, with no expression at 4 dpi, but increases slightly by 12 dpi (**Table 3.2**).

Analysis of the top 30 BlastP hits to Ds41021 (**Appendix 14**) showed that Ds41021 is somewhat conserved among Dothideomycete species. After the top hit to AreA of *F. fulva*, the other hits

had amino acid identities of 70%–50%. All top 30 hits had query coverage above 80% and an E value of 0 (**Appendix 14**). Phylogenetic analysis of the top 30 BlastP hits to Ds41021 in Dothideomycete species (**Figure 3.7**) showed that the proteins appear to cluster according to phylogenetic relationship rather than fungal lifestyle. The proteins that cluster closest to Ds41021 are from *F. fulva* and then *Z. cellare*. CLNR1 from *C. lindemuthianum* is the most phylogenetically distinct protein to Ds41021 among those analysed. Proteins from non-pathogenic fungal species make up about one third of the total proteins (**Figure 3.7**).

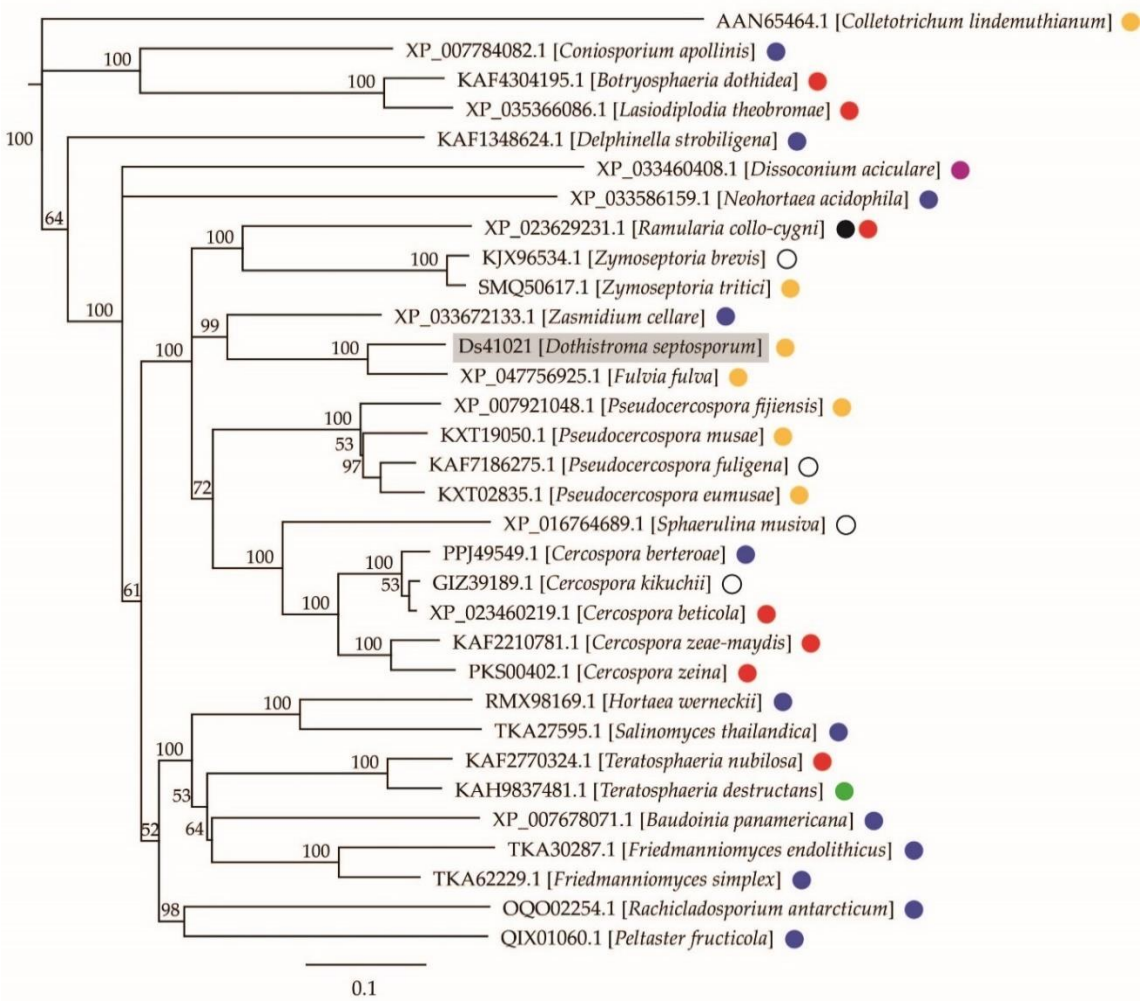

Figure 3.7. Phylogenetic tree of protein sequences of the top 30 BlastP hits from Dothideomycetes species (taxid: 147541) to *Dothistroma septosporum* protein Ds41021 (highlighted in grey) and homologue CLNR1 from *Colletotrichum lindemuthianum* (used as an outgroup). The lifestyles of the Dothideomycete fungi were determined from literature and illustrated by a coloured dot; dark blue, saprophytic or non-pathogenic; red, necrotrophic; green, biotrophic; yellow, hemibiotrophic; black, endophytic; white, pathogenic but lifestyle undetermined.; purple, fungal parasite. One species has two dots, *Ramularia collo-cygni*, because in the literature this fungus has been shown to change from endophytic growth to

necrotrophic. Phylogenetic tree was made using the Neighbor-Joining method and the Jukes-Cantor genetic distance model, with 100 bootstrap replicates. Consensus support is illustrated at each node as a percentage.

Ds41021 and the *F. fulva* AreA protein are orthologs of CLNR1 from *C. lindemuthianum* (**Table 3.1**, **Table 3.2**), an AreA orthologue and major nitrogen regulatory protein (Pellier 2003). *AreA* is a transcription factor shown to regulate nitrogen assimilation in filamentous fungi, and deletion of orthologs in a wide range of fungi disrupts virulence and fungal growth (John et al., 2021). Gene deletion mutants of *CLNR1* were blocked at the transition to necrotrophic growth and were non-pathogenic, suggesting a role for this transcription factor in regulating the necrotrophic switch. It was hypothesised that nitrogen starvation could be a cue for the transition to necrotrophic growth, or *CLNR1* could regulate secondary hyphae developmental genes (Pellier et al., 2003). Expression of *CLNR1* was not investigated by Pellier et al. (2003), but it seems unlikely that *Ds41021* would play a role in the necrotrophic switch if expression is decreased in the mid stage. However, it is possible that Ds41021 regulates genes and "sets up" for the transition to necrotrophy during the biotrophic stage. In summary, Ds41021 is a predicted GATA zinc finger transcription factor that could potentially be important for necrotrophic growth due to its homology with CLNR1 of *C. lindemuthianum*, a protein known to be required for the transition to necrotrophy.

3.3.3.5 Ds68895

Ds68895 is suggested to encode a Zn_2Cys_6 fungal transcription factor based on the presence of two Pfam domains (**Table 3.1**). Ds68895 was first identified because of homology with CLTA1, another protein of *C. lindemuthianum* also suggested to play a role in the necrotrophic switch (Dufresne et al., 2000). Ds68895 has 40% amino acid identity (77% query coverage) to CLTA1 (**Table 3.1**). Expression of *Ds68895* is moderate from *in vitro* to mid stage *in planta*, with a small expression peak at the late stage of 3.4-fold, making a 2.4-fold difference with *in vitro* (**Table 3.1**). The *F. fulva* orthologue of Ds69885 is predicted to be a positive regulator of purine utilization with 87% amino acid identity to Ds69885 (**Table 3.2**). This *F. fulva* gene is only expressed at low levels *in vitro* and very low *in planta* (**Table 3.2**).

Analysis of the top 30 BlastP hits to Ds68895 (**Appendix 15**) showed that Ds68895 is somewhat conserved among Dothideomycete species. All 30 hits had an amino acid identity of over 50%, query coverage of at least 63% and an E value of 0 (**Appendix 15**). The top 30 hits (**Appendix 15**) and *F. fulva* orthologue (**Table 3.2**) suggest Ds68895 might be a regulator of purine utilization.

Genes that degrade purine have recently been shown to be required for full virulence and prevention of nitrogen starvation (Perino, Glienke, de Oliveira Silva, & Deising, 2020). Application of a chemical inhibitor of a purine degradation gene was shown to reduce virulence of *C. lindemuthianum* and four other pathogens. This suggests that inhibiting the purine degradation pathway could be a viable disease control strategy (Perino et al., 2020).

Phylogenetic analysis of the top 30 BlastP hits to Ds68895 in Dothideomycete species (**Figure 3.8**) showed that proteins may cluster because of fungal lifestyle rather than phylogenetic relationship. Ds68895 clusters in a clade with other proteins from pathogenic fungal species, except for the protein from *Z. cellare*. However, consensus support for this clade is only 56%, and two proteins from pathogenic fungal species are found outside of the clade. Proteins from non-pathogenic fungal species make up approximately half of the total proteins. Ds68895 clusters closest with the protein from *F. fulva*, then the protein from *Z. cellare*. The *C. lindemuthianum* protein CLTA1 is most distant from Ds68895 (**Figure 3.8**).

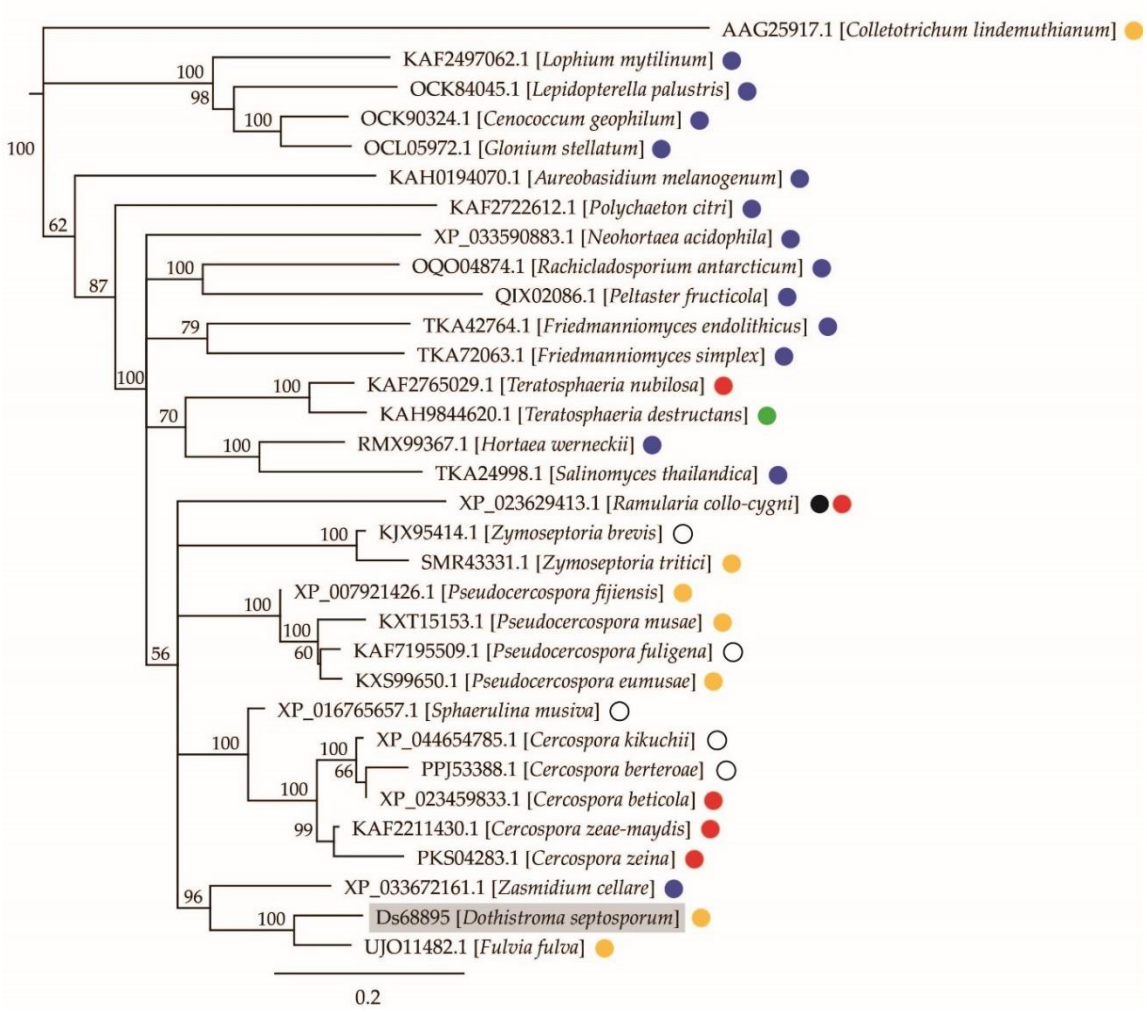

Figure 3.8. Phylogenetic tree of protein sequences of the top 30 BlastP hits from Dothideomycetes species (taxid: 147541) to Dothistroma septosporum protein Ds68895 (highlighted in grey) and homologue CLTA1 from Colletotrichum lindemuthianum (used as an outgroup). The lifestyles of the Dothideomycete fungi were determined from literature and illustrated by a coloured dot; dark blue, saprophytic or non-pathogenic; red, necrotrophic; green, biotrophic; yellow, hemibiotrophic; black, endophytic; white, pathogenic but lifestyle undetermined. One species has two dots, *Ramularia collo-cygni*, because in the literature this fungus has been shown to change from endophytic growth to necrotrophic. Phylogenetic tree was made using the Neighbour-Joining method and the Jukes-Cantor genetic distance model, with 100 bootstrap replicates. Consensus support is illustrated at each node as a percentage.

Ds68895 and the *F. fulva* predicted positive regulator of purine utilization protein, are orthologues of CLTA1 of *C. lindemuthianum* (**Table 3.1**, **Table 3.2**). CLTA1 was identified from a random insertional mutagenesis experiment, where the mutant was non-pathogenic and induced HR-like necrotic spots on the host. The mutant was blocked at the transition to necrotrophy, as hyphal growth was inhibited at 3 dpi and no secondary hyphae were

differentiated, suggesting CLTA1 regulates the necrotrophic switch (Dufresne et al., 2000). While expression analysis *in planta* was not performed, it was shown that *CLTA1* is expressed at low levels in culture and is likely not induced under nitrogen starvation (Dufresne et al., 2000). In summary, Ds68895 is a putative Zn_2Cys_6 fungal transcription factor, suggested to regulate necrotrophic growth because of homology to proteins with known roles in necrotrophy and its high gene expression in the necrotrophic stage of growth.

3.3.4 Candidate virulence factors identified for functional analysis by gene deletion and virulence assessment on the host plant *P. radiata*

The main focus of this study was to identify, then functionally characterise, candidate virulence factors by gene deletion and virulence analysis on the *P. radiata* host. Candidates were selected in this study by analysis of gene expression, homology to characterised proteins and, in the case of effectors, the ability to trigger cell death in non-host *Nicotiana* species. Both effector and transcription factor genes were identified as candidate virulence factors and selections made for gene deletion analysis. Because of space and time constraints imposed by the lengthy and complex process required for virulence assays of *D. septosporum* on *P. radiata* one candidate from each gene type was selected.

The effector selected for analysis by gene deletion was *DsCE3*. *DsCE3* is highly expressed *in planta*, particularly at the late necrotrophic stage, and the protein induces cell death in *N. benthamiana* and *N. tabacum* (**Table 3.1**). DsCE3 was also recently found, when recombinantly expressed by *Pichia pastoris* and infiltrated, to elicit some form of cell death in three different pine genotypes (Tarallo, 2022). DsCE3 is of particular interest because it is an orthologue of RcCDI1 of *R. commune*, a cell death-eliciting PAMP (**Table 3.1**) (Franco-Orozco et al., 2017). The *F. fulva* RcCDI1 and DsCE3 orthologue is also likely a PAMP. As well as being highly expressed at the late stage, *DsCE3* is also well expressed at the early biotrophic stage, suggesting the protein is produced at this stage. It is unlikely that DsCE3 is recognised as a PAMP to cause a cell death response during the biotrophic stage, because this response would likely contribute to *P. radiata* resistance. It is possible that DsCE3 could potentially be recognised as a PAMP but another effector is secreted by *D. septosporum* that suppresses or masks this recognition during the biotrophic stage. Regardless of whether DsCE3 is recognised as a PAMP by *P. radiata*, the gene that encodes this protein is highly expressed specifically *in planta* and likely contributes to virulence, possibly by triggering the necrotrophic stage. Recent work following up on the research of Hunziker (2018), suggested through AlphaFold2 predictions that DsCE3 is part of the trypsin inhibitor β-trefoil superfamily (Tarallo, 2022). This researcher hypothesised that β-trefoil

fold-containing proteins (such as DsCE3) may function in the biotrophic stage to escape host recognition, or have a toxic effect through host membrane disruption, and function in the necrotrophic stage (Tarallo, 2022). This study also identified an orthologue of DsCE3 in the pine pathogen *Cyclaneusma minus*, which elicited chlorosis or weak cell death in *N. benthamiana* and *N. tabacum* (Tarallo, 2022). Gene deletion of *DsCE3* will help elucidate what function this gene performs in *D. septosporum* and if it is required for full virulence on *P. radiata*.

The transcription factor selected for gene deletion analysis was Ds69328. *Ds69328* is a Zn_2Cys_6 transcription factor highly expressed specifically at the mid stage of *D. septosporum* infection of *P. radiata* (**Table 3.1**). The mid stage is when early necrotic lesions form and is hypothesised to be when the transition to necrotrophic growth occurs. Ds69328 is not well conserved outside of the orthologue in *F. fulva* (**Appendix 13**), in which it is not expressed at all during early infection (**Table 3.2**), suggesting a role outside of biotrophic growth. Phylogenetic analysis showed that the top 30 hits of Ds69328 clustered due to phylogenetic relationships rather than fungal lifestyle (**Figure 3.6**), suggesting that this protein may play different roles in different fungi. These results point to a possible role of Ds69328 in the necrotrophic switch in *D. septosporum*, a process that has been understudied in hemibiotrophic pathogens. Analysis of gene deletion mutants of *Ds69328* will determine whether this hypothesis is correct, and whether Ds69328 is required for virulence on *P. radiata*.

Chapter 4 - Identification of candidate virulence factors from the *Dothistroma septosporum* and *Fulvia fulva* secretomes

4.1 Introduction

The term "secretome", first coined by Tjalsma, Bolhuis, Jongbloed, Bron, and van Dijl (2000), is defined as the set of molecules secreted by a cell, tissue or organism through conventional, unconventional, or other unknown mechanisms (Agrawal, Jwa, Lebrun, Job, & Rakwal, 2010; Greenbaum, Luscombe, Jansen, Qian, & Gerstein, 2001). Proteins are the most common of all secreted molecules, and their conventional secretion requires an amino (N)-terminal signal peptide for direction through the endoplasmic reticulum and Golgi apparatus (Girard, Dieryckx, Job, & Job, 2013; Vincent & Bedon, 2014). Secretion without a signal peptide is considered unconventional and includes pathways requiring extracellular vesicles (Agrawal et al., 2010; Vincent, Rafiqi, & Job, 2020). Molecules other than proteins are also secreted by various organisms, and for plants and fungi this can include phytohormones, secondary metabolites, peptides, and nucleic acids (Vincent et al., 2020). For phytopathogenic fungi, the secretome is of particular interest because it contains an arsenal of molecules used to interact with and cause disease on plants (Girard et al., 2013).

In a recent study of the Camellia petal blight pathogen *Ciborinia camelliae*, fungal culture filtrate was tested for cell death-eliciting activity on the host plant and analysed by mass spectrometry to identify proteins acting as necrotrophic factors (Kondratev et al., 2022). A similar experiment was trialled in this study, using a *D. septosporum* mutant (*DsHexA*) deficient in the phytotoxin dothistromin, to determine if molecules present in the fungal culture filtrate can elicit cell death in the non-host *Nicotiana benthamiana*. This approach was found unsuitable for *D. septosporum*, as trace amounts of dothistromin produced by the *DsHexA* mutant appeared to cause cell death in some *N. benthamiana* infiltrations (**Appendix 16**). Fortunately, fungal secretomes can also be investigated through proteomic analysis (Liu, Stevens-Green, Johal, Buchanan, & Geddes-McAlister, 2022) and this approach was used instead in this thesis.

Proteomics has been used to analyse the secretomes of many phytopathogenic fungi and to identify candidate virulence factors (González-Fernández, Valero-Galván, Gómez-Gálvez, & Jorrín-Novo, 2015; Kettles & Kanyuka, 2016). Analysis of the secretomes from *D. septosporum* and *F. fulva* will enable identification of new candidate virulence factors and may provide further information about the *D. septosporum* candidates identified in **Chapter 3**, and the *F. fulva* candidate Ecp11-1 examined in **Chapter 2**. A well-established method for identification of fungal

virulence factors is proteomic analysis of apoplastic washing fluid from a successful interaction between the pathogen and the plant host (de Wit, Buurlage, & Hammond, 1986). Indeed, proteomic and transcriptomic analysis of apoplastic washing fluid from a *Fulvia fulva*-tomato interaction identified over 60 new candidate effectors (Mesarich et al., 2018). Analysis of apoplastic washing fluid from a compatible *D. septosporum*-pine interaction has not been performed before, as the tough epidermis of pine needles makes infiltration exceedingly difficult (R. Bradshaw, per comm). However, the recent use of tissue culture-generated pine shoots to test the effects of recombinantly expressed proteins, found that this soft tissue could be vacuum-infiltrated with liquid (Hunziker, 2018; Hunziker et al., 2021; Tarallo et al., 2022). Indeed, apoplastic washing fluid harvest was found to be successful in a preliminary trial with uninfected pine shoots (**Appendix 17**). Unfortunately, the pine shoots did not perform well in a *D. septosporum* infection trial, where many died before the infection cycle was completed (**Appendix 18**). Although proteomic analysis of apoplastic washing fluid is the ideal method for identifying secreted virulence factors, analysis of the *in vitro* proteome can also provide insights into the fungal secretome (Bradley et al., 2022; He et al., 2021; Pierre, Griffith, Morphew, Mur, & Scott, 2017; Yang et al., 2021).

In this study, proteomic analysis was performed on the culture filtrates of *D. septosporum* and *F. fulva* grown in different conditions, and comparisons were made between the two fungal secretomes. For both fungi, samples were grown in a nutrient-rich medium, as well as a nutrient-poor medium which is suggested to mimic *in planta* conditions (Fernando et al., 2019). Unlike *F. fulva* (Mesarich et al., 2018), *in planta* proteomic analysis of *D. septosporum* has not, as mentioned above, been performed previously. Therefore, to provide additional *in planta*-like conditions, some *D. septosporum* samples were cultured in medium with plant extract (pine extract, as pine needle-soaked water), a technique that has been utilized in other systems to more closely mimic *in planta* conditions (He et al., 2021). Samples from both fungi were harvested at different time points for each medium, based on prior work with *D. septosporum* in which these media had been used. For nutrient-poor medium, the time points were chosen to correspond with those from a *D. septosporum* transcriptome study (Ozturk et al., 2019). For nutrient-rich medium, two time points (day 4 and 9) were chosen to correspond with samples from a study of dothistromin biosynthesis in *D. septosporum* (Chettri et al., 2018). That study showed that, when grown in low Dothistroma medium (LDM; **Appendix 19**), 4 dpi was an early exponential phase of *D. septosporum* growth in which dothistromin gene expression and the rate of dothistromin production were rapidly increasing. At 9 dpi, the *rate* of dothistromin biosynthesis had started to decline, although dothistromin still accumulated to high levels as the

biomass increased (**Figure 4.1**) (Chettri et al., 2018). These samples might loosely correlate with the mid (early lesion) and late (sporulating lesion) *in planta* stages (Bradshaw et al., 2016; Kabir et al., 2015b), and analysis may lead to identification of proteins with a role in the necrotrophic switch.

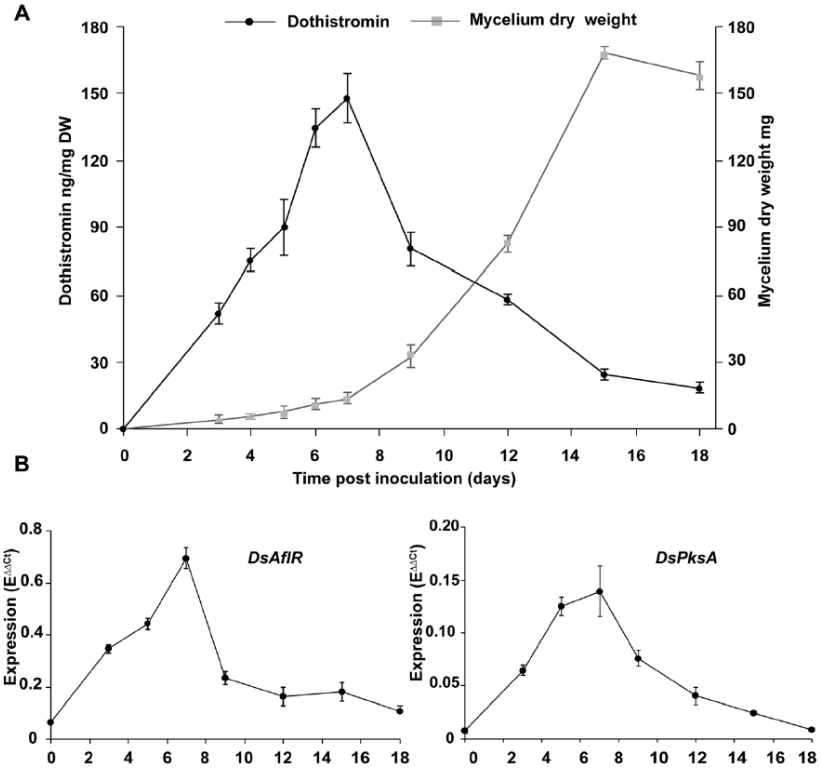

Figure 4.1. Rate of dothistromin production and expression of key biosynthesis genes in Dothistroma septosporum. (**a**) Rate of dothistromin production (ng dothistromin per mg dry weight (DW) of mycelium) is shown by a black line, while *D. septosporum* biomass accumulation (mg of dry weight of mycelium) is shown by a grey line, over a time course. (**b**) Expression of key dothistromin biosynthesis genes *DsAflR* and *DsPksA* relative to the geometric mean of two control genes (*DsTub1* and *DsTef1*), over the same time course. Taken from Chettri et al. (2018).

This chapter presents the first culture filtrate proteomes of *D. septosporum* and *F. fulva*. The comparative analysis presented here identified trends in both fungal secretomes, provided evidence to support a hemibiotrophic lifestyle of *F. fulva*, and identified proteins of interest which may play a role in virulence.

4.2 Materials and methods

4.2.1 Biological materials

The fungal strains *D. septosporum* NZE10 (de Wit et al., 2012) and *F. fulva* Race 5 (Stergiopoulos et al., 2007) were used in this study.

4.2.1.1 Fungal culturing

F. fulva was cultured routinely as described in **Chapter 2** (**Materials and methods section 2.2.1.1**). Routine culturing of *D. septosporum* was on Dothistroma medium (DM; **Appendix 19**). For inoculation, a section of mycelium was ground in water with a micro pestle then spread across a DM plate and incubated at 22°C for 7–10 days. For growth of *D. septosporum* in liquid culture, 25 mL of medium (in 125 mL conical flasks) was inoculated with spores or ground mycelium, depending on the experiment. Cultures were incubated at 22°C for 7–10 days, shaking at 160 rpm (classic series C10 platform shaker (New Brunswick Scientific)). Media used to culture *D. septosporum* are shown in **Appendix 19**.

To harvest culture filtrate of *D. septosporum* and *F. fulva* for proteome analysis, cultures were grown in 125 mL conical flasks containing 25 mL media, inoculated with 10^5 spores/mL, and incubated at 22°C, with shaking at 180 rpm (classic series C10 platform shaker (New Brunswick Scientific)). Samples were taken after 4 and 9 days for samples in 'nutrient-rich' LDM medium, following the method of Chettri et al. (2013), but after 9, and 16 days in 'nutrient-poor PMMG medium, following the method of Ozturk et al. (2019) to facilitate comparisons with those earlier studies. Culture filtrates were harvested through a sterile nappy liner or Miracloth and centrifuged at 3,400 x g for 4 min to sediment any remaining mycelial fragments. The culture filtrates were then sterilized by passage through a 0.2 µm filter (Ahlstrom-Munksjö, Helsinki, Finland), snap frozen in liquid nitrogen, and stored at -80°C.

4.2.1.2 Spore generation

Spore production in *F. fulva* was performed as described in **Chapter 2** (**Materials and methods section 2.2.1.1**). For spore production in *D. septosporum*, the fungus was cultured on DM plates then sub-cultured to Dothistroma Sporulation Medium (DSM; **Appendix 19**) by spreading ground mycelium as described above. After 7 days incubation at 22°C, spores of the fungus were then transferred to pine minimal salts medium (PMMG; **Appendix 19**) plates, made using water in which pine needles had been soaked for 24 h, to increase spore production. The transfer was done by adding 2-3 mL water to the DSM plate for 10 min, the spores suspended with a plate spreader, then spread across PMMG plates before incubating in the dark for 7 d at 22°C (Chettri

et al., 2012). Harvesting of spores was performed in the same way, except after suspending with a plate spreader, the spores were collected and filtered through a sterile nappy liner or Miracloth (EMD Millipore Corp.). If necessary, the spores were concentrated by collection at 3,500 x g for 4 min and the supernatant removed to a desired volume. Spore concentrations were then determined using a haemocytometer.

4.2.2 Analysis of the *D. septosporum* and *F. fulva* culture filtrate proteomes

4.2.2.1 Proteomic samples

Attempts to identify virulence factors from the *D. septosporum* secretome by screening culture filtrate in non-host *Nicotiana* species were unsuccessful (**Appendix 16**). Therefore, to identify candidate virulence factors, the proteomes of *D. septosporum* and *F. fulva* were analysed and compared. For the *D. septosporum* proteome, cultures were grown in eight different conditions (**section 4.3.1**): in either nutrient-rich (LDM) or nutrient-poor (PMMG) media, with or without pine extract (to mimic *in planta*-like conditions) and harvested at different time points (4-, 9- or 16-days post-inoculation). For the *F. fulva* proteome, cultures were grown in four different conditions (**section 4.3.6**): in either nutrient-rich (potato dextrose broth, PDB: Merck, New York, USA) or nutrient-poor (PMMG) media, and harvested 4-, 9- or 16-days post-inoculation.

4.2.2.2 Preparing *D. septosporum* and *F. fulva* culture filtrates for LC-MS analysis

Culture filtrates and the fungal mycelia were harvested separately (**Materials and methods section 4.2.1.1**), snap frozen in liquid nitrogen, stored at -80°C for at least two days, and then freeze-dried. The freeze-dried mycelium was weighed to provide an average dry weight for each sample.

Culture filtrates were prepared for liquid chromatography-mass spectrometry (LC-MS) analysis by trypsin digestion as described by Bradley (2022), with the addition that freeze-dried culture filtrates were suspended in 1–2 mL sterile MilliQ water.

4.2.2.3 LC-MS analysis of *D. septosporum* and *F. fulva* peptide samples (performed by Trevor Loo, Massey University)

Peptide samples were analysed by LC-MS as described by Bradley (2022), with the following additions. For the LC-MS mass spectrometer settings, the normalized collision energy was 28, and the charge exclusions were: “unassigned”, 1, and >6.

4.2.2.4 Database search (performed by Trevor Loo and Hannah McCarthy)

The raw LC-MS spectra files were used as queries against a list of predicted proteins using the Proteome Discoverer™ search engine (ThermoFisher Scientific), as described by Bradley (2022) with the following additions. For the data analysis parameters, the database used for the *D. septosporum* samples was *D. septosporum* NZE10 predicted proteins, and for *F. fulva* it was the *F. fulva* Race 5 predicted proteins. For *D. septosporum*, the predicted protein list of the NZE10 strain was obtained from the Joint Genome Institute (JGI) website (https://mycocosm.jgi.doe.gov/Dotse1/Dotse1.home.html). For *F. fulva*, the predicted protein list was obtained from BioProject PRJNA565804 on the National Center for Biotechnology Information (NCBI) website (https://www.ncbi.nlm.nih.gov/bioproject/PRJNA565804). Another addition to the methods described by Bradley (2022) was that the taxonomy setting was *Dothistroma septosporum* and *Fulvia fulva*. When analysing the raw LC-MS spectra files using Proteome Discoverer™ software, the following display filters were used: "Master is equal to master", "Description does not contain keratin", "Protein false discovery rate (FDR) confidence at least level high in protein FDR confidence combined" and "Found in samples has confidence high in at least 2 samples".

4.2.2.5 Filtering predicted proteins and PCA plot analysis

Once the list of predicted proteins was obtained, principle component analysis (PCA) plots were generating using Proteome Discoverer™ software in conjunction with standard parameters. The list of proteins was then exported to Microsoft© Excel (App v2211 Build 15831.20252), and manually filtered to remove non-*D. septosporum*/*F. fulva* proteins, based on the protein descriptions. The amino acid sequences from the predicted protein list were then merged into the Microsoft© Excel document using RStudio (v2022.07.2 Build 576) and the accession number. The list of proteins was then manually filtered again to only keep those detected in at least two biological replicates with high confidence. This list of proteins was then considered the total proteins detected from these *D. septosporum* or *F. fulva* samples.

4.2.2.6 Filtering for classically secreted proteins

The aim of this analysis was to identify potential virulence factors from among the classically secreted proteins detected in the culture filtrate. Therefore, the following filtering was performed on the total list of proteins to determine which were likely classically secreted: presence of a signal peptide predicted with SignalP v4.1 (Petersen, Brunak, von Heijne, & Nielsen, 2011), absence of transmembrane domains predicted with TMHMM v2.0 (Krogh, Larsson, von Heijne, & Sonnhammer, 2001), absence of Glycosylphosphatidylinositol (GPI) lipid

anchoring predicted using big-PI Fungal Predictor (Eisenhaber, Schneider, Wildpaner, & Eisenhaber, 2004) and absence of endoplasmic reticulum retention motifs manually predicted by the presence of carboxyl (C)-terminal “HDEL” or “KDEL” motifs at the end of the protein sequence.

4.2.2.7 Annotation of classically secreted proteins

To facilitate characterisation of the classically secreted proteins, further gene and protein annotation was performed. For *D. septosporum* proteins, gene expression was available from transcriptome data (Bradshaw et al., 2016). Because transcriptomic analysis has not been performed as part of an infection time course for the Race 5 strain of *F. fulva*, gene expression from Mesarich et al. (2014) of the 0WU top BlastP hit (performed using Geneious v9.1.8 software) to the Race 5 proteins was used. Candidate effector proteins were predicted using EffectorP v3.0 (Sperschneider & Dodds, 2021). Carbohydrate-active enzyme (CAZyme) proteins were predicted using dbCAN2 with the HMMER and DIAMOND tools (Zhang et al., 2018), where the protein was annotated as a CAZyme if predicted by at least one tool. Protein function annotations were predicted using InterProScan (Finn et al., 2017), with Geneious v9.1.8 software and the Pfam and SMART databases. To annotate proteins that had been previously identified as candidate effectors in *D. septosporum*, the following literature was examined: Hunziker (2018), Hunziker et al. (2021), Tarallo et al. (2022), Tarallo (2022). For *F. fulva*, characterised effectors were already annotated in the predicted protein list obtained from BioProject PRJNA565804, but additional candidate effectors identified by Mesarich et al. (2018) were also manually added to the data. For annotation of protein type in all pie graphs, candidate effector annotation (either from EffectorP v3.0 or previous studies) had priority over other protein types (such as CAZyme annotation).

4.2.2.8 Data manipulation and illustration

Microsoft© Excel was used to view and sort data. RStudio (v2022.07.2 Build 576) was used to merge excel files and generate Venn diagrams and heatmaps. Adobe Illustrator v24.1.1 was used to generate pie graphs and embellish figures.

4.3 Results

4.3.1 LC-MS analysis of secreted proteins from *D. septosporum*

Previous attempts to identify virulence factors from the *D. septosporum* secretome by screening culture filtrate in non-host *Nicotiana* species were unsuccessful (**Appendix 16**). Therefore, to analyse the *D. septosporum* secreted proteome and identify candidate virulence factors, LC-MS analysis of culture filtrates was performed. Cultures were grown in eight different conditions, in either nutrient-rich (LDM) or nutrient-poor (PMMG) media, as well as in the presence or absence of pine extract (to mimic *in planta*-like conditions) and harvested at different time points (**Table 4.1**).

Mycelium from the LDM Day 4 samples with and without pine extract weighed in at ~20 mg dry weight, while the Day 9 samples weighed ~200-300 mg dry weight, illustrating the significant increase in growth between these two sample time points but also showing a lower growth increase in the presence of pine extract. The PMMG samples had less than 0.5 mg of mycelial dry weight for all samples, showing that growth of *D. septosporum* in this low-nutrient medium was significantly reduced compared to that in the nutrient-rich LDM medium.

Table 4.1. *Dothistroma septosporum* culture conditions for liquid chromatography-mass spectrometry analysis and mycelium dry weights of harvested samples.

Nutrient[1]	Pine extract[2]	Harvest time (dpi)	Mycelium dry weight[3] (mg)
Rich (LDM)	No	4	22.7 ± 5.2
		9	300.3 ± 22.8
	Yes	4	22.1 ± 1.6
		9	214.4 ± 46.6
Poor (PMMG)	No	9	0.5 ± 0.6
		16	<0.5[4]
	Yes	9	<0.5[4]
		16	<0.5[4]

1 – LDM, Low Dothistroma medium; PMMG, Pine minimal salts medium.

2 - In conditions that contained pine extract (pine), the medium was made with pine needle-soaked MilliQ water (**Appendix 19**).

3 - Mean ± SD. Four biological replicates were analysed per sample.

4 – The mycelium dry weight was below the limit of detection by the scale.

The harvested culture filtrates were concentrated by freeze-drying, then analysed by sodium dodecyl-sulfate polyacrylamide gel electrophoresis (SDS-PAGE). The SDS gels showed distinct differences between the nutrient-rich (LDM) and nutrient-poor (PMMG) treatments (**Figure 4.2**). The samples grown in PMMG medium had distinct protein bands, while the LDM samples mainly had smears. This is likely due to a larger number of proteins being present in these LDM samples.

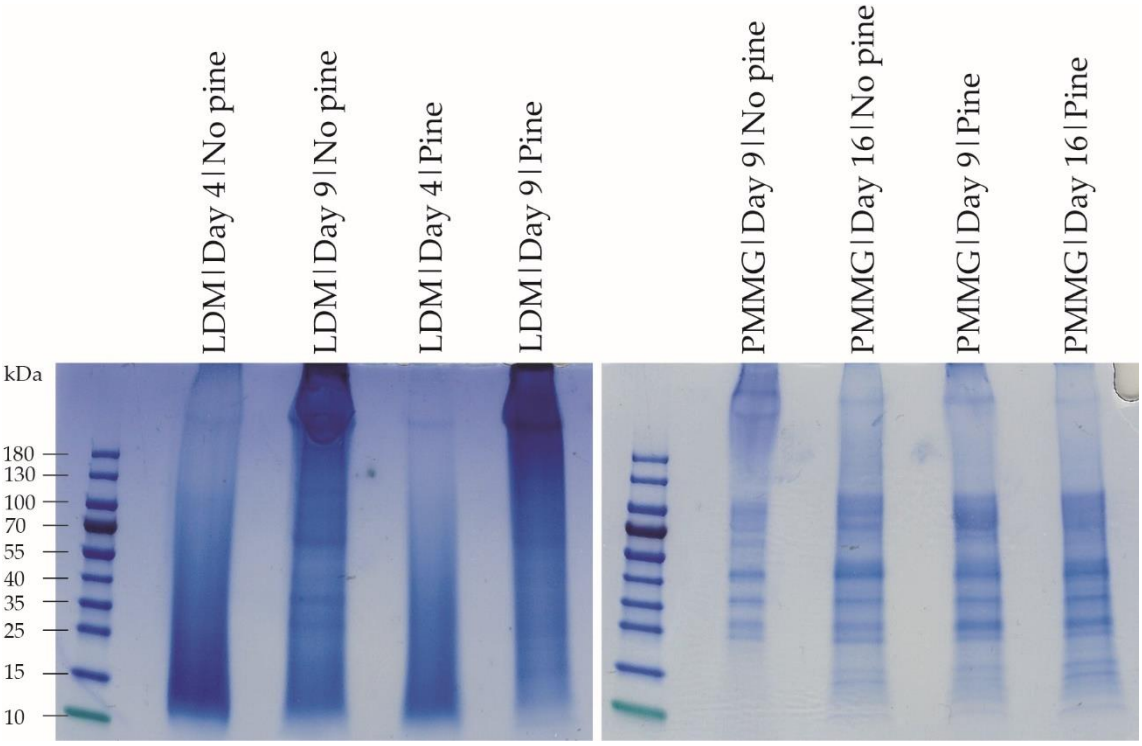

Figure 4.2. Total protein profiles of *Dothistroma septosporum* culture filtrate samples. Samples were resolved by SDS-PAGE electrophoresis on a 4-20% Mini-Protean® Tgx™ Precast Protein Gel (Bio-Rad). Growth media were nutrient-rich (low Dothistroma media, LDM) or nutrient-poor (pine minimal salts medium, PMMG), with addition of pine extract in some samples (pine needle-soaked water), and sample times in days since inoculation as labelled above the gel lanes. Ladder sizes in kilodaltons (kDa) are labelled on the left. One representative biological replicate is shown per sample.

The samples were then prepared by trypsin digestion and analysed by LC-MS (**Materials and methods section 4.2.2.2**). To compare the protein profiles between samples and biological replicates, a principal component analysis (PCA) was performed (**Figure 4.3**). In this analysis, principal component 1 (PC1) explained 34.8% of the variance and principal component 2 (PC2) explained 25%. The four biological replicates of most of the samples clustered together. However, those from PMMG|Day 16|No pine (purple) did not cluster tightly, and the

PMMG|Day 9|Pine (pink) and LDM|Day 9|Pine (red) samples each had one replicate that did not cluster with the rest (**Figure 4.3**).

Several profiles were evident from clustering between different samples (**Figure 4.3**). Profile 1 was the most heterogeneous and consisted of samples PMMG|Day 9|No pine (brown), LDM|Day 4|Pine (orange), and LDM|Day 4|No pine (blue). These were all early samples but included a mix of media types. Profile 2 consisted of samples LDM|Day 9|No pine (green) and LDM|Day 9|Pine (red), both of which shared media type and sampling time. Profile 3 consisted of samples PMMG|Day 16|No pine (purple), PMMG|Day 16|Pine (yellow), and PMMG|Day 9|Pine (pink) (all PMMG).

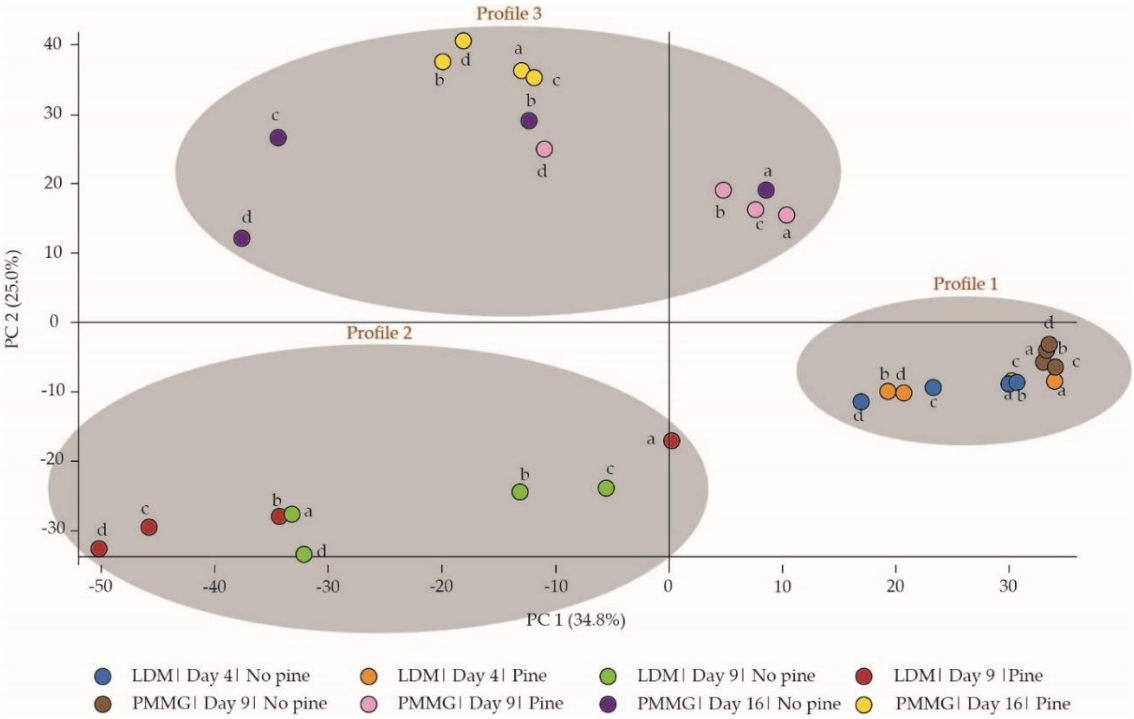

Figure 4.3. Principle component analysis (PCA) plot of *Dothistroma septosporum* proteome samples following growth of the fungus in different media and liquid chromatography-mass spectrometry (LC-MS) analysis. Clustered samples are highlighted by a grey oval and labelled as protein profiles 1–3. Biological replicates are labelled as a–d. Growth media were nutrient-rich (low Dothistroma media, LDM) or nutrient-poor (pine minimal salts medium, PMMG), with addition of pine extract in some samples (pine needle-soaked water).

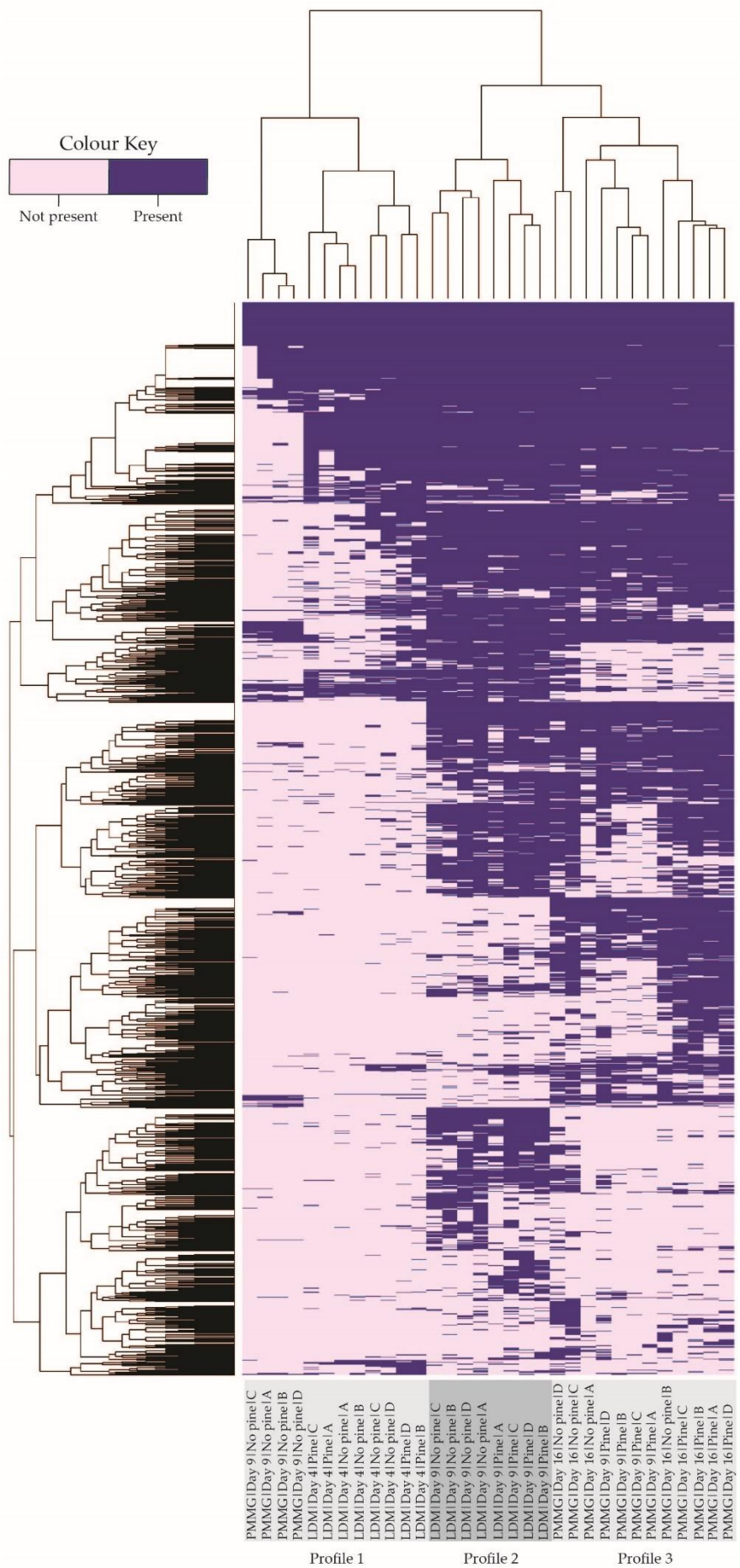
Colour Key
Not present
Present
PMMG | Day 9 | No pine | C
PMMG | Day 9 | No pine | A
PMMG | Day 9 | No pine | B
PMMG | Day 9 | No pine | D
LDM | Day 4 | Pine | C
LDM | Day 4 | Pine | A
LDM | Day 4 | No pine | A
LDM | Day 4 | No pine | B
LDM | Day 4 | No pine | C
LDM | Day 4 | No pine | D
LDM | Day 4 | Pine | D
LDM | Day 4 | Pine | B
LDM | Day 9 | No pine | C
LDM | Day 9 | No pine | B
LDM | Day 9 | No pine | D
LDM | Day 9 | No pine | A
LDM | Day 9 | Pine | A
LDM | Day 9 | Pine | C
LDM | Day 9 | Pine | D
LDM | Day 9 | Pine | B
PMMG | Day 16 | No pine | D
PMMG | Day 16 | No pine | C
PMMG | Day 16 | No pine | A
PMMG | Day 9 | Pine | D
PMMG | Day 9 | Pine | B
PMMG | Day 9 | Pine | C
PMMG | Day 9 | Pine | A
PMMG | Day 16 | No pine | B
PMMG | Day 16 | Pine | C
PMMG | Day 16 | Pine | B
PMMG | Day 16 | Pine | A
PMMG | Day 16 | Pine | D
Profile 1
Profile 2
Profile 3

Figure 4.4. Heatmap analysis of *Dothistroma septosporum* culture filtrate proteome samples identified by liquid chromatography-mass spectrometry (LC-MS) analysis. The heatmap shows presence (purple) or absence (light pink) of proteins in each sample. Proteins were considered present if they were found in at least two biological replicates with high confidence. The row dendrogram shows similarity between proteins (individual protein labels not shown), and the column dendrogram shows similarity between samples. Branch length is proportional to the degree of dissimilarity. Sample names are labelled at the bottom of the heatmap, detailing media type (LDM (low Dothistroma media) or PMMG (pine minimal salts medium)), sample time (Day 4, 9, or 16), addition of pine extract (Pine (from water-soaked needles) or No pine), and biological replicate (A to D).

After filtering (**Materials and methods section 4.2.2.5**), a total of 1966 *D. septosporum* proteins were identified from the culture filtrate samples with high confidence (**Appendix 20**). To further elucidate the patterns in protein content between each sample, heatmap analysis of the presence or absence of proteins was performed (**Figure 4.4**). The heatmap showed that the biological replicates of most samples grouped together. However, there was some mixing of replicates of LDM|Day 4|Pine and LDM|Day 4|No pine, consistent with their close clustering in the PCA plot, and suggesting that the presence of pine extract does not have much effect on the early LDM samples. Also consistent with the PCA plot analysis, replicate B of the PMMG|Day 16|No pine sample (purple) was separated from the other biological replicates and was instead between the PMMG|Day 9 and 16|Pine samples.

The same three distinct protein profiles identified from the PCA plot analysis (**Figure 4.3**) were present in the heatmap (**Figure 4.4**). Profile 1 consisted of samples PMMG|Day 9|No pine, LDM|Day 4|Pine, and LDM|Day 4|No pine, and contained the least proteins of the three profiles. Different sub-profiles were also present within profile 1 between the PMMG and LDM samples. Profile 2 included the remaining LDM samples (LDM|Day 9|No pine and LDM|Day 9|Pine), and profile 3 contained the remaining PMMG samples (samples PMMG|Day 16|No pine, PMMG|Day 16|Pine, and PMMG|Day 9|Pine). Profile 1 suggested that the addition of pine extract does not have a large effect on the early LDM samples, as already noted. Profiles 2 and 3 revealed a distinct difference in protein content between the remaining LDM and PMMG samples. The separation of the early (9 Day) PMMG samples to distinct heatmap profiles 1 (no pine) and 3 (pine) suggested that the addition of pine extract had a strong effect on these early PMMG samples.

4.3.2 Secreted proteins

A total of 1966 proteins were identified from the *D. septosporum* culture filtrate proteome samples. To determine which of these proteins were classically secreted, further filtering was performed in the expectation that this set would be enriched in effectors or virulence factors (**Material and methods section 4.2.2.6**). After filtering, 233 proteins were suggested to be classically secreted (only 11.8% of the 1966 proteins). During the process of filtering, the largest drop in protein number occurred when selecting for those with a signal peptide (**Appendix 21**). The large number of proteins that lacked a signal peptide might partly be accounted for by cell rupture during sampling, resulting in contamination with cytoplasmic proteins. Indeed, the top BlastP hits of four randomly selected proteins without a signal peptide were associated with the cytoplasm (**Appendix 22**), supporting this hypothesis.

Heatmap analysis was performed with the 233 classically secreted proteins from *D. septosporum* culture filtrate proteome samples (**Figure 4.5**). The same three heatmap profile groups were observed as for the total *D. septosporum* proteome. Interestingly, the four biological replicates of each sample grouped together, unlike the outliers seen for some of the replicates in the total protein samples. This suggests non-classically secreted proteins and/or cytoplasmic contaminant proteins were the main contributors to the variation observed between those biological replicates.

EffectorP v3.0. was used to predict how many of the classically secreted proteins were effectors. Of the 233 proteins, 157 were not candidate effectors, 53 were apoplastic effectors, 19 were cytoplasmic effectors, and four were predicted to be both apoplastic and cytoplasmic effectors (**Appendix 21**). Candidate effectors of *D. septosporum* have also been identified in other studies though prediction pipelines (Hunziker, 2018; Tarallo, 2022), as well as in **Chapter 3**. The candidate virulence factor DsCE3 (Ds71487), which was shortlisted for gene disruption analysis in **Chapter 3**, was detected in all proteomic samples (**Appendix 21**). Of the 82 proteins identified as candidate effectors in those other studies (Hunziker, 2018; Tarallo, 2022), 30 (36%) were detected in this culture filtrate proteome (**Appendix 21**). Of the seven candidate effectors previously shown to elicit cell death in *Nicotiana* species (Hunziker, 2018; Hunziker et al., 2021; Tarallo et al., 2022), four were identified in this proteome (Ds70057, Ds71487, Ds70694, and Ds158381, **Appendix 21**). These results suggest that this *in vitro* proteome includes effector proteins which have been shown to be functional *in planta*, providing confidence that new candidate effectors could be identified from this resource.

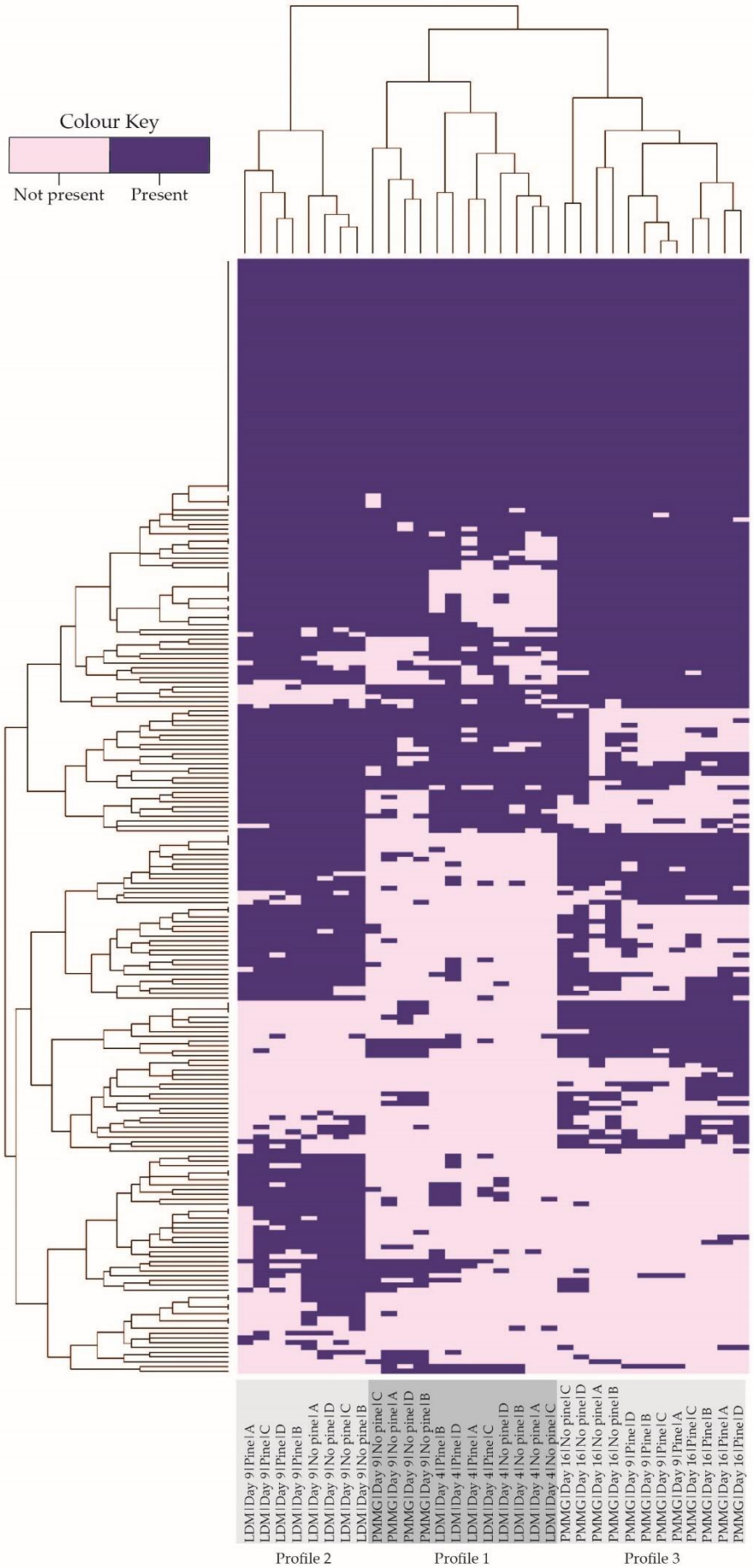
Colour Key
Not present
Present
LDM | Day 9 | Pine | A
LDM | Day 9 | Pine | C
LDM | Day 9 | Pine | D
LDM | Day 9 | Pine | B
LDM | Day 9 | No pine | A
LDM | Day 9 | No pine | D
LDM | Day 9 | No pine | C
LDM | Day 9 | No pine | B
PMMG | Day 9 | No pine | C
PMMG | Day 9 | No pine | A
PMMG | Day 9 | No pine | D
PMMG | Day 9 | No pine | B
LDM | Day 4 | Pine | B
LDM | Day 4 | Pine | D
LDM | Day 4 | Pine | A
LDM | Day 4 | Pine | C
LDM | Day 4 | No pine | D
LDM | Day 4 | No pine | B
LDM | Day 4 | No pine | A
LDM | Day 4 | No pine | C
PMMG | Day 16 | No pine | C
PMMG | Day 16 | No pine | D
PMMG | Day 16 | No pine | A
PMMG | Day 16 | No pine | B
PMMG | Day 9 | Pine | D
PMMG | Day 9 | Pine | B
PMMG | Day 9 | Pine | C
PMMG | Day 9 | Pine | A
PMMG | Day 16 | Pine | C
PMMG | Day 16 | Pine | B
PMMG | Day 16 | Pine | A
PMMG | Day 16 | Pine | D
Profile 2
Profile 1
Profile 3

Figure 4.5. Heatmap analysis of classically secreted proteins from *Dothistroma septosporum* culture filtrate proteome samples identified by liquid chromatography-mass spectrometry (LC-MS) analysis. The heatmap shows presence (purple) or absence (light pink) of proteins in each sample. The row dendrogram shows similarity between proteins (individual protein labels not shown), and the column dendrogram shows similarity between samples. Branch length is proportional to the degree of dissimilarity. Sample names are labelled at the bottom of the heatmap, detailing media type (LDM (low Dothistroma media) or PMMG (pine minimal salts medium)), sample time (Day 4, 9, or 16), addition of pine extract (Pine (from water-soaked needles) or No pine), and biological replicate (A to D).

4.3.3 Overview of classically secreted proteins present in the *D. septosporum* culture filtrate proteome

The 233 proteins predicted to be classically secreted from *D. septosporum* into culture filtrate were analysed and compared (See **Appendix 20** for details of all these proteins). The numbers of different classically secreted proteins were between ~100–200 in each treatment. Interestingly, the number of unique proteins found in each sample was very low, with the highest number of unique proteins being eight, from the LDM|Day 9|No pine sample (**Table 4.2**).

As expected, the late samples from each medium had higher numbers of secreted proteins compared to the early samples. Considering the very low mycelial dry weights recorded for the PMMG samples, a large number of proteins were secreted. Unexpectedly, addition of pine extract had inconsistent effects on protein numbers, increasing the number of secreted proteins in the early samples, but decreasing the number in late samples, in both LDM and PMMG media (**Table 4.2**). To identify any proteins common to these specific conditions, the proteome was next analysed to determine the effects of pine extract and of sampling time in samples grown in either PMMG or LDM medium.

Table 4.2. Unique classically secreted proteins of *Dothistroma septosporum* in culture per treatment.

Treatment	Number of secreted proteins per sample	Number of unique secreted proteins per sample
LDM|Day 4|No pine	103	1
LDM|Day 4|Pine	124	0
LDM|Day 9|No pine	189	8
LDM|Day 9|Pine	176	2
PMMG|Day 9|No pine	127	1
PMMG|Day 9|Pine	138	0
PMMG|Day 16|No pine	173	2
PMMG|Day 16|Pine	158	6

4.3.4 Effect of pine extract on the proteome

Classically secreted proteins were analysed to determine the effects of pine extract. To investigate this, the proteins specifically secreted in samples with and without pine extract were compared. From all samples (i.e. both LDM and PMMG media combined), there were only nine proteins unique to pine extract, whilst there were 15 in samples without pine extract, and 209 that were secreted both with and without pine extract (**Appendix 23**). Interestingly, of the nine proteins unique to pine extract, none were common to both media types (**Appendix 21**).

To determine the effect of pine extract in each specific medium, the proteins secreted in each type of medium were analysed (**Figure 4.6**). Proteins secreted in PMMG that were unique to pine extract were of particular interest because this sample type is hypothesised to mimic the pine host environment most closely among all the culture conditions used. In PMMG, there were 14 proteins unique to pine extract, and nine of these were encoded by genes upregulated *in planta* (**Table 4.3**). Four of these proteins were predicted glycoside hydrolase (GH) CAZymes. One was a predicted GH17 and may have a role in virulence as reported for a GH17 from *F. fulva* (Ökmen, Bachmann, & de Wit, 2019). Of the other upregulated genes, three encoded candidate effectors, two of which were identified in other studies (Hunziker, 2018; Tarallo et al., 2022): DsEcp20-1 (Ds51311) and DsCE37 (Ds74289). The gene expression and specific protein secretion profile of these proteins suggests they may function as virulence factors.

The LDM medium is nutrient-rich and does not mimic the host environment but there were eight proteins unique to pine extract. In contrast to what was seen for PMMG, none of these eight proteins were predicted to be CAZymes (**Figure 4.6**). Of the genes encoding these eight, only three of them were upregulated *in planta*, including one candidate effector and two "other" proteins predicted to have esterase functions (**Table 4.3**). The candidate effector (Ds70909) was

a predicted glutathione S-transferase and as glutathione transferases from *Alternaria brassicicola* were found to be essential for full virulence, likely through their detoxification role (Calmes et al., 2015), this protein is of interest.

In summary, secreted proteins were identified as unique to the presence of pine extract in each media type, but no common proteins were found between the two media types. The proteins secreted in the nutrient-poor medium included several CAZymes and candidate effectors, while those in the nutrient-rich medium included candidate effectors but no predicted CAZymes. Candidate effectors identified included the previously identified proteins DsEcp20-1 and DsCE37, and new candidate effector Ds70909, and these proteins are of interest for further investigation.

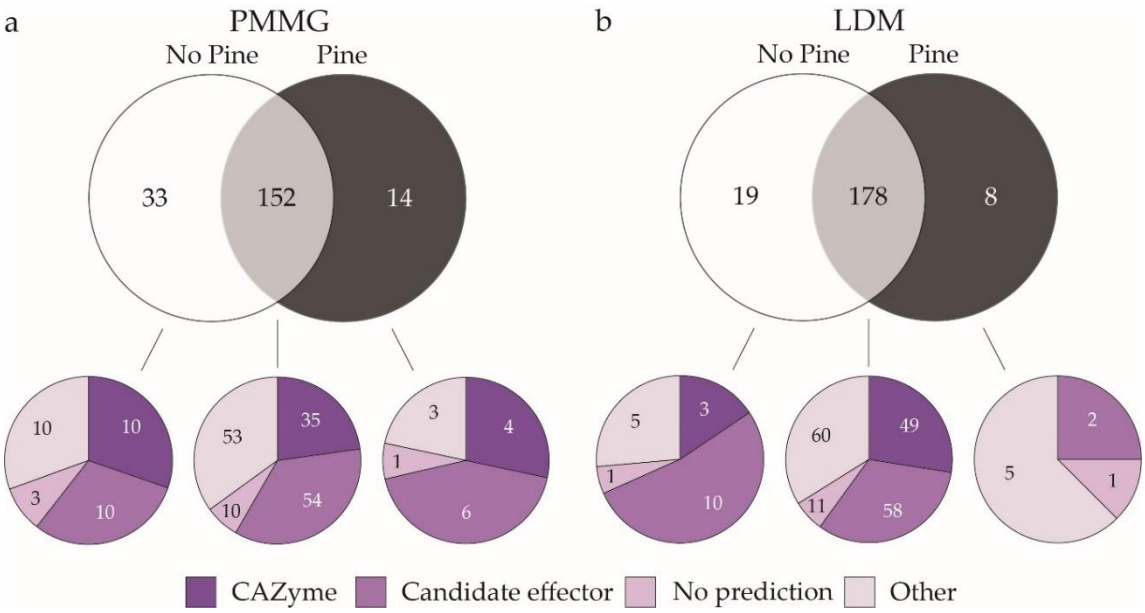

Figure 4.6. Classically secreted proteins of *Dothistroma septosporum* identified in the presence or absence of pine extract in each culture medium, and the protein type. Proteins predicted as candidate effectors by either EffectorP or by previous studies (Hunziker, 2018; Hunziker et al., 2021; Tarallo, 2022) were labelled as candidate effectors (**Materials and methods section 4.2.2.7**). CAZyme, carbohydrate-active enzyme; LDM, low Dothistroma medium; PMMG, pine minimal salts medium; Pine, extract from water-soaked pine needles.

Table 4.3. Classically secreted proteins of *Dothistroma septosporum* that were specifically produced in the presence of pine extract in each culture medium.

	Normalised expression[2]					
JGI ID[1]	Iv	Early	Mid	Late	Protein type[3]	Protein domains[4]
PMMG medium						
74289	42	165	12	18	CE (*DsCE37*)	-
129885	19	88	21	31	Other	Chloroperoxidase
49342	9	5	78	85	CAZyme	Glycosyl hydrolase family 1
72607	4	1	12	79	CAZyme	Glycosyl hydrolase family 43
25475	8	10	19	68	No pred	-
51311	19	62	53	57	CE (*DsEcp20-1*)	-
39360	3	6	16	50	CAZyme	Glycosyl hydrolase family 43
48652	13	45	35	46	CE	GDSL-like Lipase/Acylhydrolase/Carbohydrate Esterase Family 16
60011	14	33	31	24	CAZyme	Glycosyl hydrolase family 17
LDM medium						
74915	9	22	8	319	Other	Carboxylesterase, type B
70909	65	67	173	138	CE	Glutathione S-transferase, N-terminal domain
75202	12	134	15	42	Other	Calcineurin-like phosphoesterase

1 – Joint Genome Institute (JGI) protein ID from the *D. septosporum* genome page (https://mycocosm.jgi.doe.gov/Dotse1/Dotse1.home.html). PMMG, pine minimal salts medium; LDM, low Dothistroma medium.

2 – Gene expression is shown as Reads Per Million per Kilobase (RPMK) and was sourced from a transcriptome analysis performed on *D. septosporum*-infected *Pinus radiata* seedlings. Three *in planta* stages were sampled: early, mid, and late, as well as *in vitro* (Iv; growth in low Dothistroma medium (LDM) broth for 7 days, 22°C (Bradshaw et al., 2016)). Proteins were only included if the encoding gene had >2-fold increase in gene expression between *in vitro* and any *in planta* stage, and expression *in planta* >50 RPMK, or >25 RPMK for carbohydrate-active enzymes (CAZymes).

3 – Protein type determined by HMMER, InterPro, and EffectorP v3.0. analysis, as well as candidate effector (CE) predictions from other studies (Hunziker, 2018; Tarallo, 2022). For CEs, the encoding gene name was added in brackets.

4 – Predicted protein domains based on HMMER and DIAMOND prediction (https://bcb.unl.edu/dbCAN2/blast.php), as well as InterPro prediction, performed using Geneious software (v9.1.8.).

4.3.5 Effect of different time point sampling on the proteome

To investigate the effect of growth time on the presence or absence of secreted proteins, the proteins specifically secreted in early samples were compared to those in late samples. From all samples (i.e. both LDM and PMMG media combined), there were four proteins unique to early time point samples, 54 unique to late, and 175 present in both early and late samples. Interestingly, of the four proteins uniquely secreted in the early samples, none were candidate effectors, but three were CAZyme proteins (**Appendix 24**).

The proteins secreted in early and late samples were then investigated in each medium type separately. There were 205 proteins secreted in LDM, where nine were unique to the Day 4 samples, 78 unique to the Day 9, and 118 present in both Day 4 and Day 9 samples (**Figure 4.7**). The Day 4 LDM samples corresponded to the sample of Chettri et al. (2018), when dothistromin production was exponentially increasing. Therefore, these Day 4 LDM samples are thought to loosely correlate to the mid (early lesion) stage *in planta* as the rate of dothistromin biosynthesis was high at this stage when lesions were expanding (Kabir et al., 2015b). Unexpectedly, of the nine proteins unique to the Day 4 LDM samples, none were encoded by genes upregulated specifically at the mid stage *in planta*. However, three proteins were encoded by genes upregulated at the late (sporulating lesion) *in planta* stage, all of which were CAZymes (**Table 4.4**). The most highly expressed CAZyme (Ds71743) was upregulated at the early and late *in planta* stages and encodes a predicted cellulase, which likely breaks down cellulase in the plant cell walls. This CAZyme could be important for lesion expansion and is a potential virulence factor.

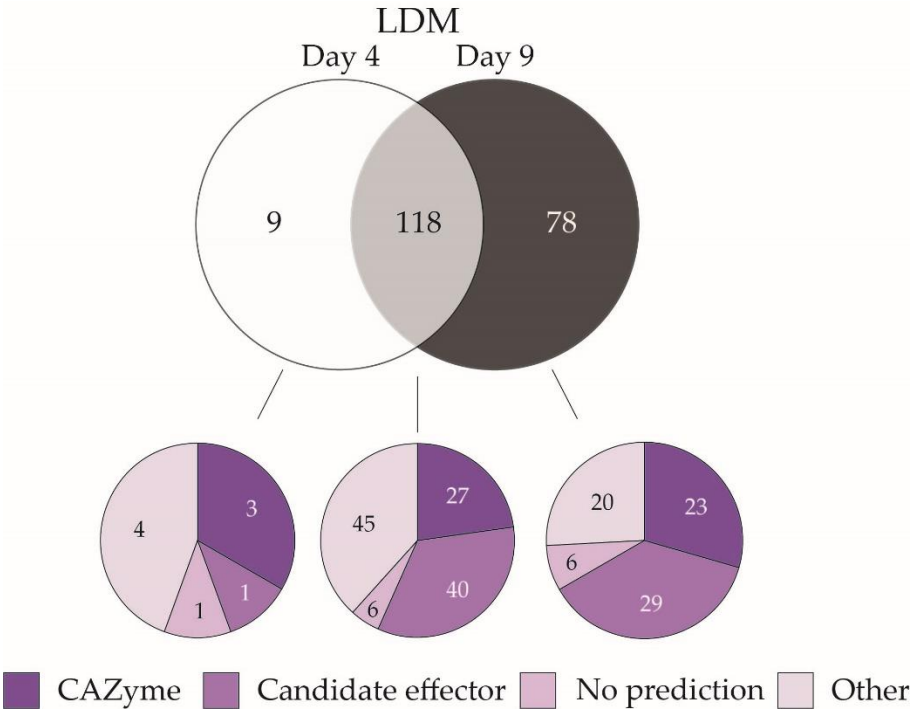

Figure 4.7. Classically secreted proteins of *Dothistroma septosporum* present in early and late LDM culture samples, and the protein type. CAZyme, carbohydrate-active enzyme; LDM, low Dothistroma medium.

The Day 9 LDM samples corresponded to the *in vitro* sample of Chettri et al. (2018), when the *rate* of dothistromin biosynthesis was decreasing, but dothistromin was still rapidly accumulating. Therefore, the Day 9 LDM samples probably correlates most closely to a period of rapid lesion expansion which occurs between the mid (early lesion) and late (sporulating lesion) *in planta* stages. For the purposes of this study a focus was made on proteins encoded by genes up-regulated at the mid and/or late stages *in planta.* Of the 78 proteins secreted in the Day 9 LDM samples, 20 were upregulated at the mid (early lesion) and/or late (sporulating lesion) stage (**Table 4.4**). Of these 20 proteins, eight were CAZymes, nine were candidate effectors, and three were "other" or "no prediction" proteins. Of the candidate effector proteins, three had been identified in other studies: DsCPL1 (Ds70155), DsEcp20-3, (Ds70694) and DsCE20 (Ds74790). The cerato-platanin protein DsCPL1 was also identified as a candidate virulence factor in **Chapter 3** and was one of the proteins detected specifically in the late PMMG sample. This protein is encoded by a gene that is very highly expressed at the mid and late stages *in planta* and was also highly expressed at the Day 9 *in vitro* stage in the study of Ozturk et al. (2019), which used the same growth conditions as this proteome study (**Table 4.4**). DsEcp20-3 is encoded by a gene upregulated at the mid and late stages (**Table 4.4**) and has been shown to elicit cell death in the pine host and in non-host *Nicotiana* species (Tarallo et al., 2022).

Of the eight Day 9 CAZymes encoded by genes upregulated at the mid and/or late *in planta* stages (**Table 4.4**), one was a predicted cellulase (Ds70420). Like the cellulase secreted specifically in the Day 4 LDM sample mentioned previously, the Ds70420 protein likely functions by facilitating lesion expansion and/or breakdown of the cell wall to allow sporulation structures to erupt through the needle. Another of the CAZyme proteins (Ds71018) was a predicted Glycoside Hydrolase Family 3 (GH3) protein that was also present in the late PMMG sample. This protein could possibly play a role in virulence by detoxifying host-derived fungi-toxic saponins, as was shown for GH3 proteins in other fungal phytopathogens (Bradley et al., 2022). These two CAZymes may be potential virulence factors and are of interest for further investigation.

Table 4.4. Classically secreted proteins produced by *Dothistroma septosporum* at different time points in LDM culture.

	Normalised expression[2]						
JGI ID[1]	Iv[3]	Iv	Early	Mid	Late	Protein type[4]	Protein domains[5]
Day 4							
71743	-	7	55	46	301	CAZyme	Glycosyl hydrolase family 5, Cellulase
69092*	-	5	21	3	68	CAZyme	Glycosyl hydrolase family 64
75559*	-	4	2	3	43	CAZyme	Auxiliary Activity Family 3, GMC oxidoreductase
Day 9							
70155*	808	257	71	507	1303	CE (*DsCPL1*)	Cerato-platanin
70231*	1593	213	7	1266	247	No pred	-
45955*	490	135	70	840	368	CE	-
71018*	26	31	32	154	310	CAZyme	Glycosyl hydrolase family 3, Fibronectin type III-like
43773	5	10	36	69	246	Other	Carboxylesterase family
70694	22	5	4	205	115	CE (*DsEcp20-3*)	-
72229	9	3	17	9	205	Other	NAD(P)-binding Rossmann-like domain
70420	6	8	22	8	192	CAZyme	Glycosyl hydrolase family 5, Cellulase
70709	15	36	33	52	169	CE	Aldose 1-epimerase
74790	32	30	18	49	159	CE (*DsCE20*)	-
89736	31	18	27	139	65	CAZyme	Glycosyl hydrolase 131 catalytic N-terminal domain[6]
161792	3	5	14	12	126	CE	Glycosyl hydrolase family 54, CBM42, Alpha-L-arabinofuranosidase B catalytic
73318	18	10	5	112	93	CAZyme	Glycosyl hydrolase family 93
40253	25	10	14	9	109	CAZyme	Auxiliary Activity Family 1, Multicopper oxidase
73225	64	57	32	14	98	CE	-
49342*	6	9	5	78	85	CAZyme	Glycosyl hydrolase family 1
72607	7	4	1	12	79	CAZyme	Glycosyl hydrolase family 43
19107	29	52	1	49	76	CE	Phosphatidylethanolamine-binding protein
39360*	1	3	6	16	50	CAZyme	Glycosyl hydrolase family 43
176781*	12	19	1	27	21	CE	Glycosyl hydrolase family 11

1 – Joint Genome Institute (JGI) protein ID from the *D. septosporum* genome page (https://mycocosm.jgi.doe.gov/Dotse1/Dotse1.home.html).

2 – Gene expression is shown as Reads Per Million per Kilobase (RPMK) and was sourced from a transcriptome analysis performed on *D. septosporum*-infected *Pinus radiata* seedlings. Three *in planta* stages were sampled: early, mid, and late, as well as *in vitro* (Iv; growth in low Dothistroma medium (LDM) broth for 7 days, 22°C (Bradshaw et al., 2016)). Proteins were only included if the encoding gene had >5-fold increase in gene expression between early and mid, early and late, or mid and late *in planta*, and expression *in planta* >50 RPMK, or >25 RPMK for carbohydrate-active enzymes (CAZymes).
3 – The *in vitro* gene expression is shown as RPMK, from *D. septosporum* mycelium grown for nine days in LDM (Ozturk et al., 2019).
4 – Protein type determined by HMMER, InterPro, and EffectorP v3.0. analysis, as well as candidate effector (CE) predictions from other studies (Hunziker, 2018; Tarallo, 2022). For candidate effectors, the encoding gene name was added in brackets.
5 – Predicted protein domains based on HMMER and DIAMOND prediction (https://bcb.unl.edu/dbCAN2/blast.php), as well as InterPro prediction, performed using Geneious software (v9.1.8.). GMC: glucose-methanol-choline. CBM24: Carbohydrate-Binding Module Family 42.
6 – HMMER and DIAMOND predictions did not suggest this protein is a CAZyme (despite the protein prediction from InterPro analysis), therefore it was classified as "other".
*Protein was also present in the corresponding early or late pine minimal salts medium (PMMG) sample.

The proteins secreted in early or late PMMG samples were also investigated. Because there was no indication from previous studies whether these *in vitro* samples correlate with any *in planta* stages, this study focused on proteins encoded by genes upregulated at any *in planta* stage to potentially identify those with a role in virulence. There were 199 proteins secreted into PMMG medium, where 11 were unique to Day 9 samples, 35 unique to Day 16, and 153 present in both Day 9 and Day 16 samples (**Figure 4.8**). Of the 11 proteins unique to the Day 9 samples, four were upregulated *in planta* (**Table 4.5**). Among these four were two CAZymes that were also detected in the early LDM samples and were upregulated at the late (sporulating lesion) *in planta* stage, along with a candidate effector (**Table 4.5**). The candidate effector gene (*Ds27299*) was the most highly expressed of all protein-coding genes unique to the Day 9 samples, and the encoded protein had a predicted Nis1 domain, which was identified from a necrosis-inducing fungal effector of *Colletotrichum orbiculare* (Yoshino et al., 2012). This candidate effector may be a potential virulence factor functioning at the necrotrophic switch.

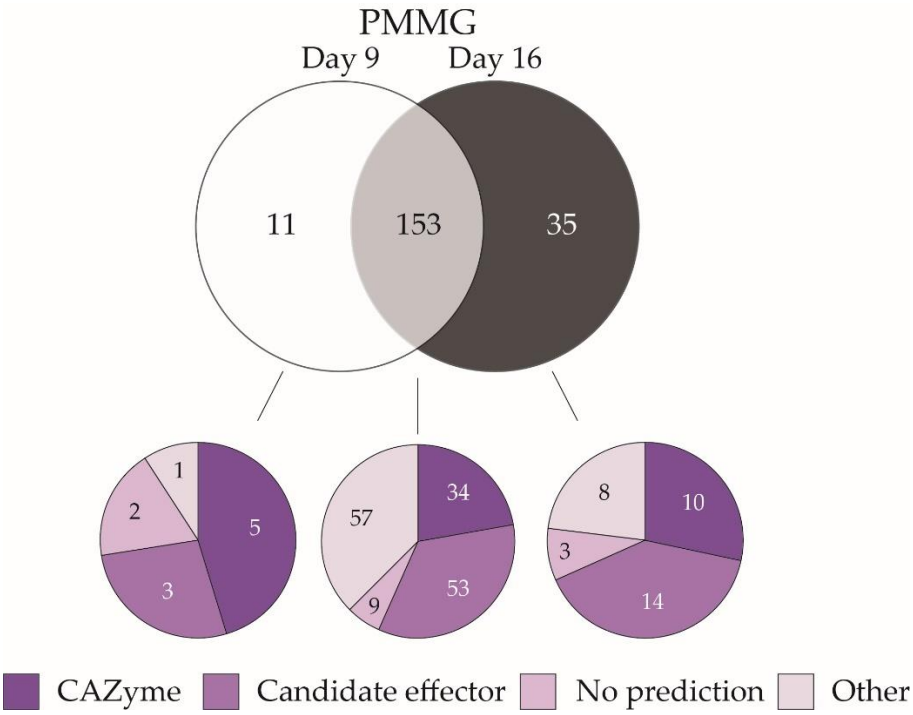

Figure 4.8. Classically secreted proteins of *Dothistroma septosporum* present in early and late PMMG culture samples, and the protein type. CAZyme, carbohydrate-active enzyme; PMMG, pine minimal salts medium.

The Day 16 PMMG samples had the same growth conditions as the *in vitro* samples of a *D. septosporum* RNAseq study (Ozturk et al., 2019), providing additional *in vitro* gene expression values. Of the 35 proteins unique to the Day 16 samples, 15 were encoded by genes upregulated *in planta*, including six CAZymes and five candidate effectors (**Table 4.5**). Interestingly, all CAZyme proteins were also detected in the late LDM samples and were upregulated at the mid (early lesion) and/or late (sporulating lesion) *in planta* stages. Of the candidate effector proteins, four were identified in other studies (Hunziker, 2018; Tarallo, 2022) (DsCPL1, DsCE1, DsCE37, and DsCE8), and DsCPL1 was also secreted in the late LDM samples. These proteins are all candidates for further study, with potential roles in the necrotrophic stage.

Table 4.5. Classically secreted proteins produced by *Dothistroma septosporum* at different time points in PMMG culture.

	Normalised expression[2]						
JGI ID[1]	Iv[3]	Iv	Early	Mid	Late	Protein type[4]	InterPro domain[5]
Day 9							
27299	-	88	79	162	1026	CE	Nis1 family
141428	-	170	895	128	96	Other	Lysophospholipase catalytic domain
69092*	-	5	21	3	68	CAZyme	Glycosyl hydrolase family 64
75559*	-	4	2	3	43	CAZyme	Auxiliary Activity Family 3, GMC oxidoreductase
Day 16							
70155*	113	257	71	507	1303	CE (*DsCPL1*)	Cerato-platanin
70231*	16	213	7	1266	247	No pred	-
44908	57	12	134	57	874	CE (*DsCE1*)	-
45955*	25	135	70	840	368	CE	-
71018*	103	31	32	154	310	CAZyme	Glycosyl hydrolase family 3, Fibronectin type III-like
20543	121	7	229	35	70	No pred	-
74289	170	42	165	12	18	CE (*DsCE37*)	-
74875	13	1	10	0	133	CE (*DsCE8*)	-
91962	2	4	3	108	22	Other	Chloroperoxidase
118184*	6	8	28	23	91	CAZyme	Glycosyl hydrolase family 3, Fibronectin type III-like
49342*	9	9	5	78	85	CAZyme	Glycosyl hydrolase family 1
25475	52	8	10	19	68	No pred	-
39360*	3	3	6	16	50	CAZyme	Glycosyl hydrolase family 43
153101*	22	6	9	33	15	CAZyme	Auxiliary Activity Family 7, FAD binding domain, Berberine and berberine like
47355*	17	5	10	15	28	CAZyme	Glycosyl hydrolase family 32

1 – Joint Genome Institute (JGI) protein ID from the *D. septosporum* genome page (https://mycocosm.jgi.doe.gov/Dotse1/Dotse1.home.html).

2 – Gene expression is shown as Reads Per Million per Kilobase (RPMK) and was sourced from a transcriptome analysis performed on *D. septosporum*-infected *Pinus radiata* seedlings. Three *in planta* stages were sampled: early, mid, and late, as well as *in vitro* (Iv; growth in low Dothistroma medium (LDM) broth for 7 days, 22°C (Bradshaw et al., 2016)). Proteins were only included if the encoding gene had >5-fold increase in gene expression between either *in vitro* stages and any *in planta* stages, and expression *in planta* >50 RPMK, or >25 RPMK for carbohydrate-active enzymes (CAZymes).

3 – *In vitro* gene expression (RPMK), from *D. septosporum* mycelium grown for 16 days in pine minimal salts medium (PMMG) (Ozturk et al., 2019).

4 – Protein type determined by HMMER, InterPro, and EffectorP v3.0. analysis, as well as candidate effector (CE) predictions from other studies (Hunziker, 2018; Tarallo, 2022). For CEs, the encoding gene name was added in brackets.
5 – Predicted protein domains based on HMMER and DIAMOND prediction (https://bcb.unl.edu/dbCAN2/blast.php), as well as InterPro prediction, performed using Geneious software (v9.1.8.). GMC: glucose-methanol-choline.
*Protein was also present in the corresponding early or late low Dothistroma medium (LDM) sample.

In summary, the sampling time was found to have an effect on the proteome. The Day 4 LDM sample appeared to contain more proteins with genes upregulated in the late stage, rather than the mid stage *in planta*, which was not predicted based on the previous *in vitro* research these sample timings were modelled on Chettri et al. (2018). A predicted cellulase was identified as the most highly expressed CAZyme in this sample, which may contribute to lesion expansion. The Day 9 LDM sample had a large number of unique proteins, including several candidate effectors that are of interest for future research (DsCPL1, DsEcp20-3, and DsCE20). A new candidate effector (Ds27299), belonging to the characterised Nis1 family, was identified from the proteins secreted specifically in the early PMMG samples, while the late PMMG samples contained several candidate virulence factors that may function in the necrotrophic stage.

4.3.6 LC-MS analysis of secreted proteins from *F. fulva*

To identify proteins secreted by *F. fulva* in culture filtrate and make a comparison with the *D. septosporum in vitro* secretome, proteomic analysis was performed with *F. fulva* culture filtrate samples. Plant extract was not added to medium in this case because an *in planta* proteome had been performed previously with apoplastic washing fluid from a compatible *F. fulva*-tomato interaction (Mesarich et al., 2018). To enable comparison with the *D. septosporum* proteome, cultures were grown in a comparable nutrient-rich medium (PDB), and the same nutrient-poor medium (PMMG) and sampled at the same time points (**Table 4.6**).

Samples were harvested as for the *D. septosporum* proteome (**Materials and methods section 4.2.1.1**), and the dry weight of the mycelium was measured (**Table 4.6**). As expected, cultures grown in nutrient-poor medium (PMMG) had a lower mycelium dry weight than those grown in the nutrient-rich medium (PDB). Interestingly, the dry weight recorded from the nutrient-poor samples was a lot higher than the corresponding *D. septosporum* samples (**section 4.3.1**), suggesting that *F. fulva* grows better in PMMG than *D. septosporum*.

The culture filtrate samples were harvested, freeze-dried and analysed by SDS-PAGE. The SDS gels showed a distinct difference in band intensity between the nutrient-rich and nutrient-poor

medium samples (**Figure 4.9**). Unexpectedly, the greater band intensity, which suggested greater protein content, was observed from the nutrient-poor (PMMG) samples (**Figure 4.9**). This contrasts to the *D. septosporum* culture filtrate samples, which had stronger band intensity in SDS gels with nutrient-rich samples (**section 4.3.1**). However, the *D. septosporum* PMMG samples had very minimal fungal growth, evident from the mycelial dry weight (**Table 4.1**), which is likely why these samples had only a faint protein banding profile. The freeze-dried culture filtrates were also resuspended in non-standardized volumes of water, therefore making any comparisons in protein band intensity a qualitative assessment, rather than quantitative.

Table 4.6. *Fulvia fulva* culture conditions for liquid chromatography-mass spectrometry analysis and mycelium dry weights of harvested samples.

Nutrient[1]	Harvest time (dpi)[2]	Mycelium Dry Weight[3] (mg)
Rich (PDB)	4	66.8 ± 3.5
	9	125 ± 15.2
Poor (PMMG)	9	19.2 ± 9.1
	16	22.7 ± 7.5

1 – PDB, potato dextrose broth; PMMG, pine minimal salts medium.

2 – Days post inoculation (dpi).

3 – Mean ± SD. Four biological replicates were analysed per sample.

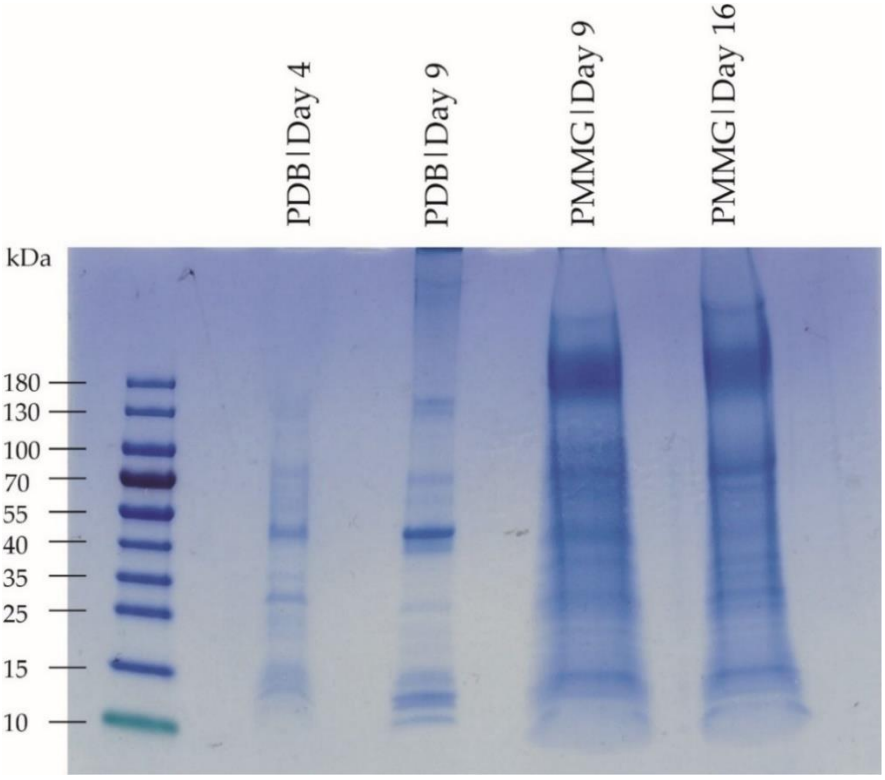

Figure 4.9. Total protein profiles of *Fulvia fulva* culture filtrate samples. Samples were resolved by SDS-PAGE electrophoresis on a 4-20% Mini-Protean® Tgx™ Precast Protein Gel (Bio-Rad). Medium type of nutrient-rich (potato dextrose broth (PDB)) or nutrient-poor (pine minimal salts medium (PMMG)) medium, and sample time (4, 9, or 16 days) of the samples are labelled above the gel pictures. Ladder sizes in kilodaltons (kDa) are labelled on the left of the gel pictures. One representative biological replicate is shown per sample.

The samples were prepared by trypsin digestion and analysed by LC-MS (**Materials and methods section 4.2.2.2**). To compare the protein profiles between samples and biological replicates, a principal component analysis (PCA) was performed (**Figure 4.10**). In this analysis, principal component 1 (PC1) explained 51.7% of the variance and principal component 2 (PC2) explained 17.5%. The biological replicates clustered together for all samples except PMMG|Day 9 (red).

Several profiles were evident from clustering between different samples (**Figure 4.10**). Both PDB medium samples PDB|Day 4 (blue) and PDB|Day 9 (orange) clustered close together but remained as separate profiles (Profiles 1 and 2, respectively). The two biological replicates "c" and "d" of sample PMMG|Day 9 (red) clustered separately as Profile 3. The remaining biological replicates "b" and "a" of sample PMMG|Day 9 (red) clustered with the PMMG|Day 16 (green) samples as Profile 4.

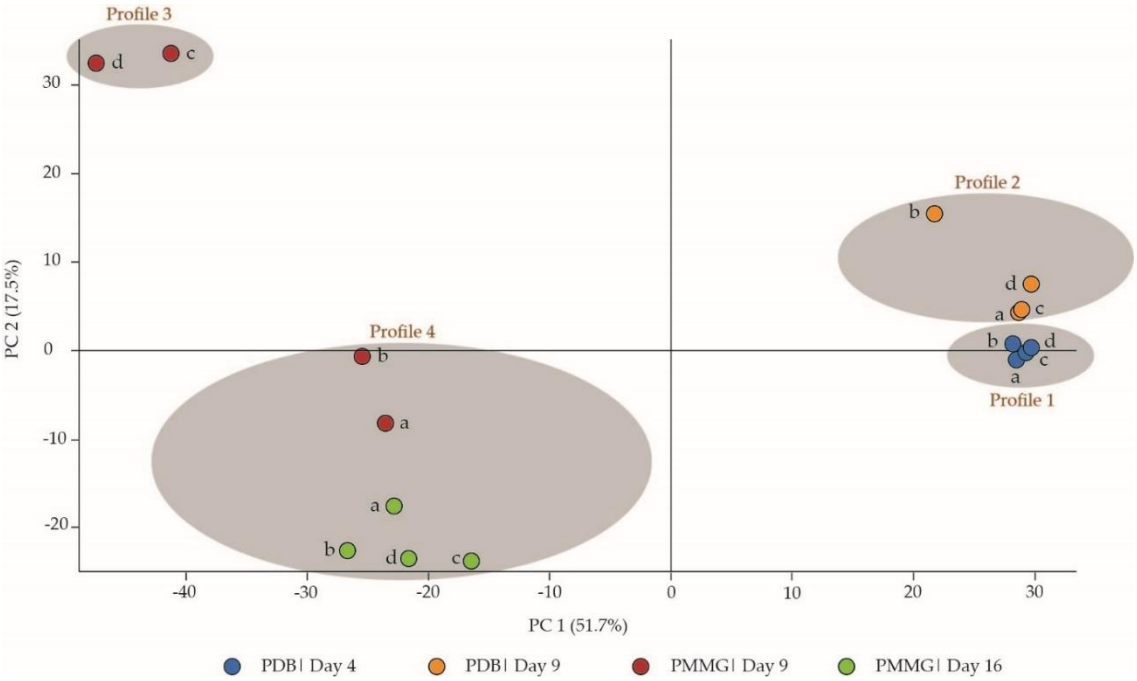

Figure 4.10. Principle component analysis (PCA) plot of *Fulvia fulva* proteome samples following growth of the fungus in different media and liquid chromatography-mass spectrometry (LC-MS) analysis. Clustered samples are highlighted by a grey oval and labelled as protein profiles 1–4. Biological replicates are labelled as a–d. Growth media were nutrient-rich (potato dextrose broth, PDB) or nutrient-poor (pine minimal salts medium, PMMG).

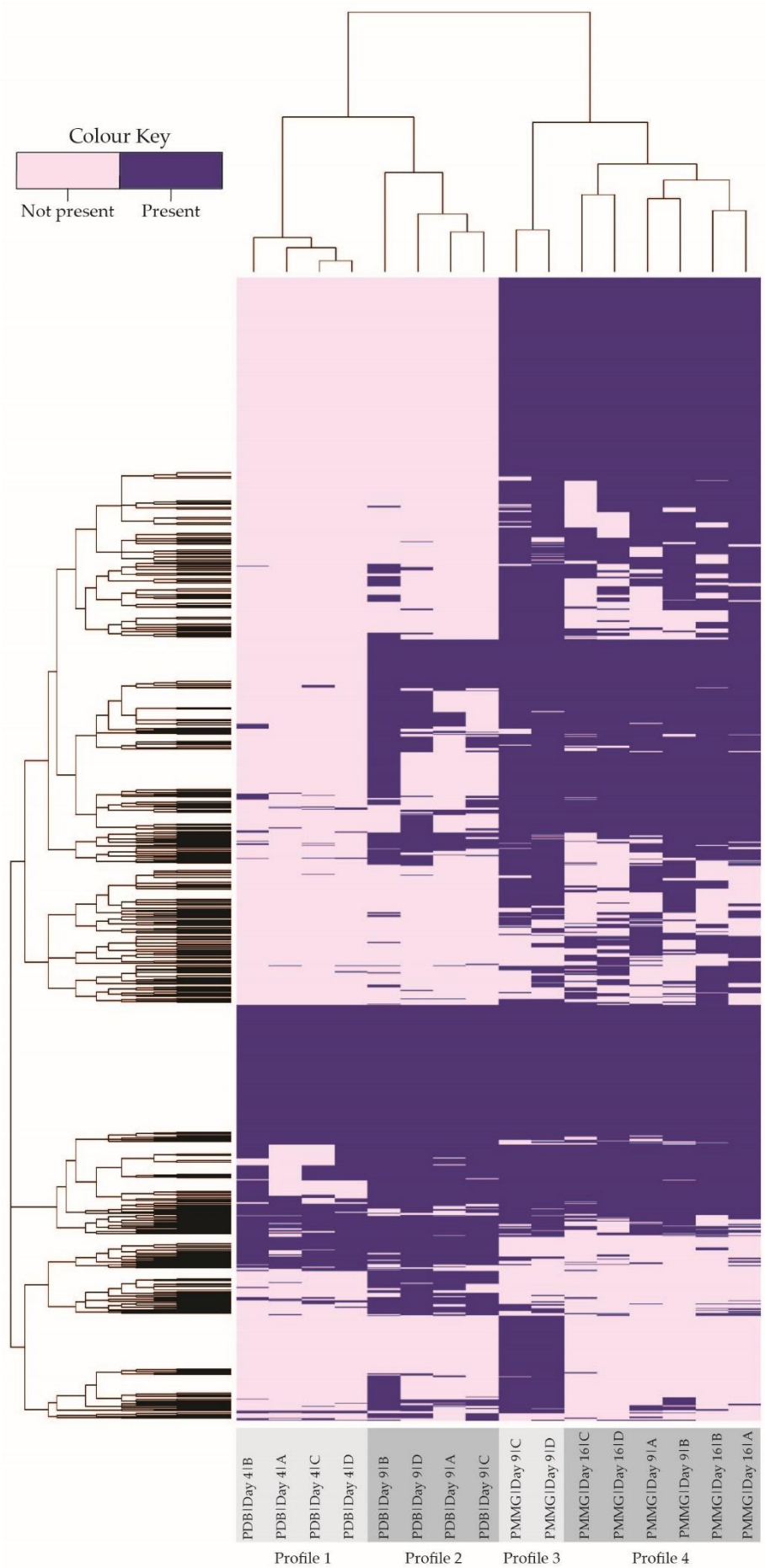
Colour Key
Not present
Present
PDB | Day 4 | B
PDB | Day 4 | A
PDB | Day 4 | C
PDB | Day 4 | D
PDB | Day 9 | B
PDB | Day 9 | D
PDB | Day 9 | A
PDB | Day 9 | C
PMMG | Day 9 | C
PMMG | Day 9 | D
PMMG | Day 16 | C
PMMG | Day 16 | D
PMMG | Day 9 | A
PMMG | Day 9 | B
PMMG | Day 16 | B
PMMG | Day 16 | A
Profile 1
Profile 2
Profile 3
Profile 4

Figure 4.11. Heatmap analysis of *Fulvia fulva* culture filtrate proteome samples identified by liquid chromatography-mass spectrometry (LC-MS) analysis. The heatmap shows presence (purple) or absence (light pink) of proteins in each sample. Proteins were considered present if they were found in at least two biological replicates with high confidence. The row dendrogram shows similarity between proteins (individual protein labels not shown), and the column dendrogram shows similarity between samples. Branch length is proportional to the degree of dissimilarity. Sample names are labelled at the bottom of the heatmap, detailing media type (potato dextrose broth (PDB) or pine minimal salts medium (PMMG)), sample time (Days 4, 9, or 16), and biological replicate (A to D).

A total of 1674 *F. fulva* proteins were identified from the culture filtrate samples with high confidence (**Appendix 25**), a lower number than identified in the *D. septosporum* proteome (**section 4.3.1**). To further elucidate the patterns in protein content between each sample, heatmap analysis of the presence or absence of proteins was performed (**Figure 4.11**). The heatmap showed that the PMMG samples appear to have a far greater number of protein types present than the PDB samples, which is consistent with the SDS gel results (**Figure 4.9**). The biological replicates of the PDB samples clustered together, but not those of the PMMG samples, which is consistent with the PCA results (**Figure 4.10**). Furthermore, the same four protein profiles identified from the PCA plot were present in the heatmap analysis. It is interesting that the two biological replicates "c" and "d" of PMMG|Day 9 (profile 3) appeared to have a greater protein content than the other two replicates.

4.3.7 Secreted proteins

A total of 1674 proteins were identified from the *F. fulva* culture filtrate samples. To determine how many of these proteins were classically secreted, filtering was performed as for the *D. septosporum* proteome (**Materials and methods section 4.2.2.6**). After filtering, 252 proteins were suggested to be classically secreted (only 15% of the 1674 proteins), which was slighter higher than for the *D. septosporum* secretome. Interestingly, more than 70 proteins without signal peptides had predicted associations with mitochondria (**Appendix 25**), suggesting that cell rupture may have occurred during sampling.

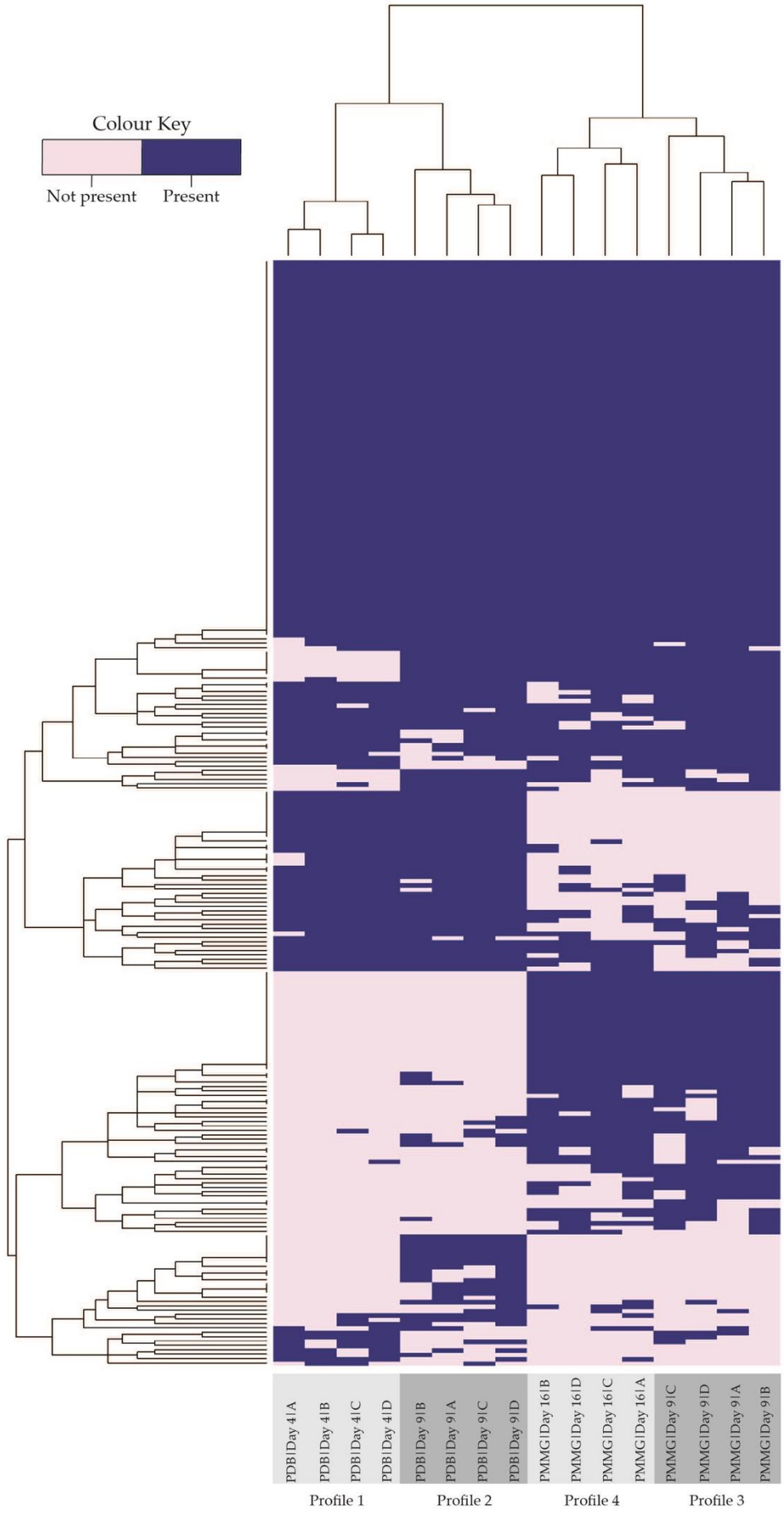
Colour Key
Not present
Present
PDB | Day 4 | A
PDB | Day 4 | B
PDB | Day 4 | C
PDB | Day 4 | D
PDB | Day 9 | B
PDB | Day 9 | A
PDB | Day 9 | C
PDB | Day 9 | D
PMMG | Day 16 | B
PMMG | Day 16 | D
PMMG | Day 16 | C
PMMG | Day 16 | A
PMMG | Day 9 | C
PMMG | Day 9 | D
PMMG | Day 9 | A
PMMG | Day 9 | B
Profile 1
Profile 2
Profile 4
Profile 3

Figure 4.12. Heatmap analysis of classically secreted proteins from *Fulvia fulva* culture filtrate proteome samples identified by liquid chromatography-mass spectrometry (LC-MS) analysis. The heatmap shows presence (purple) or absence (light pink) of proteins in each sample. The row dendrogram shows similarity between proteins (individual protein labels not shown), and the column dendrogram shows similarity between samples. Branch length is proportional to the degree of dissimilarity. Sample names are labelled at the bottom of the heatmap, detailing media type (potato dextrose broth (PDB) or pine minimal salts medium (PMMG)), sample time (Day 4, 9, or 16), and biological replicate (A to D).

Heatmap analysis was performed with the 252 classically secreted proteins from *F. fulva* culture filtrate proteome samples (**Figure 4.12**). There was a clear distinction between the nutrient-rich and nutrient-poor media samples. Consistent with the SDS gel results (**Figure 4.9**) and the heatmap of all *F. fulva* proteins (**Figure 4.11**), the PMMG samples appeared to have a higher number of different protein types than the PDB samples. This was in contrast to the *D. septosporum* proteome, where the PMMG samples appeared to have lower numbers of protein types than the LDM samples (**section 4.3.1**). The biological replicates of each sample clustered together in this analysis, as was found for the *D. septosporum* secretome (**section 4.3.2**), suggesting that major variation observed between some replicates was due to non-classically secreted and/or cytoplasmic contaminant proteins. This resulted in the four protein profiles being specific to the sample type and containing all four biological replicates. This contrasts to the *D. septosporum* proteome, where only three protein profiles were present, each containing more than one sample type (**section 4.3.2**).

EffectorP v3.0. was used to predict how many of these classically secreted proteins were effectors. Of the 252 proteins, 168 were not predicted to be candidate effectors, 57 were apoplastic effectors, 18 were cytoplasmic effectors, and nine were predicted to be both apoplastic and cytoplasmic effectors (**Appendix 26**). Similar to *D. septosporum* (**section 4.3.2**), the greatest number of candidate effectors were predicted to be apoplastic, likely because both fungi colonize the apoplast (Kabir et al., 2015b; Thomma et al., 2005). A total of 75 apoplastic effectors or candidate effectors have also been identified in *F. fulva* so far (**Materials and methods section 4.2.2.7**) (Mesarich et al., 2018) and, of these, 27 (36%) were detected in this culture filtrate proteome (**Appendix 27**). These numbers are very similar to what was observed in the *D. septosporum* culture filtrate proteome (**section 4.3.2**). The majority of these previously identified candidate effector proteins were detected in all proteomic samples, including candidate effector CfEcp11-1 (**Appendix 27**), which was investigated in **Chapter 2**. There were only seven previously identified candidate effector proteins not detected in all proteomic

samples, and the samples they were detected in were highly variable (**Appendix 27**). These results show that, similar to the *D. septosporum* proteome, the *F. fulva in vitro* proteome includes effector proteins that are known to be functional *in planta*, and therefore suggests that new candidate effectors can be identified from this resource.

4.3.8 Overview of secreted proteins present in the *F. fulva* culture filtrate proteome

The 252 proteins predicted to be classically secreted from *F. fulva* into the culture filtrate were analysed and compared (See **Appendix 26** for details of all these proteins). The number of classically secreted proteins found in each treatment was between approximately 160–200 (**Table 4.7**). Similar to the *D. septosporum* proteome, the number of unique proteins found in each treatment was very low, with the highest number of unique proteins being 18, from the PDB|Day 9 sample. Interestingly, the highest number of unique proteins was also identified in the *D. septosporum* proteome from the late time sample in nutrient-rich medium (**section 4.3.3**). To identify any proteins common to the early and late samples, the proteome was analysed to determine the effect of sample time, and this was addressed below.

Table 4.7. Unique classically secreted proteins of *Fulvia fulva* in culture per treatment.

Treatment	Number of secreted proteins per sample	Number of unique proteins per sample
PDB|Day 4	161	4
PDB|Day 9	188	18
PMMG|Day 9	192	6
PMMG|Day 16	187	3

4.3.9 Effect of time on the proteome

To investigate the effect of growth time on the secreted proteins, the proteins specifically secreted in early samples were compared to those in late samples. From all samples (i.e. both PDB and PMMG media combined), there were 12 proteins specifically secreted in early time point samples, 21 secreted in late, and 219 secreted in both early and late samples (**Appendix 28**). Interestingly, similar to the *D. septosporum* proteome, a greater proportion of CAZyme proteins were secreted specifically in the early samples than the late samples.

The proteins secreted specifically in early or late samples were then investigated in each media type separately. Interestingly, no proteins that were encoded by a gene upregulated *in planta* were common between the early and late samples of the two media types, which contrasts with the *D. septosporum* proteome. There were 196 *F. fulva* proteins secreted in the PDB media type,

of which eight were secreted specifically in the Day 4 sample, 35 in Day 9, and 153 in both Day 4 and Day 9 samples (**Figure 4.13**). Of the eight proteins secreted specifically in the Day 4 sample, two were encoded by genes that were highly upregulated *in planta*, specifically at 4 dpi (**Table 4.8**). The first (UJO15715.1) was a predicted chloroperoxidase; the second (UJO17753.1) was the candidate effector CfEcp14-2, which has no predicted protein domains. These two proteins could potentially play a role during early infection. Of the 35 proteins secreted specifically in the Day 9 sample, 11 were encoded by genes that were upregulated *in planta* (**Table 4.8**). Five of these proteins were candidate effectors, including the previously identified candidate avirulence proteins CfEcp14-1 (UJO17283.1) and CfEcp50-1 (UJO23906.1). Another chloroperoxidase (UJO16216.1), upregulated at Day 4, was also present in this sample.

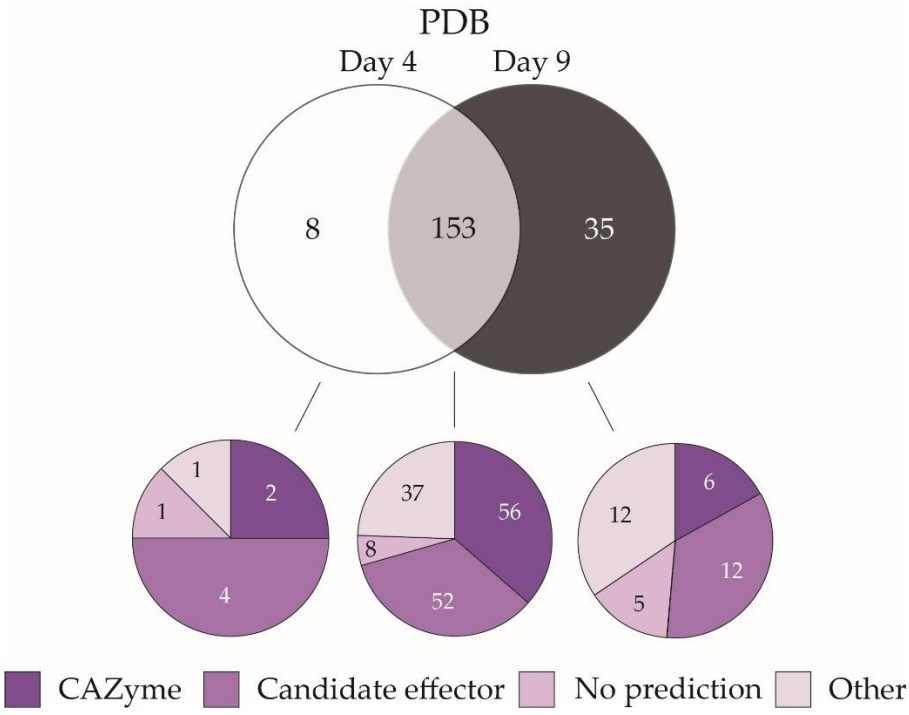

Figure 4.13. Classically secreted proteins produced by *Fulvia fulva* in early and late proteome samples in potato dextrose broth (PDB) culture media, and the protein type. CAZyme, carbohydrate-active enzyme.

Table 4.8. Classically secreted proteins produced by Fulvia fulva at different time points in PDB culture samples.

	Normalised expression[2]					
Accession[1]	Iv	4 dpi	8 dpi	12 dpi	Protein type[3]	Protein domains[4]
Day 4						
UJO15715.1	10	749	5	8	Other	Chloroperoxidase
UJO17753.1	4	400	3	3	CE (*CfEcp14-2*)	-
Day 9						
UJO19814.1	24	95	863	610	CE	-
UJO17283.1	13	668	523	272	CE (*CfEcp14-1*)	-
UJO19274.1	15	0	230	164	CE (*CfEcp50-1*)	Hydrophobic surface binding protein A
UJO17233.1	17	169	10	153	Other	Domain of unknown function
UJO11660.1	0	0	26	166	Other	Arginase family
UJO16216.1	14	143	30	44	Other	Chloroperoxidase
UJO11563.1	1	0	78	109	CE	-
UJO18208.1	0	0	57	62	CE	Carbohydrate Esterase Family 5, Cutinase
UJO16150.1	1	60	2	2	CAZyme	Carbohydrate-Binding Module Family 13, Domain of unknown function
UJO12550.1	8	0	9	52	Other	Isochorismatase family
UJO18904.1	0	50	33	51	Other	Fasciclin domain

1 – GenBank protein accession from the NCBI website (https://www.ncbi.nlm.nih.gov/).

2 – Gene expression is shown for the 0WU orthologue of the Race 5 gene (identified as the top BlastP hit, **Materials and methods section 4.2.2.7**) as fragments per kilobase of exon per million fragments mapped (FPKM) and was sourced from a transcriptome study of a compatible interaction of H-Cf-0 tomato plants inoculated with *F. fulva* 0WU strain and sampled 4, 8, and 12 days post-inoculation (dpi), as well as *in vitro* (Iv; growth in potato dextrose broth for 4 days, 22°C (Mesarich et al., 2014)). Proteins were only included if the encoding gene had >5-fold increase in gene expression between *in vitro* (Iv) and any *in planta* stage, and expression *in planta* >50 RPMK, or >25 RPMK for carbohydrate-active enzymes (CAZymes).

3 – Protein type determined by HMMER, InterPro, and EffectorP v3.0. analysis. Effectors were also identified from the protein description of the predicted secreted protein list (**Materials and methods section 4.2.2.7**), and candidate effectors (CEs) identified by Mesarich et al. (2018) were also included. For CEs, the encoding gene name was added in brackets.

4 – Predicted protein domains based on HMMER and DIAMOND prediction (https://bcb.unl.edu/dbCAN2/blast.php), as well as InterPro prediction, performed using Geneious software (v9.1.8.).

There were 203 proteins secreted in PMMG medium, of which 16 were secreted specifically in the Day 9 sample, 11 in Day 16, and 176 in both Day 9 and Day 16 samples (**Figure 4.14**). Of the 16 proteins secreted specifically in the Day 9 sample, five were upregulated *in planta* (**Table 4.9**). Three of these upregulated genes encoded CAZymes, one of which (UJO13947.1) was a predicted GH17. Another GH17 from *F. fulva* has been shown to release a DAMP through enzymatic activity and was downregulated at the biotrophic stage but upregulated in the later stages when *F. fulva* grows saprophytically (Ökmen et al., 2019). It is possible that UJO13947.1 also plays a role in virulence, but possibly during the biotrophic stage when the gene was upregulated. The other two proteins encoded by genes upregulated *in planta* were candidate effectors, including CfEcp50-1 (UJO19274.1), also found in PBD Day 9 samples (**Table 4.8**) and one with no predicted domains (UJO15145.1).

Of the 35 proteins secreted specifically in the Day 16 sample, only two were encoded by genes that were upregulated *in planta* (**Table 4.9**). Both were CAZyme proteins, encoded by genes with low expression compared to other CAZymes in the Day 9 samples. The low number of proteins encoded by genes upregulated *in planta* in this sample could be because the late Day 16 time point does not relate well with the transcriptome data, where the latest time point is 12 dpi *in planta* (Mesarich et al., 2014).

In summary, sampling time and type of medium had an effect on the *F. fulva* proteome. In contrast to the *D. septosporum* proteome, few proteins were similar between the PDB and PMMG media at the corresponding early or late time points. However, effector Ecp50-1 was detected in the Day 9 samples of both media even though Day 9 was the 'early' sample for PMMG and the 'late' sample for PDB. As observed from analysis of the *D. septosporum* proteome, a greater proportion of CAZyme proteins were found in the early time points compared with the late times. Proteins of interest, including candidate effectors, were identified from all samples except the late PMMG, thought to be due to this sample not correlating with the available transcriptome data.

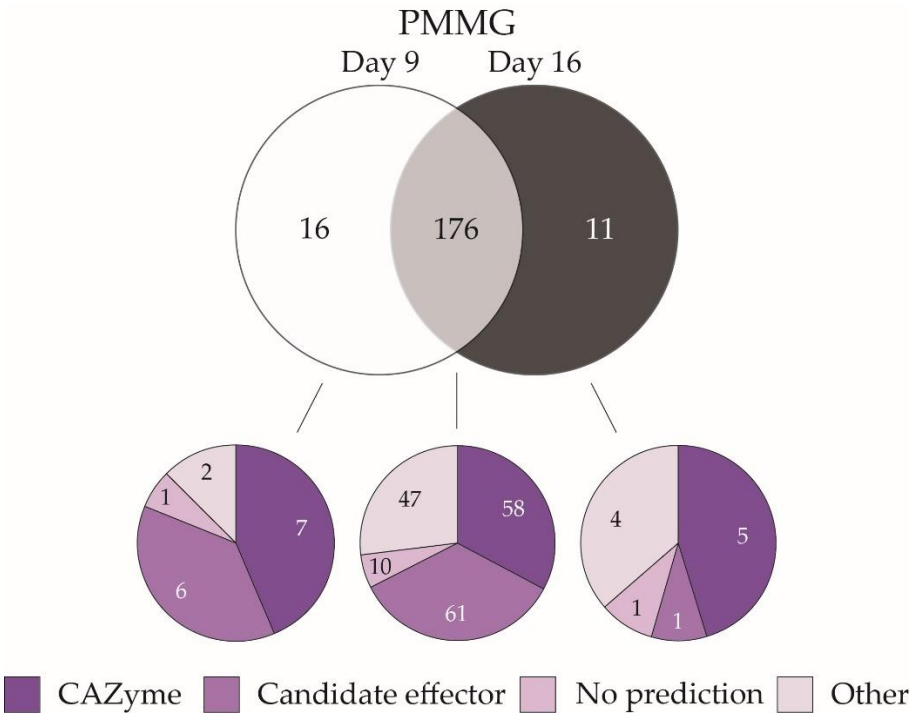

Figure 4.14. Classically secreted proteins produced by *Fulvia fulva* in early and late proteome samples in PMMG culture media, and the protein type. CAZyme, carbohydrate-active enzyme; PMMG, pine minimal salts medium.

Table 4.9. Classically secreted proteins produced by *Fulvia fulva* at different time points in PMMG culture samples.

	Normalised expression[2]					
Accession[1]	Iv	4 dpi	8 dpi	12 dpi	Protein type[3]	Protein domains[4]
Day 9						
UJO13947.1	4	152	287	280	CAZyme	Glycoside Hydrolase Family 17
UJO19640.1	5	168	21	275	CAZyme	Glycoside Hydrolase Family 43
UJO19274.1	15	0	230	164	CE (*CfEcp50-1*)	Hydrophobic surface binding protein A
UJO25033.1	4	180	3	3	CAZyme	Auxiliary Activity Family 7, FAD binding domain, Berberine and berberine like
UJO15145.1	7	92	1	1	CE	-
Day 16						
UJO22794.1	3	36	91	54	CAZyme	Glycoside Hydrolase Family 47
UJO18559.1	4	75	1	3	CAZyme	Polysaccharide Lyase Family 26, YetA-like protein

1 – GenBank protein accession from the NCBI website (https://www.ncbi.nlm.nih.gov/).

2 – Gene expression is shown for the 0WU orthologue of the Race 5 gene (identified as the top BlastP hit, **Materials and methods section 4.2.2.7**) as fragments per kilobase of exon per million fragments mapped (FPKM) and was sourced from a transcriptome study of a compatible interaction of H-Cf-0 tomato plants inoculated with *F. fulva* 0WU strain and sampled 4, 8, and 12 days post-inoculation (dpi), as well as *in vitro* (Iv; growth in potato dextrose broth for 4 days, 22°C (Mesarich et al., 2014)).

3 – Protein type determined by HMMER, InterPro, and EffectorP v3.0. analysis. Effectors were also identified from the protein description of the predicted secreted protein list (**Materials and methods section 4.2.2.7**), and candidate effectors (CEs) that were identified by Mesarich et al. (2018) were also included. For CEs, the encoding gene name was added in brackets.

4 – Predicted protein domains based on HMMER and DIAMOND prediction (https://bcb.unl.edu/dbCAN2/blast.php), as well as InterPro prediction, performed using Geneious software (v9.1.8.).

Proteins were only included if the encoding gene had >5-fold increase in gene expression between *in vitro* (Iv) and any *in planta* stage, and expression *in planta* >50 RPMK, or >25 RPMK for carbohydrate-active enzymes (CAZymes).

4.3.10 Proteome comparison between *D. septosporum* and *F. fulva*

To identify homologous proteins secreted in culture filtrate by either *D. septosporum* or *F. fulva*, or by both fungi, the proteomes were compared. From all proteins secreted by each fungus, 132 were specific to *D. septosporum*, 151 to specific to *F. fulva*, and 101 were homologous and secreted by both fungi (**Figure 4.15**). Of the homologous proteins, approximately 40% were candidate effectors.

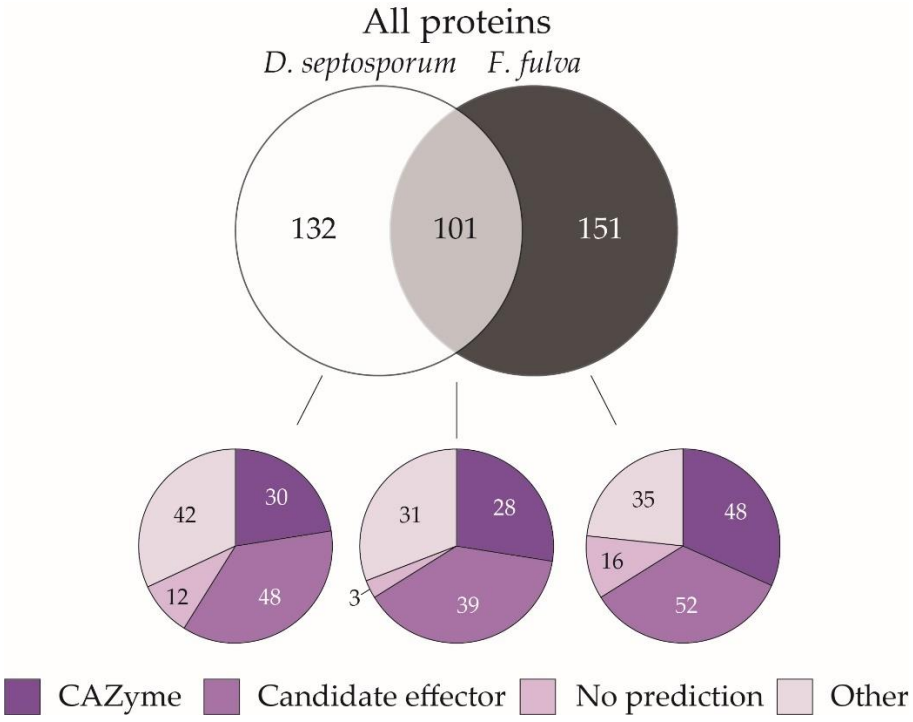

Figure 4.15. Comparison of classically secreted proteins produced by *Dothistroma septosporum* and *Fulvia fulva* in culture filtrate proteomes, and the protein type. CAZyme, carbohydrate-active enzyme.

The number of homologous proteins secreted in the PMMG Day 9 and Day 16 samples (the two conditions both fungi were cultured in) was examined. From the homologous proteins secreted in the PMMG Day 9 sample, six proteins were secreted by *D. septosporum*, 36 by *F. fulva*, and 52 were secreted by both fungi (**Figure 4.16**). Of the six homologous proteins secreted specifically by *D. septosporum*, two were upregulated *in planta* (**Appendix 29**). These included a predicted secretory lipase and a carbohydrate esterase which was also a candidate effector. These predicted functions in combination with the upregulated encoding gene expression at the late *in planta* stage, suggest that these proteins could play a role in necrotrophy. Of the 36 homologous proteins secreted specifically by *F. fulva* in the PMMG Day 9 sample, eight were

encoded by genes upregulated *in planta* (**Appendix 29**). Five of these proteins were candidate effectors, including the previously identified CfEcp20-1 (UJO14225.1), CfEcp20-3 (UJO16284.1), and CfEcp45 (UJO22670.1) (Mesarich et al., 2018).

Of the 52 homologous proteins secreted in the PMMG Day 9 sample by both *D. septosporum* and *F. fulva*, 10 were encoded by genes upregulated *in planta* in both fungi (**Table 4.10**). Of these 10 proteins, one was only detected in the Day 9 sample, a predicted CAZyme. The other nine proteins were detected in both the Day 9 and 16 samples. Of these nine proteins, three were "other" proteins, two were CAZymes, and four were candidate effectors. Two of the "other" proteins were predicted chloroperoxidases, which catalyse the chlorination of organic compounds (Ortiz-Bermúdez, Srebotnik, & Hammel Kenneth, 2003). Three other chloroperoxidases were identified as secreted by *D. septosporum* or *F. fulva* (**sections 4.3.4**, **4.3.5**, and **4.3.9**), and it would of interest to determine what role these proteins play in each fungus. One of the four candidate effectors was Ecp2-1 (Ds158381/UJO11627.1), a well characterised effector that is encoded by a gene highly expressed at all stages *in planta* in *F. fulva*, and at the mid stage in *D. septosporum*. Another of the candidate effectors was PhiA-2 (69113/UJO14439.1), which was identified as a candidate effector in *D. septosporum* by Hunziker (2018) and suggested through homology in other species to be important for sporulation (Hunziker, 2018; Melin, Schnürer, & Wagner, 2003).

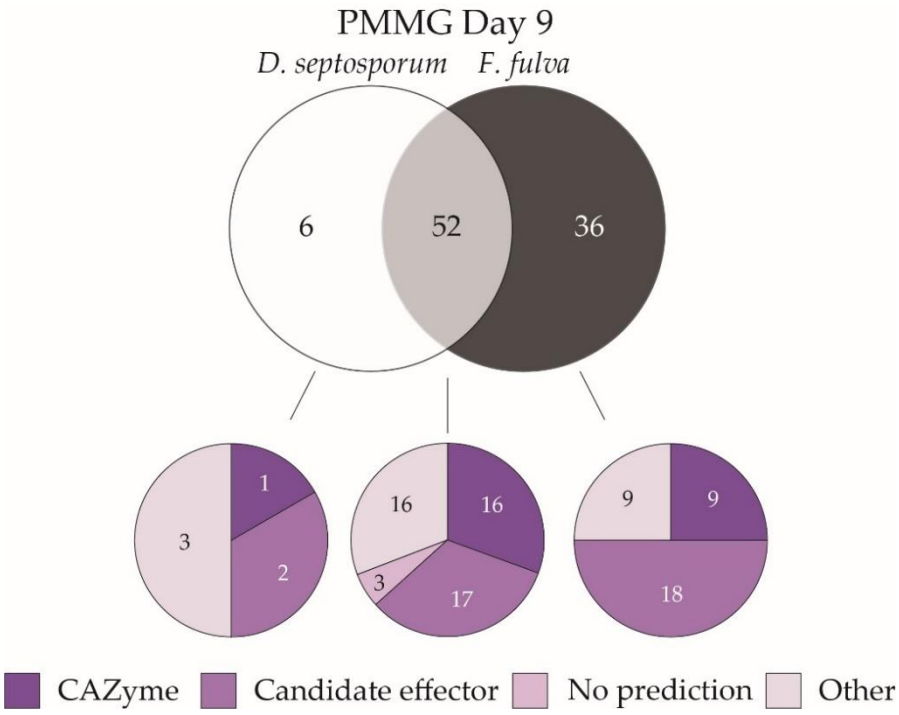

Figure 4.16. Homologous, conventionally secreted proteins of *Dothistroma septosporum* and *Fulvia fulva* produced in pine minimal salts medium (PMMG) Day 9 samples, and the protein type. For *D. septosporum*, the PMMG Day 9 samples without pine extract were compared.

Table 4.10. Homologous, classically secreted proteins produced by both *Dothistroma septosporum* and *Fulvia fulva* in PMMG.

	Normalised expression[2]					
JGI ID/Accession[1]	Iv	Early/4 dpi	Mid/8 dpi	Late/12 dpi	Protein type[3]	Protein domains[4]
PMMG Day 9						
75559/UJO24912.1	4/16	2/133	3/559	43/329	CAZyme	Auxiliary Activity Family 3, GMC oxidoreductase
PMMG Day 16						
70155/UJO22670.1	257/15	71/142	507/447	1303/240	CE (*FfEcp45/DsCPL1*)	Cerato-platanin
71018/UJO22853.1	31/7	32/217	154/2	310/133	CAZyme	Glycoside Hydrolase Family 3, Fibronectin type III-like
47355/UJO23674.1	5/1	10/169	15/24	28/95	CAZyme	Glycoside Hydrolase Family 32
PMMG Day 9 and PMMG Day 16						
158381/UJO11627.1	1/39	8/20415	244/85886	18/61577	CE (*Ff/DsEcp2-1*)	Ecp2 domain
72090/UJO24417.1	74/15	3629/897	134/37	496/29	CE	Ferritin-like domain
70420/UJO23128.1	8/0	22/752	8/5	192/17	CAZyme	Glycoside Hydrolase Family 5, Cellulase
75727/UJO15156.1	13/10	415/749	45/5	44/8	Other	Chloroperoxidase
73553/UJO20286.1	17/45	83/654	90/25	62/27	CE	-
69113/UJO14439.1	53/25	83/82	257/63	342/208	CE	-
75970/UJO16216.1	5/14	503/143	122/30	337/44	Other	Chloroperoxidase
74371/UJO21024.1	29/7	30/105	53/3	149/11	CAZyme	Glycoside Hydrolase Family 35, Beta-galactosidase
75835/UJO15271.1	10/8	314/105	17/7	367/53	Other	Carboxylesterase family

1 – For *D. septosporum* proteins, the Joint Genome Institute (JGI) protein ID from the *D. septosporum* genome page (https://mycocosm.jgi.doe.gov/Dotse1/Dotse1.home.html) is shown. For *F. fulva* proteins, the GenBank protein accession from the NCBI website (https://www.ncbi.nlm.nih.gov/) is shown.

2 – For *D. septosporum* proteins, the encoding gene expression is shown as Reads Per Million per Kilobase (RPMK) and was sourced from a transcriptome analysis performed on *D. septosporum*-infected *Pinus radiata* seedlings. Three *in planta* stages were sampled: early, mid, and late, as well as *in vitro* (Iv; growth in low Dothistroma medium (LDM) broth for 7 days, 22°C (Bradshaw et al., 2016)). For *F. fulva* proteins, gene expression is shown for the 0WU orthologue of the Race 5 gene (identified as the top BlastP hit, **Materials and methods section 4.2.2.7**) as fragments per kilobase of exon per million fragments mapped (FPKM) and was sourced from a transcriptome study of a compatible interaction of H-Cf-0 tomato plants inoculated with *F. fulva* 0WU strain and sampled 4, 8, and 12 days post-inoculation (dpi), as well as *in vitro* (Iv; growth in potato dextrose broth (PDB) for 4 days, 22°C (Mesarich et al., 2014)). Proteins were only included if the encoding gene from *D. septosporum* and *F. fulva* had >5-fold increase in gene expression between *in vitro* and any *in planta* stage, and expression *in planta* >50 RPMK, or >25 RPMK for carbohydrate-active enzymes (CAZymes).

3 – Protein type determined by HMMER, InterPro, and EffectorP v3.0. analysis. For *D. septosporum*, candidate effectors (CEs) predicted from other studies (Hunziker, 2018; Tarallo, 2022) were included. For *F. fulva*, effectors were also identified from the protein description of the predicted secreted protein list (**Materials and methods section 4.2.2.7**), and CEs identified by Mesarich et al. (2018) were also included. For CEs, the encoding gene name was added in brackets.
4 – Predicted protein domains based on HMMER and DIAMOND prediction (https://bcb.unl.edu/dbCAN2/blast.php), as well as InterPro prediction, performed using Geneious software (v9.1.8.). GMC: glucose-methanol-choline.

From the homologous proteins secreted in the PMMG Day 16 sample, 11 proteins were secreted specifically by *D. septosporum*, 14 by *F. fulva*, and 69 were secreted by both fungi (**Figure 4.17**). Details of the proteins secreted specifically by each fungus are shown in **Appendix 30**. Of the 69 proteins secreted by both *D. septosporum* and *F. fulva*, 12 were upregulated *in planta* by both species (**Table 4.10**). Nine of these proteins were also detected in the Day 9 sample and were discussed above. Of the remaining three proteins, one was the candidate effector CfEcp45 (UJO22670.1) which was detected in the Day 9 sample as secreted only by *F. fulva*. The other two proteins were CAZymes predicted to contain GH domains, including GH3, which has been shown to be important for virulence in *F. fulva* and other fungal phytopathogens (Bradley et al., 2022).

In summary, 101 homologous proteins were secreted by *D. septosporum* and *F. fulva* in the nutrient-poor PMMG samples, some of which were specific to the time point. Candidate effectors, including Ecp2-1 and PhiA-2, were identified to be secreted by both fungi and were upregulated *in planta*, making them of particular interest for further analysis.

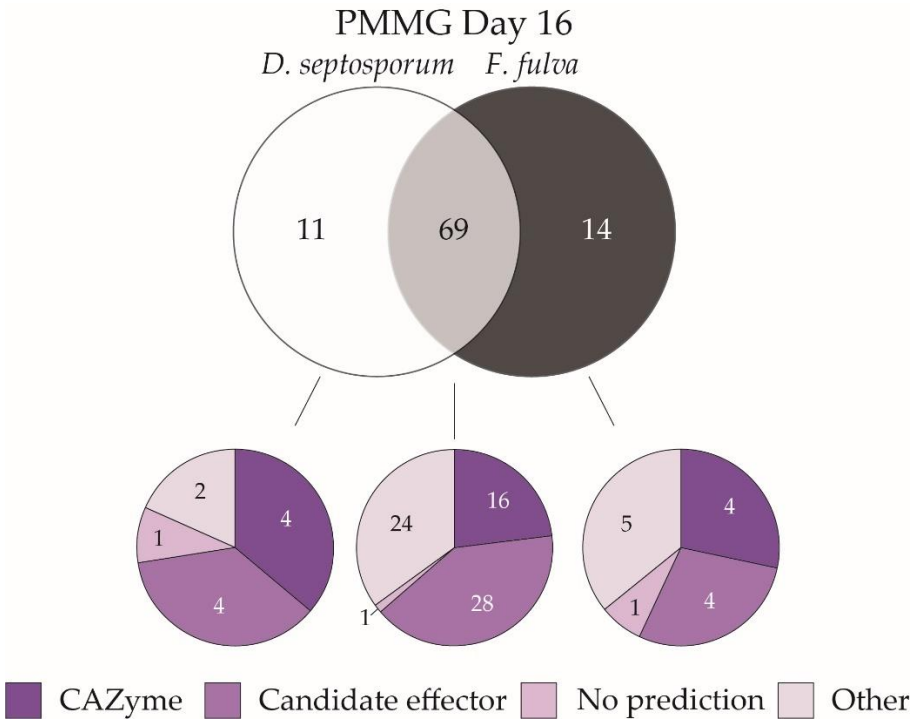

Figure 4.17. Homologous, classically secreted proteins produced by *Dothistroma septosporum* and *Fulvia fulva* proteins in pine minimal salts medium (PMMG) Day 16 samples, and the protein type.

4.4 Discussion

This chapter presents the first *in vitro* proteomes of *D. septosporum* and *F. fulva*, and their comparative analysis. Samples were analysed from nutrient-rich or nutrient-poor medium, at different time points and, for the *D. septosporum* samples, with and without the addition of pine extract. Proteomic analysis of *D. septosporum* culture filtrates revealed that pine extract had an effect on the secretome, and several candidate effectors, including known cell death elicitors, were secreted in the culture filtrate. Proteomic analysis of *F. fulva* culture filtrate identified many previously identified candidate effectors. Comparison of these two fungal secretomes identified ~100 homologous proteins that were secreted during growth in the same (PMMG) medium, including those with a potential role in virulence. This discussion will focus on trends observed from both secretomes, highlight key findings and proteins of interest, outline the limitations in this analysis, and provide suggestions for future work.

4.4.1 *D. septosporum* and *F. fulva* secreted abundant proteins in both nutrient-rich and nutrient-poor media

The different *in vitro* conditions had a strong effect on fungal growth and secreted protein content. For *D. septosporum*, fungal growth was greatly reduced in the nutrient-poor PMMG medium compared to the nutrient-rich LDM medium, as was evident from the dry mycelium weight (**section 4.3.1**). This trend was also observed for *F. fulva*, but this fungus was able to grow better than *D. septosporum* in the nutrient-poor PMMG medium (**Table 4.6**). Despite this, the number of proteins secreted by both fungi in the PMMG samples was considerable, suggesting that the low-nutrient medium was adequate to support protein production. Interestingly, for both proteomes, the number of unique proteins secreted in each sample was relatively low but was highest in the late nutrient-rich samples (9 d).

While the numbers of different types of secreted proteins were similar between the different samples, heatmap and PCA plot analysis identified differences in the protein content between samples. For *D. septosporum*, the largest differences in protein type were between the different time points of the nutrient-rich media samples, and between the early nutrient-poor media samples with and without the addition of pine extract (**Figure 4.5**). For *F. fulva*, the largest difference in protein type was between the nutrient-rich and nutrient-poor medium samples (**Figure 4.12**). It would be interesting to determine if these protein profiles remained consistent if protein quantity was considered as well as protein content. A limitation of this culture filtrate proteome was that proteins were only detected as present or absent. If this experiment was to be repeated, quantitative analysis could provide valuable insight into which proteins were

secreted in the highest abundance across different time points and media types. Regardless, as has been found in other studies (Bradley, 2022; Paper, Scott-Craig, Adhikari, Cuomo, & Walton, 2007), analysis of different media types has provided a detailed picture of the *in vitro* secretome of *D. septosporum* and *F. fulva*.

The culture filtrate proteomes of both *D. septosporum* and *F. fulva* contained many classically secreted proteins. Because the purpose of this experiment was to identify potential virulence factors, classically secreted proteins were the focus for analysis. However, it should be noted that for both proteomes, the classically secreted proteins made up only a small proportion of the total proteins detected. The large number of proteins detected that did not contain a signal peptide could be due to cytoplasmic contamination, as has been reported from other proteomic studies (Bradley, 2022; Gómez-Pérez et al., 2022). This was supported by the identification of several proteins with suggested association with the cytoplasm from *D. septosporum* (**Appendix 20**), and with mitochondria from *F. fulva* (**Appendix 25**). However, it is possible that some of the proteins without a signal peptide are secreted through nonconventional means (Vincent et al., 2020; Wang et al., 2017), and the inability to differentiate these proteins from cytoplasmic contaminants is another limitation of this analysis.

4.4.2 The *in vitro* proteomes of *D. septosporum* and *F. fulva* contain homologous proteins and support classification of *F. fulva* as a hemibiotroph

A high number of homologous proteins were classically secreted in the culture filtrate proteomes of both *D. septosporum* and *F. fulva*. When both fungi were cultured in the same conditions, the proportion of homologous secreted proteins was 50–70%, and highest in the later time point (**Figure 4.16**, **Figure 4.17**). This was an expected result, considering that 70% of gene content is homologous between these two fungi (de Wit et al., 2012). However, the culture filtrate proteome analysis further highlights the close relationship of *D. septosporum* and *F. fulva* and adds to the considerable comparative work that has been performed between these two fungi (Mesarich et al., 2023).

The culture filtrate proteome supports evidence for a hemibiotrophic lifestyle of *F. fulva*. *F. fulva* had long been regarded as a model species for biotrophic pathogens (de Wit et al., 2012), but over the last decade it has become apparent that this pathogen exhibits a more hemibiotrophic lifestyle (Hane et al., 2019; Mesarich et al., 2023; Ökmen et al., 2019). Necrosis and death of tomato leaves often occurs at the late stage of infection, often at time points beyond those observed in a typical two-to-three-week infection time course in a controlled laboratory greenhouse, which is typical for hemibiotrophs (Thomma et al., 2005). Furthermore, the genome

content of CAZyme-encoding genes in *F. fulva* is unusually high for a biotrophic pathogen (de Wit et al., 2012; Karimi-Jashni et al., 2022). Indeed, the number of different predicted CAZyme proteins detected in this culture filtrate proteome was proportionally equal to those detected in the proteome of *D. septosporum*, which is well established as a hemibiotroph (Kabir et al., 2015b). This was particularly evident in the samples where both fungi were cultured in the same conditions and supports the current classification of *F. fulva* as a hemibiotrophic pathogen. Unfortunately, this culture filtrate proteome was limited in the ability to identify proteins with possible roles in the necrotrophic stage, due to transcriptome data only being available for the biotrophic stage of *F. fulva* (Mesarich et al., 2014).

4.4.3 Proteins with a possible role in virulence were identified from the *D. septosporum* and *F. fulva in vitro* proteomes

Many of the classically secreted proteins from *D. septosporum* and *F. fulva* culture filtrate were candidate effectors, even though this was an *in vitro* rather than *in planta* study. For *F. fulva*, an *in planta* proteome was already available (Mesarich et al., 2018). For *D. septosporum*, attempts to establish an *in planta* experiment involving harvest of apoplastic washing fluid from pine was unsuccessful (**Appendix 17**). Instead, a nutrient-poor medium supplemented with pine extract was used to provide *in planta*-like conditions. Despite this limitation, several characterised effectors were detected from the culture filtrates of both fungi. Of particular interest is that some of these effectors were detected from the nutrient-rich media, as well as the nutrient-poor. Could it be possible that these proteins may play dual roles in virulence and *in vitro* growth? Proteins with dual functions have been identified in other fungal phytopathogens. Protein FvLcp1, from the maize pathogen *Fusarium verticillioides*, was suggested to bind chitin through LysM domains, as well as promoting biosynthesis of the mycotoxin fumonisin (Zhang et al., 2022). The Lysin (LysM) domain-containing effector Mg3LysM from *Zymoseptoria tritici*, causal agent of Septoria tritici blotch disease of wheat, was found to bind fungal chitin to block chitin-induced plant defences as well as contributing to lesion formation and asexual sporulation during infection (Marshall et al., 2011). Another gene from *Z. tritici*, *Zt6*, encodes a ribonuclease and was found to have toxicity towards wheat cells as well as other organisms, such as bacteria and yeast. The protein encoded by this gene was suggested to have a dual role as an elicitor of wheat cell death as well as function in antimicrobial competition (Kettles et al., 2018). Effectors with additional antimicrobial roles may be produced in culture as well as during infection of the host. Indeed, several *Venturia pyrina* homologues of *Verticillium dahliae* antimicrobial effector Ave1 (Snelders et al., 2020) are secreted in culture when grown in cellophane membranes (Cooke et al., 2014). For *F. fulva*, almost all candidate effectors were detected in all proteomic

samples (**Appendix 27**). Therefore, it is possible that some of these candidate effectors are secreted in culture because they have an antimicrobial role as well as a role in virulence. Regardless, the identification of characterised effectors from the culture filtrates of both fungi indicate that these *in vitro* proteomes are valuable for identifying effectors and other secreted proteins of interest.

To identify proteins with a possible role in virulence, those encoded by a gene upregulated *in planta* and above a defined expression threshold, were shortlisted. The *F. fulva* proteome was performed with the Race 5 strain because it is faster growing than the 0WU type-strain, has an available chromosome-level genome assembly (Zaccaron et al., 2022), and because it was also used for gene disruption analysis of *CfEcp11-1* in **Chapter 2**. However, this limited the analysis of the *F. fulva* proteome because transcriptome analysis has not been performed as part of an infection time course with this strain. Instead, gene expression was determined from the Race 5 homologues of the 0WU strain, for which transcriptome analysis based on an infection time course has been performed (Mesarich et al., 2014). From these shortlisted proteins, those with a potential role in virulence and secreted by *D. septosporum* or both *D. septosporum* and *F. fulva*, are discussed below. Due to the limited data available for the proteins secreted by *F. fulva* (gene expression only over the biotrophic stage, and no plant extract added), the only proteins of interest were those previously identified as candidate effectors in other studies. Therefore, while this proteome did not identify any new candidate virulence factors by examining the *F. fulva* proteome alone, it did further characterise the secretion of previously identified candidate effectors.

4.4.3.1 Homologous candidate effector and CAZyme proteins of interest were identified in the proteomes of *D. septosporum* and *F. fulva*

Several proteins of interest were secreted *in vitro* by both *D. septosporum* and *F. fulva*. In **section 4.3.10**, homologous proteins secreted under the same nutrient-poor conditions were analysed from the two fungi. Besides Cf/DsEcp2-1, which has been well characterised in both species (de Wit et al., 2012; Guo, Hunziker, et al., 2020), the other previously identified candidate effector type secreted by both fungi was CfEcp45/DsCPL1 (**Table 4.11**). These homologous proteins are predicted cerato-platanins encoded by genes upregulated *in planta* in both species, but most highly at the mid infection stage by *D. septosporum*. Cerato-platanins have been shown to play a role in virulence in other fungal phytopathogens (Eranthodi et al., 2022; S. Li et al., 2019; Pazzagli et al., 2014), and DsCPL1 was shortlisted as a candidate virulence factor of *D. septosporum* in **Chapter 3**. This protein was hypothesised to play a role in the necrotrophic

switch due to its gene expression profile and cell death-eliciting orthologue present in another pine pathogen, *Heterobasidion annosum sensu stricto* (Chen et al., 2015; Hunziker, 2018). The secretion of these homologous proteins by both fungi suggests an important role in virulence, and it would be of interest to test each protein in the corresponding host for a cell death-eliciting function.

Previously unidentified candidate virulence factors were secreted *in vitro* by both *D. septosporum* and *F. fulva*. Of the homologous proteins secreted under nutrient-poor conditions, proteins with predicted ferritin-like domains (Ds72090/UJO24417.1) were identified from both culture filtrates (**Table 4.11**). Iron is an essential element for both plants and fungi, and acquisition of iron plays an important role in pathogen virulence (Liu, Kong, Wu, & Ling, 2021; Verbon et al., 2017; Wang et al., 2020). These proteins may function in sequestering iron from the host apoplast, similar to how several *Verticillium dahliae* CFEM (Common in Fungal Extracellular Membrane) proteins are suggested to sequester iron from the host xylem, both to support fungal growth and starve the host of this important element (Wang et al., 2022). Indeed, both of the *D. septosporum* and *F. fulva* ferritin-like proteins are encoded by genes highly upregulated at the start of infection (**Appendix 21** and **26**), which coincides with the start of apoplastic colonisation (Bradshaw et al., 2016; Kabir et al., 2015b; Thomma et al., 2005). The secretion of these homologues by both fungi suggests these proteins may play a role in virulence and are of interest for further investigation.

Several homologous CAZymes of interest were secreted *in vitro* by both *D. septosporum* and *F. fulva*. These included two GH5 proteins (**Table 4.11**) which, as predicted cellulases, likely degrade the plant cell wall and play an important role in virulence (Ma et al., 2019; Ma et al., 2022; Prasanth, Viswanathan, Malathi, & Sundar, 2022). However, the high number of predicted GH5 proteins in both fungi (de Wit et al., 2012) suggests that there is likely to be redundancy in function and no single GH5 is an essential virulence factor. Regardless, secretion of both homologous GH5 proteins *in vitro* suggests that these proteins may be of interest for future CAZyme analysis of these fungi. Other homologous CAZymes secreted by both fungi included predicted Glycoside Hydrolase Family 3, 32, and 35 proteins, as well as predicted Auxiliary Activity Family 3 proteins (**Table 4.11**). These CAZyme families are not well studied, apart from GH3, of which some GH3 proteins in other phytopathogenic fungi function to detoxify host-derived saponins (Bradley et al., 2022). Although a specific role may be unknown, many different CAZymes have been shown to function as elicitors or virulence factors (Ma et al., 2015; Quoc & Chau, 2017), and the secretion of these homologues in both *D. septosporum* and *F. fulva* suggests an important role in both fungi.

Table 4.11. Proteins of particular interest identified from the culture filtrate proteomes of *Dothistroma septosporum* and *Fulvia fulva*.

Accession[1]	Protein prediction	Gene upregulation *in planta*	Thesis section(s)
D. septosporum			
Biotrophic stage			
51311 (*DsEcp20-1*)	Candidate effector	All stages	4.3.4, 4.4.3.2
72090	Ferritin-like domain	Early stage	4.3.10, 4.4.3.1
Necrotrophic switch			
71018	Glycoside Hydrolase Family 3, Fibronectin type III-like	Mid and late stage	4.3.5, 4.3.10, 4.4.3.1
70694 (*DsEcp20-3*)	Candidate effector	Mid stage	4.3.5, 4.4.3.2
27299	Nis1 family	Mid and late stage	4.3.5, 4.4.3.2
70155 (*DsCPL1*)	Candidate effector, Cerato-platanin	Mid and late stage	4.3.5, 4.3.10, 4.4.3.1
Necrotrophic stage			
70420	Glycoside Hydrolase Family 5, Cellulase	Late stage	4.3.5, 4.3.10, 4.4.3.1
74371	Glycoside Hydrolase Family 35, Beta-galactosidase	Late stage	4.3.10, 4.4.3.1
F. fulva			
Biotrophic stage			
UJO22670.1 (*CfEcp45*)	Candidate effector, Cerato-platanin	8 dpi	4.3.10, 4.4.3.1, 4.5
UJO24417.1	Candidate effector, Ferritin-like domain	4 dpi	4.3.10, 4.4.3.1
UJO22853.1	Glycosyl hydrolase family 3, Fibronectin type III-like	4 and 12 dpi	4.3.10, 4.4.3.1, 4.5
UJO21024.1	Glycoside Hydrolase Family 35, Beta-galactosidase	4 dpi	4.3.10, 4.4.3.1
UJO23128.1	Glycoside Hydrolase Family 5, Cellulase	4 dpi	4.3.10, 4.4.3.1

1 – If the protein is a previously identified candidate effector, the gene name is given in brackets.

4.4.3.2 Candidate effector and CAZyme proteins of interest were identified in the *D. septosporum* culture filtrate proteome

Several previously identified candidate effector proteins of interest were secreted *in vitro* by *D. septosporum*, including DsEcp20-1 and DsEcp20-3 (**Table 4.11**). These two proteins were first shortlisted as candidate effectors by Hunziker (2018), as well as likely orthologues of effector candidates CfEcp20-1 and CfEcp20-3 of *F. fulva* (Mesarich et al., 2018). These proteins have since been described as part of a conserved apoplastic effector family, and DsEcp20-3 (but not DsEcp20-1) was shown to elicit cell death in non-host *Nicotiana* species as well as the *P. radiata* host (Tarallo et al., 2022). Furthermore, another member of this effector family from *F. fulva*, CfEcp20-2, was recently shown to be required for full virulence on the tomato host (Karimi-Jashni et al., 2022). In the *D. septosporum* culture filtrate proteome, DsEcp20-1 was secreted specifically in *in planta*-like conditions (nutrient-poor medium with pine extract) and is suggested to play a role in virulence. In contrast, DsEcp20-3 was secreted specifically in the late nutrient-rich sample and is encoded by a gene upregulated at the mid *in planta* stage. Taken together, these results suggest that DsEcp20-3 may function at the necrotrophic switch although, because it is part of an effector family, there is likely to be redundancy in function.

A previously unidentified candidate effector of *D. septosporum* was detected in the culture filtrate proteome: protein Ds27299, which has a Nis1 family domain (**Table 4.11**). Proteins with the Nis1 domain are part of a family of core effectors, conserved across a wide range of fungi (Irieda et al., 2019; Yoshino et al., 2012). Nis1 proteins from several different fungal pathogens have been shown to interact with and inhibit PRR (pattern recognition receptor)-associated kinases to suppress pathogen-associated molecular pattern (PAMP)-triggered immunity (PTI) (Irieda et al., 2019). The Nis1 protein from *Colletotrichum orbiculare* was shown to play a role in virulence on the *N. benthamiana* host, and the *Magnaporthe oryzae* Nis1 protein was shown to be crucial for infection on barley and rice (Irieda et al., 2019). The *D. septosporum* Nis1 protein was detected specifically in the early nutrient-poor sample and is encoded by a gene upregulated at the late stage *in planta* (**Table 4.11**). Interestingly, *F. fulva* also has a predicted Nis1 protein (UJO21232.1), but it was not detected in the culture filtrate proteome (**Appendix 25**). It would be of interest to perform gene disruption analysis with the *D. septosporum Nis1* gene and test the mutant for virulence on the pine host.

4.4.4 Conclusions

In summary, analysis of the *D. septosporum* and *F. fulva* culture filtrate secretomes provided unique insights into these two closely related pathogens. This analysis provided further evidence

to support a hemibiotrophic lifestyle for *F. fulva* and, should transcriptome data become available for the necrotrophic stage, this secretome could facilitate identification of necrotrophic effectors from this pathogen. Characterised effector proteins as well as new candidate virulence factors were identified from both fungi, illustrating that analysis of *in vitro* secretomes of fungal phytopathogens can be a valuable tool for identifying proteins with a possible role in virulence. The next logical step after identification of candidate virulence factors, is to characterise protein function and test for a role in virulence. Due to time constraints, candidate virulence factors identified from this chapter could only be examined by gene deletion analysis in one fungus. In the next chapter, two *D. septosporum* candidate virulence factors, one of which was detected in this culture filtrate proteome, will be disrupted by CRISPR/Cas9 and assessed for virulence in the *P. radiata* host.

MASSEY UNIVERSITY
TE KUNENGA KI PŪREHUROA
UNIVERSITY OF NEW ZEALAND

GRADUATE RESEARCH SCHOOL

STATEMENT OF CONTRIBUTION
DOCTORATE WITH PUBLICATIONS/MANUSCRIPTS

We, the student and the student's main supervisor, certify that all co-authors have consented to their work being included in the thesis and they have accepted the student's contribution as indicated below in the Statement of Originality.

Student name:	Hannah Margaret McCarthy
Name and title of main supervisor:	Prof. Rosie E. Bradshaw
In which chapter is the manuscript/published work?	Chapter 5
What percentage of the manuscript/published work was contributed by the student?	60%

Describe the contribution that the student has made to the manuscript/published work:

Methodology, investigation, writing—original draft preparation, writing—review and editing, and visualisation.

Please note the published work only accounts for approximately 25% of Chapter 5 - the other 75% of Chapter 5 is entirely the work of Hannah McCarthy.

Please select one of the following three options:

(●) The manuscript/published work is published or in press

Please provide the full reference of the research output:

McCarthy HM, Tarallo M, Mesarich CH, McDougal RL, Bradshaw RE. Targeted Gene Mutations in the Forest Pathogen Dothistroma septosporum Using CRISPR/Cas9. Plants (Basel). 2022 Apr 8;11(8):1016. doi: 10.3390/plants11081016. PMID: 35448744; PMCID: PMC9025729.

( ) The manuscript is currently under review for publication

Please provide the name of the journal:

( ) It is intended that the manuscript will be published, but it has not yet been submitted to a journal

Student's signature:	Hannah McCarthy Digitally signed by Hannah McCarthy Date: 2023.02.24 09:19:49 +13'00'	Main supervisor's signature:	Bradshaw, Rosie Digitally signed by Bradshaw, Rosie Date: 2023.02.24 09:12:52 +13'00'

This form should be placed at the beginning of each relevant thesis chapter.

Chapter 5 - Functional analysis of candidate Dothistroma septosporum virulence factors by CRISPR/Cas9 gene editing

5.1 Introduction

Of the tools available to characterise gene function, targeted mutation by gene deletion or disruption is among the most definitive in identifying a role in virulence. This approach is based on the careful analysis of interaction phenotypes observed between pathogen mutants and their plant hosts and is of utmost importance to our understanding of how plant pathogens cause disease. The pathogen–host interactions database (PHI-base) exemplifies this approach by providing an inventory of curated pathogen gene mutations that affect disease phenotypes (Urban et al., 2020). The increased availability of genome sequences and associated *in planta* transcriptome data has facilitated the identification of candidate genes from plant pathogens that can be tested for roles in virulence, pathogenicity, or other types of interactions. However, the application of molecular tools such as targeted gene deletion or disruption in forest pathology is almost nonexistent compared to their use in agricultural and horticultural settings (Dort, Tanguay, & Hamelin, 2020).

Genomic and transcriptomic resources for *D. septosporum* (Bradshaw et al., 2016; de Wit et al., 2012) have enabled the identification of candidate virulence factor genes (Hunziker et al., 2021) (**Chapter 3**). In **Chapter 4**, the *D. septosporum in vitro* secreted proteome was presented as a new resource to identify candidate virulence factors. Targeted gene deletion has been performed regularly in *D. septosporum* using the traditional method of homologous recombination based on protoplast transformation, followed by virulence assessment on the *P. radiata* host, with the aim of determining gene function. For example, genes involved in biosynthesis of the anthraquinone toxin dothistromin were deleted by this method and revealed dothistromin to be a virulence factor in DNB (Kabir et al., 2015a). Other deleted *D. septosporum* genes include potential virulence and avirulence genes (Guo, Hunziker, et al., 2020; Ozturk et al., 2019), as well as those involved in gene regulation (Chettri et al., 2012; Chettri et al., 2018). However, in *D. septosporum* the homologous recombination method is inefficient, with only a small proportion of transformants being gene deletion mutants.

To improve the efficiency of targeted gene mutation in *D. septosporum* and given the success of CRISPR/Cas9 gene editing in *F. fulva* in **Chapter 1**, this technology was trialled as one of the objectives for this thesis. Clustered regularly interspaced short palindromic repeats, or CRISPR, is part of an adaptive immune system in prokaryotes that protects against invasion from phages

and plasmids (Barrangou et al., 2007; Mojica et al., 2005). CRISPR operates through two main components: Cas nuclease proteins which cut the DNA to produce a double-strand break (DSB) and CRISPR RNAs (crRNAs) which direct the Cas protein (Brouns et al., 2008) to the protospacer adjacent motif (PAM) site (Deveau et al., 2008). In prokaryotes, genetic memory of previous viral invasions can be stored as CRISPR spacers and used to make crRNAs to defend against subsequent invasions (Barrangou et al., 2007; Deveau et al., 2008). For the use of CRISPR/Cas9 as a gene editing technology, the crRNA is adapted to a single guide RNA (sgRNA) (Jinek et al., 2012) and designed to match to an existing PAM site in the target gene, allowing specific gene editing (Gasiunas, Barrangou, Horvath, & Siksnys, 2012; Jinek et al., 2012).

Since the first report of CRISPR/Cas9 gene editing in filamentous fungi (Liu, Chen, Jiang, Zhou, & Zou, 2015), this technology has been used in many different fungal species (Schuster & Kahmann, 2019), including plant pathogens (Dort et al., 2020; Gosavi et al., 2020). Pathogenic Dothideomycete species where CRISPR/Cas9 technology has been successfully applied include *Alternaria alternata* (Wenderoth et al., 2017), *Leptosphaeria maculans* (Idnurm et al., 2017), *Parastagonospora nodorum* (Khan, McDonald, Williams, & Solomon, 2020) and *Venturia inaequalis* (Rocafort, Arshed, et al., 2022). Notably, in *P. nodorum*, CRISPR/Cas9 gene editing technology was recently used to characterise the *SnTox5* gene, showing that it encodes a virulence factor responsible for inducing programmed cell death and facilitating mesophyll colonization in wheat (Kariyawasam et al., 2021).

In **Chapters 3** and **4**, candidate virulence factors of *D. septosporum* were identified through bioinformatic and proteomic analysis. The transcription factor gene *Ds69328* and candidate effector gene *DsCE3* were selected to be functionally analysed by gene disruption and virulence assessment on the *P. radiata* host. Because CRISPR/Cas9 technology had not been applied to *D. septosporum* previously, it was first trialed using the dothistromin regulator gene *DsAflR*, which has a visible phenotype when disrupted. Subsequently, CRISPR/Cas9 was used to disrupt candidate virulence factor genes *Ds69328* and *DsCE3*, and the transformants tested for virulence on the *P. radiata* host. The work presented in this chapter will aid future characterisation of candidate virulence factors from *D. septosporum*, as well as from other Dothideomycete species.

5.2 Materials and methods

5.2.1 Culturing of *Dothistroma septosporum*

Wild type (WT) *D. septosporum* strain NZE10 (de Wit et al., 2012) was used in this study. The WT fungus, CRISPR/Cas9 transformants, and complementation transformants were routinely cultured as described in **Chapter 4** (**Materials and methods section 4.2.1.1**). To facilitate visual phenotype screening for dothistromin production in *DsAflR* transformants, the DM medium was supplemented with 100 µg/mL $CuSO_4.5H_2O$ to elevate dothistromin production. For spore production, *D. septosporum* was cultured as described in **Chapter 3** (**section 3.2.1.1**).

5.2.1.1 Single spore or mycelium purification

To obtain pure cultures, CRISPR/Cas9 transformants of *DsAflR*, *Ds69328*, and *DsCE3* (transformant 2 only) were single spore-purified. To achieve this, spores were harvested (**Chapter 4**, **Materials and methods section 4.2.1.2**) from a DM plate and 50 µL of spore suspension streaked onto a new DM plate using an inoculation loop. After incubation, a single colony was cultured onto a DM plate to generate enough spores to repeat the spore streak a second time. For the other *DsCE3* CRISPR/Cas9 and complementation transformants, purification was performed with ground mycelium, as this method was considerably faster. In this process 50 µL of ground mycelium was streaked with an inoculation loop onto a DM plate, then a resulting single colony was ground in 50 µL of sterile MilliQ water and streaked again onto a new DM plate to make two rounds of purification.

5.2.1.2 Culturing for genomic DNA (gDNA) extraction

For gDNA extraction, *D. septosporum* was cultured in one of two ways. One method was to culture *D. septosporum* on DM agar overlaid with cellophane for 7 days at 22°C then scrape off the grown mycelium for gDNA extraction. The other method was to inoculate *D. septosporum* in 25 mL of DM broth in a 125 mL flask, using ~200 µL ground mycelium and incubated with shaking at 160 rpm (classic series C10 platform shaker (New Brunswick Scientific)) for 7 days at 22°C. Mycelium was then harvested by filtration through a sterile nappy liner or Miracloth (EMD Millipore Corp.).

5.2.2 gDNA extraction from *D. septosporum*

gDNA was extracted from *D. septosporum* using three different methods, depending on the purpose. For high-quality gDNA, required for methods such as Southern hybridization and qPCR, a hexadecyltrimethylammonium bromide (CTAB) DNA extraction method developed by Doyle (1987) was used, with adaptions detailed by Guo (2015). For methods that did not require high-

quality DNA, such as PCR screening of CRISPR/Cas9 transformants, a rapid gDNA extraction method was used. gDNA from the *DsAflR* CRISPR/Cas9 transformants was extracted using the simple salts/ethanol precipitation method of Liu et al. (2000). However, this method produced gDNA of very low quality. Therefore, for PCR screening of the other CRISPR/Cas9 transformants (*Ds69328*, *DsCE3*, and complements), gDNA was extracted using a further modified version of the CTAB method (Doyle & Doyle, 1987). For this, mycelium was ground in a microcentrifuge tube with a micro pestle. Then, 600 µL CTAB buffer was added and mixed, and the tubes incubated at 65°C for 40 min with occasional mixing by inversion. After cooling at room temperature for 2 min, 600 µL of chloroform was added and mixed by inversion then, after a 2 min incubation, the tubes were centrifuged at 13,000 rpm (HeraeusTM Pico 17 microcentrifuge (Thermo Fisher Scientific)) for 5 min. The supernatant was transferred to a new tube and centrifuged again at the same speed. The supernatant was then transferred to a new tube, 600 µL isopropanol added and mixed by inversion, and the tubes kept at -20°C for at least 20 min. The tubes were then centrifuged at 6,500 rpm for 5 min to sediment the DNA. About 80% of the isopropanol was removed by careful pipetting, without disturbing the DNA pellet. Then 600 µL 70% ethanol was added, mixed by inversion, and centrifuged again at the same speed. The 70% ethanol was removed, then this ethanol wash step was repeated one more time. Traces of ethanol were removed by pipetting and the tubes air-dried for 10 min. The DNA was resuspended in 30–50 µL MilliQ water, then 0.5–1 µL 20 mg/mL RNase added and the tubes incubated at 37°C for 10 min. The gDNA was then stored at -20°C. gDNA concentration and quality were determined using a Nanodrop® ND-1000 UV-Vis spectrophotometer and Nanodrop® software version 3.1.0 (Nanodrop Technologies Inc.).

5.2.3 Construction of CRISPR/Cas9 plasmid with sgRNA

Selection of the CRISPR sgRNA is an important part of the CRISPR/Cas9 transformation process that can impact the transformation efficiency. Two sgRNAs targeting the *DsAflR* gene, and one targeting each of *Ds69238* and *DsCE3*, were selected from the first exon (**Table 5.1**); this location maximizes the effects of any frameshift mutations that might be caused during DSB repair (Doench et al., 2014). The sgRNAs were identified using the "find CRISPR sites" tool in Geneious (v9.1.8 software) and those with the highest on-target activity score and an off-target score of 100% were selected (**Table 5.1**). After the sgRNAs were selected, they were designed and inserted into the CRISPR plasmid Cas9HygAMAccdB, using methods described previously (Rocafort, Arshed, et al., 2022). Plasmids were extracted (**Chapter 2**, **Materials and methods section 2.2.2.2**), screened by PCR (**Chapter 2**, **Materials and methods section 2.2.2.5**), and sequenced (**Chapter 2**, **Materials and methods section 2.2.2.8**). PCR and sequencing were

performed using primer M139, which binds in the Cas9HygAMAccdB plasmid, and the reverse sgRNA protospacer primer which binds to the sgRNA (all primers used in this work are listed in **Appendix 31**). All plasmids used in this study are listed in **Appendix 32**.

Table 5.1. CRISPR/Cas9 sgRNA protospacers used to target *Dothistroma septosporum* genes.

sgRNA protospacer target	Sequence (5'–3') [1]	Binding site (bp)	Direction	Off-target sites [2]	Off-target score [3]	On-target activity score [4]
AflR 1	TCACGCGGCTCAGAGTCGAGCGG	Exon 1 (10–32)	Forward	0	100%	0.692
AflR 2	ACAAGAAGCAGCAGATAGGAGGG	Exon 1 (267–289)	Forward	0	100%	0.703
Ds69328	GAATACACAGAAGCACGCGGAGG	Exon 1 (59–81)	Forward	0	100%	0.780
DsCE3	GACTGCGCCAGCAAATACAACGG	Exon 1 (97–119)	Forward	0	100%	0.800

1 - Underlined bases are the protospacer adjacent motif (PAM) sites.

2 - Off-target sites found in the coding sequence (CDS) of the *D. septosporum* NZE10 genome, using Geneious (v9.1.8).

3 - Off-target score calculated using Geneious (v9.1.8) by scoring against the *D. septosporum* genome, based on Hsu et al. (2013), where scores are between 1 and 100 and a high score indicates low off-target activity.

4 - On-target activity score based on sequence features of the sgRNA, calculated using Geneious (v9.1.8). The score is from 0–1, with a score closer to 1 indicating higher on-target activity; based on Doench et al. (2016).

5.2.4 Construction of donor DNA plasmid for CRISPR/Cas9 transformation

The donor DNA (dDNA) plasmid, which acts a template for homologous recombination repair, was constructed with two 1 kb homologous flanks of the gene of interest (*Ds69328* or *DsCE3*), with the geneticin resistance gene *nptII* cassette (P*trpC*-*nptII*-T*trpC*) in between. The homologous flanks started 3 bp from the DSB on either side (which occurs 3 bp downstream from the PAM site) (Jinek et al., 2012) and were amplified from WT *D. septosporum* gDNA by PCR (**Chapter 2**, **Materials and methods section 2.2.2.5**). Primer positions are shown in the results (**section 5.3.3**), and the primer sequences are listed in **Appendix 31**. The *nptII* cassette was amplified from the plasmid *pII99* (Lara-Ortíz, Riveros-Rosas, & Aguirre, 2003), while the plasmid *pAN7-1* (Punt et al., 1990), which is a Gibson Assembly-compatible plasmid, was the backbone for the dDNA plasmid assembly. All PCRs were performed with Phusion High-Fidelity DNA polymerase (New England Biolabs), and the products were extracted by column or gel extraction (**Chapter 2**, **Materials and methods section 2.2.2.3**). The fragments were then assembled via Gibson Assembly (Gibson et al., 2009), using 0.02 pmol/fragment, and transformed into DH5α *E. coli* cells by chemical transformation (**Chapter 2**, **Materials and methods section 2.2.3.1**). The correct assembly was verified by sequencing (**Chapter 2**, **Materials and methods section 2.2.2.8**, primers listed in **Appendix 31**), and a schematic of the *DsCE3* dDNA plasmid is shown in **Appendix 33**. All plasmids used in this study are listed in **Appendix 32**. The dDNA plasmid was then linearized with the *Nde*I (New England Biolabs) restriction enzyme (**Chapter 2**, **Materials and methods section 2.2.2.11**) prior to fungal transformation.

5.2.5 Construction of complementation plasmids

The complementation plasmids were constructed by sticky-end restriction enzyme cloning. The target gene and surrounding sequence (up to 1 kb on each side, depending on proximity of neighbouring genes) was amplified using primers with restriction sites *Apa*I or *Xba*I added at their 5' ends, using Phusion High-Fidelity DNA Polymerase (as per the manufacturer's protocols), and the products purified by column or gel extraction (**Chapter 2**, **Materials and methods section 2.2.2.3**). Because *DsCE3* had a *Xba*I restriction site within the coding sequence, the sequence was first amplified with overlapping primers which mutated the *Xba*I site without disrupting the amino acid sequence (primers listed in **Appendix 31**).

Plasmid pBC-phleo (Silar, 1995), containing the phleomycin resistance gene *Phleo*, was digested with restriction enzymes *Apa*I and *Xba*I (**Chapter 2**, **Materials and methods section 2.2.2.11**) and gel-extracted (**Chapter 2**, **Materials and methods section 2.2.2.3**). The PCR products and

digested plasmid were ligated using T4 ligase (NEB) as per the manufacturer's protocol, with a 16°C overnight incubation. The ligation mixture was transformed into DH5α *E. coli* cells by chemical transformation (**Chapter 2**, **Materials and methods section 2.2.3.1**), and transformants screened by PCR with the same primers used to amplify the genes. Plasmid DNA was then extracted (**Chapter 2**, **Materials and methods section 2.2.2.2**), and sequencing performed with the same primers (primers listed in **Appendix 31**). A schematic of the *DsCE3* complementation plasmid is shown in **Appendix 34**. All plasmids used in this study are listed in **Appendix 32**.

5.2.6 CRISPR/Cas9 gene disruption of *D. septosporum* genes

5.2.6.1 Generation of *D. septosporum* protoplasts and PEG transformation

Protoplasts were generated from *D. septosporum* as reported previously (Bradshaw, Bidlake, Forester, & Scott, 1997), except flasks were inoculated with mycelium fragments and incubated at 22°C for 6–7 days. To digest the cell walls, 10 mg/mL Glucanex lysing enzyme (Novozymes, Copenhagen, Denmark) was used, and the flasks incubated at 30°C for 12–16 h, with shaking at 100 rpm (Ecotron, INFORS-HT, Switzerland). Transformation was performed as reported previously (Bradshaw et al., 1997) but with several modifications. Protoplasts were diluted to 1.25 x 10^8 protoplasts/mL in STC (Sorbitol, Tris-HCl, and $CaCl_2$) buffer (Bradshaw et al., 1997), then to 80 µL of this protoplast suspension, 20 µL 40% polyethylene glycol (PEG) solution (40% PEG 4000, 50 mM $CaCl_2$, 50 mM Tris-HCl, 1M sorbitol) was added. The Cas9HygAMAccdB plasmid and dDNA plasmid (if using) were added to the protoplast solution, vortexed briefly and left on ice for 30 min. Then, a further 900 µL 40% PEG solution was added, mixed, and the mixture left at room temperature (~20°C) for 20 min.

The protoplasts were then plated by mixing 100 µL of the protoplast suspension with 3.5 mL molten (50°C) regeneration medium (RG: 50 g/L malt extract (Oxoid, Basingstoke, UK), 23 g/L nutrient broth (Oxoid), 0.8 M sucrose, 0.8% bacteriological agar (Pure Science)) and overlaying an RG plate (15 mL, 1.5% bacteriological agar). Plates were incubated overnight at 22°C, then a 5 mL overlay of 0.8% RG was added containing antibiotics for the entire plate. Plates were incubated at 22°C for at least 2 weeks before transformants appeared.

For disruption of *DsAflR*, 5 µg Cas9HygAMAccdB plasmid (1 µg/µL) was used, with the transformation plates containing 70 µg/mL hygromycin B (Roche), for selection of the plasmid. For disruption of *Ds69328*, 3 µg of Cas9HygAMAccdB plasmid and 5 µg of linearized dDNA plasmid was used, while for *DsCE3*, 3 µg of Cas9HygAMAccdB plasmid and 3.9 µg of dDNA plasmid was used. For both *Ds69328* and *DsCE3*, the transformation plates contained 70 µg/mL

hygromycin B and 100 µg/mL geneticin (Life Technologies, California, USA), for selection of the Cas9HygAMAccdB plasmid and dDNA, respectively. For complementation of *Ds69328* and *DsCE3*, 5 µg of complementation plasmid was used, and plates contained 100 µg/mL geneticin and 30 µg/mL Zeocin™/phleomycin (InvivoGen, California, USA), for selection of the dDNA and complementation plasmid, respectively.

5.2.6.2 Sub-culturing CRISPR/Cas9 and complementation transformants

Transformants that grew on the *DsAflR* transformation plates were transferred to 12-well DM plates, sub-cultured to standard DM plates, and then purified (**Materials and methods section 5.2.1.1**) on DM plates (all media contained 70 µg/mL hygromycin B). After PCR and sequence analysis of the *DsAflR* transformants, it was suggested that culturing on hygromycin selection for an extended period may have resulted in high selection pressure for maintaining the Cas9HygAMAccdB plasmid, which contained the hygromycin resistance cassette. Therefore, in subsequent transformations the transformants were immediately sub-cultured to media without hygromycin.

For disruption of *Ds69328* and *DsCE3*, the transformants were transferred from the transformation plates to 12-well DM plates, then sub-cultured to standard DM plates (all media containing 100 µg/mL geneticin to select for insertion of the *nptII* cassette, as part of the dDNA) for purification (**Materials and methods section 5.2.1.1**). For complementation of *Ds69328* and *DsCE3*, transformants were transferred from the transformation plates to DM and purification performed (all media contained 30 µg/mL zeocin and 100 µg/mL geneticin, **Materials and methods section 5.2.1.1**). After purification, all transformants were maintained on DM without selection.

5.2.6.3 Screening CRISPR/Cas9 and complementation transformants

Transformants were screened by PCR (**Chapter 2**, **Materials and methods section 2.2.2.5**), and PCR products sequenced (**Chapter 2**, **Materials and methods section 2.2.2.8**). All primers used are listed in **Appendix 31**.

Confirmation of gene disruption was achieved by Southern hybridization. DNA for the probe was PCR amplified from WT *D. septosporum* gDNA using Phusion High-Fidelity DNA polymerase (New England Biolabs). The PCR product was gel or column-purified (**Chapter 2**, **Materials and methods section 2.2.2.3**) and, if necessary, several reactions combined to obtain ~100 ng total DNA then speed vacuum-concentrated as needed. The probe DNA was digoxigenin (DIG)-

labelled using a DIG High Prime DNA Labelling and Detection Starter Kit I (Roche), and labelling efficiency determined according to the manufacturer's instructions.

For Southern hybridization, ~2 µg of gDNA from WT and transformed *D. septosporum* strains was digested at 37°C overnight with restriction enzymes (New England Biolabs): *Hin*dIII or *Xho*I for *DsAflR* transformants, *Eco*RV or *Hin*dIII for *Ds69328*, and *Eco*RI or *Hin*dIII for *DsCE3*, then resolved overnight at 30V on a 0.8% agarose gel. After that, DNA was transferred to a positively charged nylon membrane (Roche) and blotted overnight according to Southern (1975). DNA transfer and fixation, hybridization of the DIG-labelled probe, and immunological detection was performed by enzyme immunoassay using the DIG High Prime DNA Labelling and Detection Starter Kit I (Roche), following the manufacturer's instructions with the following modifications. Prior to hybridization, the membrane was washed with 2 x SSC and fixed under a UV crosslinker Cex-800 (Ultra Lum, California, USA). Hybridization was performed in a glass hybridization tube at 42°C overnight in a 400 HY hybridization oven (Bachofer, Baden-Württemberg, Germany).

5.2.6.4 Thin layer chromatography of *DsAflR* transformants

The presence of dothistromin in *DsAflR* transformants was assayed by thin layer chromatography (TLC) as reported previously (Chettri et al., 2012), except that flasks were inoculated with mycelium fragments, incubated for 7 days, and the TLC was run in toluene:acetone (80:20) solvent acidified with 1% formic acid.

5.2.6.5 Copy number determination by quantitative PCR

To determine the copy number of complementation genes in complementation transformants, qPCR analysis (**Chapter 2**, **Materials and methods section 2.2.2.6**) was performed with 50 ng WT and complementation transformant gDNA using primers that amplify the target gene (*Ds69328* or *DsCE3*) and a single-copy reference gene (*DsAflR*, JGI ID: 75566). From the standard curves (**Chapter 2**, **Materials and methods section 2.2.2.6**) the primer efficiencies (E) were determined to be: *DsAflR* (E=1.93), *Ds69328* (E=2), *DsCE3* (E=1.98). Primer sequences are listed in **Appendix 31**. The Ct ratio between the target and reference gene of the WT and the complementation transformant gDNA was calculated (**Materials and methods section 2.2.2.7**) to determine the copy number.

5.2.7 Morphology assessment of *D. septosporum* transformants

To determine whether the gene-disrupted and complementation transformants had different *in vitro* growth characteristics compared to the WT, sporulation and radial growth were measured. To assess sporulation, 50 µL of spore solution (1 x 10^5 spores/mL) was spread over PMMG plates,

with three replicate plates per strain. After seven days of incubation at 22°C, 2 mL of sterile MilliQ water was added, and after 10 min the spores were dispersed with a plate spreader. The spores were harvested by pipetting and the spore concentration determined with a haemocytometer, with the tube weighed to determine volume and thus calculate the total number of spores per plate.

For radial growth assessment, a DM plate with a confluent mat of *D. septosporum* mycelia was used to generate agar plugs using a sterile cork borer (7 mm diameter). Three DM plates, each with three agar plugs, were inoculated per strain and incubated for three weeks at 22°C. Radial growth was then measured at one and three weeks post-inoculation across two perpendicular axes and the growth rate calculated as mm/day. For both sporulation and radial growth assessments, T-tests were performed in Microsoft© Excel (as a two-tailed distribution, with two-sample equal variance), to determine if any strains were significantly different to WT.

5.2.8 Virulence assay of *D. septosporum* transformants on *P. radiata*

5.2.8.1 *P. radiata* seedlings

To test the virulence of *D. septosporum* CRISPR/Cas9 mutants and complementation transformants compared to WT, they were inoculated onto *P. radiata* seedlings. The pine seeds were provided by the Radiata Pine Breeding Company (RPBC) and were from a cross of two parents with similarly low levels of *D. septosporum* resistance. The seeds were germinated at Scion (Rotorua, New Zealand) and the seedlings grown in small root trainer pots (2 x 2 cm^2). The pine seedlings were then transferred to Massey University (Palmerston North, New Zealand), where they were transplanted to pots (9 x 9 cm^2) with standard garden potting mix. The pine seedlings were grown in a glasshouse at ambient temperature, except for 8 weeks outside in a shade house over the summer. At the time of inoculation, the pine seedlings were ~16 months old and ~40 cm tall.

Pine seedlings were brought into the laboratory on the day of inoculation. Where possible, four replicate pines were each sprayed with approximately 50 mL of 1.6 $x10^6$ *D. septosporum* spores/mL. For several strains, a concentration of 1.6 x 10^6 spores/mL was not obtained and, due to time constraints, spore harvesting could not be repeated so it was necessary to inoculate fewer replicate seedlings and/or lower spore concentrations. Details of the pine replicates, volume and concentration of spores used for each *D. septosporum* strain are in **section 5.3.9**.

5.2.8.2 Inoculation of *P. radiata* seedlings with *D. septosporum* spores

Inoculation of the pine seedlings was performed as described by Kabir, Ganley, and Bradshaw (2013). Spores were harvested (**Chapter 4**, **Materials and methods section 4.2.1.2**) and sprayed onto seedlings using a sterile universal bottle with a plastic bottle sprayer head screwed onto the lid. After the pines were sprayed, they were air-dried for 20 min, then each pine was covered with a clean plastic sleeve (Petri dish bag) to maintain a high level of needle wetness for the first five days.

5.2.8.3 Inoculation chamber set-up and infection course

The pines were incubated in growth chambers (**Figure 5.1**) that consisted of a large plastic container with a plastic frame over the top, covered in sheets of plastic. An opening was cut in the plastic sheet at the top of the chamber to allow ventilation when opened. Two custom-made water misters/foggers were placed in the bottom of each growth chamber, and water added to cover the misters. The pines were placed on top of plastic tip boxes so that they were raised above the water level, and were distributed so that the biological replicates were separated into different chambers. To maintain a high level of needle wetness, the water in the bottom of the chambers was maintained at the optimum level, and sterile water was sprayed over the top of the pines once or twice a day, as required.

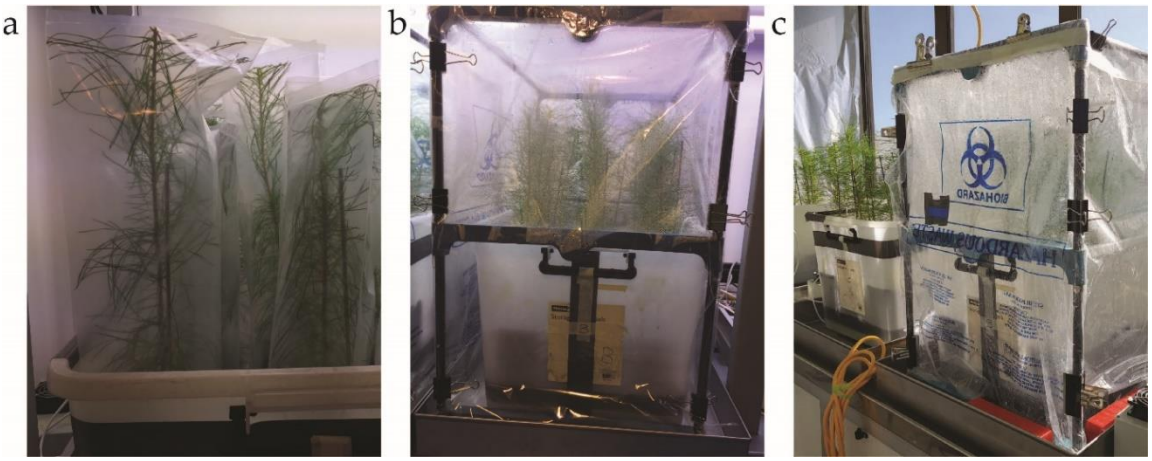

Figure 5.1. Growth chambers for virulence assessment of *Dothistroma septosporum* CRISPR/Cas9 mutants and complementation strains on Pinus radiata seedlings. (**a**) After inoculation, each pine was covered in a plastic sleeve for five days to maintain high needle wetness. (**b**) Growth chamber consisting of a plastic container, covered by a plastic frame and sheets of plastic (biohazard bags). (**c**) One growth chamber with

plastic frame removed (left) and another (right) covered by the plastic frame with misters functioning (condensation is visible).

Due to the only plant growth room with natural light at Massey University being unavailable at the start of the experiment, for the first two weeks of the experiment the pines were maintained in the growth chambers in another plant growth room with an artificial light source (12 h light/12 h dark photoperiod with 180 µmol/m^2/s) at 22°C. During this period only about two thirds of the pines had been inoculated due to some strains not producing enough spores in the first harvest. After two weeks, the remainder of the pines were inoculated and all the pines and growth chambers were moved to the plant growth room with natural light (~15 to 750 µmol/m^2/s depending on the weather) at 22°C with ~80% humidity and maintained there for the rest of the time. For the staggered inoculations ('Experiments 1 and 2'), each Experiment had seedlings inoculated with WT *D. septosporum* of a similar spore concentration to the transformed strains so that comparisons could be made. Details of the experimental set up and inoculations are shown in **Appendix 35a**.

5.2.8.4 Sample harvesting and virulence assessment by visual analysis and fungal biomass determination

Ten weeks after inoculation, the needles were removed from each tree and separated (through visual inspection) into three categories: (1) green and healthy needles with no Dothistroma needle blight (DNB) symptoms, (2) needles with DNB symptoms (as described in **Chapter 1 section 1.3.2**), or (3) dead needles (no DNB symptoms, and needles dead and/or dry). The dead needles were discarded, while the healthy needles were stored at 4°C until counted. The needles with DNB symptoms were also stored at 4°C for up to two days before examining by eye and with a dissecting microscope to confirm the DNB lesions. The numbers of needles with visual DNB symptoms were counted and compared with the total number of needles (healthy plus infected DNB needles) to calculate the percentage of needles with disease lesions. Lesions were harvested for gDNA extraction by cutting 1–2 mm either side with a scalpel and collecting in a pre-weighed microcentrifuge tube. The number of lesions harvested was recorded.

The cut lesions were snap-frozen in liquid nitrogen, freeze-dried, and the dry weight determined. gDNA was first extracted using the modified CTAB method (**Materials and methods section 5.2.2**), but the resulting gDNA could not be amplified by qPCR unless the samples were diluted 10-fold, presumably due to contaminants that were co-purified as part of the extraction process (**Appendix 35c**). Several modifications of the CTAB method, as well as different gDNA extraction

kits were tested, and the Plant Genomic DNA Mini Kit (Geneaid, New Taipei City, Taiwan) was found to be the most successful. Therefore, gDNA from the rest of the samples was extracted using this kit, following the manufacturer's instructions. The gDNA concentrations were quantified using a Qubit™ dsDNA HS Assay Kit (Thermo Fisher Scientific) in an Invitrogen™ Qubit™ 3 Fluorometer (performed by the Massey Genome Service). The gDNA was then used in qPCR analysis (**Chapter 2**, **Materials and methods section 2.2.2.6**) and the resulting Ct values used to estimate the fungal biomass in two different ways. The first method involved relative quantification of the fungal biomass compared to the pine using primers (detailed in **Appendix 35c**) targeting the *D. septosporum* target gene polyketide synthase A (*DsPksA,* JGI ID: 48345) and the *P. radiata* reference gene cinnamyl alcohol dehydrogenase (*CAD*), as described by Chettri et al. (2012). Because the Ct values from amplification of *CAD* were very high, it was suggested that the *P. radiata* gDNA in the dead (lesion) needle tissue may have degraded. Therefore, another analysis method was used that did not involve comparison with the pine *CAD* Ct values. This method involved absolute quantification of the fungal biomass based on *DsPksA* amplification and use of a *DsPksA* standard curve (Ct value vs gDNA concentration, **Chapter 2**, **Materials and methods section 2.2.2.6**, **Appendix 35d**). For both of these methods, the fungal biomass was normalised in two different ways: by the number of lesions used for gDNA extraction, and also by the dry weight of lesion material used in the DNA extraction.

5.3 Results

5.3.1 Establishment of CRISPR/Cas9 gene editing in *D. septosporum*

In **Chapter 3**, candidate virulence factors *Ds69328* and *DsCE3* were selected for characterisation by gene disruption and virulence analysis. As CRISPR/Cas9 had not been performed in *D. septosporum* previously, a preliminary trial targeting *DsAflR* was performed to determine the efficiency of this gene editing method and to optimise this protocol for *D. septosporum*. This preliminary trial was performed without a repair template and, to facilitate screening, *DsAflR* was selected due to the visual phenotype exhibited by deletion mutants (Chettri 2013). Following the success of CRISPR/Cas9 disruption of *DsAflR*, the results of which were recently published (McCarthy, Tarallo, Mesarich, McDougal, & Bradshaw, 2022), candidate virulence factors *Ds69328* and *DsCE3* were disrupted using donor DNA (dDNA) with a selective marker, and virulence analysis was performed on the *P. radiata* host.

5.3.1.1 Transformation of *D. septosporum* with CRISPR/Cas9 and sgRNAs targeting *DsAflR* yielded a high percentage of dothistromin-deficient transformants

CRISPR/Cas9 editing of *DsAflR* was performed using two different sgRNA protospacers to increase the chance of obtaining a disrupted transformant. Both protospacers had high on-target activity scores of ~0.7 and targeted the start of exon 1 (**Figure 5.2**). After CRISPR/Cas9 transformation, nine transformants from sgRNA *AflR*1 grew on the transformation plates, and 128 transformants from sgRNA *AflR*2. After two rounds of sub-culturing on DM with hygromycin selection, one transformant was obtained from sgRNA *AflR*1, and 47 transformants from sgRNA *AflR*2.

From a preliminary phenotypic screen, three transformants had a dothistromin-producing phenotype similar to the WT fungus and therefore appeared to have an intact *DsAflR* gene. However, 45 transformants (including the one from sgRNA *AflR*1) were suggested to be *DsAflR* mutants because they had a dothistromin-deficient phenotype, as indicated by the absence of red-brown pigmentation in the surrounding media they were cultured on. One of these transformants (#118) had a delayed dothistromin-deficient phenotype, producing dothistromin at the first sub-culture but exhibiting a dothistromin-deficient phenotype in all following sub-cultures (**Appendix 38**). It is likely that because transformants were maintained on DM agar with hygromycin selection until purification, the Cas9HygAMAccdB plasmid was under selection and Cas9 was still active to disrupt *DsAflR*. Representative samples of transformants with dothistromin-producing and dothistromin-deficient phenotypes, as well as TLC analysis showing presence or absence of dothistromin production, are shown in **Figure 5.3**.

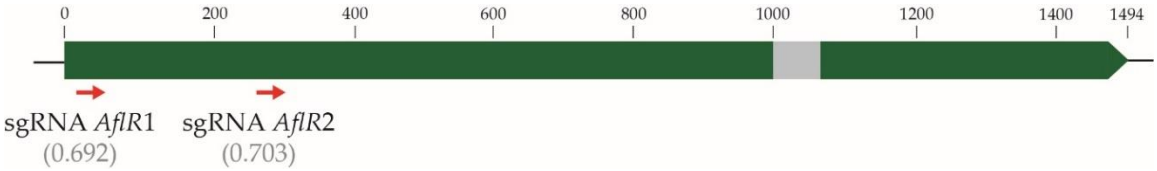

Figure 5.2. Schematic of single guide RNA (sgRNA) protospacer locations in *DsAflR*. The *DsAflR* gene is shown with the two exons as green bars and the intron as a grey bar. The two sgRNA protospacers are shown by red arrows illustrating they are in a 5'–3' direction. Protospacer sgRNA *AflR*1 targets position 10–32 bp from the start of the coding sequence, while sgRNA *AflR*2 targets 267–289 bp. On-target activity score is shown in grey underneath the protospacer name. Base pair numbers are shown above the *DsAflR* gene.

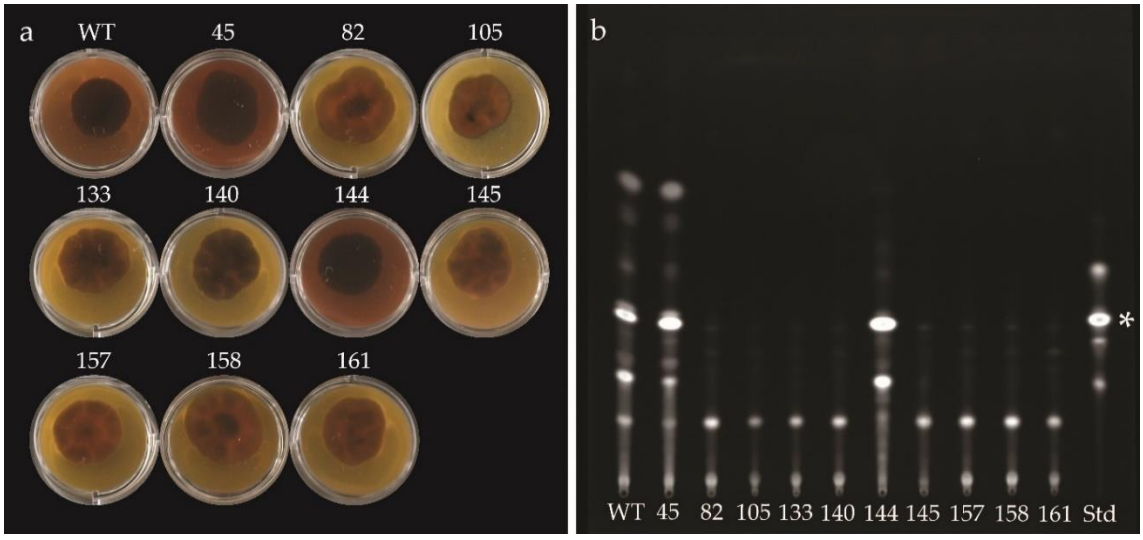

Figure 5.3. Presence or absence of dothistromin from wild type (WT) *Dothistroma septosporum* and CRISPR/Cas9 *DsAflR* transformants selected for investigation. (**a**) Visual analysis of dothistromin production when grown on Dothistroma medium (DM) supplemented with 100 µg/mL $CuSO_4.5H_2O$ (known to enhance dothistromin production; **Appendix 39**). The presence of dothistromin is shown by red-brown pigmentation of the media, as seen in DM supporting growth of the WT fungus and transformants 45 and 144. Transformants were photographed four weeks post-inoculation. (**b**) Thin layer chromatography (TLC) analysing dothistromin production in *DsAflR* transformants and WT fungus. The position of dothistromin is shown in the standard (Std), highlighted with a white asterisk. Dothistromin is visible in the samples representing the WT fungus and transformants 45 and 144.

As a starting point to verify which transformants were *DsAflR* mutants, and to identify what types of mutations were caused by CRISPR/Cas9 gene editing, PCR screening was performed

using primers HM89/HM90 that bind either side of *DsAflR* (**Figure 5.4**). Only four transformants gave a PCR product the same size as the WT fungus (1.6 kb); three of these had a dothistromin-producing phenotype in a visual screen (37, 45, and 144), while transformant 140 was dothistromin-deficient. Two transformants (145 and 158) gave larger PCR products than the WT fungus, whilst all other transformants screened either did not have a PCR product or had several non-specific PCR products. Together these results suggested that over 90% of the CRISPR/Cas9 transformants had a mutation in the *DsAflR* gene that led to the dothistromin-deficient phenotype.

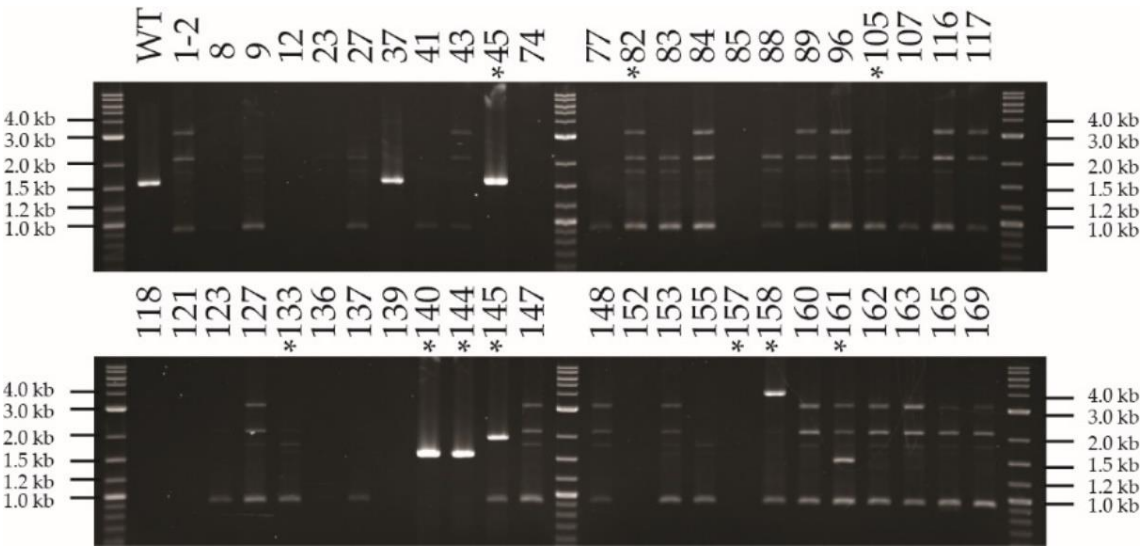

Figure 5.4. PCR screen of *Dothistroma septosporum DsAflR* CRISPR/Cas9 transformants to amplify the full-length *DsAflR* gene sequence. PCR was performed with gDNA using primers HM89 and HM90 that bind either side of *DsAflR*. Wild type (WT) and transformant number are at the top of the gel images. All transformants were obtained with sgRNA *AflR*2, except 1–2 which was with sgRNA *AflR*1. Those that were selected for further study are labelled with an asterisk. Because a crude gDNA extraction method (**Materials and methods section 5.2.2**) was used which generated low-quality gDNA, amplification of *β-tubulin* (JGI ID: 68998) was also performed as a control (**Appendix 40**). This gene was amplified successfully from the gDNA of all transformants except 134 (removed from the *DsAflR* screen).

5.3.1.2 A single nucleotide deletion and insertions ranging from 387 bp to 2.8 kb were identified among *DsAflR* CRISPR/Cas9 transformants of *D. septosporum*

The different types of mutations caused by CRISPR/Cas9 gene editing were investigated in a subset of ten transformants (all from sgRNA *AflR*2). Subset selection was based on transformants that gave a specific PCR product of WT size or larger, as well as a representative selection of

transformants that displayed different patterns of non-specific PCR amplification. The dothistromin phenotypes and TLC profiles of these ten transformants, showing the presence or absence of dothistromin, are shown in **Figure 5.3**.

A PCR analysis was then carried out using gDNA from the ten transformants (**Figure 5.5**) and selected PCR products were sequenced (**Figure 5.6**). Southern blot analysis with two restriction enzymes was also performed to confirm the results (**Figure 5.7**). As in the preliminary screen, a PCR with primers HM89/HM90 gave a 1.6 kb product with gDNA from the WT fungus and transformants 45, 140, and 144 (**Figure 5.5b**). Sequencing of these PCR products confirmed that transformants 45 and 144 have the WT *DsAflR* sequence and are therefore not *DsAflR* disruptants, as suggested from their dothistromin-producing phenotype and TLC profile (**Figure 5.3**). Transformant 140 did not appear to produce dothistromin (**Figure 5.3**) despite the WT-sized PCR product, and sequencing identified a single adenine nucleotide deletion at the double-strand break (DSB) site, resulting in a frame-shift mutation (**Figure 5.6b**). These results were further supported by WT-sized fragments obtained from transformants 45, 140, and 144 in Southern hybridizations (**Figure 5.7**).

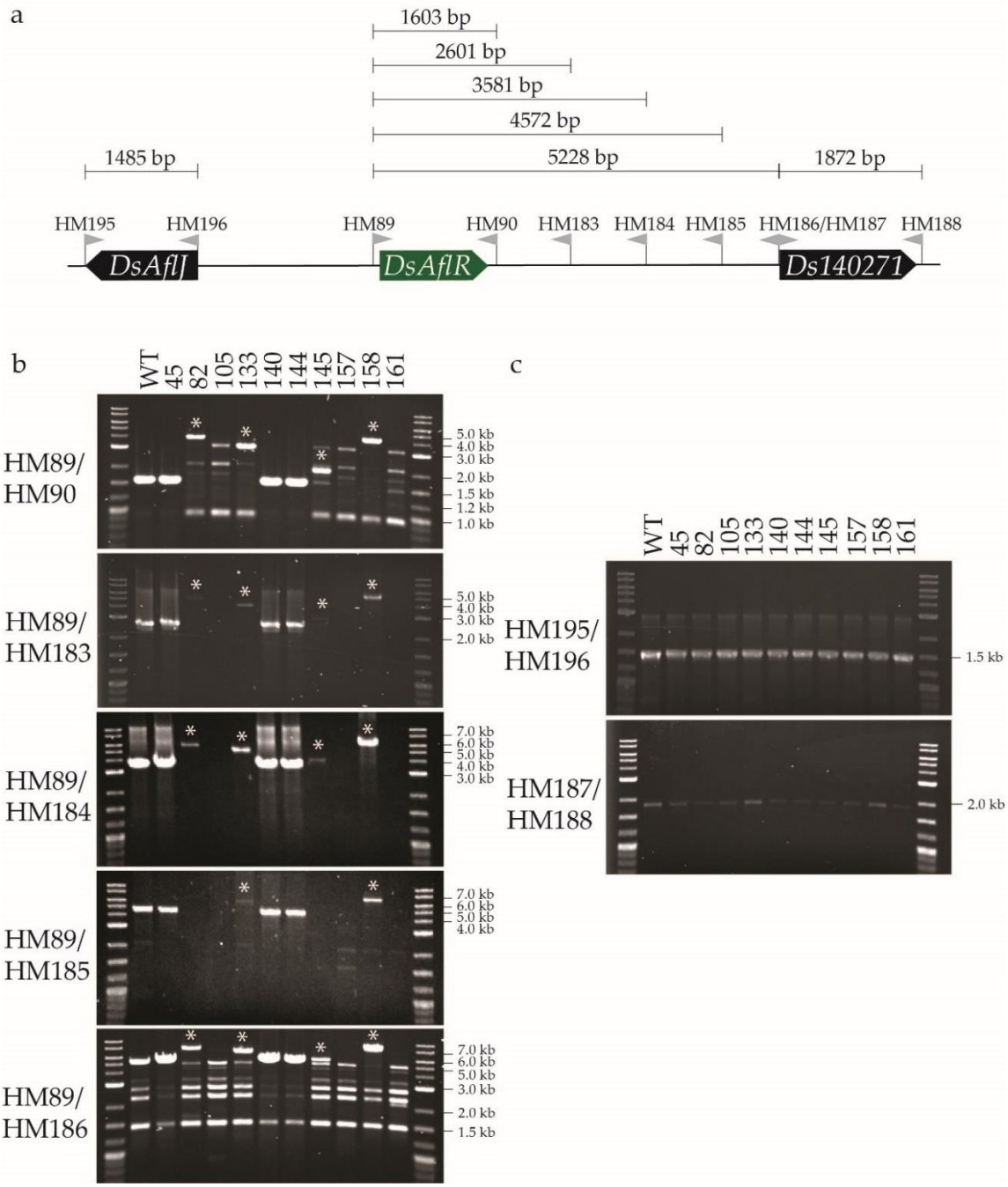

Figure 5.5. PCR screening to characterise *Dothistroma septosporum DsAflR* CRISPR/Cas9 transformants. (**a**) Primers used to screen the *DsAflR* region. The green bar is *DsAflR*, and the black bars are flanking genes, labelled with either their name or JGI protein ID. Positions of primers are illustrated by grey flags with the primer name above. Distances between the primer pairs are shown above the primers. (**b**) PCR screen of the *DsAflR* gene and the intergenic region between *DsAflR* and *Ds140271*. (**c**) PCR screen of the genes upstream and downstream of *DsAflR*. The name of each transformant screened is shown at the top of each group of gel pictures. PCR products larger than wild type (WT)-sized PCR products are labelled with a white asterisk. Relevant labels of the DNA ladder are shown to the right of each gel picture and the primers used in each PCR are shown on the left.

A PCR product larger than that from the WT fungus (1.6 kb) was amplified from transformants 82 (4.2 kb), 133 (3.5 kb), 145 (2.3 kb) and 158 (4.4 kb), consistent with the preliminary PCR screen (**Figure 5.5b**). Insertions of various sizes, ranging from 387 nt to 2.8 kb, were estimated from the *DsAflR* PCR (HM89/HM90) product sizes, with additional evidence from full sequence analysis of smaller PCR products (**Figure 5.6**). The site of insertion in these transformants was at the DSB site or up to 2 nt downstream towards the protospacer adjacent motif (PAM) site (**Figure 5.6b**). Southern hybridization analysis of gDNA digested with *Hin*dIII or *Xho*I showed that each of these four insertion transformants (82, 133, 145, 158) lacked a band corresponding to the WT *DsAflR* gene, confirming their status as *DsAflR* mutants (**Figure 5.7**). Transformants 82, 133, and 158 had the expected *Xho*I fragments but smaller *Hin*dIII hybridizing bands than expected indicative of extra *Hin*dIII sites in the inserted DNA. Transformant 145 was unusual in showing larger hybridizing bands for both *Hin*dIII and *Xho*I digests (**Figure 5.7**), despite being the transformant with the smallest insertion of 387 bp. These results are unusual and not supported by the previous PCR analysis, suggesting that whole genome sequencing would be required to determine the full extent of CRISPR/Cas9 editing in this transformant.

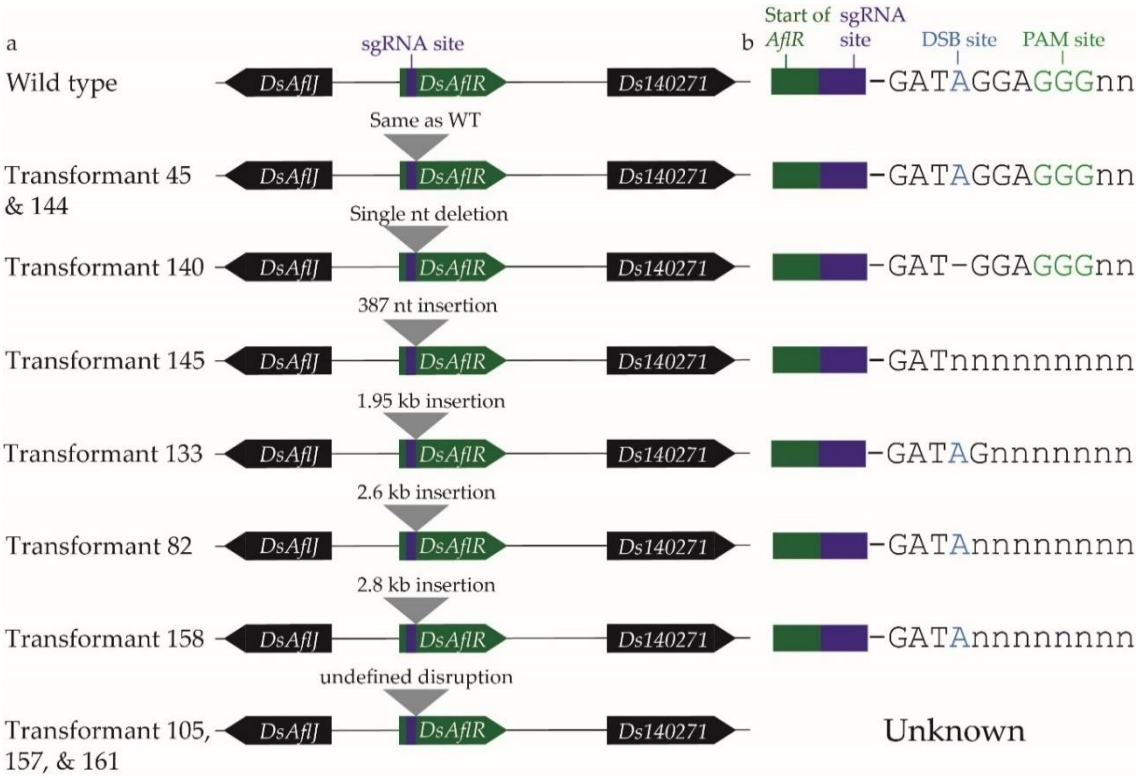

Figure 5.6. Summary of mutations identified from *Dothistroma septosporum DsAflR* CRISPR/Cas9 transformants. (**a**) Visual representation of the *DsAflR* locus including flanking genes in each transformant. The purple bar in *DsAflR* is the CRISPR/Cas9 sgRNA *AflR*2 binding site. Mutations, if present,

are indicated by a grey triangle and labelled with the type of mutation identified through phenotype, PCR analysis, and PCR amplicon sequencing. (**b**) The specific locations within the sgRNA *AflR*2 binding site where CRISPR/Cas9 disruptions were observed. The sgRNA *AflR*2 binding site is 23 bp; the end with the double-strand break (DSB) site (in blue) and protospacer adjacent motif (PAM) site (in green) are shown as nucleotides, and the rest is illustrated by a purple bar. Where a transformant had an insertion, the insertion start position is shown through truncation of the sgRNA *AflR*2 binding site sequence. The single nucleotide deletion in transformant 140 is shown by a dash in the sequence. For transformants 105, 157, and 161, no PCR amplification was achieved in the *DsAflR* region, therefore no sequencing was performed (labelled "unknown").

gDNA from transformants 105, 157, and 161 did not give a specific PCR product (**Figure 5.5b**), consistent with the preliminary PCR screen. It is possible that these transformants contain a large indel (insertion or deletion) that could not be captured by the PCR screen using primers HM89/HM90. To investigate this, primers were designed to amplify the genes either side of *DsAflR*: *DsAflJ* and *Ds140271*. As expected, the WT fungus and all transformants for which a PCR product was obtained from the *DsAflR* screen showed amplification of these two neighbouring genes. Interestingly, gDNA of transformants 105, 157, and 161 also amplified *DsAflJ* and *Ds140271* (**Figure 5.5c**). This suggested that if these transformants each contained a large indel, it did not disrupt the genes located either side of *DsAflR*.

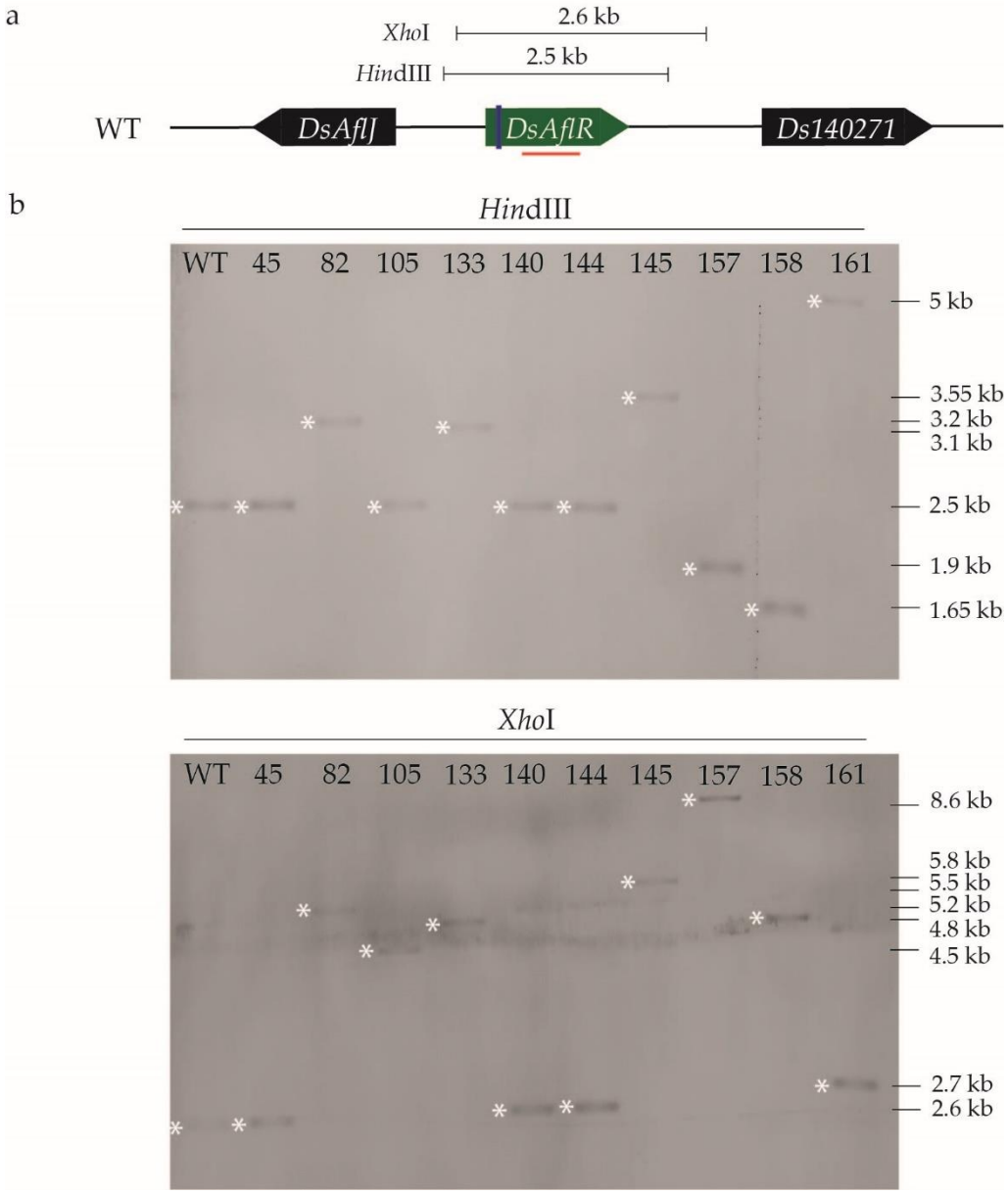

Figure 5.7. Southern hybridization analysis of *Dothistroma septosporum DsAflR* CRISPR/Cas9 transformants. (**a**) Schematic of the wild type (WT) *DsAflR* locus and positions of the restriction sites and probe. The green bar is *DsAflR*, the black bars are flanking genes, the purple line within *DsAflR* is the sgRNA *AflR*2 site, and the red line is where the probe binds. Restriction sites and distances between them are shown above. (**b**) Southern hybridization of digested genomic DNA from WT *D. septosporum* and *DsAflR* CRISPR/Cas9 transformants of this fungus using *Hin*dIII and *Xho*I. A digoxigenin (DIG)-11-dUTP-labelled probe bound to a region of *DsAflR* downstream of the sgRNA *AflR*2 site. Hybridizing fragments are marked with an asterisk and sizes are labelled on the right.

To identify the hypothesized indel in these three transformants (105, 157, 161), primers were designed at ~1 kb intervals between *DsAflR* and *Ds140271* (**Figure 5.5a**). PCR amplification of the set of 10 transformants using the HM89 forward primer with each of the nested reverse

primers HM183, HM184, HM185 and HM186 (**Figure 5.5b**) gave PCR products consistent with those expected based on PCR results with the *DsAflR* gene HM89/HM90 primers. In some cases, the PCR products were very faint, or non-specific bands were observed, the latter occurring in all samples for the widely spaced HM89/HM186 primer pair (the largest distance apart in this primer series). Interestingly, for the putative large-indel transformants 105, 157, and 161, none of the PCRs involving the region spanning between *DsAflR* and *Ds140270* gave a specific product. Southern hybridization analysis of transformants 105, 157, and 161 confirmed disruption of the WT *DsAflR* locus as expected. It also revealed different sized fragments among the three transformants for each restriction enzyme (**Figure 5.7**), suggesting these transformants were the products of independent insertion events with different sized inserts and additional restriction enzyme recognition sites. It was not possible to estimate the insert sizes based on the information available. In summary, these results show that a variety of disruptions in *DsAflR* were produced from CRISPR/Cas9 gene editing in *D. septosporum*.

5.3.1.3 Insertions in *D. septosporum DsAflR* transformants match components of the CRISPR/Cas9 plasmid

Transformants with insertions that gave a product larger than that from the WT fungus in the *DsAflR* PCR (primers HM89/HM90) were analysed by PCR amplicon sequencing. The 387 bp insertion from transformant 145 was identified to match part of the CRISPR/Cas9 plasmid (Cas9HygAMAccdB) used in transformation, specifically the C-terminal region of the hygromycin B resistance gene (*hph*) and the *trpC* terminator of the *hph* cassette (**Figure 5.8**). Partial sequencing of the larger insertions in transformants 82 and 158 also showed matches to the *hph* cassette (**Figure 5.8**). PCR product size and sequence information suggested that the insertion in transformant 82 included the *gpdA* promoter and the full *hph* coding sequence, whilst the insertion in transformant 158 appeared to include the entire *hph* cassette, but in the opposite orientation to the other two transformants (**Figure 5.8**). Transformants 82 and 158 thus both contained regions of the *hph* cassette known to contain a *Hin*dIII recognition site, accounting for the additional *Hin*dIII site predicted from the Southern hybridization results (**Figure 5.7**). Transformant 133 contained an insertion that matched different parts of the CRISPR/Cas9 plasmid, including regions of the AMA1 autonomously replicating sequence and parts of the *Cas9* and ampicillin resistance (*AmpR*) genes, interspersed with a segment of DNA that was not from the plasmid but matched bacterial insertion (IS1) sequences, including those from *Escherichia coli*. Together, these results showed that in several transformants, partial copies of the plasmid used for CRISPR/Cas9 editing in *D. septosporum* were inserted at the DSB.

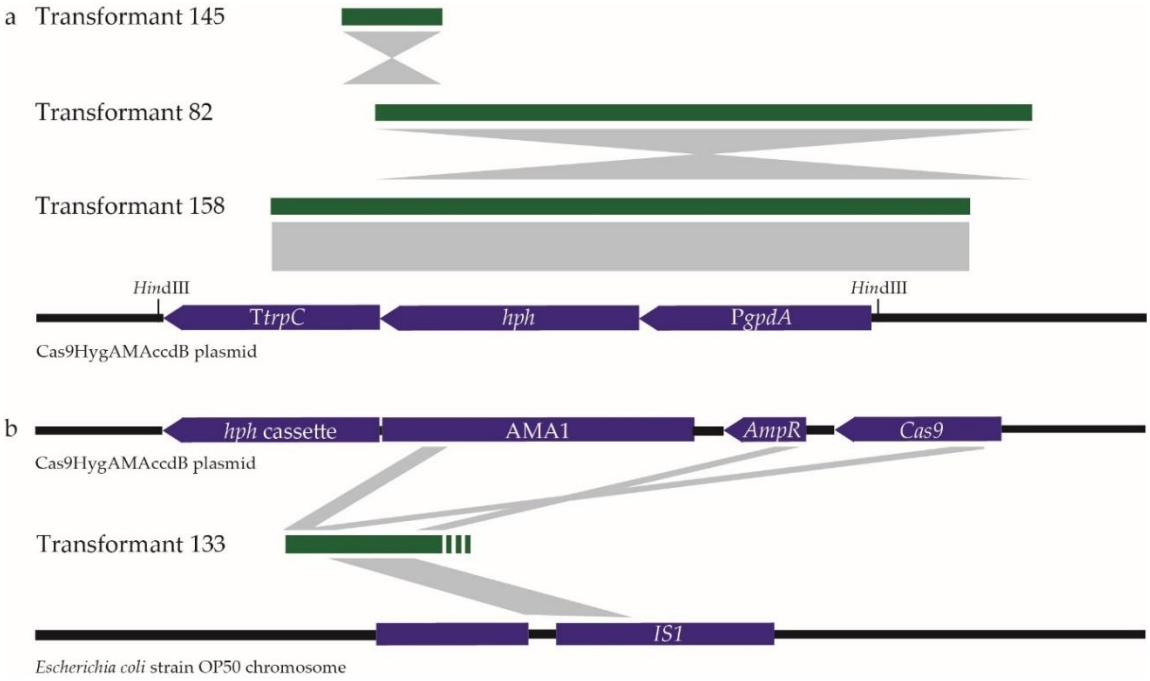

Figure 5.8. Insertions in *Dothistroma septosporum* CRISPR/Cas9 *DsAflR* transformants and matching sequences. (**a**) Insertions in transformants 145, 82 and 158 that match part of the *hph* (hygromycin B resistance gene) cassette from the CRISPR/Cas9 plasmid (Cas9HygAMAccdB). (**b**) Part of insertion in transformant 133 that matches different regions of the CRISPR/Cas9 plasmid as well as a region in an *Escherichia coli* strain OP50 chromosome. The insertions were identified by PCR analysis and PCR amplicon sequencing. Insertions are indicated by green bars that align to matching regions of the Cas9HygAMAccdB plasmid or *E. coli* chromosome. The grey rectangles or triangles underneath and above the insertions indicate the orientation relative to that of the *DsAflR* gene. *Hin*dIII restriction enzymes sites near the *hph* cassette are labelled. The black line indicates part of the Cas9HygAMAccdB plasmid sequence or *E. coli* chromosome, and genes or plasmid components are shown by labelled purple bars (*TtrpC* terminator, *hph* cassette, *PgpdA* promoter, AMA1 autonomously replicating sequence, *AmpR* β-lactamase (ampicillin resistance) gene, *Cas9* gene). PCRs performed to support the expected insertion sizes and content of transformants 82 and 158 are shown in **Appendix 41**.

5.3.2 CRISPR/Cas9 gene editing in *D. septosporum* using donor DNA-directed repair

5.3.2.1 Generation of *D. septosporum DsCE3* and *Ds69328* gene disruption transformants

Previous success disrupting *DsAflR* in *D. septosporum* using CRISPR/Cas9 suggested that this gene editing method could be used to target the candidate virulence factors identified in **Chapter 3**. The two candidate genes selected were effector *DsCE3* and transcription factor *Ds69328.* Unlike *DsAflR*, where a visual phenotype was used to screen the transformants, gene

disruption of these two candidates was not expected to generate a known visual phenotype. Therefore, to aid screening, transformation was performed with a dDNA repair construct which was designed with the geneticin resistance cassette flanked by DNA sequence of the targeted gene. Once a gene is disrupted by Cas9, the DSB should be repaired using the dDNA template and homologous recombination will result in insertion of the geneticin resistance gene into the DSB site. This should result in disruption of the targeted gene and the disruption transformants being resistant to geneticin, enabling targeted screening to be performed.

CRISPR/Cas9 transformation was performed with one sgRNA protospacer for each gene. Both protospacers target the first exon of the gene and have a high on-target activity score of 0.78 for *Ds69328* and 0.8 for *DsCE3* (**Figure 5.9**). Transformation of *D. septosporum* protoplasts was performed using the PEG transformation method (**Materials and methods section 5.2.6.1**), adding both the Cas9HygAMAccdB and dDNA plasmids, and plating on transformation plates with hygromycin and geneticin. After incubating for 2–3 weeks, many colonies were observed from the *DsCE3* transformation plates. In contrast, the *Ds69328* transformation plates had very limited growth after 3–4 weeks incubation. From the *DsCE3* transformation plates, 72 transformants were sub-cultured to new selective plates containing geneticin, of which 59 had grown after 7 days. From the *Ds69328* transformation plates, eight transformants were sub-cultured, where two were large and the others were very small. After this incubation step, only the two large colonies grew on the geneticin selective plates.

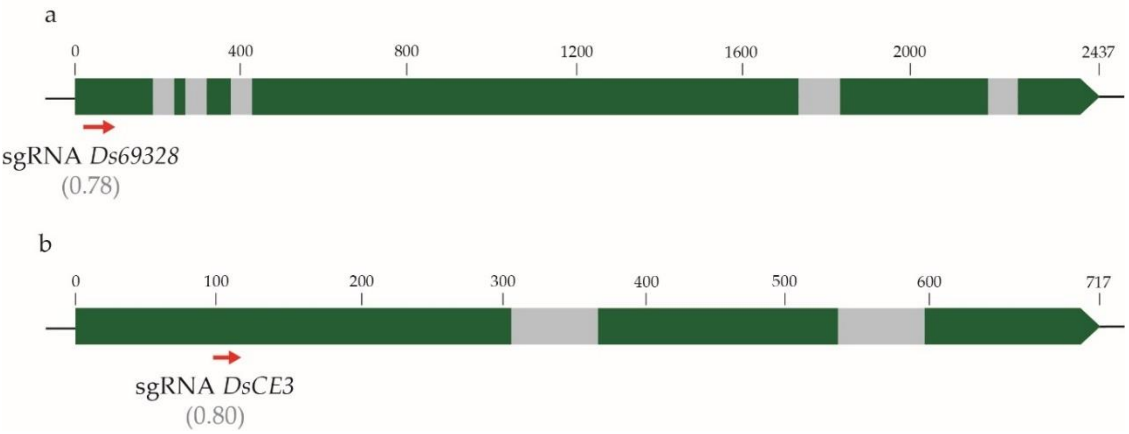

Figure 5.9. Schematic of single guide RNA (sgRNA) protospacer location in *Ds69328* and *DsCE3* of *Dothistroma septosporum*. (**a**) sgRNA protospacer targeting base pairs 59–81 in *Ds69328* with an on-target score of 0.78. (**b**) sgRNA protospacer targeting base pairs 97–119 in *Ds69328* with an on-target score of 0.80. Exons are shown as green bars and grey bars are introns. The sgRNA protospacers are shown

by red arrows illustrating they are in a 5'–3' direction. On-target activity score is shown in grey underneath the protospacer name. Base pair numbers are shown above the genes.

5.3.3 PCR screening of CRISPR/Cas9 *DsCE3* and *Ds69328* transformants

Initial screening of the *DsCE3* and *Ds69328* transformants was performed by PCR analysis of gDNA extracted by the rapid modified CTAB method (Doyle & Doyle, 1987) (**Materials and methods section 5.2.2**). The two CRISPR/Cas9 *Ds69328* transformants were screened using two primer pairs that bind outside the flanking regions used in the dDNA and inside the geneticin cassette (**Figure 5.10a**). These PCRs both amplified the expected sized products in both transformants (**Figure 5.10b**), suggesting that targeted disruption of *Ds69328* with the geneticin cassette had occurred.

Of the *DsCE3* CRISPR/Cas9 transformants, 12 were randomly selected for screening using two primer pairs of the same design as for *Ds69238* (**Figure 5.11a**). All 12 transformants amplified a product of the expected size for one primer pair (HM204/HM239), but only nine amplified from the other primer pair (HM238/HM203) (**Figure 5.11b**). These results suggest that targeted disruption of the *DsCE3* gene with the geneticin cassette occurred for nine out of the 12 *DsCE3* transformants screened.

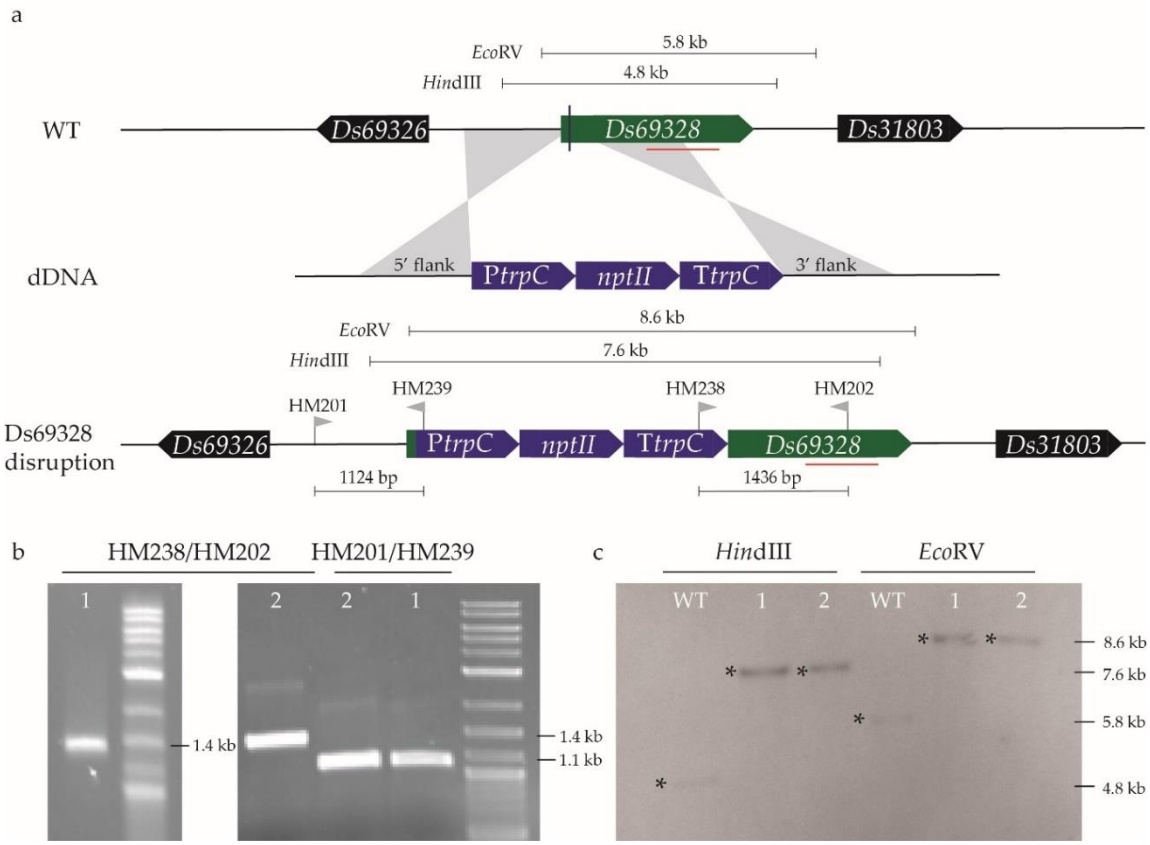

Figure 5.10. PCR screening and Southern hybridization of CRISPR/Cas9 *Ds69328* transformants from *Dothistroma septosporum*. (**a**) Schematic of the wild type (WT) *Ds69328* locus, donor DNA (dDNA) containing the 5' and 3' flanks, and the *Ds69328* disruption locus. The green bar is *Ds69328*, the black bars are adjacent genes, and the blue bars are parts of the geneticin cassette including the promotor (P*trpC*), geneticin resistance gene (*nptII*), and terminator (T*trpC*). The vertical blue bar in *Ds69328* indicates the single guide RNA (sgRNA) site, and the horizontal red line indicates where the Southern hybridization probe binds. Positions of the restriction sites and expected restriction fragment sizes from Southern hybridization with the probe are shown above the WT and *Ds69328* disruption locus. Positions of primers are illustrated by grey flags with the primer name above. (**b**) Screening of *Ds69328* disruptions by PCR amplification. Primers used are shown above and the PCR product sizes are shown on the right of each gel picture. *Ds69328* disruption transformant numbers are shown at the top of each gel picture. (**c**) Southern hybridization of digested genomic DNA from WT *D. septosporum* and *Ds69328* CRISPR/Cas9 transformants (1 and 2) using *Hin*dIII and *Eco*RV. A digoxigenin (DIG)-11-dUTP-labelled probe bound to a region of *Ds69328* downstream of the sgRNA site. WT or *Ds69328* disruption transformant numbers are shown at the top of the Southern hybridization picture. Hybridizing fragments are marked with a black asterisk and fragment sizes are labelled on the right.

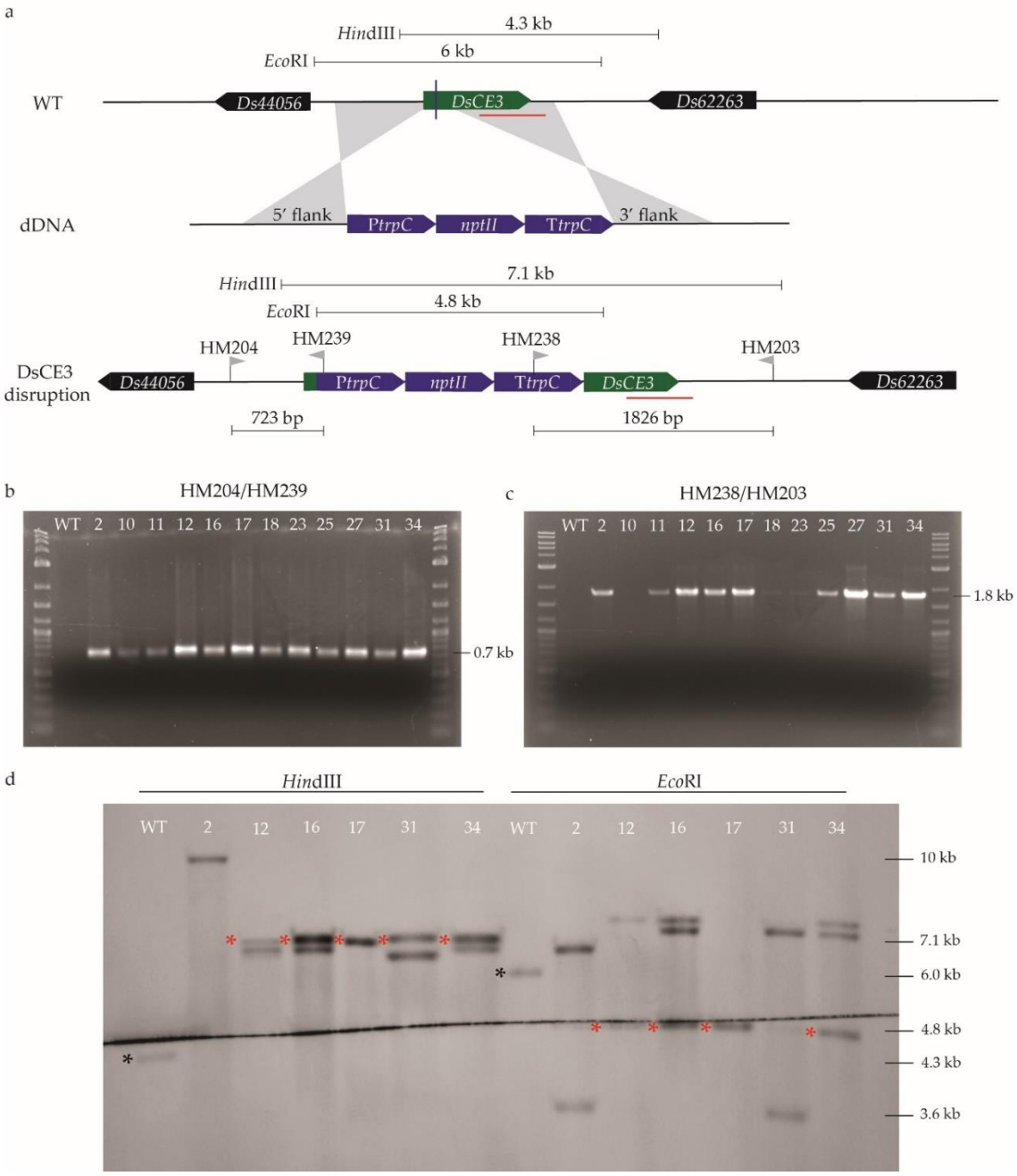

Figure 5.11. PCR screening and Southern hybridization of CRISPR/Cas9 *DsCE3* transformants from *Dothistroma septosporum*. (**a**) Schematic of the wild type (WT) *DsCE3* locus, donor DNA (dDNA) containing 5' and 3' flanks and the *DsCE3* disruption locus. The green bar is *DsCE3*, the black bars are adjacent genes, and the blue bars are parts of the geneticin cassette including the promotor (P*trpC*), geneticin resistance gene (*nptII*), and terminator (T*trpC*). The vertical blue bar in *DsCE3* indicates the single guide RNA (sgRNA) site and the horizontal red line indicates where the Southern hybridization probe binds. Positions of restriction sites and expected fragment sizes from Southern hybridization with the probe are shown above the WT and *DsCE3* disruption locus. Positions of primers are illustrated by grey flags with the primer name above. (**b-c**) Screening of *DsCE3* disruptions with PCR amplification. Primers used are shown above and the PCR product sizes are shown on the right of each gel picture. WT or *DsCE3*

disruption transformant numbers are shown at the top of each gel picture. (**d**) Southern hybridization of digested genomic DNA from WT *D. septosporum* and *DsCE3* CRISPR/Cas9 transformants (2, 12, 16, 17, 31, and 34) of this fungus using *Hin*dIII and *Eco*RI. A digoxigenin (DIG)-11-dUTP-labelled probe bound to a region of *DsCE3* downstream of the sgRNA site. WT or *DsCE3* disruption transformant numbers are shown at the top of the Southern hybridization picture. Hybridizing fragments from WT are marked with a black asterisk, and fragments of the correct size from *DsCE3* disruption transformants with a red asterisk. Hybridizing fragment sizes are labelled on the right.

5.3.4 Southern hybridization analysis of *DsCE3* and *Ds69328* transformants

Initial screening results by PCR analysis suggested that successful disruption of *DsCE3* and *DS69328* occurred. To further support this result, Southern hybridization was performed for each set of transformants. For the two *Ds69328* transformants, Southern hybridization was performed with the two restriction enzymes *Hin*dIII and *Eco*RV. The WT and the two *Ds69328* transformants all had hybridising fragments of the expected sizes with both enzymes (**Figure 5.10c**), consistent with disruption of *Ds69328* with the geneticin cassette.

For the *DsCE3* disruption, six transformants that amplified the correct product in the PCR screen were analysed by Southern hybridization with *Hin*dIII and *Eco*RI. The WT had hybridising fragments of the expected size with both enzymes (**Figure 5.11c**). However, all but one of the *DsCE3* transformants had multiple fragments of different sizes. Transformants 12, 16 and 34 had the expected fragment sizes with both enzymes, as well as other fragments of the incorrect size (**Figure 5.11c**). Transformants 2 and 31 did not have the expected fragment sizes with one or both enzymes. Only transformant 17 had a single hybridising fragment of the expected size for both enzymes. These results suggest that disruption of *DsCE3* with the geneticin cassette occurred successfully for four of the six transformants screened, but additional disruption to the genome could have occurred in three of these.

5.3.5 Growth characteristics of *D. septosporum* WT and CRISPR/Cas9 gene disruption mutants

Screening by PCR and Southern hybridisation analysis suggested that several *D. septosporum* CRISPR/Cas9 transformants had been successfully disrupted in the target gene. To determine whether this disruption had an impact on their morphology, radial growth rate and sporulation were measured. The WT fungus grew 0.64 mm/day and produced a total of 1.7×10^6 spores per plate. For the two *Ds69328* mutants, radial growth and sporulation assessment was not significantly different to the WT (**Table 5.2**). For the six *DsCE3* mutants, two (Δ*DsCE3* #16 and

#34) were not significantly different from WT in radial growth or sporulation, whilst four (Δ*DsCE3* #2, 12, 17, and 31) showed a small but significant reduction in radial growth, but not sporulation, compared to the WT (**Table 5.2**).

Table 5.2. Growth characteristics of wild type (WT) and gene disrupted *Dothistroma septosporum* strains.

Strain name	Growth rate (mm/day)[1]	P (T-test)[2]	Total spores per plate[3]	P (T-test)[2]
WT	0.64 ± 0.08	-	$1.7 \pm 1.7 \times 10^6$	-
Δ*Ds69328* #1	0.64 ± 0.04	0.86	$3.7 \pm 2.1 \times 10^6$	0.16
Δ*Ds69328* #2	0.61 ± 0.02	0.35	$3.4 \pm 0.6 \times 10^6$	0.06
Δ*DsCE3* #2	0.56 ± 0.08	**0.05**	$1.4 \pm 0.8 \times 10^6$	0.75
ΔDsCE3 #12	0.52 ± 0.04	**0.00**	$2.3 \pm 0.6 \times 10^6$	0.41
Δ*DsCE3* #16	0.63 ± 0.10	0.91	$9.1 \pm 0.3 \times 10^6$	0.38
Δ*DsCE3* #17	0.56 ± 0.04	**0.02**	$2.7 \pm 0.7 \times 10^6$	0.22
Δ*DsCE3* #31	0.54 ± 0.06	**0.01**	$2.1 \pm 1.0 \times 10^6$	0.66
Δ*DsCE3* #34	0.58 ± 0.06	0.11	$1.3 \pm 0.2 \times 10^6$	0.60

1 – Mean (± SD) radial growth at 3 weeks, from three replicate plates, each with three agar plugs (n=9).
2 – T-tests were calculated in Microsoft© Excel (T.test function), as a two-tailed test and a two-sample equal variance test. A T-test value ≤0.05 indicates a significant difference compared to WT; those values are highlighted in bold.
3 – Mean (± SD) number of spores per plate, from three replicate plates per strain (n=3). Spores were harvested in ~2 mL water and the concentration determined using a cytometer. The weight of the tube was measured to determine the exact volume of spore suspension harvested, and the total number of spores in that volume was calculated from the spore concentration. Full data are shown in **Appendix 36**.

5.3.6 Complementation of *D. septosporum* CRISPR/Cas9 mutants

Virulence of the successfully disrupted candidate virulence factor transformants was tested on *P. radiata*. To determine whether a change in virulence in the transformants can be recovered by complementation of the disrupted gene, complementation transformants were generated. Complementation was performed by direct insertion of a plasmid containing the targeted gene sequence and, where possible, up to 1 kb upstream sequence containing the promoter region. The complementation plasmids were generated by restriction enzyme cloning (**Materials and methods section 5.2.5**) and then PEG transformation of *D. septosporum* protoplasts was performed (**Materials and methods section 5.2.6.1**).

For complementation of the *Ds69328* #2 gene-disrupted mutant, the complementation sequence contained the *Ds69328* gene as well as ~1 kb upstream, making the sequence ~4 kb (**Figure 5.12a**). After transformation, 10 colonies were observed on the transformation plates

and sub-cultured to selective media. gDNA was then extracted from eight transformants, and PCR screening performed with the primers shown in **Figure 5.10a**. The expected 2119 bp product was amplified from the WT, and from all screened transformants except transformant *Ds69328* #2-C6 (**Figure 5.12b**). These results suggested that complementation of transformant *Ds69328* #2 occurred as expected in all but one transformant.

Because the *DsCE3* gene-disrupted mutants had different radial growth rates (**Table 5.3**), two complements were developed: one in mutant *DsCE3* #17 (significantly different radial growth rate to WT), and the other in mutant *DsCE3* #34 (not significantly different). Complementation was performed using sequence that contained the *DsCE3* gene as well as ~0.8 kb upstream, however the downstream sequence was restricted to ~0.5 kb due to the proximity of another gene (*Ds62263*) (**Figure 5.12a**). After transformation, eight transformants were obtained from complementation of mutant *DsCE3* #17. PCR screening of the eight transformants with the primers shown in **Figure 5.10a** was performed on extracted gDNA. The complementation plasmid DNA amplified the expected size 1830 bp product, as did the WT gDNA. All eight complementation transformants also amplified the expected product, but transformant *DsCE3* #17-C5 also amplified a smaller ~1.5 kb product (**Figure 5.12c**). These results suggested that complementation of mutant *DsCE3* #17 occurred as expected in all but one transformant.

After transformation of gene disruption mutant *DsCE3* #34 with a complementation plasmid, ~20 colonies were observed on the transformation plates. gDNA was extracted from 11 transformants and PCR screening was performed with the same primers and in the same PCR as with the *DsCE3* #17 complements. The expected size of PCR product was amplified from all transformants screened except transformant *DsCE3* #34-C2 (**Figure 5.12d**). These results suggested that complementation of mutant *DsCE3* #34 occurred as expected in all but one transformant.

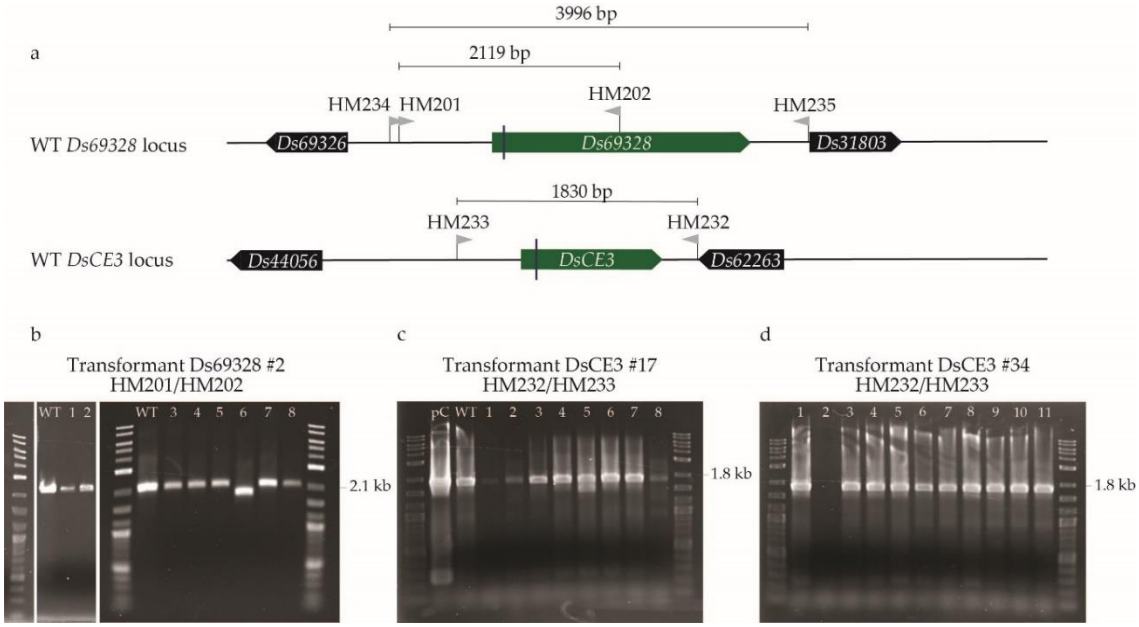

Figure 5.12. Complementation design and PCR screening of *Dothistroma septosporum Ds69328* and *DsCE3* mutants transformed with complementation plasmids. (**a**) Schematic of *Ds69328* and *DsCE3* wild type (WT) loci illustrating primer positions for amplification of sequence used to complement the gene disruption mutants. The green bars are *Ds69328* and *DsCE3*, the black bars are flanking genes, and the vertical blue lines in *Ds69328* and *DsCE3* indicate the single guide RNA (sgRNA) sites. Primer positions are shown by grey flags, and PCR product sizes above the primers. For *Ds69328*, the sequence amplified by primers HM234/HM235 was used to construct the complementation plasmid, while primers HM201/HM202 were used to screen the transformants for complementation. For *DsCE3*, the primers HM232/HM233 were used to amplify the sequence for construction of the complementation plasmid (pC) as well as to screen the transformants for complementation. (**b–c**) PCR screening of putative complementation mutants with primers shown in (a). Primers used are shown above the gels, and relevant DNA ladder sizes are shown to the right. (**b**) Screening of complementation transformants of the *Ds69328* #2 disruption mutant. (**c**) Screening of complementation transformants of the *DsCE3* #17 disruption transformant. (**d**) Screening of complementation transformants of the *DsCE3* #34 disruption mutant.

5.3.7 Gene copy number determination in complementation *D. septosporum* strains

PCR analysis shown in the previous section suggested that successful complementation of *Ds69328* and *DsCE3* mutants had occurred. To determine how many copies of the complementation construct were inserted after transformation, qPCR was performed to compare amplification of the targeted gene with that of *DsAflR*, a known single-copy gene in the *D. septosporum* NZE10 genome (Chettri et al., 2013). Because the CRISPR/Cas9 gene disruption analysis causes insertion of the geneticin cassette at the DSB site, and the qPCR primers were

not designed over the DSB site, the disrupted gene will still amplify in the qPCR analysis. Therefore, in the search for a complementation strain that has only one copy of the target gene inserted, the copy number will be two: one disrupted gene and one undisrupted complementing gene.

The qPCR analysis with *Ds69328* as the target gene showed a ratio of 1 for the WT gDNA (**Table 5.3**), suggesting that one copy of *Ds69328* is present in the WT genome. Analysis of gDNA from the complementation strains found that *Ds69328* #2-C1 had five copies, *Ds69328* #2-C2 had 15 copies, and *Ds69328* #2-C3 had two copies of *Ds69328* (**Table 5.3**). The qPCR analysis with *DsCE3* as the target gene also showed that the WT gDNA had a ratio of 1. Analysis of the complementation strains showed that *DsCE3* #17-C8 had two copies, *DsCE3* #34-C1 had nine copies, and *DsCE3* #34-C10 had three copies of *DsCE3* (**Table 5.3**). These results show that multiple copies of *Ds69328* and *DsCE3* were inserted from the complementation transformation. The strains *Ds69328* #2-C3 and *DsCE3* #17-C8 were selected for virulence analysis because they contain only one additional copy of the target gene. Due to a single copy *DsCE3* #34-C10 complementation strain not being obtained, it was decided to continue with just the *DsCE3* #17-C8 complement.

Table 5.3. Target gene copy number determination in complementation strains.

Target gene / Strain	Ct reference	ΔCt reference[1]	Ct target	ΔCt target[1]	Ratio[2]	Copy number[3]
Ds69328						
WT	19.6	-	19.1	-	-	1
Ds69328 #2-C1	23.2	-3.5	20.3	-1.1	4.8	5
Ds69328 #2-C2	20.4	-0.8	16.1	3.1	14.6	15
Ds69328 #2-C3	20.5	-0.9	19.1	0.0	1.8	**2**
DsCE3						
WT	19.6	-	19.4	-	-	1
DsCE3 #17-C8	22.8	-3.2	21.4	-2.0	2.1	**2**
DsCE3 #34-C1	21.2	-1.6	17.7	1.7	9.2	9
DsCE3 #34-C10	20.9	-1.3	19.0	0.4	3.1	3

1 – The ΔCt is the difference in Ct between the complement and the wild type (WT) when amplifying each of the target and reference genes by PCR. The single copy reference gene used was *DsAflR* (JGI ID: 75566), previously verified by Southern hybridization (Chettri et al., 2013). Results are the averages of four technical replicates.

2 – The ratio was calculated using a method detailed in **Chapter 2**, **Materials and methods section 2.2.2.7**. The primer efficiencies were calculated using standard curves, as detailed in **Chapter 2**, **Materials and methods section 2.2.2.6**, and were 1.93 for *DsAflR*, 1.98 for *DsCE3*, and 2.0 for *Ds69328*.

3 – The copy number is rounded, so for example a ratio of 14.6 gives a copy number of 15. Because the disrupted gene is still present in the genome and is amplified by the qPCR primers, a complementation

strain where one copy of the target gene was inserted will give a copy number of two. The copy numbers of the two complementation strains to be used for virulence assays are shown in bold.
The full data used to calculate the values displayed in this table are shown in **Appendix 37**.

5.3.8 Growth characteristics of *D. septosporum* WT and CRISPR/Cas9 complementation strains

PCR screening and copy number qPCR analysis suggested that complementation of the *Ds69328* and *DsCE3* mutants had successfully occurred. To determine whether this complementation had an impact on the morphology of *D. septosporum*, radial growth and sporulation were measured (**Table 5.4**). The WT was observed to grow 0.54 mm/day and produce a total of 1.3 x 10^5 spores per plate. The *Ds69328* #2-C3 strain had a significantly higher growth rate than the WT, while sporulation assessment was not significantly different. The *DsCE3* #17-C8 strain was not significantly different to WT in radial growth or sporulation.

Table 5.4. Growth characteristics of wild type (WT) and complementation *Dothistroma septosporum* strains.

Strain name	Growth rate (mm/day)[1]	P (T-test)[2]	Total spores per plate[3]	P (T-test)[2]
WT	0.54 ± 0.03	-	1.3 ± 0.3 x 10^5	-
Ds69328 #2-C3	0.63 ± 0.07	**0.00**	4.1 ± 2.7 x 10^5	0.15
DsCE3 #17-C8	0.57 ± 0.05	0.21	3.0 ± 1.7 x 10^5	0.16

1 – Mean (± SD) radial growth at 3 weeks, from three replicate plates, each with three agar plugs (n=9).
2 – T-tests were calculated in Microsoft© Excel (T.test function), as a two-tailed test and a two sample equal variance test. A T-test value ≤0.05 indicates a significant difference compared to WT; those values are highlighted in bold.
3 – Mean (± SD) number of spores per plate, from three replicate plates per strain (n=3).
Full data are shown in **Appendix 37**.

5.3.9 Virulence analysis of *D. septosporum* WT, CRISPR/Cas9 mutants, and complementation strains on *P. radiata* seedlings

Successful disruption of candidate virulence factor genes *Ds69328* and *DsCE3* was performed by CRISPR/Cas9 editing, and complementation strains were developed. To determine whether these genes contribute towards virulence of *D. septosporum*, *P. radiata* seedlings were inoculated with WT, CRISPR/Cas9 mutants, and complementation strains. Due to delays in obtaining sufficient spore concentrations for some strains, a staggered inoculation was

performed with two experiments. Also, due to some strains not producing enough spores, even after a subsequent harvest, some strains were inoculated with different spore concentrations and volumes (**Table 5.5**). Pine seedlings were sprayed with *D. septosporum* spores and incubated in growth chambers for 10 weeks. Pine needles were then harvested, examined with a dissecting microscope, and the disease symptoms recorded.

Table 5.5. Inoculation conditions for virulence assessment of *Dothistroma septosporum* wild type (WT), gene disruption, and complementation strains.

Target gene / Strain	Inoculation concentration (spores/mL)	Inoculation volume per seedling (mL)	Total spores sprayed per seedling[2]	Biological replicates
Experiment 1				
WT	6.0×10^5	21.6	1.3×10^7	3
Δ*Ds69328* #1	5.6×10^5	10.0	5.6×10^6	3
Δ*Ds69328* #2[1]	$0.5/1.6 \times 10^6$	16.0/12.5	$0.8/2.0 \times 10^7$	2/2
Ds69328 #2-C3[1]	$0.8/1.2 \times 10^6$	13.5/16.5	$1.0/2.0 \times 10^7$	2/2
Experiment 2				
WT	1.6×10^6	13.0	2.1×10^7	5
Δ*DsCE3* #17	1.6×10^6	11.5	1.8×10^7	4
Δ*DsCE3* #34	1.6×10^6	12.5	2.0×10^7	4
DsCE3 #17-C8	1.6×10^6	16.25	2.6×10^7	4

1 – Four replicates were used but two were inoculated with different spore numbers from the other two.
2 – Note that not all spores sprayed would have landed on the seedlings due to their thin needles.

Examining the percentage of needles that had *D. septosporum*-like lesions through dot plot and statistical analysis (**Figure 5.13**, **Table 5.6**) identified several trends, although there was a high level of variability between the biological replicates of all samples. One biological replicate from the *Ds69328* #2-C3 strain was a clear outlier. This sample (*Ds69328* #2-C3 rep D) had a much lower number of healthy needles compared to the other replicates (**Appendix 35b**), suggesting that the number of dead needles (which were not counted) was much higher. Visual identification of *D. septosporum* lesions was difficult on dead needles as usually only regions of sporulation were visible (as opposed to the distinct lesions observed in green needles), and these could not be clearly distinguished from saprophytic contamination present on some of the dead needles.

Dot plot analysis of the disrupted and complementation *Ds69328* strains suggested no difference to the WT (**Figure 5.13**). These results were supported by the statistical analysis, where no strains were significantly different to WT or the complement (**Table 5.6**). Dot plot analysis of the *DsCE3* strains suggested that disruption caused an increase in the percentage of

needles with lesions, while complementation caused a decrease (**Figure 5.13**). These results were supported by the statistical analysis, where both the disrupted strains were significantly different and had a higher percentage of needles with lesions, compared to both the WT and the complementation strains. The complementation strain was also significantly different and had a lower percentage of needles with lesions, compared to the WT (**Table 5.6**). These results suggested that disruption of *Ds69328* had no impact on virulence, while disruption of *DsCE3* may have increased virulence.

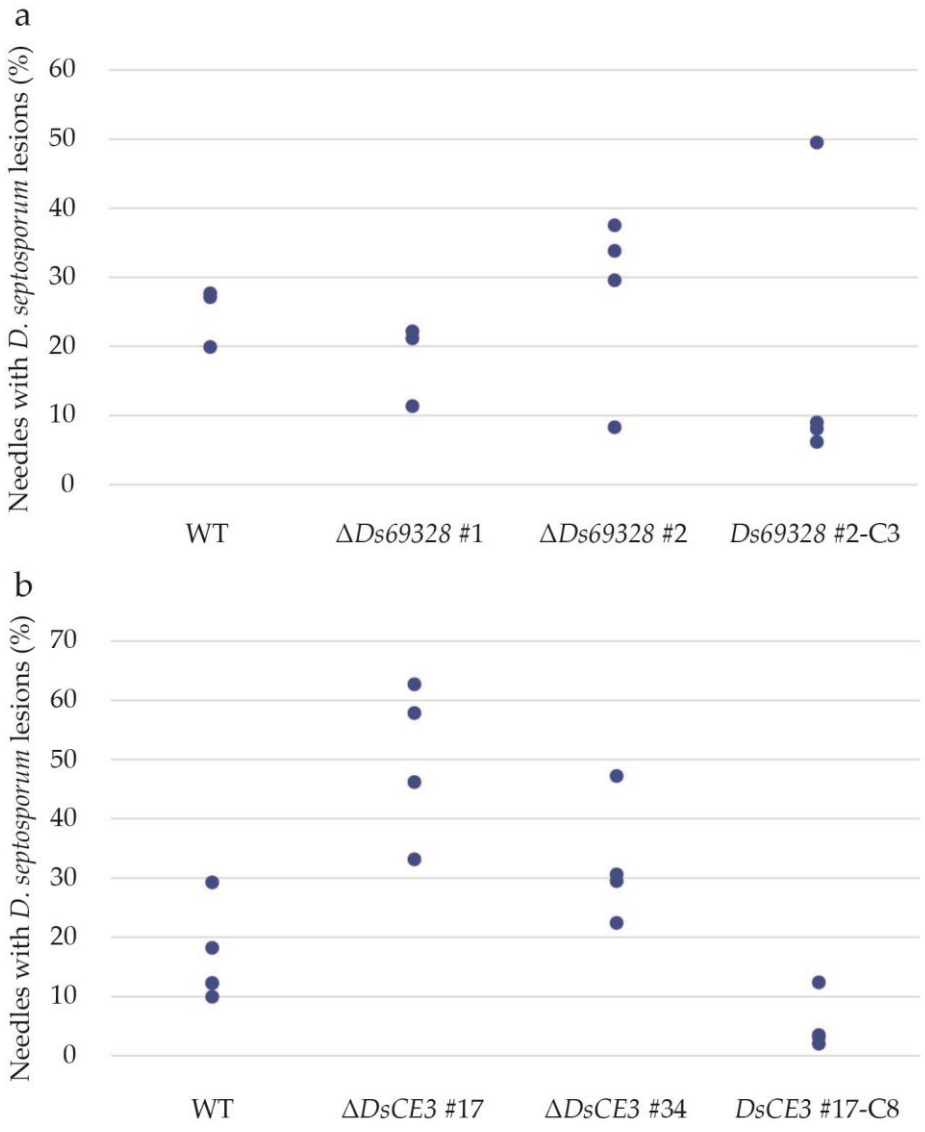

Figure 5.13. Dot plot of percentages of needles with *Dothistroma septosporum* lesions. Results are shown for Experiment 1 (**a**) and 2 (**b**). Percentages were calculated as the number of needles with lesions out of the total number of needles (excluding dead needles) per tree. Wild type, WT.

Table 5.6. Percentages of *Pinus radiata* needles with Dothistroma needle blight (DNB) symptoms when inoculated with wild type (WT), gene disruption, and complementation strains of *Dothistroma septosporum*.

Target gene / Strain	Biological replicates	Needles with DNB symptoms (%)[1]	P (T-test) WT/COMP[2]
Experiment 1			
WT	3	24.92 ± 3.53	-
Δ*Ds69328* #1	3	18.25 ± 4.88	0.19/1.00
Δ*Ds69328* #2	4	27.33 ± 11.33	0.78/0.49
Ds69328 #2-C3	4	18.21 ± 18.11	0.62/-
Experiment 2			
WT	5	16.40 ± 6.99	-
Δ*DsCE3* #17	4	50.01 ± 11.41	**0.00/0.00**
Δ*DsCE3* #34	4	32.46 ± 9.10	**0.03/0.00**
DsCE3 #17-C8	4	5.28 ± 4.14	**0.04**/-

1 – Mean (± SD) percent of needles with *D. septosporum* lesions out of total counted needles.
2 – T-tests were performed with the WT and with the corresponding complement. T-tests were calculated in Microsoft© Excel (T.test function), as a two-tailed test and a two sample equal variance test. A T-test value ≤0.05 indicates a significant difference (in bold).
Full data are shown in **Appendix 35b**.

After visual analysis of the *P. radiata* needles, DNB-like lesions were excised from the needles and gDNA was extracted (**Materials and methods section 5.2.8.4**). Unfortunately, the well-established CTAB gDNA extraction method, which had been used previously for virulence assessment of *D. septosporum*-inoculated *P. radiata* seedlings (Chettri et al., 2012; Guo, Hunziker, et al., 2020), produced gDNA of a low quality that was only amplified by qPCR in a few samples (**Appendix 35c**). Prior to gDNA extraction of the excised lesions, this method had been trialled successfully with healthy *P. radiata* needles. Therefore, this suggests that the dry and dead needle tissue in and around the lesions resulted in the CTAB method producing low-quality gDNA. Several different gDNA extraction methods and modifications of the CTAB method were then attempted until one (Geneaid kit) was found that produced gDNA of sufficient quality to be reliably amplified by qPCR. Therefore, all other samples were gDNA-extracted using the Geneaid kit (**Materials and methods section 5.2.8.4**). Unfortunately, the samples extracted by the CTAB method appeared to have much higher *D. septosporum* gDNA concentrations than the other biological replicates (some over 10-fold higher, **Appendix 35c**), probably because it was a crude extraction method that produced low-quality gDNA and did not involve column purification like the Geneaid kit. Because these samples were extracted through a different method and presented outlying *D. septosporum* gDNA values, these samples were not considered to be reliable and were excluded from the subsequent biomass analysis. This

resulted in the exclusion of six samples in total and unfortunately for Experiment 2 WT and *DsCE3* #17-C8 strains, two biological replicates were excluded from each (**Table 5.7**).

The amount of *D. septosporum* biomass per lesion and per dry weight of infected pine tissue was then estimated though qPCR analysis. Relative quantification was performed using the target *D. septosporum* gene *DsPksA* and the reference *P. radiata* gene *CAD* (**Materials and methods section 5.2.8.4**), and dot plot and statistical analyses were performed (**Appendix 42**, **Appendix 43**). The results from this relative quantification biomass analysis suggested that the only strain significantly different to the WT (in both ng per lesion and ng per dry weight) was *Ds69328* #2-C3 (**Appendix 43**). However, the Ct values obtained using the *CAD* primers were very high, suggesting that the amount of *P. radiata* DNA present in the sample was very low (**Appendix 35c**). It was hypothesised that because many of the infected needles also appeared dry and dead around the lesions, the *P. radiata* gDNA may have degraded, meaning that this biomass analysis may be inaccurate. The amount of *D. septosporum* biomass present in the samples was then estimated using a different method that does not involve comparison with the *P. radiata* reference gene. Instead, the *D. septosporum* gDNA concentration in the qPCR was determined from the *D. septosporum* target gene *DsPksA* standard curve and normalised to the number of lesions used for gDNA extraction, and to the dry weight of lesion material used in the DNA extraction (**Materials and methods section 5.2.8.4**).

Dot plot and statistical analysis of the *D. septosporum* biomass results illustrated several trends in the data (**Figure 5.14, Table 5.7**). Firstly, a large difference in fungal biomass was observed between the WT strains of the two Experiments. The WT from Experiment 1 had a much lower fungal biomass than the WT from Experiment 2, which was a different trend from the visual analysis of percentage of needles with DNB symptoms (**Figure 5.13**, **Table 5.6**). Secondly, high variation was prevalent in the majority of samples (**Figure 5.14**, **Table 5.7**), as was also observed from the visual needle lesion analysis (**Figure 5.13**, **Table 5.6**). Interestingly, the biological replicate from the *Ds69328* #2-C3 strain which was an outlier in the visual needle analysis (**Figure 5.13**), was not an outlier in the biomass analysis. This suggests that there may have been inaccuracies when identifying and counting needles with lesions in this sample.

From the visual needle analysis, disruption and complementation of *Ds69328* appeared to have no impact on virulence (**Figure 5.13**, **Table 5.6**). However, the dot plot analysis of the fungal biomass suggested an increase in virulence in these strains (**Figure 5.14**). Statistical analysis (**Table 5.7**) showed that one disrupted strain, Δ*Ds69328* #2, was significantly different to the WT in fungal biomass per dry weight of pine needles, as well as to both the WT and the

complementation strain when calculated as fungal biomass per lesion. The complementation strain, *Ds69328* #2-C3, was also significantly different to the WT in both fungal biomass analyses. The other disrupted strain, Δ*Ds69328* #1, was not significantly different to either WT or the complementation strain (**Table 5.7**) and had very high variability between the biological replicates (**Figure 5.14**). These results suggest that disruption and complementation of *Ds69328* caused an increase in fungal biomass, however this result is not conclusive due to the high variability between replicates, different results between the two disruption mutants, and the unusually low biomass in the WT.

Visual analysis of the percentage of needles with DNB symptoms suggested that disruption of *DsCE3* caused an increase in virulence, while complementation caused a reduction (**Figure 5.13**, **Table 5.6**). Dot plot analysis of the fungal biomass suggested that strains disrupted in *DsCE3* had a slightly lower fungal biomass than WT, while the complementation strains had a much lower fungal biomass (**Figure 5.14**). Statistical analysis suggested that, when considering the fungal biomass per dry weight of infected needles (**Table 5.7**), the disrupted strain Δ*DsCE3* #17 was significantly different to both WT and the complementation strain, while strain Δ*DsCE3* #34 was only significantly different to the complement. The complementation strain was also significantly different to the WT with a much lower fungal biomass. The fungal biomass per lesion results showed greater variation between biological replicates than the fungal biomass per dry weight of pine needles, which may explain the absence of any significant differences between samples (**Figure 5.14**). These results suggest that disruption and complementation of *DsCE3* caused a decrease in fungal biomass. These results are more conclusive than for *Ds69328* because both *DsCE3* mutants were reduced in fungal biomass compared to the WT, and the WT was inoculated with a similar spore inoculum to the transformants and had a more expected level of fungal biomass compared to published studies with the same WT isolate (Kabir et al., 2013). However, the complementation did not restore virulence to the WT level, and analysis of the disruption mutants by visual needle assessment appeared to show an opposite trend to the fungal biomass results.

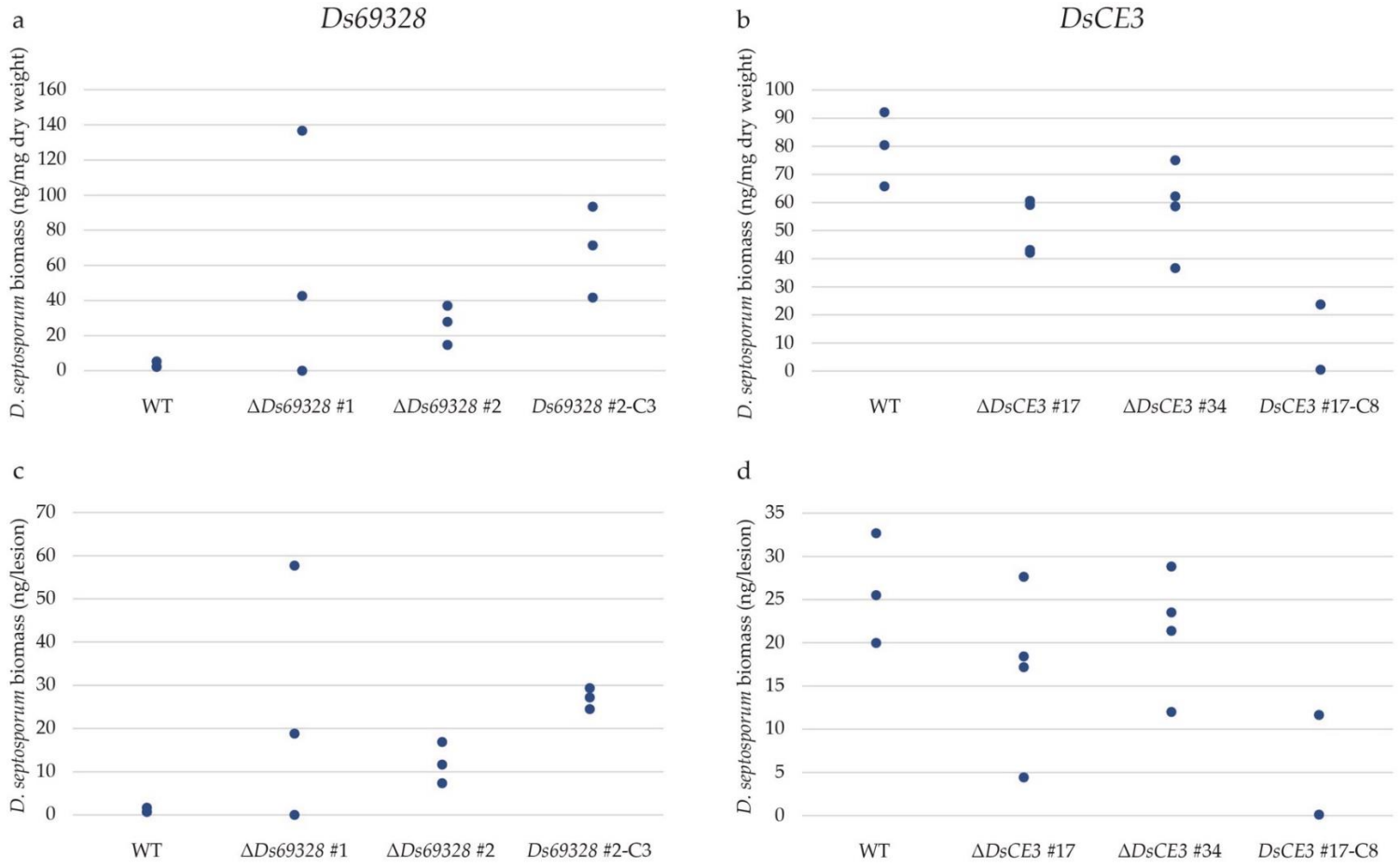

Figure 5.14. Dot plot analysis of fungal biomass in wild type (WT), gene disruption and complementation strains of *Dothistroma septosporum* in infected *Pinus radiata*. Results are shown for Experiment 1 (**a** and **c**), and 2 (**b** and **d**). Biomass was calculated as ng of *D. septosporum* gDNA per mg dry weight of infected needles (**a** and **b**), or per lesion (**c** and **d**). *D. septosporum* gDNA concentration was calculated using the Ct values from the *DsPksA* target gene of *D. septosporum* and comparing with the *DsPksA* primers standard curve (**Materials and methods section 5.2.8.4**). Each dot represents one biological replicate (i.e., one *P. radiata* tree).

Table 5.7. Biomass of wild type (WT), gene disruption, and complementation strains of *Dothistroma septosporum* on infected *Pinus radiata*.

Target gene / Strain	Biological replicates	Fungal biomass (ng/mg DW)[1]	P (T-test) WT/COMP[1]	Fungal biomass (ng/lesion)[2]	P (T-test) WT/COMP[2]
Experiment 1					
WT	3	3.32 ± 1.46	-	1.02 ± 0.46	-
Δ*Ds69328* #1	3	89.69 ± 47.06	0.09/0.64	38.28 ± 19.45	0.08/0.50
Δ*Ds69328* #2	3	26.60 ± 9.15	**0.02**/0.06	11.96 ± 3.89	**0.02**/**0.01**
Ds69328 #2-C3	3	68.84 ± 21.16	**0.01**/-	27.00 ± 1.98	**0.00**/-
Experiment 2					
WT	3	79.47 ± 10.78	-	26.06 ± 5.19	-
Δ*DsCE3* #17	4	51.29 ± 8.64	**0.02**/**0.02**	16.92 ± 8.26	0.21/0.24
Δ*DsCE3* #34	4	58.16 ± 13.83	0.12/**0.03**	21.44 ± 6.08	0.41/0.07
DsCE3 #17-C8	2	12.1 ± 11.6	**0.01**/-	5.88 ± 5.78	0.05/-

1 – Results are the mean ± standard deviation of fungal gDNA (ng) per dry weight (DW) of infected needles (mg).

2 – Results are the mean ± standard deviation of fungal gDNA (ng) per lesion.

T-tests were performed with the WT and with the corresponding complement. T-tests were calculated in Microsoft© Excel (T.test function), as a two-tailed test and a two sample equal variance test. A T-test value ≤0.05 indicates a significant difference (in bold).

Fungal gDNA was determined through amplification of *D. septosporum* target gene *DsPksA* (JGI ID: 48345), and comparison of the Ct value with the *DsPksA* standard curve (**Materials and methods section 5.2.8.4**). Full data are shown in **Appendix 35d**.

5.4 Discussion

The aim of this thesis was to identify and characterise virulence factors from Dothideomycete species, including *D. septosporum*. In **Chapters 3** and **4**, candidate virulence factors were identified from *D. septosporum* through bioinformatic and proteomic studies. The transcription factor gene *Ds69328* and candidate effector gene *DsCE3* were chosen for characterisation by gene disruption. While targeted gene knockouts had previously been performed routinely in *D. septosporum* through homologous recombination, this method was inefficient and required extensive screening of transformants. The success of CRISPR/Cas9 gene editing in other Dothideomycete species (Idnurm et al., 2017; Khan et al., 2020; Rocafort, Arshed, et al., 2022; Wenderoth et al., 2017) prompted a trial of this method in *D. septosporum*. The well characterised gene *DsAflR* was used for this trial because disruption results in a visual phenotype and facilitated screening.

For the CRISPR/Cas9 trial disrupting *DsAflR*, the transformation was performed with the CRISPR/Cas9 plasmid and no repair template, meaning the DSB was likely repaired by non-homologous end-joining (NHEJ). Two different sgRNAs were used in the *DsAflR* transformation but, despite having similar on-target scores and the transformations being performed under the same conditions in the same experiment, significantly different numbers of transformant colonies were obtained. While variability in sgRNA activity has been reported previously (Doench et al., 2016; Doench et al., 2014; Li et al., 2018; Rocafort, Arshed, et al., 2022), our transformation strategy selected for uptake and retention of the autonomously replicating CRISPR/Cas9 plasmid rather than sgRNA activity. Therefore, the difference in the number of transformants obtained when using each sgRNA might have been due to differences in plasmid uptake and persistence.

Gene editing of *D. septosporum* was highly efficient using CRISPR/Cas9 with NHEJ repair, with >90% of transformants successfully disrupted in *DsAflR*. CRISPR/Cas9 editing using NHEJ has been performed in other Dothideomycete species with a range of efficiencies reported, from 100% in *P. nodorum* using preassembled ribonuclear protein (RNP) (Khan et al., 2020), to 16.7% in *V. inaequalis* using an autonomously replicating plasmid (Rocafort, Arshed, et al., 2022), and approximately 10% in *Alternaria alternata* using a CRISPR/Cas9 plasmid (Wenderoth et al., 2017). These different gene disruption efficiencies could be due to any combination of the factors that are known to influence CRISPR/Cas9 editing efficiency, such as sgRNA design (Doench et al., 2016; Doench et al., 2014; Konstantakos, Nentidis, Krithara, & Paliouras, 2022), transformation method (El-Sayed, Abdel-Ghany, & Ali, 2017), and amount of Cas9 protein

produced (Schuster & Kahmann, 2019). Another major factor is accessibility of the target gene through chromatin organisation (Kuscu, Arslan, Singh, Thorpe, & Adli, 2014; Wu et al., 2014; Yarrington et al., 2018), and is possibly why some genes can be successfully disrupted while others cannot (Urquhart & Idnurm, 2019; Wang & Rollins, 2021).

Disruption of *DsAflR* produced a range of different transformant types including one with a single nucleotide deletion, four with insertions ranging from 387 bp to 2.8 kb, and three with undefined disruptions (**Figure 5.6**). NHEJ is thought to be an error-prone DNA repair mechanism that mostly results in small insertions or deletions (INDELs) (El-Sayed et al., 2017; Kim & Kim, 2014). However, INDELs ranging from several hundred base pairs to 1–2 kb in size, as well as those too large to amplify by PCR, have also been reported in other studies (Foster et al., 2018; Rocafort, Arshed, et al., 2022; Wenderoth et al., 2017).

Several *D. septosporum DsAflR* transformants were shown to contain insertions that matched part of the CRISPR/Cas9 plasmid used in transformation, specifically all or part of the hygromycin B resistance gene *hph* (**Figure 5.8**), despite the CRISPR/Cas9 plasmid containing a fungal autonomously replicating sequence (Rocafort, Arshed, et al., 2022). Insertion of a CRISPR plasmid into fungal transformants was first reported by Fuller, Chen, Loros, and Dunlap (2015) who found insertion of partial and complete copies of the transforming plasmid. Subsequent studies found insertion of the complete CRISPR/Cas9 plasmid consistently at the DSB site (Zheng et al., 2017) or insertion of large plasmid fragments (Boontawon et al., 2021; Li et al., 2018). Fuller et al. (2015) suggested that insertion of the CRISPR plasmid, or of partially degraded parts of the plasmid, could occur at the DSB site through the NHEJ mechanism. More recent research suggested that integration of CRISPR plasmids can occur following their cleavage with nucleases found in protoplast lysates in transformation, which allows incorporation by the NHEJ mechanism, essentially using the cleaved plasmid product as a nonhomologous dDNA molecule (Li et al., 2018). Interestingly, all the studies that reported insertion of partial or complete copies of a CRISPR plasmid (Boontawon et al., 2021; Fuller et al., 2015; Zheng et al., 2017) used protoplast transformation and hygromycin B selection. In this study, *DsAflR* transformants were successively sub-cultured four times on hygromycin B selective media, providing strong selection for stable integration of the *hph* gene. To reduce such integration events, in subsequent experiments the transformants were sub-cultured to non-selective media (or media without hygromycin) after the first round of selection on transformation plates.

The preliminary CRISPR/Cas9 trial disrupting *DsAflR* was highly successful, therefore the next CRISPR/Cas9 targets were candidate virulence factors *Ds69328* and *DsCE3*. Because these genes

have not been disrupted previously, and were not expected to produce a visual phenotype, a dDNA repair template containing the geneticin resistance cassette was used in a marker-based strategy to facilitate screening. Introduction of a dDNA template enables homologous recombination repair to occur, which is generally considered a more accurate repair system (Ceccaldi, Rondinelli, & D'Andrea, 2016; El-Sayed et al., 2017). dDNA-based CRISPR/Cas9 gene editing, using homologous flanks of various sizes, has been used successfully in the phytopathogenic species *P. nodorum* (Khan et al., 2020) and *Magnaporthe oryzae* (Foster et al., 2018). The effector gene *ToxA* of *P. nodorum* was successfully disrupted using 1 kb flanks and also with micro-homology flanks of 50 bp, although efficiency dropped from 70% to 25% when using the smaller flanks (Khan et al., 2020). Two genes were targeted in *M. oryzae* using a dDNA repair template, where one had 100% efficiency and the other had ~70–80%. The gene that had 100% efficiency using long homologous flanks, was also targeted in a separate transformation with micro-homology flanks of 30–40 bp and found to be successfully disrupted at a similar efficiency (Foster et al., 2018).

Disruption of candidate virulence factors *Ds69328* and *DsCE3* using CRISPR/Cas9 and a dDNA repair template with 1 kb homologous flanks was highly successful. While only two *Ds69328* transformants grew after sub-culturing, both were found to be disrupted. These transformants were analysed by PCR and Southern hybridization which suggested that disruption of *Ds69328* and homologous recombination repair with the geneticin resistance cassette had occurred successfully in both.

Of the *DsCE3* transformants, 59 grew after sub-culturing. Disruption of *DsCE3* was also efficient (75%) with nine of the 12 screened transformants shown to be successfully disrupted. While PCR analysis indicated that homologous recombination with the dDNA repair template occurred as expected, Southern hybridization analysis suggested otherwise. Four of the six transformants screened had a hybridisation fragment of the expected size, however three of those had additional fragments of unexpected sizes from both *Hin*dIII and *Eco*RI digestions (**Figure 5.11**). These additional fragments could be due to poor stringency of the probe, or partial digestion of the gDNA; however, the diversity of fragment sizes between the transformants makes these explanations unlikely. It is possible that these fragments are due to additional modification of the *DsCE3* locus by off-target activity of Cas9, or unexpected repair outcomes from homologous recombination of the dDNA. A recent study of CRISPR/Cas12a-based ribonucleoprotein disruption in *M. oryzae* using microhomology-mediated end-joining (MMEJ) and non-homologous dDNA reported five different repair outcomes, hypothesised to be caused by at least three different DNA repair mechanisms (Huang, Schol, Villanueva, Heidstra, & Joosten,

2021). To determine what effects the CRISPR/Cas9 process had at the DSB site and possibly elsewhere in the genome it would be necessary to perform whole-genome sequencing. However, these results emphasise the importance of performing Southern hybridization analysis alongside PCR screening.

Growth characteristics of the *Ds69328* and *DsCE3* transformants were analysed, and four of the six *DsCE3* transformants showed significantly slower radial growth compared to the WT (**Table 5.2**). These transformants were not the same four that had unexpected Southern hybridisation fragments. In fact, these transformants represent each different type of Southern hybridization result (expected fragment only, expected and additional fragments, unexpected fragments only), suggesting there is no correlation between growth rate and transformant type. All other transformants were not significantly different to the WT in radial growth or sporulation and several were selected for complementation. Growth characteristics of the complementation strains were examined, and the *Ds69328* #2-C3 strain found to have significantly faster radial growth than the WT (**Table 5.4**). It should also be noted that the radial growth and total spore count of the WT was different between the independent experiments shown in **Tables 5.2** and **5.4**. Because of this inconsistency, it is possible that significant differences between the transformants and the WT may be unreliable. In future, it is recommended to test a greater number of biological replicates, and to ensure that all strains are cultured directly from the glycerol stock as multiple rounds of sub-culturing can reduce *D. septosporum* growth and sporulation.

To determine whether the candidate virulence factors *Ds69328* and *DsCE3* contribute to *D. septosporum* infection on *P. radiata*, a virulence assessment was performed. Seedlings of a susceptible pine variety were inoculated with WT, gene disruption and complementation strains of *Dothistroma septosporum* and incubated for 10 weeks. A limitation of the *D. septosporum* virulence assessment is that several aspects of the experiment were not consistent for all samples. Firstly, due to some isolates not producing sufficient spores when required, a second set of inoculations had to be performed two weeks later. Secondly, due to the main plant growth room being out of use, and due to time constraints, the first set of pines to be inoculated was maintained in a different plant growth room with artificial light of a lower intensity than the main growth room. The first week of infection is a crucial period, as this is when the *D. septosporum* spores germinate (Kabir et al., 2015b). Because the pines were maintained in different conditions during this critical period, this may have contributed to variation between the samples, such as the between the WTs of experiment 1 and 2. Thirdly, the desired spore concentration was not obtained from all strains even after the time delay and, due to further

time constraints, this could not be repeated. Consequently, some variation in the number of spores used for inoculation is present between samples. Therefore, while this experiment can provide some insight into the role of *DsCE3* and *Ds69328* in virulence, ideally this assessment should be repeated with consistent experimental conditions, to confirm the results.

After the 10-week incubation, the needles were harvested, and virulence assessed visually through the percentage of needles with lesions, and quantitively through fungal biomass analysis. The main result that was consistent between the two virulence assessments was that high levels of variation were present between biological replicates. In previous *D. septosporum* virulence assessments, clonal *P. radiata* seedlings were used but, due to unavailability, this study used non-clonal seedlings. The level of variability between biological replicates in experiments that used clonal seedlings (Chettri et al., 2012; Guo, Hunziker, et al., 2020; Ozturk et al., 2019) is far lower than what was observed in this study. Therefore, it is likely that the variability in disease symptoms between the biological replicates was partly due to genetic variability in the pine seedlings. Space constraints prevented the use of more than four replicates per treatment and it was unfortunate that some of those replicates were unusable for the biomass analysis due to problems with the CTAB-based gDNA extraction method.

The virulence of the WT strain was different between Experiment 1 and 2. The WT from Experiment 1 had a slightly higher percentage of needles with DNB symptoms than the WT from Experiment 2 (**Table 5.6**), but had a much lower fungal biomass (**Table 5.7**). While a lower concentration of spore inoculum was obtained for the Experiment 1 WT, the total number of spores inoculated per seedling was very similar to that for the Experiment 2 WT (**Table 5.5**). It is possible that the staggered inoculation and growth room change (discussed above) may have resulted in the reduced fungal biomass for the Experiment 1 WT. These inconsistent results mean that comparisons with the WT may be inaccurate, especially for the *Ds69328* strains which were compared with the Experiment 1 WT. Should this experiment be repeated in the future, it is recommended that a higher number of biological replicates are tested, especially for the WT.

Visual assessment of disease symptoms is not as objective as fungal biomass quantification, and this has been shown in several studies. Dothistromin, the phytotoxic secondary metabolite produced by *D. septosporum* was originally thought to not be essential for virulence, because virulence assessment of *P. radiata* infected with dothistromin mutants had been performed visually (Schwelm et al., 2009). However, once virulence assessment was performed by fungal biomass quantification, it was shown that dothistromin is indeed a virulence factor of *D. septosporum* (Kabir et al., 2015a). Recently, *DsEcp2-1*-disrupted mutants appeared to be the

same as WT when virulence was assessed visually but shown to be significantly increased in virulence when fungal biomass was assessed, suggesting the gene encodes an avirulence factor (Guo, Hunziker, et al., 2020). In the experiments outlined in this thesis, the pines were harvested and visual assessments made on different dates, depending on their inoculation date. Visual assessment of needles with and without DNB symptoms involved making judgements about needles that were borderline for the set criteria, especially when the needle was dead and DNB symptoms were unclear. It is possible that there was some variation in subjective decisions required when assessing needles with borderline symptoms. Therefore, the fungal biomass results presented in this study should be considered a more objective representation of the virulence of the *Ds69328* and *DsCE3* mutant strains, compared to the visual needle lesion assessment.

Virulence assessment through fungal biomass analysis suggested that the complementation strains of both genes did not restore virulence to the same level as the WT, suggesting that complementation had not occurred as anticipated. It is possible that the complementation copies were randomly inserted into a region of the genome under chromatin regulation, and were very lowly expressed, or not expressed at all. However, this seems unlikely as the tight packing of chromatin which makes access difficult for the gene transcription machinery (Lawrence, Daujat, & Schneider, 2016), would also make access difficult for random gene insertion. It is also possible that because the target genes were only disrupted and not knocked out, the presence of two gene copies might have induced quelling in both copies. Quelling is RNAi-mediated silencing of multiple gene copies and has been reported after introduction of a homologous transgene when the endogenous gene is still present (Lax et al., 2020; Li, Chang, & Liu, 2010). Further work would be required to determine if this scenario is possible and, to the best of my knowledge, it has not been reported in other CRISPR/Cas9 studies. Another explanation is that the autonomously replicating CRISPR/Cas9 plasmid was not lost after selection was removed, and that *Cas9* had remained active in the genome. If this had occurred, then the complementation copy of the gene, which contained the PAM site, could have been targeted by Cas9 to introduce a mutation. The complementation transformants were screened by PCR, but this type of analysis would only show large indels, rather than single nucleotide indels that could cause frameshift mutations. Again, whole-genome sequencing would be informative.

Insertion of part of the CRISPR/Cas9 plasmid, usually containing the hygromycin resistance gene, occurred in several *DsAflR*-disrupted mutants, but this was thought to be due to the strong selection pressure being applied when the transformants were maintained on hygromycin

selection for too long. Therefore, when disruption of *Ds69328* and *DsCE3* was performed, the transformants were removed from hygromycin selection immediately, and only cultured on geneticin. If the *Cas9* gene was still present, it is possible that the transformants were not cultured for long enough without selection for the autonomously replicating plasmid to be lost, or that the *Cas9* gene was inserted into the genome. Regardless, the results from this study suggest that complementation should be performed with a gene copy mutated at the PAM site.

Although interpretation of the results of this experiment is limited by the unexpected phenotypes of the complementation strains, inconsistencies in infection between the WTs, and variability between replicates, suggestions can still be made about the potential roles of *Ds69328* and *DsCE3* in virulence. Virulence assessment through fungal biomass analysis suggested that disruption of *Ds69328* caused an increase in fungal biomass. However, this was in comparison with the WT with very low fungal biomass, so no firm conclusions can be made about the role of this gene in virulence of *D. septosporum*. Should this experiment be repeated and support this result, a possible role for *Ds69328* could be in regulating the expression of avirulence factors. The regulated genes could encode proteins which function as PAMPs, release DAMPs, or are effector proteins which are recognised by a receptor in the host. This would be an interesting result, because identification of avirulence factors can lead to identification of host immune receptors and could aid pine resistance breeding efforts. In contrast, disruption of *DsCE3* was suggested to cause a decrease in fungal biomass. Therefore, *DsCE3* may function as a virulence factor that contributes to virulence but is not essential, as *D. septosporum* was still able to produce sporulating lesions and complete its lifecycle. As discussed in **Chapter 3**, DsCE3 was hypothesised to function as a PAMP that triggers cell death, aiding the switch to necrotrophic growth. Ideas for future research to test this hypothesis and to characterise the role *DsCE3* plays in virulence of *D. septosporum*, are discussed in **Chapter 6**.

In summary, highly efficient CRISPR/Cas9 gene editing of *D. septosporum* was established in this study. This method was used to disrupt a well characterised gene *DsAflR*, with a known phenotype, as well as two uncharacterised candidate virulence factors, *Ds69328* and *DsCE3*. Although there were confounding factors that limited the interpretation, virulence assessment of *D. septosporum* mutants indicated that DsCE3 may function as a virulence factor. Priorities for future work will be discussed further in **Chapter 6**.

Chapter 6 – Conclusions and future work

6.1 Introduction

The diseases caused by *D. septosporum* and *F. fulva* are important threats to plant health. The incidence and severity of Dothistroma needle blight (DNB) has increased drastically over the last few decades (Drenkhan et al., 2016), partly attributed to climate change (Woods et al., 2016). The current control measures of silviculture and copper fungicide application have limited effectiveness (Brown & Webber, 2008; Hirst et al., 1999) and, as disease incidence continues to increase, it has become imperative that new control measures are sought. Identification of virulence factors from *D. septosporum* and corresponding resistance (*R*) genes in the pine host could facilitate pine breeding programs by providing molecular markers for disease resistance in pine.

In contrast, tomato leaf mould disease, which was originally controlled through fungicide application, then later through introgression of tomato *R* genes, had not been considered a significant threat for many years. However, *F. fulva* adapted to these genes rapidly so that, by the 1980's, all six major deployed *R* genes had been overcome (Lindhout, Korta, Cislik, Vos, & Gerlagh, 1989) and some of these resistant strains had become the most dominant in the population within a decade (Wang, Meng, Xu, Wang, & Li, 2007). Like with DNB, there is now an urgent need to discover new virulence factors from *F. fulva* and develop new resistant varieties.

To meet this need, the focus of this thesis was to identify and characterise virulence factors from *D. septosporum* and *F. fulva*. Characterising previously identified *F. fulva* effector candidate CfEcp11-1 (Mesarich et al., 2018), was one of the aims of this study. In **Chapter 2**, two novel homologues of CfEcp11-1 were identified, and chimeric protein sequences were designed as part of a multidisciplinary collaboration to determine what regions and amino acids of this protein are required for receptor recognition. CRISPR/Cas9 gene editing was performed for the first time in this fungus to successfully disrupt both copies of *CfEcp11-1*, and these mutants are currently being characterised for a role in virulence by our collaborators.

Another aim was to identify candidate virulence factors from *D. septosporum* and address the current knowledge gap about hemibiotrophic pathogens by identifying candidates with a possible role in the necrotrophic switch. In **Chapter 3**, a prediction pipeline was used to identify ten candidates which were analysed through homology, predicted protein function and gene expression profiles, to predict their role in virulence. These results were followed up by identification of new candidate virulence factors from culture filtrate proteomes of *D.*

septosporum and *F. fulva*. **Chapter 4** presents the first comparative proteomic analysis of *D. septosporum* and *F. fulva*. This analysis identified several new candidate virulence factors and provided further insight to previously identified candidates, such as those from **Chapters 2** and **3**, and their possible roles in virulence.

Finally, the last aim of this thesis was to characterise the roles of two of the identified candidate virulence factors of *D. septosporum* by gene disruption and virulence assessment on the pine host. In **Chapter 5**, CRISPR/Cas9 gene editing was applied to *D. septosporum* for the first time and used to disrupt the two candidate virulence genes *Ds69328* and *DsCE3*. Virulence assessments suggested a role for DsCE3 as a virulence factor. However, due to the limitations discussed in **Chapter 5**, repetition of these experiments is required to obtain more reliable evidence. The aims completed in this thesis will facilitate future research to identify and characterise candidate virulence factors from *D. septosporum* and *F. fulva*, as well as other fungal species. The next logical steps to continue the research presented in this thesis are discussed below.

6.2 CfEcp11-1 of *F. fulva* is a LARS effector with homologues in other fungal species

CfEcp11-1 was first identified from apoplastic washing fluid of a compatible interaction between *F. fulva* and tomato by Mesarich et al. (2018). In the study by Mesarich et al. (2018), CfEcp11-1 was shown to elicit a hypersensitive response (HR) in several wild tomato cultivars, and to have low amino acid identity with avirulence effector AvrLm3 of *L. maculans*. In this thesis, two new CfEcp11-1 homologues were identified from *F. oxysporum* and more recently another 49 structural analogues of CfEcp11-1 were identified and named the Leptosphaeria AviRulence and Suppressing (LARS) effector family (Lazar et al., 2022). Interestingly, despite the many LARS family effectors identified in Dothideomycetes and other fungal classes, this study did not identify a homologue in the closely related fungus, *D. septosporum*. In the study by Lazar et al. (2022), an HMM search was performed first to identify protein analogues, and then structural analogy was confirmed by AlphaFold2 predictions. It has recently been shown that analysis of the primary sequence information of effectors is often insufficient to identify important relationships with effector families. Indeed, many effectors have low sequence similarity but predicted structural similarity to other effectors (Rocafort, Bowen, et al., 2022; Seong & Krasileva, 2023). Recently, LARS family effectors were identified from the apple scab causal agent *Venturia inaequalis* through structural similarity predicted by AlphaFold2 (Rocafort, Bowen, et al., 2022). It would be of interest in the future to perform AlphaFold2 predictions of

D. septosporum candidate effectors, to determine if this fungus contains any LARS family effectors.

Prior work suggested that CfEcp11-1 could be recognised by the *L. maculans* host *B. napus*, but AvrLm3 was not recognised in tomato. In **Chapter 2**, these results were followed up by the design of chimeric and mutant AvrLm3 and CfEcp11-1 proteins to determine what protein regions and amino acids are required for receptor recognition by Cf-Ecp11-1 in tomato. Several CfEcp11-1 homologues were also designed to be screened for a response in tomato. However, due to limitations of the available plant growth room (discussed in **Chapter 2**), Potato virus X (PVX) screening could not be performed at Massey University. Instead, genes encoding the chimeric proteins were sent to collaborators in the Netherlands, where the state-of-the-art growth room facilities are likely to have success, and these results are expected in the near future. The same chimeric constructs are also being tested in *B. napus* by our collaborators in France, and once these experiments have been performed, it will be interesting to compare the results from each host.

It has been shown that, similar to AvrLm3, CfEcp11-1 recognition by Rlm3 in *B. napus* can be masked by AvrLm4-7 (Lazar et al., 2022). It would be valuable to determine if this interaction also occurs with the putative tomato Cf-Ecp11-1 receptor. This could be tested by heterologous secretion of the CfEcp11-1 protein in *Pichia pastoris*, as performed previously (Lazar et al., 2022), and infiltration into *AvrLm4-7*-agroinfiltrated tomato plants. If AvrLm4-7 can mask recognition of CfEcp11-1 by the tomato Cf-Ecp11-1 receptor, CfEcp11-1 should not trigger HR when infiltrated. This experiment would further characterise the role of CfEcp11-1 and the extent of its conservation with AvrLm3. The chimeric proteins collaboratively designed and presented in this thesis include tagged versions of CfEcp11-1. Previous work which suggested AvrLm3 was not recognised in tomato was performed with an untagged construct (as tagging was found to disrupt recognition in *B. napus*) and, therefore, the presence of the protein could not be confirmed by Western blot analysis. It will be valuable to test these tagged CfEcp11-1 constructs, because if any of the CfEcp11-1 proteins are found to be unaffected by the tag, AvrLm3 (as a structural analogue of CfEcp11-1) can be tagged in the same way and tested again for recognition in tomato. These results are expected in the future from our collaborators.

Despite being recognised as an avirulence factor in tomato, there are several lines of evidence that suggest CfEcp11-1 is an important protein for *F. fulva*. Firstly, it was shown in **Chapter 4** that CfEcp11-1 was detected in all culture filtrate proteome samples, suggesting this protein may be required for growth in culture. This could be tested by analysing growth characteristics,

such as radial growth and sporulation, of the *CfEcp11-1*-disrupted strains, as was performed in **Chapter 5** for the *D. septosporum* mutants. Secondly, the recognition of CfEcp11-1 as an avirulence factor would provide strong selection for the loss or modification of the encoding gene to avoid triggering host defences. Two functional copies of *CfEcp11-1* are present in the genome, as well as a pseudogenized copy, suggesting that retention of *CfEcp11-1* function is important for *F. fulva* (Zaccaron et al., 2022). Could the duplication of *CfEcp11-1* suggest that modification to avoid Cf-Ecp11-1 recognition is currently underway? Could this have already occurred with the pseudogenized copy, but resulted in loss of function? It would be interesting to analyse the ratio of non-synonymous to synonymous mutations in the pseudogenized copy, to investigate what evolutionary processes resulted in this outcome. The identification of duplicated copies of *CfEcp11-1* highlights the importance of performing chromosome-level genome assemblies of plant-pathogenic fungi. The third line of evidence that CfEcp11-1 is important for *F. fulva* is that CfEcp11-1 is recognised in many wild tomato species (Mesarich et al., 2018). Could *Cf-Ecp11-1* have been maintained in so many wild varieties because it is an important effector cannot be easily lost or mutated? Finally, as part of a well conserved effector family (Lazar et al., 2022), it is likely that CfEcp11-1 and CfEcp11-1 homologues play an important role in their respective fungal species. Therefore, one of the objectives of this thesis was to characterise CfEcp11-1 through gene disruption and virulence assessment on the tomato host (without the Cf-Ecp11-1 receptor).

CRISPR/Cas9 was performed successfully in *F. fulva* for the first time, and both single- and double-copy *CfEcp11-1* mutants were obtained. Unfortunately, due to limitations of the available plant growth rooms and time constraints, these mutants were not tested as part of the work described in this thesis. However, they have been sent to our collaborators in the Netherlands, and the results of the virulence assays will be published together with the chimeric gene screening results. It will be interesting to determine whether the single- and double-copy mutants differ in virulence, and if they function redundantly, or contribute additively to virulence. Our collaborators are also working to clone the tomato *Cf-Ecp11-1* receptor gene, which would facilitate resistance breeding work and provide valuable information about CfEcp11-1. Identifying what type of receptor recognises CfEcp11-1 may help suggest what type of protein CfEcp11-1 is and what function it performs in *F. fulva*. Based on previously identified Cf R proteins, it is likely that Cf-Ecp11-1 is also a receptor-like protein (RLP). Should this analysis determine that CfEcp11-1 contributes to the virulence of *F. fulva*, there are several complementation experiments that would be informative. The *CfEcp11-1*-disrupted mutant could be complemented with *AvrLm3*, or any of the other *CfEcp11-1* homologues found to

trigger cell death in tomato, to determine whether these homologous genes can restore virulence. The mutants could also be complemented with a gene encoding one of the chimeric *CfEcp11-1* proteins that do not trigger HR in tomato. This would indicate whether the same amino acids or gene regions required for receptor recognition are also required for virulence.

6.3 Candidate virulence factors identified from *D. septosporum* and *F. fulva* through bioinformatic and proteomic analysis

Candidate effectors from *D. septosporum* were previously identified through prediction pipelines in two separate studies (Hunziker, 2018; Tarallo, 2022). In **Chapter 3**, the results of these two studies, homology to virulence factors from other species including *F. fulva*, and gene expression data, were used to develop a new candidate virulence factor prediction pipeline with a key focus on the necrotrophic switch. Ten candidates were shortlisted using this analysis, six of which were novel to this study. This pipeline was unique as it included predicted transcription factor genes, while previous studies focused solely on effector candidates (Hunziker, 2018; Tarallo, 2022). As discussed in **Chapter 1**, many genes suggested to play a role in the necrotrophic switch are predicted transcription factors. Some of the most promising transcription factors identified in **Chapter 3** are listed in **Table 6.1**, including DsPf2, Ds74812, and Ds69328. These candidates could be characterised in the future by generating gene disruption mutants and performing comparative transcriptome analysis with the wild type (WT). This experimental approach was used to study *PnPf2* of *Parastagonospora nodorum* and identified its possible role in the necrotrophic switch by regulating expression of necrotrophic effector genes (Jones et al., 2019).

Candidate effectors were also identified from the prediction pipeline in **Chapter 3**. The majority were identified in previous studies and found to elicit cell death in the non-host *Nicotiana* species or the *P. radiata* host (Hunziker, 2018; Hunziker et al., 2021; Tarallo, 2022; Tarallo et al., 2022). In **Chapter 4**, candidate effector proteins, such as DsEcp57-1, DsGH11, DsCPL1, and DsCE3 (**Table 6.1**), were further characterised by their secretion in different *in vitro* conditions. As well as the *D. septosporum* proteome, the *F. fulva in vitro* proteome was also presented in **Chapter 4**, and comparisons were made between the two. Novel candidate virulence factors from *D. septosporum* and *F. fulva*, which were not identified in **Chapter 2**, **Chapter 3**, or previous studies, were identified through this comparative proteomic analysis (**Table 6.1**). These culture filtrate proteomes showed that, contrary to popular belief, effector proteins can be expressed in culture, at least for *D. septosporum* and *F. fulva*. These results illustrate the value of performing

in vitro proteomic analysis and present a useful tool for the identification of candidate effector proteins.

The proteomic analysis could be improved by the addition of transcriptome analysis of the complete hemibiotrophic lifecycle of *F. fulva* Race 5. Because *F. fulva* was considered a biotroph until quite recently (Mesarich et al., 2023) and, due to the late onset of necrotrophy caused by this species in its tomato host, gene expression analysis is not currently available for the necrotrophic stage. With the addition of such gene expression data, this *in vitro* proteome as well as the *in planta* proteome (Mesarich et al., 2018) could be re-analysed to identify necrotrophic effectors for the first time in this pathogen. Of course, it would also be invaluable in the future to repeat the *F. fulva in planta* proteome to include apoplastic washing fluid extracted from the necrotrophic stage. *F. fulva* necrotrophic stage expression data would also enable additional comparisons to be performed with the *D. septosporum* proteome and may lead to identification of new *F. fulva* homologues with roles in virulence.

As detailed in **Chapter 1**, proteomic analysis of *D. septosporum* was previously a gap in the available resources for this pathogen. The *in vitro* proteome presented in **Chapter 4** has therefore provided valuable information about this pathogen; however, an *in planta* proteome is yet to be completed. **Chapter 4** illustrated that apoplastic washing fluid could be collected from clonal *P. radiata* shoots, but infection with *D. septosporum* proved problematic. It would be valuable in the future to optimize *D. septosporum* infection on these clonal *P. radiata* shoots, so that proteomic analysis could be performed with apoplastic washing fluid extracts. It was hypothesized that *D. septosporum* was growing on the *P. radiata* media and producing dothistromin that killed the clonal *P. radiata* shoots. Therefore, future trials could include removing the *P. radiata* shoots for inoculation and ensuring the spores dry on the shoots before replacing them back into the medium in the jars. Antibiotics could also be added to the media to prevent growth of *D. septosporum*, provided there was no detrimental effect to the *P. radiata* shoots or the *D. septosporum* on the shoots. It should also be determined how long the *P. radiata* shoots remain healthy for once the jars are opened, as *D. septosporum* infection can take 10–12 weeks on 1–2 year old seedlings (Kabir et al., 2015b). It may be necessary to provide additional moisture to the jars for the *P. radiata* shoots, as well as to maintain high needle wetness for *D. septosporum* infection. Should these trials prove unsuccessful, another option to provide *in planta*-like proteomic analysis, would be to grow *D. septosporum* in *P. radiata* apoplastic washing fluid and analyse extracts of this culture. This experimental approach was recently used to identify candidate virulence factors from the proteome of the kauri dieback pathogen, *Phytophthora agathidicida* (Bradley, 2022).

Table 6.1. Candidate virulence factors identified in this study that are of interest for further research.

Name	Predicted function[1]	Features[2]	Chapter where discussed
D. septosporum – biotrophic stage			
DsEcp57-1	Candidate effector	E & M, all LDM samples	Chapters 3, 4
DsGH11	Glycoside hydrolase family 11	*in planta*, D9 LDM & all PMMG	Chapters 3, 4
Ds74289	Candidate effector	E, D16 PMMG pine extract	Chapter 4
D. septosporum – necrotrophic switch			
DsCE3	Candidate effector, cell death elicitor	L, all samples	Chapters 3, 4, 5
Ds69328	Zn_2Cys_6 fungal transcription factor	M	Chapters 3 & 5
DsCE15	Cell death eliciting effector	M & L	Chapter 3
Ds27299	Nis1 domain	M & L, LDM & D9 PMMG	Chapter 4
DsPf2	Zn_2Cys_6 fungal transcription factor	No	Chapter 3
Ds74812	Basic-leucine zipper transcription factor	M	Chapter 3
D. septosporum – necrotrophic stage			
DsCPL1	Cerato-platanin effector	M & L, all late samples, homologue	Chapters 3, 4
DsEcp20-3	Candidate effector, cell death elicitor	M & L, D9 LDM	Chapter 4
Ds158381 (Ecp2-1)	Avirulence effector	M, PMMG, homologue	Chapter 4
Ds70909	Glutathione S-transferase	M & L, spec pine extract in LDM	Chapter 4
Ds71743	Cellulase	L, D4 LDM & PMMG	Chapter 4
F. fulva			
CfEcp11-1	Candidate avirulence effector	*in planta*, all samples	Chapters 2, 4
CfEcp14-2	Candidate effector	*in planta*, D4 PDB	Chapter 4
CfEcp14-1	Candidate avirulence protein	*in planta*, D9 PDB	Chapter 4
CfEcp50-1	Candidate effector	*in planta*, D9 PDB & D9 PMMG	Chapter 4
UJO13947.1	Glycoside hydrolase family 17	*in planta*, PDB & D9 PMMG	Chapter 4
UJO11627.1 (CfEcp2-1)	Effector	*in planta*, all samples, homologue	Chapter 4

1 – Predicted protein function from multiple sources, as discussed through thesis.

2 – Features include: gene expression, the encoding *D. septosporum* gene was upregulated *in planta*, not upregulated at all (No), or upregulated at the specific *in planta* stages; E, early; M, mid; L, late (Bradshaw 2016). The gene encoding the *F. fulva* 0WU orthologue of the Race 5 gene named in column 1 was upregulated *in planta* (Mesarich 2014). Proteins were detected in proteome samples with the specific properties: D4, day 4; D9, day 9; D16, day 16; LDM, low Dothistroma medium; PMMG, pine minimal salts medium; PDB, potato dextrose broth; pine extract, sample had the addition of pine extract; homologue; all samples, protein was detected in all sample types indicated; spec, specific to the sample types indicated; homologue; a homologue from *D. septosporum* or *F. fulva* was also detected.

6.4 DsCE3 is a candidate virulence factor of *D. septosporum*

Candidate virulence factors of *D. septosporum* were identified in **Chapter 3**, and two were selected for gene disruption analysis in **Chapter 5**, including DsCE3. This protein was first identified as a candidate effector by Hunziker (2018), where it was shown to elicit cell death in *N. benthamiana* and *N. tabacum*. It was also recently shown through recombinant expression and infiltration that DsCE3 can elicit a form of cell death on *P. radiata* (Tarallo, 2022). *DsCE3* is highly upregulated at the late *in planta* stage and was detected in all proteomic samples in **Chapter 4**. Gene disruption suggested that *DsCE3* may be important for radial growth as four of the six transformants tested had slower growth than the WT. Virulence assessment on the *P. radiata* host suggested that *DsCE3* may be important for virulence. The two disrupted transformants had a significantly higher percentage of needles with DNB symptoms, but a significantly lower fungal biomass compared to the WT. Fungal biomass analysis is more objective than visual needle analysis, as discussed in **Chapter 5**, therefore these results suggested that *DsCE3* may function as a virulence factor. However, complementation did not restore virulence, therefore it would be valuable to repeat this virulence assay with correctly complemented transformants in the future.

If virulence assessment of *DsCE3* was repeated, several aspects of the experiment should be changed. Firstly, the gene disrupted strain Δ*DsCE3* #34 should be replaced with a new transformant with only the expected sizes of Southern hybridizing fragments. The additional or incorrect fragments observed from this strain and all others, except Δ*DsCE3* #17, suggest that the DSB was repaired in an unexpected way, or there were ectopic effects, which may have affected the virulence of these strains. Complementation would also need to be repeated; how this could be performed to minimise the chances of complementing genes being silenced, is discussed in **section 6.6**. For virulence assessment on the *P. radiata* host, it is important that clonal pine seedlings are used to reduce variability between biological replicates. Ideally, all seedlings would also be inoculated with the same spore concentration and volume. It is also

recommended that a larger number of *P. radiata* replicates are inoculated with the *D. septosporum* WT.

The function DsCE3 performs in *D. septosporum* is currently unknown. DsCE3 is an orthologue of the cell death-eliciting pathogen-associated molecular pattern (PAMP) RcCDI1, from the barley scald disease pathogen *Rhynchosporium commune* (Franco-Orozco et al., 2017; Hunziker, 2018). An orthologue of DsCE3 was also recently identified from pine pathogen *Cyclaneusma minus* (protein Cm2492) and shown to elicit chlorosis or weak cell death in *Nicotiana* species (Tarallo, 2022). DsCE3 was suggested through AlphaFold2 predictions to be part of the trypsin inhibitor β-trefoil superfamily (Tarallo, 2022). It would be useful to test this prediction by performing trypsin inhibition assays, as were performed by Sabotič et al. (2012). Proteins with a β-trefoil fold can have a variety of functions, including as protease inhibitors (Renko, Sabotič, & Turk, 2012; Sabotič, Renko, & Kos, 2019) and fungal lectins (Juillot et al., 2016; Schubert et al., 2012; Varrot, Basheer, & Imberty, 2013). Fungal effectors, such as *F. fulva* Avr2, are protease inhibitors and can inhibit plant defence proteases (Jashni, Mehrabi, Collemare, Mesarich, & de Wit, 2015). In contrast, several fungal protease inhibitors and lectins have been shown to have toxic properties in other microorganisms or the host plant, the latter of which may promote virulence for necrotrophic pathogens (Asano, Miwa, Maeda, Kimura, & Nishiuchi, 2013; Sabotič et al., 2019; Schubert et al., 2012; Varrot et al., 2013; Wohlschlager et al., 2011).

It is possible that DsCE3 elicits cell death in *Nicotiana* species and *P. radiata* through recognition as a PAMP. This hypothesis is supported by homology to the characterised PAMP RcCDI1 and by the cell death-eliciting activity of DsCE3. One way to test if DsCE3 is recognised as a PAMP would be to express DsCE3 in *Nicotiana* species via an *Agrobacterium tumefaciens*-mediated transient expression assay (ATTA) and analyse the expression of plant PTI-associated genes, such as *BAK1* and *SOBIR1*, through qPCR as has been performed previously (Tarallo, 2022). DsCE3 could also be expressed via ATTA in *Nicotiana* species in which *SOBIR1* has been deleted (Huang et al., 2021) and the response compared with that in WT *Nicotiana*. Absence of a cell death response in the *SOBIR1* mutant would indicate that DsCE3 recognition requires SOBIR1, and therefore that DsCE3 could be considered a PAMP. It would be beneficial to determine if DsCE3 is recognised as a PAMP, because a cognate *P. radiata* receptor could potentially be identified and bred into new *P. radiata* cultivars to enhance disease resistance.

Instead of acting as a PAMP, DsCE3 might elicit cell death in *Nicotiana* species and the *P. radiata* host because of its toxicity, like the *Fusarium graminearum* lectin FFBL (Asano et al., 2013). Fungal lectins have been suggested to kill other microorganisms by disrupting cell membranes

(Juillot et al., 2016; Schubert et al., 2012; Wohlschlager et al., 2011). Therefore, it is possible that DsCE3 could disrupt plant cell membranes to promote necrotrophy and therefore virulence. This could be investigated by performing localization studies in *Nicotiana* species where DsCE3 is tagged at the N- or C-terminus with a fluorescent protein, such as mCherry or green fluorescent protein (GFP), and the pine tissues is labelled with a plasma membrane marker such as FM4-64 (Rigal, Doyle, & Robert, 2015), to determine if the protein localizes to the plant cell membrane. It would be valuable to determine whether DsCE3 elicits cell death through fungal lectin-based toxicity, because it is possible that some pine species may secrete a protein to suppress the cell death-eliciting activity of DsCE3. There is a precedent for this in the Thi2.4 protein of *Arabidopsis* species that can suppress the *F. graminearum* lectin FFBL (Asano et al., 2013). An orthologue of Thi2.4 in pine would potentially be of interest as a target for resistance breeding.

Other fungal protease inhibitors and lectins have been shown to have toxic properties towards other microorganisms, to provide defence against fungal parasites and predators or aid in competition (Sabotič et al., 2019; Schubert et al., 2012; Varrot et al., 2013; Wohlschlager et al., 2011). Therefore, it is also possible that as well as having toxicity towards plant cells, DsCE3 may also be toxic to competing microorganisms present on *P. radiata* needles. One way this could be tested would be to identify a suitable *D. septosporum* competitor, such as a fungal saprophyte or bacterial or fungal endophyte, and to determine growth of the competitor microorganism *in vitro* in the presence of the *DsCE3* disrupted strain compared to the WT.

The hypothesis presented in **Chapter 3**, was that DsCE3 can be recognised in *P. radiata* and *N. benthamiana* as a PAMP to elicit HR, and that during a compatible interaction on the host, another effector is present to mask or suppress DsCE3 recognition during the biotrophic stage. This masking or suppressing activity could also be stopped at the end of the biotrophic stage, so the cell death elicited by DsCE3 recognition could trigger the switch to necrotrophy. Regardless of whether DsCE3 elicits cell death through recognition as a PAMP or fungal lectin-based toxicity, it is possible that this protein is involved in the necrotrophic switch. If virulence assessment of DsCE3 was repeated in the future to confirm the role of DsCE3 as a virulence factor, it may also be valuable, when performing visual analysis of infected needles, to also count how many lesions were sporulating compared to the wild type. If DsCE3 contributes to the necrotrophic switch, fewer sporulating lesions would be expected from the mutant.

6.5 Ds69328 is a candidate virulence factor of *D. septosporum*

The other candidate virulence factor identified in **Chapter 3** and selected for gene deletion analysis in **Chapter 5** was Ds69328. *Ds69328* is predicted to encode a Zn_2Cys_6 fungal

transcription factor that was identified as a potential necrotrophic switch factor from the transcriptome analysis of *D. septosporum* infection of *P. radiata* (Bradshaw et al., 2016). This gene was suggested to play a role in the transition to necrotrophy because it was highly upregulated specifically at the mid stage *in planta* (Bradshaw et al., 2016). The analysis performed in **Chapter 3** showed that Ds69328 is not well conserved in Dothideomycete species, other than *F. fulva*, and does not share homology to characterised proteins. As discussed in **Chapter 3**, several fungal transcription factors have been identified as contributing to virulence by regulating the expression of effector proteins or secondary metabolites. Therefore, it is possible that Ds69328 performs the same function in *D. septosporum*. Virulence assessment on the *P. radiata* host tentatively suggested that Ds69328 may have an avirulence function, as one mutant had increased fungal biomass compared to the WT. However, these results were unreliable, for several reasons discussed in **section 6.5**, illustrating the difficulty of performing a virulence assay with a slow-growing foliar pine pathogen, and the experiments will need to be repeated in the future.

If virulence assessment of the *Ds69328* mutants on *P. radiata* was repeated, several aspects of the experiment should be changed, most of which were discussed in **section 6.5**. Complementation will need to be repeated because, as with the *DsCE3* mutants, complementation strains were not restored to the WT phenotype. This lack of complementation was also found for complementation strains of three other *D. septosporum* CRISPR mutants that were tested within the same virulence assessment by another researcher (Tarallo, 2022). Several hypotheses were discussed in **Chapter 5** as to why complementation did not restore virulence. The most likely was that an active *Cas9* gene and sgRNA was present in the genome, due to the CRISPR/Cas9 plasmid being retained either autonomously or integrated into the genome, resulting in mutation of the extra 'complementation' gene copy. The presence of the *Cas9* gene in transformants could be determined by Southern hybridization or genome sequencing. Transformants without *Cas9* would be preferable candidates for virulence assessment because the presence of an active Cas9 protein increases the chance for off-target effects (Ibraheim et al., 2021; Li et al., 2019). However, for future experiments, complementation should be performed with a gene copy mutated at the PAM site to guard against any unwanted Cas9 activity.

Should Ds69328 be confirmed in the future to play a role during *P. radiata* infection, it would be valuable to sequence the transcriptome of a *Ds69328* mutant and compare it with that of the WT. This was recently performed with transcription factor *PnPf2* of *Parastagonospora nodorum*, where it was found that this gene regulates the expression of several necrotrophic effectors and

may contribute towards the necrotrophic switch (Jones et al., 2019). Transcriptome analysis of a *Ds69328* mutant may identify differentially expressed gene compared to the WT and could lead to the identification of new candidate effectors, which would be invaluable for future research.

6.6 Future perspectives

This research identified several new candidate virulence factors from *D. septosporum* and *F. fulva* and further characterised candidates through *in vitro* secretion and gene deletion analysis. These candidates may be valuable for future control strategies. RNAi-based silencing of virulence factors, either through host-induced gene silencing (HIGS) or spray-induced gene silencing (SIGS), can be an effective control strategy against fungal pathogens (Guo et al., 2019; Sang & Kim, 2020; Song & Thomma, 2018). If a role in virulence is confirmed in the future, Ds69328 may be a suitable target for RNA silencing by spray-induced gene silencing (SIGS), as this gene is not well conserved and has a low chance of off-target effects in beneficial microbiota. Because DsCE3 is well conserved in other fungal species of a variety of lifestyles, the best use of this candidate virulence factor to develop control strategies of DNB would be to identify a cognate receptor or DsCE3-suppressing protein in *P. radiata*. To identify a DsCE3 receptor, a range of pine germplasm with known levels of DNB resistance would need to be screened for HR by infiltration of heterologously produced DsCE3 protein. This would facilitate breeding for resistance, while identification of the corresponding *P. radiata* gene would be invaluable to act as a molecular marker in this process. Yeast two-hybrid assays, co-immunoprecipitation (co-IP) or proximity labelling experiments (Kanja & Hammond-Kosack, 2020; Qin, Cho, Cavanagh, & Ting, 2021) could also be performed with DsCE3 to aid identification of the *P. radiata*-interacting protein. In summary, the research presented in this thesis has provided valuable insight into the infection strategies of these two pathogens and will hopefully aid future disease resistance strategies in pine and tomato.

Appendix

Appendices for Chapter 2

Appendix 1. Plasmids used in Chapter 2.

Plasmid name	Purpose	Antibiotic selection[1]	Reference
pFBTS1	Backbone and hygromycin resistance gene (*hph*) cassette for *CfEcp11-1* homologous recombination plasmid	Kan	Bolton et al. 2008
pFBTS1-*CfEcp11*-1-HR	Homologous recombination transformation of *CfEcp11-1*	Kan/Hyg	This study
pMAI105	Single guide RNA (sgRNA) and *Cas9* expression vector	Hyg	Chambers et al. 2021
pMAI105-*CfEcp11-1*	sgRNA targeting *CfEcp11-1*	Hyg	This study
pSfinx	Potato Virus X (PVX)-based transient expression in *Agrobacterium tumefaciens*	Kan	Takken et al. 2000
pSfinx-*CfEcp11-1*	PVX-based transient expression of *CfEcp11-1*	Kan	This study
pSfinx-*AvrLm3*	PVX-based transient expression of *AvrLm3*	Kan	This study
pSfinx-*CfEcp11-1*_Region1AvrLm3_CfEcp11-1	PVX-based transient expression of region-swapped *CfEcp11-1*	Kan	This study
pSfinx-*CfEcp11-1*_Region2AvrLm3_CfEcp11-1	PVX-based transient expression of region-swapped *CfEcp11-1*	Kan	This study
pSfinx-*AvrLm3*_Region1CfEcp11-1_AvrLm3	PVX-based transient expression of region-swapped *AvrLm3*	Kan	This study
pSfinx-*AvrLm3*_Region2CfEcp11-1_AvrLm3	PVX-based transient expression of region-swapped *AvrLm3*	Kan	This study
pSfinx-*CfEcp11-1*_G132R_W135Y	PVX-based transient expression of amino acid-substituted *CfEcp11-1*	Kan	This study

pSfinx-*CfEcp11-1*_Q59H_G132R_W135Y	PVX-based transient expression of amino acid-substituted *CfEcp11-1*	Kan	This study
pSfinx-*AvrLm3*_G131R_F134Y	PVX-based transient expression of amino acid-substituted *AvrLm3*	Kan	This study
pSfinx-*AvrLm3*_I58H_G131R_F134Y	PVX-based transient expression of amino acid-substituted *AvrLm3*	Kan	This study
pSfinx-*Fusarium_oxysporum*_BFJ63	PVX-based transient expression of *Fusarium oxysporum BFJ63*	Kan	This study
pSfinx-*Fusarium_oxysporum*_BFJ70	PVX-based transient expression of *F. oxysporum BFJ70*	Kan	This study
pSfinx-*Zymoseptoria_ardabiliae*_667	PVX-based transient expression of *Zymoseptoria ardabiliae 667*	Kan	This study
pSfinx-*Zymoseptoria_ardabiliae*_1237	PVX-based transient expression of *Z. ardabiliae 1237*	Kan	This study
pSfinx-*CfEcp11-1*_N-term_6xHis	PVX-based transient expression of tagged *CfEcp11-1*	Kan	This study
pSfinx-*CfEcp11-1*_Mid1_6xHis	PVX-based transient expression of tagged *CfEcp11-1*	Kan	This study
pSfinx-*CfEcp11-1*_Mid2_6xHis	PVX-based transient expression of tagged *CfEcp11-1*	Kan	This study
pSfinx-*CfEcp11-1*_C-term_6xHis	PVX-based transient expression of tagged *CfEcp11-1*	Kan	This study
pSfinx-*CfEcp11-1*_N-term_3xFLAG	PVX-based transient expression of tagged *CfEcp11-1*	Kan	This study
pSfinx-*CfEcp11-1*_Mid1_3xFLAG	PVX-based transient expression of tagged *CfEcp11-1*	Kan	This study
pSfinx-*CfEcp11-1*_Mid2_3xFLAG	PVX-based transient expression of tagged *CfEcp11-1*	Kan	This study
pSfinx-*CfEcp11-1*_C-term_3xFLAG	PVX-based transient expression of tagged *CfEcp11-1*	Kan	This study

1 – Antibiotic selection; Hyg, hygromycin; Kan, kanamycin.

Appendix 2. Primers used in Chapter 2.

Ptimer name	Sequence 5'–3'	Purpose
CfEcp11-1 gene copy number determination		
HM265	CTTACTCCCTCGACTGCAAG	Amplification of *CfEcp11-1*
HM266	AAAGGGAGTCGTAAGAGCAG	
qCfactin-F	GGCACCAATCAACCCAAAG	Amplification of *Fulvia fulva actin* (Mesarich et al., 2014)
qCfactin-R	TACGACCAGAAGCGTACAG	
CfEcp11-1 homologous recombination (HR) plasmid construction		
HM39	CTGCAGCTGTGGAGCC	Amplification of the hygromycin resistance gene (*hph*) cassette from pFBTS1
HM40	AGCTTGATATCTGTTAGTAATC	

HM55	CTGCGCAACTGTTGGGAACTTCGAGATGCGATAACTTA	Amplification of the left *CfEcp11-1* flank
HM42	ATGCGGCTCCACAGCTGCAGCGTAGGATGAGAGTCC	
HM43	TTACTAACAGATATCAAGCTCAATAGGATCTCCAAGATG	Amplification of the right *CfEcp11-1* flank
HM56	CGTTATCCCCTGATTCTGTGTTAGTTTTTATAAGATAATTAT	
HM53	CACAGAATCAGGGGATAACG	Amplification of the pFBTS1 backbone
HM54	TTCCCAACAGTTGCGCAG	
HM1	GCTAGGGCTTGAAGCCTCGAG	Sequencing of *CfEcp11-1* flanks in HR plasmid
HM3	GCTACTAGGACGACTCCGTAAAC	
HM15	CGAAATTGCCGTCAACCAAGCTCT	Sequencing of *hph* cassette in HR plasmid
HM16	TGTTTATCGGCACTTTGCATCGGC	
HM109	GCTTCTGGATTTCCGATC	Sequencing of pFBTS1 backbone in HR plasmid
HM110	TGCTCACATGAGATCTC	
Screening *CfEcp11-1* HR transformants		
qCfactin-F	GGCACCAATCAACCCAAAG	Amplification of *F. fulva actin* (Mesarich et al., 2014) as gDNA control
qCfactin-R	TACGACCAGAAGCGTACAG	
HM146	GCTTTTCTACTATCTCCCTTC	Amplification of boundary between left *CfEcp11-1* flank and *hph*
HM147	CCTCGGACGCAAATC	
HM148	GTGCCGCTTCAATTCATG	Amplification of boundary between *hph* and right *CfEcp11-1* flank
HM149	CTACTCCCTCTCTATTACCC	
CRISPR/Cas9 *CfEcp11-1* disruption plasmid construction		
CfEcp11-1 sgRNA oligonucleotide	ATCAACAACTTCATCTGCCCTGGTGCTGATGAGTCCGTGAG GACGAAACGAGTAAGCTCGTCCACCAGTTCAGAATACCTG GGTTTTAGAGCTAGAAATAGC	Single guide RNA (sgRNA) to be inserted into pMAI105
MAI0556	CCACATCCATACCCATCAACAACTTCATCTGC	Amplification of the sgRNA oligonucleotide (Chambers et al., 2021)
MAI0310	ATTTTAACTTGCTATTTCTAGCTCTAAAAC	
MAI0667	TTGCCCGCGTTGCTGTTG	Sequencing after assembly of the pMAI105-*CfEcp11-1* plasmid (Chambers et al., 2021)
Screening CRISPR/Cas9 *CfEcp11-1*-disrupted transformants		
HM205	GACAATCCAGCGTCTATC	Amplification of the *CfEcp11-1* PAM site
HM206	CACGGTACGATGTTAAGC	

Addition of *PR1α* to *CfEcp11-1* and *AvrLm3* chimeric genes		
HM119	ACTCTTGCCGTGCCCAAAATCTCGACTGCAAGGCCGTAGC	Overlap amplification of *CfEcp11-1* chimeric genes
HM120	GCTACATGCGGCCGCCTATTGAGAACCACAGTGAA	
HM145	ACTCTTGCCGTGCCCAAAATCTTGAATGCCACGCTGTT	Overlap amplification of *AvrLm3* chimeric genes
HM135	GCTACATGCGGCCGCTTACTGATGATCGCAGTGTA	
HM123	ACTCTTGCCGTGCCCAAAATCTGGACTGTCGGTCTATCGC	Overlap amplification of *F. oxysporum BFJ63* chimeric genes
HM136	GCTACATGCGGCCGCCTATTGATGCGCACAGTGAA	
HM141	ACTCTTGCCGTGCCCAAAATTATGCTCTCGACTGC	Overlap amplification of *F. oxysporum BFJ70* chimeric genes
HM142	GCTACATGCGGCCGCTTAATGAGCCGCAC	
HM143	ACTCTTGCCGTGCCCAAAATCATGACTGCCGATC	Overlap amplification of *Z. ardabiliae 667* chimeric genes
HM144	GCTACATGCGGCCGCTCAACGTTGGTGTCC	
HM129	ACTCTTGCCGTGCCCAAAATCACGACTGCCGGGCCATCTC	Overlap amplification of *Z. ardabiliae 1237* chimeric genes
HM139	GCTACATGCGGCCGCTCATTGCGATTTACAGTGAA	
PR1A-AscI-fw	GCTACATGGCGCGCCATGGGATTTGTTCTCTTTTC	Amplification of *PR1α* signal peptide (Mesarich et al., 2014)
PR1A-rv	ATTTTGGGCACGGCAAGAG	
N31	CAACACAGCCCATAGGGTC	Amplification and sequencing of the insert in pSfinx
OX10	CAATCACAGTGTTGGCTTGC	

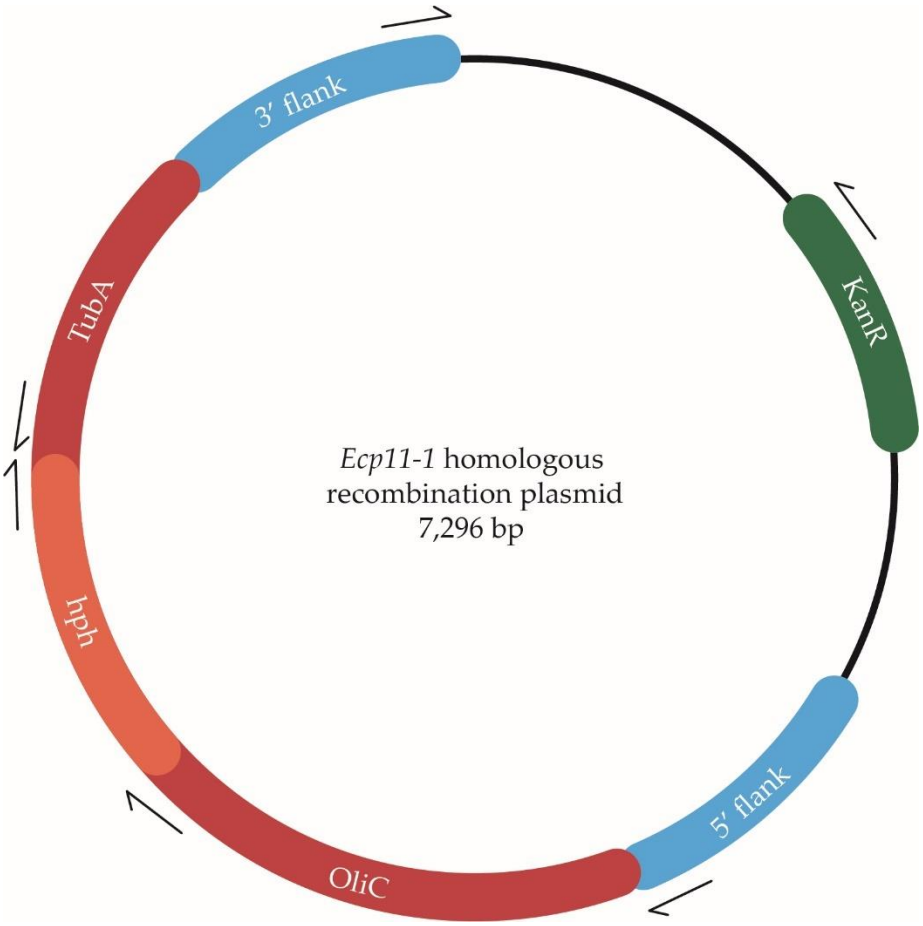

Appendix 3. Schematic of the CfEcp11-1 homologous recombination plasmid. Key features: *KanR*, kanamycin resistance gene (part of pFBTS1 backbone); *OliC*, *hph* promoter; *hph*, hygromycin resistance gene; *TubA*, *hph* terminator (*hph* cassette amplified from pFBTS1), 5' flank, *CfEcp11-1* flank; 3' flank, *CfEcp11-1* flank; bp, base pairs. Arrows illustrate gene orientation.

Appendix 4. Media for *Agrobacterium tumefaciens*-mediated transient transformation

Preparation of induction and minimal media

Component name	Stock solution	Volume for 500 mL IM[1]	Volume for 500 mL MM[2]
K_2HPO_4	1M	2 mL	4.5 mL
KH_2PO_4	1M	5.3 mL	5.3 mL
NaCl	5M	250 µL	250 µL
$MgSO_4$	1M	250 µL	250 µL
$CaCl_2$*	1M	340 µL	340 µL
$FeSO_4$*	0.0025 g/l	500 µL	500 µL
$(NH_4)_2SO_4$	1M	1.9 mL	1.9 mL
Glucose	20%	2.25 mL	5 mL
MES*[3]	1M	20 mL	-
Glycerol	50%	5 mL	-
MilliQ water	-	462 mL	482 mL

1 – 500 µL of 200 mM acetosyringone (dissolved in 100% DMSO, sterilized with a 0.2 µm filter and frozen in aliquots) was added just before use. IM, induction media.

2 – MM, minimal media.

3 – MES (2-(N-morpholino) ethanesulfonic acid) was dissolved in 80 mL water and the pH adjusted to 6.3 with 5 M KOH. The volume was then made up to 100 mL, the solution sterilized with a 0.2 µm filter (Ahlstrom-Munksjö, Helsinki, Finland) and then stored at 4°C.

*Solutions were sterilized with a 0.2 µm filter and added after autoclaving.

For preparation of IM agar, 15 g/L of bacteriological agar (Pure Science) was added.

20x salts solution for selection media

Component name	Volume for 250 mL
$NaNO_3$	30 g
KCl	2.6 g
$MgSO_4.7H_2O$	2.6 g
KH_2PO_4	7.6 g
MilliQ water	250 mL

Solution was autoclaved and stored at 4°C.

Trace elements for selection media

Component name	Volume for 100 mL
$ZnSO_4.7H_2O$	2.2 g
H_3BO_3	1.1 g
$MnCl_2.4H_2O$	0.5 g
$FeSO_4.7H_2O$	0.5 g
$CoCl_2.5H_2O$	0.16 g
$CuSO_4.5H_2O$	0.16 g
$(NH_4)_6Mo_7O_{24}.4H_2O$	0.11 g
Na_4EDTA	5 g
MilliQ water	80 mL

Each chemical was added in order to the water, dissolving before the next addition. The solution was heated to boiling, cooled to 60°C, and then adjusted to pH 6.5–6.8 with KOH. The solution was cooled to room temperature, the volume adjusted to 100 mL, autoclaved, and then stored in the dark at 4°C.

Selection media agar

Component name	Volume for 500 mL
20x salts	50 mL
Trace elements	1 mL
Glucose	10 g
Agar	15 g
MilliQ water	449 mL

After autoclaving, 50 µg/mL hygromycin and 200 µM cefotaxime was added.

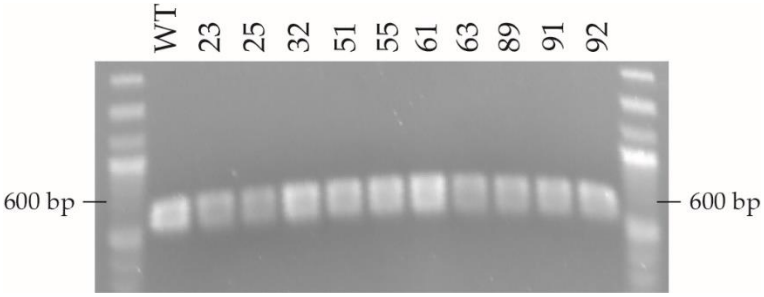

Appendix 5. PCR screen of genomic DNA from *Fulvia fulva* Race 5 wild type (WT) and CRISPR/Cas9 *CfEcp11-1* transformants. PCR performed with primers HM205/HM206 and Phusion High-Fidelity DNA polymerase, to amplify a 607 bp fragment from *CfEcp11-1*. Results are shown from ten out of the 15 transformants screened, as a representative result (all transformants screened amplified a WT-sized *CfEcp11-1* product).

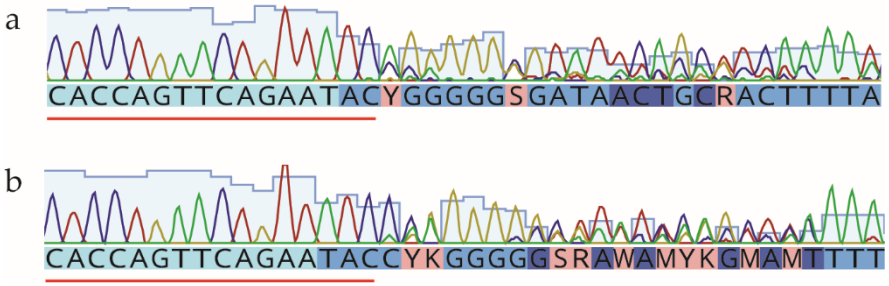

Appendix 6. Sequencing results of *CfEcp11-1* transformant #92 before and after single spore purification. A portion of the sequence up to and after the single guide RNA (sgRNA) binding site (red line) from transformant #92 before (**a**) and after (**b**) single spore purification.

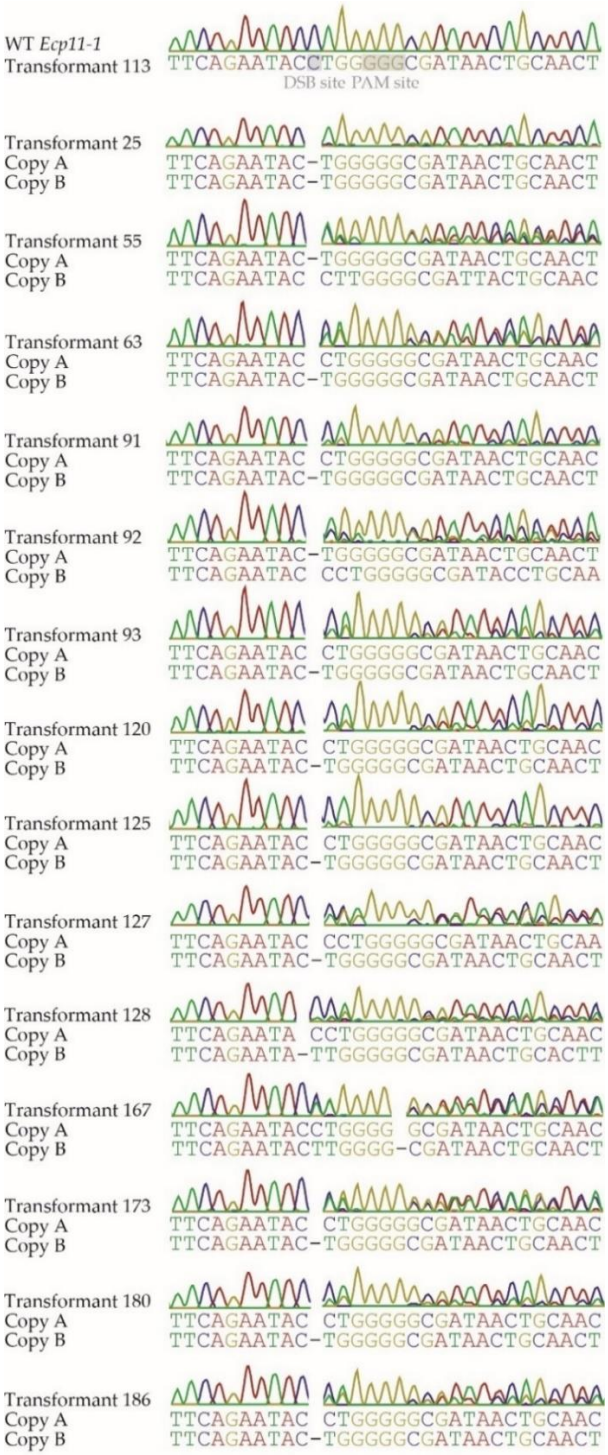

Appendix 7. Sequencing results of *Fulvia fulva CfEcp11-1* from wild type (WT) and CRISPR/Cas9 transformants. A segment of *CfEcp11-1* nucleotide sequence is shown that covers the double-strand break (DSB) site and protospacer adjacent motif (PAM) site. The sequencing chromatogram is shown above, and the nucleotide sequence based off the chromatogram is below. Nucleotide deletions are shown by a dash. The two copies of *CfEcp11-1* are labelled copy A and B, but it is not known which sequence codes for which copy. Sequencing was performed with primers HM205/HM206 on gel-extracted PCR products by the Massey University Genome service.

Appendix 8. *CfEcp11-1* gene copy number determination in mutant #25 by quantitative PCR (qPCR) analysis.

Target gene / Strain	Ct reference	ΔCt reference[1]	Ct target	ΔCt target[1]	Ratio[2]	Copy number[3]
WT	19.6	-	18.8	-	-	2
#25	20.7	-1.1	20.7	-1.9	0.6	1

1 – The ΔCt is the difference in cycle threshold (Ct) between the complement and the wild type (WT) when amplifying each of the target and reference genes by qPCR. The single copy reference gene used was *actin* (JGI ID: 189818, Mesarich 2014, Zaccaron 2022).

2 – The ratio was calculated using a using a method detailed in **Materials and methods section 2.2.2.7**. The primer efficiencies were calculated using standard curves (**Materials and methods section 2.2.2.6**), and were 1.78 for *actin*, 1.75 for *CfEcp11-1*.

3 – The gene copy number is rounded, so for example a ratio of 0.6 gives a copy number of 1.

Results are the averages of four technical replicates.

The full data used to calculate the values displayed in this table are shown in **Appendix 9**.

Appendix 9. Cycle threshold (Ct) values used to determine *CfEcp11-1* gene copy number.

Strain	Technical replicate	Ct	Average	SD
Reference gene (*actin*)				
Wild type (WT)	1	19.5	19.6	0.0
	2	19.6		
	3	19.6		
	4	19.6		
#25	1	20.7	20.7	0.0
	2	20.7		
	3	20.7		
	4	20.6		
Target gene (*CfEcp11-1*)				
WT	1	18.8	18.8	0.1
	2	18.8		
	3	18.7		
	4	18.7		
#25	1	20.8	20.7	0.0
	2	20.7		
	3	20.7		
	4	20.7		

Appendices for Chapter 3

Appendix 10. Top 30 BlastP hits to *Dothistroma septosporum* DsPf2 (Ds68376) in Dothideomycete species.

Protein description and species name	Query cover	E value	aa ID[2]	GenBank accession
Putative sucrose utilization protein SUC1 [*Fulvia fulva*]	100%	0	89%	XP_047756992.1
Uncharacterised protein [*Zasmidium cellare*]	96%	0	82%	XP_033673811.1
Hypothetical protein [*Pseudocercospora eumusae*]	98%	0	81%	KXT03587.1
Uncharacterised protein [*Cercospora kikuchii*]	96%	0	81%	XP_044654715.1
Putative sucrose utilization protein SUC1 [*Cercospora beticola*]	96%	0	80%	XP_023458891.1
Hypothetical protein [*Pseudocercospora musae*]	96%	0	80%	KXT08232.1
Uncharacterised protein [*Pseudocercospora fijiensis*]	92%	0	83%	XP_007921440.1
Uncharacterised protein [*Sphaerulina musiva*]	92%	0	81%	XP_016765098.1
Hypothetical protein [*Cercospora zeae-maydis*]	87%	0	84%	KAF2211497.1
Putative sucrose utilization protein SUC1 [*Cercospora zeina*]	96%	0	79%	PKR95748.1
Hypothetical protein [*Cercospora berteroae*]	87%	0	84%	PPJ53363.1
Uncharacterised protein [*Zymoseptoria tritici*]	96%	0	74%	XP_003857279.1
Related to transcription activator amyR [*Ramularia collo-cygni*]	92%	0	75%	XP_023623725.1
C6 zinc finger domain containing protein [*Zymoseptoria brevis*]	91%	0	76%	KJX93866.1
Hypothetical protein [*Polychaeton citri*]	93%	0	73%	KAF2719390.1
Hypothetical protein [*Teratosphaeria nubilosa*]	90%	0	77%	KAF2770028.1
Hypothetical protein [*Salinomyces thailandica*]	80%	0	80%	TKA32344.1
Putative sucrose utilization protein SUC1 [*Teratosphaeria destructans*]	90%	0	78%	KAH9826854.1
Hypothetical protein [*Hortaea werneckii*]	92%	0	74%	RMZ02587.1
Hypothetical protein [*Aureobasidium namibiae*]	92%	0	69%	XP_013431386.1
$Zn(II)_2Cys_6$ transcriptional factor FTR1 [*Aureobasidium melanogenum*]	92%	0	69%	APZ77650.1
Hypothetical protein [*Friedmanniomyces simplex*]	80%	0	79%	TKA69480.1
Unnamed protein product [*Aureobasidium vineae*]	92%	0	68%	CAD0093542.1
Hypothetical protein [*Delphinella strobiligena*]	80%	0	76%	KAF1353489.1
Unnamed protein product [*Aureobasidium uvarum*]	92%	0	68%	CAD0112806.1
Unnamed protein product [*Aureobasidium mustum*]	92%	0	68%	CAD0090979.1
Hypothetical protein [*Rachicladosporium antarcticum*]	78%	0	77%	OQO12691.1
Hypothetical protein [*Acidomyces sp. 'richmondensis'*]	92%	0	68%	KXL45373.1
Hypothetical protein [*Aureobasidium pullulans*]	92%	0	69%	THV66391.1
Hypothetical protein [*Aureobasidium subglaciale*]	92%	0	69%	XP_013347669.1

1 – Amino acid identity (aa ID).

Appendix 11. *Dothistroma septosporum* basic-leucine zipper (bZIP) transcription factor gene expression at early and mid stages of pine infection

JGI ID[1]	Gene expression at early stage[2]	Gene expression at mid stage[2]	Fold change[3]
Ds74812	4.51	100.91	22.4
Ds69427	90.56	82.76	0.9
Ds70140	107.75	248.60	2.3
Ds73911	46.09	47.09	1.0
Ds20214	154.79	157.06	1.0
Ds30380	349.50	256.35	0.7
Ds40499	52.87	49.53	0.9
Ds46768	582.35	280.88	0.5
Ds48303	27.26	23.44	0.9
Ds67816	218.20	89.26	0.4
Ds69470	146.72	129.11	0.9
Ds47817	4.25	2.50	0.6
Ds68488	60.95	189.88	3.1
Ds68942	51.36	90.64	1.8
Ds72123	282.77	236.28	0.8
Ds48335	39.68	3.59	0.1
Ds67668	47.32	26.62	0.6

1 – Joint Genome Institute (JGI) protein ID from the *D. septosporum* page (https://mycocosm.jgi.doe.gov/Dotse 1/Dotse1.home.html), of all *D. septosporum* bZIP transcription factors. Proteins were identified as predicted bZIP transcription factors from annotation of the bZIP transcription factor Pfam domain (PF00170) on the *D. septosporum* JGI site. Candidate virulence factor Ds74812 is highlighted in grey.

2 – Expression of the corresponding gene is shown as Reads Per Million per Kilobase (RPMK) and was sourced from the *D. septosporum* transcriptome study by Bradshaw et al. (2016); expression at the early and mid stages *in planta* are shown.

3 – Fold change in expression from early to mid stage *in planta*.

Appendix 12. Top 30 BlastP hits to *Dothistroma septosporum* Ds74812 in Dothideomycete species.

Protein description and species name	Query Cover	E value	aa ID[1]	GenBank Accession
Hypothetical protein [*Pyrenophora teres f. teres*]	99%	2E-94	44%	EFQ85926.1
Hypothetical protein [*Pyrenophora teres f. maculata*]	99%	3E-94	44%	CAA9959532.1
Hypothetical protein [*Bipolaris oryzae*]	99%	1E-84	43%	XP_007693775.1
Uncharacterised protein [*Boeremia exigua*]	98%	1E-78	42%	XP_046001785.1
Hypothetical protein [*Pseudocercospora eumusae*]	96%	1E-76	44%	KXS94344.1
Hypothetical protein [*Bipolaris victoriae*]	99%	9E-72	42%	XP_014550351.1
Hypothetical protein [*Pseudocercospora musae*]	87%	3E-70	43%	KXT02612.1
Uncharacterised protein [*Lindgomyces ingoldianus*]	41%	1E-21	41%	XP_033540103.1
Hypothetical protein [*Clohesyomyces aquaticus*]	35%	3E-19	41%	ORY01112.1
Hypothetical protein [*Macrophomina phaseolina*]	88%	2E-17	27%	KAH7042264.1
Hypothetical protein [*Zopfia rhizophila*]	21%	2E-15	40%	KAF2194534.1
Hypothetical protein [*Botryosphaeria dothidea*]	28%	2E-14	36%	KAF4311780.1
Uncharacterised protein [*Zasmidium cellare*]	32%	3E-14	34%	XP_033659207.1
Putative transcriptional regulator protein [*Neofusicoccum parvu*]	28%	7E-11	32%	EOD48397.1
Uncharacterised protein [*Alternaria atra*]	30%	2E-10	31%	XP_043169940.1
Hypothetical protein [*Myriangium duriaei*]	58%	8E-10	30%	KAF2157805.1
Hypothetical protein [*Cercospora zeina*]	17%	1E-09	51%	PKR98510.1
Uncharacterised protein [*Aplosporella prunicola*]	31%	4E-09	32%	XP_033395483.1
Transcription factor ZEB2 [*Lasiodiplodia theobromae*]	36%	6E-09	29%	KAB2575192.1
Uncharacterised protein [*Ramularia collo-cygni*]	27%	7E-08	32%	XP_023626890.1
Hypothetical protein [*Elsinoe australis*]	35%	9E-08	28%	PSK46154.1
Hypothetical protein [*Lepidopterella palustris*]	23%	3E-07	35%	OCK73221.1
Uncharacterised protein [*Trematosphaeria pertusa*]	26%	1E-06	31%	XP_033680317.1
Toxin biosynthesis protein [*Diplodia corticola*]	32%	2E-06	37%	XP_020125612.1
bZIP-1 domain-containing protein [*Pyrenophora tritici-repentis*]	15%	8E-06	36%	KAA8622026.1
Uncharacterised protein [*Exserohilum turcica*]	14%	1E-05	43%	XP_008030677.1
Hypothetical protein [*Bimuria novae-zelandiae*]	20%	2E-05	32%	KAF1971483.1
Hypothetical protein [*Venturia nashicola*]	17%	5E-05	38%	TID21672.1
Peptide transporter ptr2 [*Didymella keratinophila*]	27%	7E-05	31%	KAF3049120.1
Hypothetical protein [*Patellaria atrata*]	21%	1E-04	32%	KAF2840036.1

1 – Amino acid identity (aa ID).

Appendix 13. Top 30 BlastP hits to *Dothistroma septosporum* Ds69328 in Dothideomycete species.

Protein description and species name	Query Cover	E value	aa ID[1]	GenBank Accession
Uncharacterised protein [*Fulvia fulva*]	71%	0	84%	XP_047758835.1
Uncharacterised protein [*Zasmidium cellare*]	87%	6E-163	49%	XP_033662262.1
Unnamed protein product [*Zymoseptoria tritici*]	84%	1E-143	46%	SMR46147.1
Hypothetical protein [*Cercospora zeina*]	82%	2E-142	46%	PKR97968.1
Uncharacterised protein [*Cercospora kikuchii*]	86%	5E-139	45%	XP_044660814.1
Hypothetical protein [*Zymoseptoria brevis*]	84%	3E-137	44%	KJY00790.1
Hypothetical protein [*Cercospora berteroae*]	84%	4E-130	45%	PPJ57276.1
Hypothetical protein [*Pseudocercospora fuligena*]	83%	2E-125	43%	KAF7190308.1
Hypothetical protein [*Cercospora beticola*]	79%	1E-119	44%	XP_023457095.1
Uncharacterised protein [*Ramularia collo-cygni*]	86%	1E-118	41%	XP_023625780.1
Hypothetical protein [*Pseudocercospora musae*]	83%	2E-118	43%	KXT17958.1
Hypothetical protein [*Cercospora zeae-maydis*]	79%	4E-117	45%	KAF2216648.1
Uncharacterised protein [*Sphaerulina musiva*]	75%	1E-112	40%	XP_016763907.1
Hypothetical protein [*Pseudocercospora eumusae*]	67%	5E-88	44%	KXS94388.1
Uncharacterised protein [*Dissoconium aciculare*]	68%	2E-47	29%	XP_033462222.1
FSTF[2] domain-containing protein [*Neohortaea acidophila*]	68%	4E-41	27%	XP_033589342.1
Hypothetical protein [*Acidomyces sp. 'richmondensis'*]	84%	8E-41	27%	KXL49990.1
Hypothetical protein [*Delphinella strobiligena*]	68%	7E-39	28%	KAF1353334.1
Hypothetical protein [*Cryomyces minteri*]	81%	5E-33	28%	TKA73539.1
Uncharacterised protein [*Pseudovirgaria hyperparasitica*]	83%	1E-31	26%	XP_033604412.1
Hypothetical protein [*Hortaea werneckii*]	68%	3E-31	25%	OTA36472.1
Hypothetical protein [*Peltaster fructicola*]	88%	2E-29	24%	QIW96677.1
Hypothetical protein [*Aureobasidium pullulans*]	69%	8E-28	26%	THW57661.1
Hypothetical protein [*Aureobasidium subglaciale*]	69%	6E-27	26%	XP_013344639.1
Hypothetical protein [*Rhizodiscina lignyota*]	69%	5E-26	25%	KAF2101209.1
Fungal transcriptional regulatory protein [*Aureobasidium namibiae*]	68%	7E-26	26%	XP_013429574.1
Hypothetical protein [*Friedmanniomyces simplex*]	57%	1E-24	26%	TKA82903.1
Hypothetical protein [*Aureobasidium melanogenum*]	68%	1E-24	25%	KAH0342441.1
Hypothetical protein [*Friedmanniomyces endolithicus*]	68%	3E-24	24%	TKA40445.1
Hypothetical protein [*Aulographum hederae*]	89%	5E-24	23%	KAF1985238.1

1 – Amino acid identity (aa ID).

2 – Fungal-specific transcription factor (FSTF).

Appendix 14. Top 30 BlastP hits to *Dothistroma septosporum* Ds41021 in Dothideomycete species.

Protein description and species name	Query Cover	E value	aa ID[1]	GenBank Accession
NR[2] protein AreA [*Fulvia fulva*]	99%	0	89%	XP_047756925.1
Uncharacterised protein [*Zasmidium cellare*]	96%	0	70%	XP_033672133.1
NR[2] protein AreA [*Pseudocercospora fuligena*]	99%	0	70%	KAF7186275.1
Hypothetical protein [*Pseudocercospora eumusae*]	99%	0	69%	KXT02835.1
Hypothetical protein [*Pseudocercospora musae*]	97%	0	69%	KXT19050.1
Uncharacterised protein [*Sphaerulina musiva*]	96%	0	64%	XP_016764689.1
GLN3p transcription factor [*Pseudocercospora fijiensis*]	89%	0	68%	XP_007921048.1
Uncharacterised protein [*Cercospora beticola*]	99%	0	62%	XP_023629231.1
NR[2] protein AreA [*C. beticola*]	92%	0	65%	XP_023460219.1
Hypothetical protein [*Cercospora kikuchii*]	92%	0	65%	GIZ39189.1
Hypothetical protein [*Cercospora berteroae*]	92%	0	64%	PPJ49549.1
Hypothetical protein [*Cercospora zeae-maydis*]	93%	0	63%	KAF2210781.1
Hypothetical protein [*Teratosphaeria nubilosa*]	98%	0	59%	KAF2770324.1
NR[2] protein AreA [*Teratosphaeria destructans*]	97%	0	61%	KAH9837481.1
Unnamed protein product [*Zymoseptoria tritici*]	95%	0	64%	SMQ50617.1
NR[2] protein AreA [*Cercospora zeina*]	94%	0	61%	PKS00402.1
Hypothetical protein [*Salinomyces thailandica*]	97%	0	58%	TKA27595.1
NR[2] protein AreA [*Zymoseptoria brevis*]	94%	0	63%	KJX96534.1
Uncharacterised protein [*Baudoinia panamericana*]	97%	0	59%	XP_007678071.1
Hypothetical protein [*Hortaea werneckii*]	97%	0	57%	RMX98169.1
Hypothetical protein [*Friedmanniomyces endolithicus*]	84%	0	61%	TKA30287.1
Hypothetical protein [*Rachicladosporium antarcticum*]	99%	0	54%	OQO02254.1
Hypothetical protein [*Peltaster fructicola*]	83%	0	57%	QIX01060.1
Uncharacterised protein [*Dissoconium aciculare*]	99%	0	51%	XP_033460408.1
Hypothetical protein [*Friedmanniomyces simplex*]	70%	0	65%	TKA62229.1
Hypothetical protein [*Coniosporium apollinis*]	98%	0	50%	XP_007784082.1
Uncharacterised protein [*Neohortaea acidophila*]	81%	0	58%	XP_033586159.1
Zinc finger GATA-type protein [*Lasiodiplodia theobromae*]	83%	0	54%	XP_035366086.1
Hypothetical protein [*Delphinella strobiligena*]	89%	0	51%	KAF1348624.1
Zinc finger GATA-type protein [*Botryosphaeria dothidea*]	82%	0	52%	KAF4304195.1

1 – Amino acid identity (aa ID).

2 – Nitrogen regulatory (NR).

Appendix 15. Top 30 BlastP hits to *Dothistroma septosporum* Ds68895 in Dothideomycete species.

Protein description and species name	Query Cover	E value	aa ID[1]	GenBank Accession
Positive regulator of purine utilization [*Fulvia fulva*]	99%	0	87%	UJO11482.1
Uncharacterised protein [*Pseudocercospora fuligena*]	99%	0	73%	XP_033672161.1
Positive regulator of purine utilization [*P. fuligena*]	99%	0	72%	KAF7195509.1
Hypothetical protein [*Cercospora beticola*]	99%	0	69%	XP_023459833.1
Uncharacterised protein [*Cercospora kikuchii*]	99%	0	70%	XP_044654785.1
Hypothetical protein [*Pseudocercospora eumusae*]	99%	0	71%	KXS99650.1
Hypothetical protein [*Pseudocercospora musae*]	99%	0	68%	KXT15153.1
Hypothetical protein [*Zymoseptoria brevis*]	99%	0	69%	KJX95414.1
Unnamed protein product [*Zymoseptoria tritici*]	98%	0	68%	SMR43331.1
Hypothetical protein [*Cercospora zeae-maydis*]	87%	0	74%	KAF2211430.1
Hypothetical protein [*Cercospora berteroae*]	98%	0	67%	PPJ53388.1
Hypothetical protein [*Cercospora zeina*]	98%	0	67%	PKS04283.1
Hypothetical protein [*Friedmanniomyces endolithicus*]	98%	0	64%	TKA42764.1
Hypothetical protein [*Rachicladosporium antarcticum*]	98%	0	63%	OQO04874.1
Hypothetical protein [*Hortaea werneckii*]	99%	0	64%	RMX99367.1
Hypothetical protein [*Friedmanniomyces simplex*]	87%	0	68%	TKA72063.1
Hypothetical protein [*Teratosphaeria nubilosa*]	83%	0	73%	KAF2765029.1
FSTF[2] domain [*Teratosphaeria destructans*]	99%	0	64%	KAH9844620.1
Hypothetical protein [*Salinomyces thailandica*]	98%	0	64%	TKA24998.1
Fungal_trans-domain-containing protein [*Sphaerulina musiva*]	75%	0	76%	XP_016765657.1
FSTF[2] domain-containing protein [*Neohortaea acidophila*]	99%	0	59%	XP_033590883.1
Related to GAL4-like TA [*Ramularia collo-cygni*]	90%	0	68%	XP_023629413.1
Hypothetical protein [*Polychaeton citri*]	98%	0	54%	KAF2722612.1
Hypothetical protein [*Peltaster fructicola*]	99%	0	53%	QIX02086.1
Uncharacterised protein [*Pseudocercospora fijiensis*]	63%	0	77%	XP_007921426.1
Hypothetical protein [*Cenococcum geophilum*]	88%	0	54%	OCK90324.1
Hypothetical protein [*Aureobasidium melanogenum*]	85%	0	54%	KAH0194070.1
Hypothetical protein [*Lepidopterella palustris*]	79%	0	58%	OCK84045.1
Hypothetical protein [*Glonium stellatum*]	85%	0	55%	OCL05972.1
Hypothetical protein [*Lophium mytilinum*]	86%	0	53%	KAF2497062.1

1 – Amino acid identity (aa ID).

2 – Fungal-specific transcription factor (FSTF).

3 – Transcriptional activator (TA).

Appendices for Chapter 4

Appendix 16. Screening *DsHexA Dothistroma septosporum* culture filtrate for cell death-eliciting molecules

To determine if there are cell death-eliciting molecules other than dothistromin secreted by *D. septosporum*, culture filtrate of the *DsHexA* mutant (which does not produce dothistromin) was infiltrated into *Nicotiana benthamiana* leaves to test for a cell death response, alongside the wild type (WT) control that does produce dothistromin. In a preliminary trial, culture filtrate was harvested from *D. septosporum* grown in nutrient-rich Dothistromin medium (DM) or nutrient-poor pine minimal salts (PMMG) medium and inoculated by either ground mycelium or spores.

Infiltration of uninoculated media did not elicit cell death in any *N. benthamiana* leaves tested. WT culture filtrate, which contains dothistromin, elicited cell death in 100% of infiltration spots from all samples except PMMG media inoculated with spores, where the cell death occurred in 50% of infiltration spots. Infiltration of culture filtrate from the *DsHexA* mutant elicited cell death in ~30–60% of infiltration spots (**Appendix 16a**) from all samples except PMMG media inoculated with mycelium, where no cell death was observed. These preliminary results suggested that cell death-eliciting molecules were present in the *DsHexA* culture filtrate.

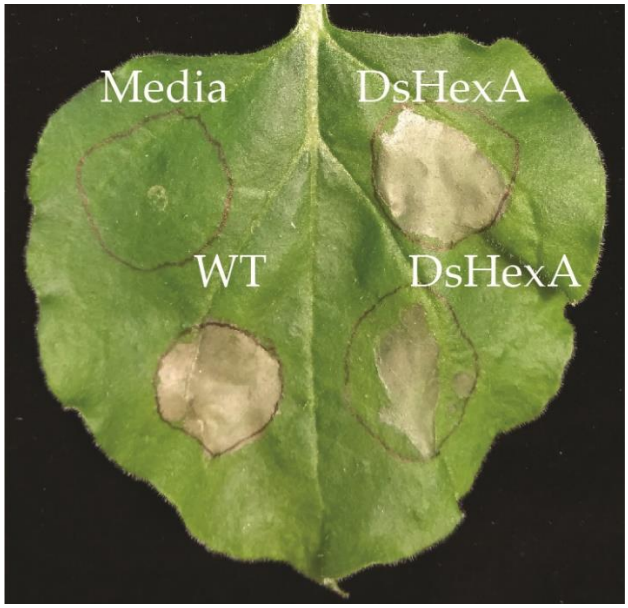

Appendix 16a. Example of cell death response from infiltration of *Dothistroma septosporum* culture filtrate into *Nicotiana benthamiana* leaves. *N. benthamiana* (cultivar Wisconsin 38) plants were grown in heat-sterilized soil (Daltons premium seed mix) in a light and temperature-controlled room at 22°C, under

a 12:12 light/dark cycle. *D. septosporum DsHexA* cultures were grown in DM (Dothistroma medium) or PMMG (pine minimal salts medium) and inoculated with ground mycelium (~1 cm^2 mycelium ground in ~200 µL MilliQ water with a micro pestle) or ~10^4 spores/mL (**Materials and methods section 4.2.1.2**). Culture filtrate was harvested (**Materials and methods section 4.2.1.1**) and stored at 4°C, before infiltrating into ~4 week-old *N. benthamiana* leaves using a needless 1 mL syringe (Terumo Corporation, Binan, Laguna, Philippines). Images are representative of two leaves infiltrated from each of four plants (n=8). Photos were taken 96 hours post-infiltration.

To determine what type of molecule caused cell death in the *DsHexA* culture filtrate, the samples were treated with 1 mg/mL Proteinase K (A & A Biotechnology) at 37°C for 1.5 and 4 h or heated to 50°C or 80°C for 4 h. The WT culture filtrate (containing dothistromin) elicited cell death in 100% of infiltration spots, while the untreated *DsHexA* culture filtrate only elicited weak cell death in ~20–40% of infiltration spots. The heat-treated *DsHexA* culture filtrate (50°C and 80°C) elicited weak cell death in ~30–40%, while the Proteinase K treated (incubated for 1.5 and 4 h) elicited weak cell death in ~10–30% of infiltration spots. Therefore, the heat and Proteinase K treatments appeared to not affect *DsHexA* culture filtrate-elicited cell death, but the untreated *DsHexA* culture filtrate also elicited very weak cell death compared to the last experiment.

Due to the minimal effect of Proteinase K and heat treatments on the *DsHexA* culture filtrate, it was hypothesised that the inconsistent cell death response could be caused by residual amounts of dothistromin being produced by the *DsHexA* mutant (~4 ng/mL, (Chettri et al., 2013)). A dilution series (5-, 25-, 125-, and 625-fold) of the WT culture filtrate, suggested to produce ~200 ng/mL dothistromin (based on previous analysis by Chettri et al. (2013)), was tested in *N. benthamiana* leaves to determine if low concentrations of dothistromin can elicit cell death. Cell death was observed in leaves infiltrated with 5-, 25-, and 125-fold diluted WT culture filtrate (**Appendix 16b**). This suggests that a low dothistromin concentration of ~10 ng/mL, which is likely produced from the *DsHexA* mutant, is sufficient to elicit cell death. These results showed that infiltration of *N. benthamiana* leaves with *DsHexA* culture filtrate is not a suitable method for identifying new cell death-eliciting molecules produced by *D. septosporum*, due to the residual levels of dothistromin produced in the strain.

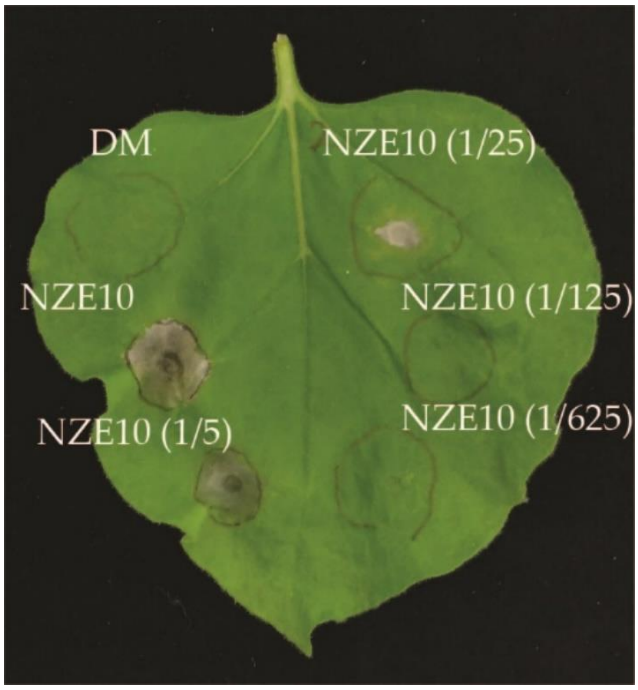

Appendix 16b. Example of cell death response in *Nicotiana benthamiana* leaf after infiltration of diluted wild type culture filtrate. Dilution folds used are in brackets. Images are representative of three leaves infiltrated from three plants (n = 9). Photos were taken 96 hours post-infiltration. DM, Dothistroma medium.

Appendix 17. Harvesting apoplastic washing fluid from clonal *Pinus radiata* shoots

The forward genetic approach of identifying cell death eliciting virulence factors from *D. septosporum* culture filtrate was unsuccessful due to trace amounts of dothistromin being present in the *DsHexA* mutant. Another forward genetics approach is harvesting apoplastic washing fluid from the host plant after inoculation with the pathogen and infiltrating into *Nicotiana* species to determine if there is a cell death response that might be due to fungal cell death elicitor molecules. Harvesting apoplastic washing fluid from pine needles has not been performed before as the tough epidermis of the needles makes infiltration very difficult (R. Bradshaw per com). Recently, *P. radiata* tissue-culture generated shoots, which have young and softer needles, have been used successfully for protein infiltration experiments (Hunziker, 2018; Tarallo et al., 2022), suggesting that apoplastic washing fluid harvest could be possible from these shoots.

A preliminary trial was performed to determine whether apoplastic washing fluid could be harvested from tissue-culture generated clonal *P. radiata* shoots (**Appendix 16c**). About 2 mL of

apoplastic washing fluid was harvested from 21 shoots, showing that apoplastic washing fluid can be successfully harvested.

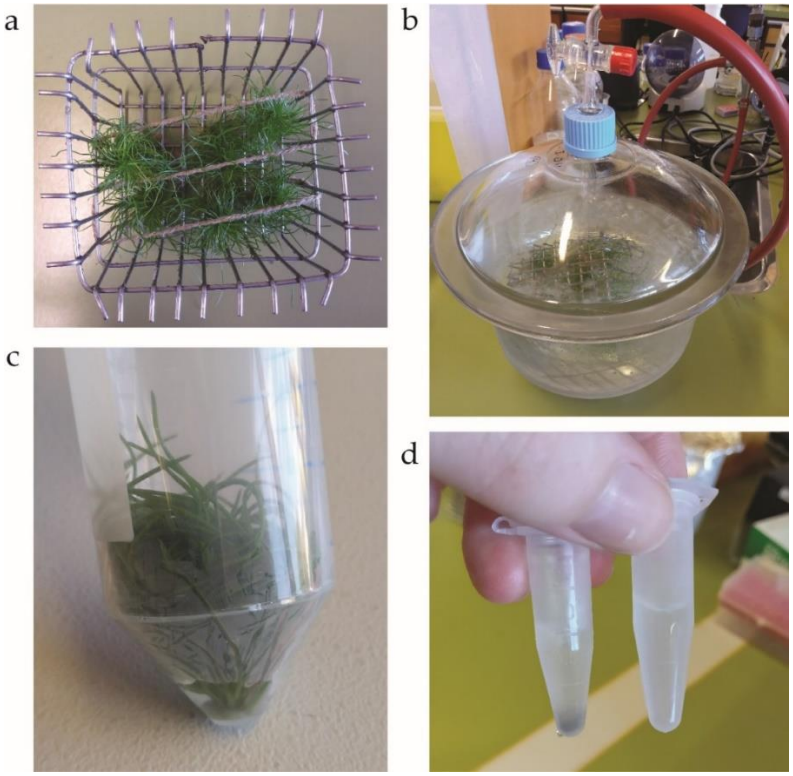

Appendix 16c. Extracting apoplastic washing fluid from *Pinus radiata* shoots by vacuum infiltration. A total of 21 clonal *P. radiata* shoots (developed by tissue culturing at Scion and maintained in modified Quoirin and Lepoivre medium with charcoal (LPch: Hargreaves et al. (2004); Tarallo (2022))) from three jars were secured in a wire cage (**a**). The cage was placed into a glass vacuum chamber filled with pre-chilled ice water, submerging the shoots. Vacuum was applied for 3 min, a total of three times (**b**). Shoots were removed and patted dry, then individually placed into a falcon tube, and centrifuged at 1,000 x g for 20 min at 4°C (**c**). Apoplastic washing fluid released from centrifugation of all shoots was then collected and filter-sterilized with a 0.2 µm filter (**d**).

Appendix 18. Pathogenicity trial in clonal *Pinus radiata* shoots with GFP *Dothistroma septosporum*

Apoplastic washing fluid was successfully harvested from clonal *P. radiata* shoots. To perform the first step of a forward genetics approach to identify virulence factors from *D. septosporum*, apoplastic washing fluid would be harvested from *P. radiata* shoots inoculated with *D. septosporum*, and then infiltrated into *N. benthamiana* leaves to look for a cell death response. To determine whether *D. septosporum* could infect and grow on tissue-culture generated clonal *P. radiata* shoots, a preliminary trial was performed. In this trial, the shoots were inoculated

with a *D. septosporum* mutant containing the enhanced green fluorescent protein (*eGFP*) gene (in-house lab stock FJT175, (Mosen, 2022)) so that disease symptoms could be identified through GFP fluorescence.

Jars containing *P. radiata* shoots in modified Quoirin and Lepoivre medium with charcoal (LPch) medium were inoculated with *D. septosporum GFP* spores at a concentration of 5 x 10^6 spores/mL and incubated at 22°C in an environmentally controlled growth room (16 h light 8 h dark period with approximately 100 µE/m^2/s), for 6 weeks for disease symptoms to develop. After 6 weeks incubation, considerable growth of *GFP D. septosporum* was observed on the LPch medium, as well as the *P. radiata* shoots. Some white fungal non-GFP fluorescing contaminants were also observed on the LPch media. From the six shoots examined, 61% of needles were dead, and 20% of needles had GFP-fluorescing lesions **(Appendix 16d**). All fluorescing lesions were early lesions, and no sporulating lesions were observed.

Appendix 16d. Condition of *GFP Dothistroma septosporum*-inoculated *Pinus radiata* needles

Needle condition	Average number of needles (± SD)[1]	Percentage of total needles (%)[1]
Alive, no lesion	32.3 ± 9.1	19
Dead	103.5 ± 33.7	61
GFP lesion	33.7 ± 13.8	20
Total needles	169.5 ± 28.4	-

1 - Results are from six individual *P. radiata* shoots from two separate jars (n=6), 6 weeks post-inoculation.

These results showed that 6 weeks after inoculating with *GFP D. septosporum* spores, over half of the *P. radiata* needles were dead (with no visible *D. septosporum* lesions), and only early lesions were observed on the living needles (Kabir et al., 2015b). It is possible that *D. septosporum* was secreting dothistromin into the LPch media, and the toxin was killing the *P. radiata* shoots. Regardless, the *D. septosporum* life cycle was not completed in this trial, making this an unsuitable system for virulence assessment of *D. septosporum* transformants. It could be possible to optimize this system by preventing growth of *D. septosporum* on the LPch medium (for example, removing the shoots from the medium when inoculating and ensuring they are dry before replacing); however, due to the considerable expense in purchasing clonal *P. radiata* shoots, this method was not continued.

Appendix 19. Media used for culturing *Dothistroma septosporum* and/or *Fulvia fulva*.

Media	Materials
Dothistroma medium (DM)	50 g/l malt extract (Oxoid) 23 g/l nutrient broth (Oxoid) 15 g/l agar, bacteriological (Pure Science)
Low DM	25 g/l malt extract (Oxoid) 20 g/l nutrient broth (Oxoid) 15 g/l agar, bacteriological (Pure Science)
Dothistroma sporulation medium (DSM)	15 g/l malt extract (Oxoid) 15 g/l yeast extract (Merck) 15 g/l agar, bacteriological (Pure Science)
Pine minimal salts medium (PMMG)[1]	10% w/v fresh pine needles in MilliQ water 0.2 g/l magnesium sulphate heptahydrate 0.9 g/l di-potassium hydrogen orthophosphate 0.2 g/l potassium chloride 1.0 g/l ammonium nitrate 0.002 g/l iron sulphate* 0.002 g/l zinc sulphate heptahydrate 0.002 g/l manganese chloride 2 g/l asparagine* 2% glucose* 15 g/l agar, bacteriological (Pure Science)

1 – Whole (not cut) pine needles were collected on the Massey University Manawatū campus and soaked in MilliQ water for 24 h. The pine-soaked water was then filtered through nappy liner twice to remove needles and sediment. The other reagents were added (except those with an asterisk), and the pH adjusted to 5.9 with HCL. The solutions with an asterisk were filter-sterilized with a 0.2 µm filter (Ahlstrom-Munksjö, Helsinki, Finland) and added after autoclaving.

Appendix 20. All proteins detected in the *Dothistroma septosporum* culture filtrate proteome.

Appendix 21. Classically secreted proteins identified from the *Dothistroma septosporum* culture filtrate proteome.

Appendices 20 and 21 can be accessed online at https://drive.google.com/drive/folders/1Yj-ODEEZSEvwmmeFGjBs8X1Ewo5AFmk0?usp=drive_link

Appendix 22. Top BlastP hits of selected *Dothistroma septosporum* proteins without a signal peptide.

JGI ID[1]	NCBI accession[2]	Protein name	Organism	Query cover	E value	% Identity
68111	XP_047757253.1	Peroxiredoxin, mitochondrial	*Fulvia fulva*	100%	6e-164	100.00%
71772	XP_047759039.1	Aspartate aminotransferase, cytoplasmic	*F. fulva*	100%	0.0	92.84%
73584	XP_047764079.1	Glycine dehydrogenase (decarboxylating), mitochondrial	*F. fulva*	100%	0.0	96.35%
48482	XP_047769544.1	40S ribosomal protein S4	*F. fulva*	100%	0.0	98.85%

1 - Joint Genome Institute (JGI) protein ID from the *D. septosporum* page (https://mycocosm.jgi.doe.gov/Dotse1/Dotse1.home.html), and the protein used as a query in the BlastP analysis.

2 – Protein accession from the NCBI website (https://www.ncbi.nlm.nih.gov), and the top BlastP hit (excluding the hit from *D. septosporum*).

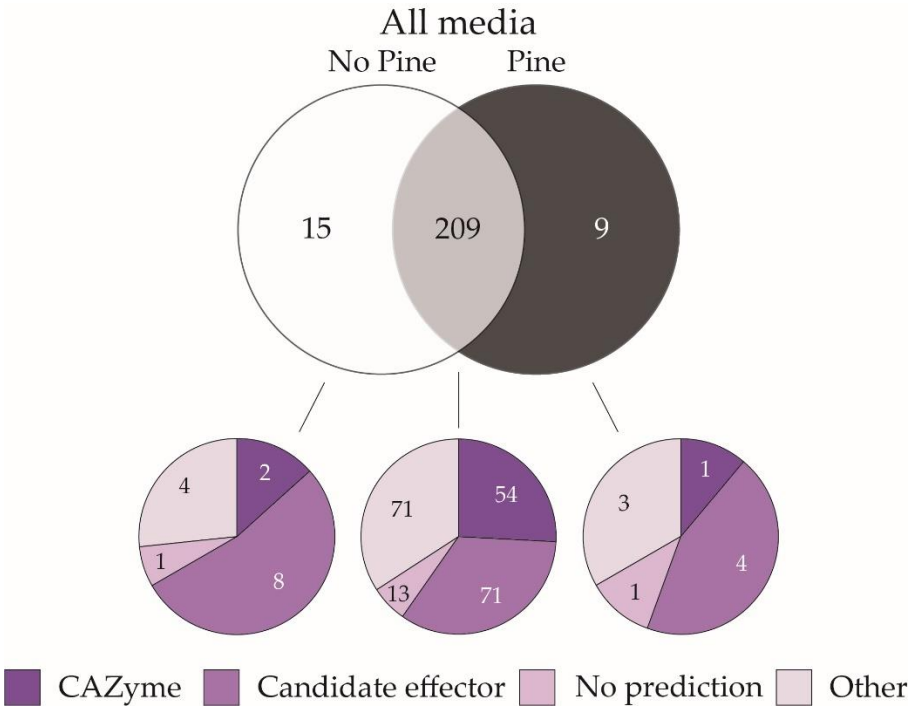

Appendix 23. Classically secreted proteins produced by *Dothistroma septosporum* in culture in the presence or absence of pine extract, and the protein type.

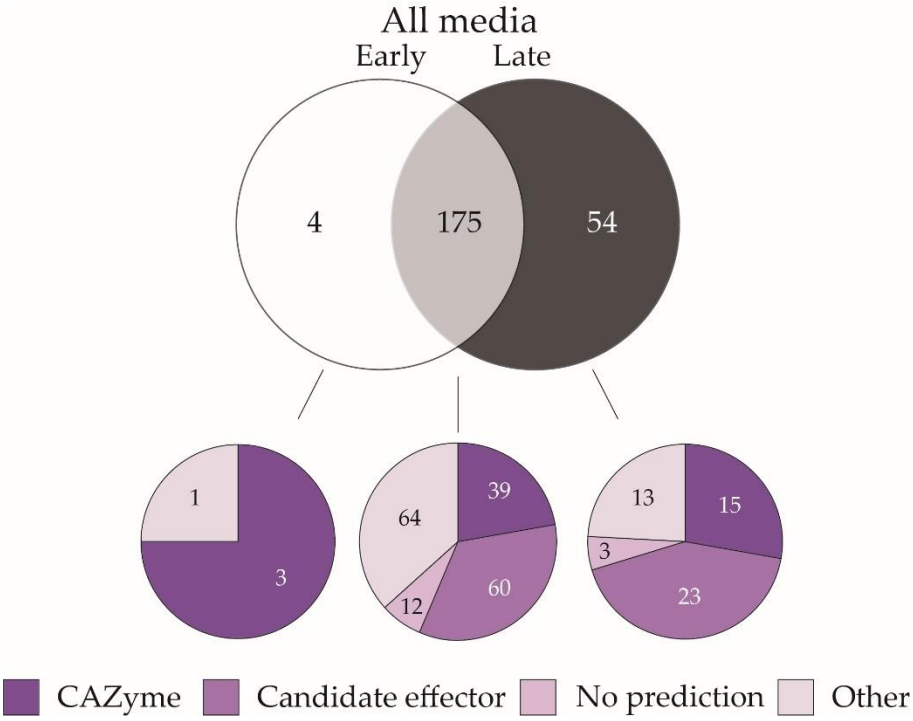

Appendix 24. Classically secreted proteins produced by *Dothistroma septosporum* in culture in early and late medium samples, and the protein type.

Appendix 25. All proteins detected in the *Fulvia fulva* culture filtrate proteome.

Appendix 26. Classically secreted proteins identified from the *Fulvia fulva* culture filtrate proteome.

Appendices 25 and 26 can be accessed online at https://drive.google.com/drive/folders/1Yj-ODEEZSEvwmmeFGjBs8X1Ewo5AFmk0?usp=drive_link

Appendix 27. Candidate effector proteins secreted in *Fulvia fulva* culture filtrate samples.

		Gene expression[2]				PDB[3]		PMMG[3]	
Name	Accession[1]	*In vitro*	4 dpi	8 dpi	12 dpi	4	9	9	16
CfAvr4E	UJO20373.1	130	0	800	393				
CfEcp2-1	UJO11627.1	39	20415	85886	61577				
CfEcp2-3	UJO18033.1	26	12203	45037	30757				
CfEcp4	UJO12859.1	296	237	6054	8553				
CfEcp5	UJO14573.1		-						
CfEcp6	UJO19933.1	58	1588	8396	2381				
CfEcp11-1	UJO17184.1	15	5073	2633	7182				
CfEcp14-1	UJO17283.1	13	668	523	272				
CfEcp14-2	UJO17753.1	4	400	3	3				
CfEcp19-1	UJO20124.1	5	2734	20472	30553				
CfEcp20-1	UJO14225.1	0	3805	19477	7443				
CfEcp20-3	UJO16284.1	5	661	201	598				
CfEcp21-1	UJO20599.1	4	2524	12485	9734				
CfEcp22	UJO23831.1		-						
CfEcp29	UJO19794.1	5	0	197	190				
CfEcp30	UJO19183.1	965	141	7	1468				
CfEcp32-1	UJO15491.1	97	547	1025	602				
CfEcp33	UJO16986.1	12	0	647	256				
CfEcp45	UJO22670.1	15	142	447	240				
CfEcp50-1	UJO19274.1	15	0	230	164				
CfEcp51	UJO23906.1	25	0	1	52				
CfEcp52	UJO10840.1	1	0	72	171				
CfEcp53-1	UJO17305.1	31	0	8	159				
CfEcp57-1	UJO13739.1	1491	1531	771	1179				
CfEcp58-1	UJO12458.1	130	0	5	9				
CfEcp59-1	UJO15825.1	59	0	0	8				
CfEcp60-1	UJO22710.1	59	0	4	4				

1 – GenBank protein accession from the NCBI website (https://www.ncbi.nlm.nih.gov/).

2 – Gene expression is shown for the 0WU orthologue of the Race 5 gene (identified as the top BlastP hit, **Materials and methods section 4.2.2.7**) as fragments per kilobase of exon per million fragments mapped (FPKM) and was sourced from a transcriptome study of a compatible interaction of H-Cf-0 tomato plants inoculated with *F. fulva* 0WU strain and sampled 4, 8, and 12 days post-inoculation (dpi), as well as *in vitro* (Iv; growth in potato dextrose broth (PDB) for 4 days, 22°C (Mesarich et al., 2014)). For two proteins, no gene expression data is shown because an 0WU orthologue was not found.

3 – The proteome samples the protein was present in are shaded in green (only considered present if the protein was identified from at least two of the four biological replicates). The media the sample was grown in is shown at the top as PDB or PMMG (pine minimal salts media), followed by the harvesting time (day 4, 9, or 16).

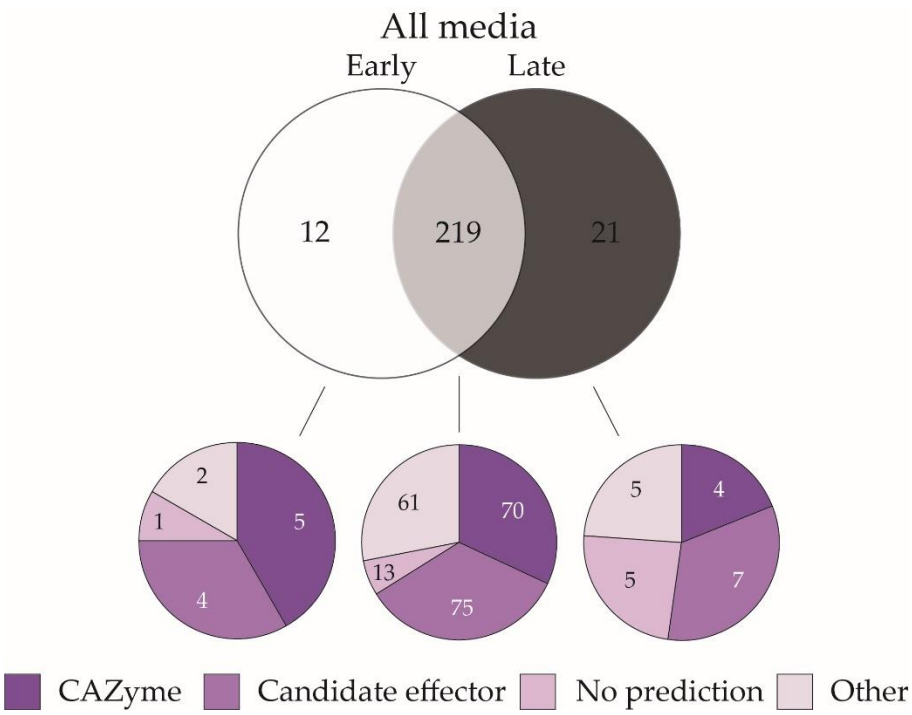

Appendix 28. Classically secreted proteins produced by *Fulvia fulva* in culture in early and late medium samples, and the protein type.

Appendix 29. Homologous proteins in sample PMMG Day 9 classically secreted individually by *Dothistroma septosporum* or *Fulvia fulva*.

	Normalised expression[2]					
Accession[1]	Iv	Early/4 dpi	Mid/8 dpi	Late/12 dpi	Protein type[3]	Protein domains[4]
D. septosporum						
75726	34	42	47	379	Other	Secretory lipase
70379*	1	6	19	202	CE	Carbohydrate Esterase Family 1
F. fulva						
UJO14225.1*	0	3805	19477	7443	CE (*FfEcp20-1*)	-
UJO10962.1	228	1379	1124	1124	CE	EMP24_GP25L
UJO16284.1*	5	661	201	598	CE (*FfEcp20-3*)	-
UJO22670.1	15	142	447	240	CE (*FfEcp45*)	Cerato-platanin
UJO13947.1	4	152	287	280	CAZyme	Glycoside Hydrolase Family 17
UJO24220.1	1	237	68	285	CE	Chordin domain
UJO22853.1	7	217	2	133	CAZyme	Glycoside Hydrolase Family 3, Fibronectin type III-like
UJO23674.1	1	169	24	95	CAZyme	Glycoside Hydrolase Family 32

1 –For *D. septosporum* proteins the Joint Genome Institute (JGI) protein ID from the *D. septosporum* genome page (https://mycocosm.jgi.doe.gov/Dotse1/Dotse1.home.html) is shown. For *F. fulva* proteins the GenBank protein accession from the NCBI website (https://www.ncbi.nlm.nih.gov/) is shown.

2 – For *D. septosporum* proteins, the encoding gene expression is shown as Reads Per Million per Kilobase (RPMK) and was sourced from a transcriptome analysis performed on *D. septosporum*-infected *Pinus radiata* seedlings. Three *in planta* stages were sampled: early, mid, and late, as well as *in vitro* (Iv; growth in low Dothistroma medium (LDM) broth for 7 days, 22°C (Bradshaw et al., 2016)). For *F. fulva* proteins, gene expression is shown for the 0WU orthologue of the Race 5 gene (identified as the top BlastP hit, **Materials and methods section 4.2.2.7**) as fragments per kilobase of exon per million fragments mapped (FPKM) and was sourced from a transcriptome study of a compatible interaction of H-Cf-0 tomato plants inoculated with *F. fulva* 0WU strain and sampled 4, 8, and 12 days post-inoculation (dpi), as well as *in vitro* (Iv; growth in potato dextrose broth for 4 days, 22°C (Mesarich et al., 2014)). Proteins were only included if the encoding gene had >5-fold increase in gene expression between *in vitro* and any *in planta* stage, and expression *in planta* >50 RPMK, or >25 RPMK for carbohydrate-active enzymes (CAZymes).

3 – Protein type determined by HMMER, InterPro, and EffectorP v3.0. analysis. For *D. septosporum*, candidate effectors (CEs) predicted from other studies (Hunziker, 2018; Tarallo, 2022) were included. For *F. fulva*, effectors were also identified from the protein description of the predicted secreted protein list (**Materials and methods section 4.2.2.7**), and CEs that were identified by Mesarich et al. (2018) were also included. For CEs, the encoding gene name was added in brackets.

4 – Predicted protein domains based on HMMER and DIAMOND prediction (https://bcb.unl.edu/dbCAN2/blast.php), as well as InterPro prediction, performed using Geneious software (v9.1.8.).

*Protein was also present in the PMMG Day 16 sample.

Appendix 30. Homologous proteins in sample PMMG Day 16 classically secreted individually by *Dothistroma septosporum* and *Fulvia fulva*.

	Normalised expression[2]					
Accession[1]	Iv	Early/4 dpi	Mid/8 dpi	Late/12 dpi	Protein type[3]	Protein domains[4]
D. septosporum						
70379*	1	6	19	202	CE	Carbohydrate Esterase Family 1
180786	18	97	6	30	No pred	-
F. fulva						
UJO14225.1*	0	3805	19477	7443	CE (*FfEcp20-1*)	-
UJO16284.1*	5	661	201	598	CE (*FfEcp20-3*)	-
UJO24912.1	16	133	559	329	CAZyme	Auxiliary Activity Family 3, GMC oxidoreductase

1 –The accession for *D. septosporum* proteins is the Joint Genome Institute (JGI) protein ID from the *D. septosporum* genome page (https://mycocosm.jgi.doe.gov/Dotse1/Dotse1.home.html). The protein accession for *F. fulva* proteins is the Gene bank protein ID from the NCBI website (https://www.ncbi.nlm.nih.gov/).

2 – For *D. septosporum* proteins, the encoding gene expression is shown as Reads Per Million per Kilobase (RPMK) and was sourced from a transcriptome analysis performed on *D. septosporum*-infected *Pinus radiata* seedlings. Three *in planta* stages were sampled: early, mid, and late, as well as *in vitro* (Iv; growth in low Dothistroma medium (LDM) broth for 7 days, 22°C (Bradshaw et al., 2016)). For *F. fulva* proteins, gene expression is shown for the 0WU orthologue of the Race 5 gene (identified as the top BlastP hit, **Materials and methods section 4.2.2.7**) as fragments per kilobase of exon per million fragments mapped (FPKM) and was sourced from a transcriptome study of a compatible interaction of H-Cf-0 tomato plants inoculated with *F. fulva* 0WU strain and sampled 4, 8, and 12 days post-inoculation (dpi), as well as *in vitro* (Iv; growth in potato dextrose broth for 4 days, 22°C (Mesarich et al., 2014)). Proteins were only included if the encoding gene had >5-fold increase in gene expression between *in vitro* and any *in planta* stage, and expression *in planta* >50 RPMK, or >25 RPMK for carbohydrate-active enzymes (CAZymes).

3 – Protein type determined by HMMER, InterPro, and EffectorP v3.0. analysis. For *D. septosporum*, candidate effectors (CEs) predicted from other studies (Hunziker, 2018; Tarallo, 2022) were included. For *F. fulva*, effectors were also identified from the protein description of the predicted secreted protein list (**Materials and methods section 4.2.2.7**), and CEs that were identified by Mesarich et al. (2018) were also included. For CEs, the encoding gene name was added in brackets.

4 – Predicted protein domains based on HMMER and DIAMOND prediction (https://bcb.unl.edu/dbCAN2/blast.php), as well as InterPro prediction, performed using Geneious software (v9.1.8.). GMC: glucose-methanol-choline

*Protein was also present in the PMMG Day 9 sample.

Appendices for Chapter 5

Appendix 31. Primers used in Chapter 5.

Name	Sequence 5'–3'	Purpose
CRISPR single guide RNA (sgRNA) preparation for insertion into Cas9HygAMAccdB plasmid		
HM95	GTCTCACGCGGCTCAGAGTCGAG	Amplification of sgRNA *DsAflR1*
HM96	AACCTCGACTCTGAGCCGCGTGA	
HM97	GTCACAAGAAGCAGCAGATAGGA	Amplification of sgRNA *DsAflR2*
HM98	AACTCCTATCTGCTGCTTCTTGT	
HM150	GTCGAATACACAGAAGCACGCGG	Amplification of sgRNA *Ds69328*
HM151	AACCCTCCGCGTGCTTCTGTGTATTC	
HM189	GTCGACTGCGCCAGCAAATACAA	Amplification of sgRNA *DsCE3*
HM190	AACTTGTATTTGCTGGCGCAGTC	
M139	TTTTCTCTTCCATTTACGC	Screening for sgRNA insertion (Rocafort et al., 2022)
Donor DNA (dDNA) plasmid construction		
HM167	GGGTTTTCCCAGTCACGACGCGGCCGCCACAATGCCAACCTCG	Amplification of *Ds69328* left homologous flank
HM168	GGAACAACTGGCATGAATTCCTTCTGTGTATTCCATG	
HM169	GTTTAGAGGTAATCCTTCTTTCTAGAACGCGATCAACACACTC	Amplification of *Ds69328* right homologous flank
HM170	CAATTTCACACAGGAAACAGCGCGGCCGCCAATTCCGTCGATGTG	
HM191	GGGTTTTCCCAGTCACGACGACAGTATTGTCGAGC	Amplification of *DsCE3* left homologous flank
HM192	GGAACAACTGGCATGAATTCTGCTGGCGCAGTC	
HM193	GTTTAGAGGTAATCCTTCTTTCTAGACAACTCCGCTCTTG	Amplification of *DsCE3* right homologous flank
HM194	CAATTTCACACAGGAAACAGCCGCAAACCACCATC	
pRS427 fw	GTCGTGACTGGGAAAACCC	Amplification of the pAN7-1 backbone
pRS427 rv	GCTGTTTCCTGTGTGAAATTG	
nptII fw	GAATTCATGCCAGTTGTTCC	Amplification of the *nptII* cassette in pII99

nptII rv	TCTAGAAAGAAGGATTACCTCTAAAC	
pRS426 seq 1	GGCGATTAAGTTGGGTAACG	Sequencing dDNA plasmids for correct assembly
pRS426 seq 2	GTGGAATTGTGAGCGGATAAC	
nptII_1	ATAGCCGAATAGCCTCTCC	
nptII_2	GAATGGGCTGACCGCTTCC	
DB056	AGATGGATTGCACGCAGGTTC	
Complementation plasmid construction		
HM230	GGACTCAAGAACGGCG	Mutation of *Xba*I site in *DsCE3*
HM231	CGCCGTTCTTGAGTCC	
HM232	ATGCATGGGCCCGCTACACTGCGCACC	Amplification of *DsCE3* and flanks
HM233	ATGCATTCTAGAGGCCTGGTGATCTTCG	
HM234	ATGCATGGGCCCCCGCACATAAGGCCAG	Amplification of *Ds69328* and flanks
HM235	ATGCATTCTAGAGTCACGCGTGCAAGG	
Screening CRISPR/Cas9 transformants		
HM103	CGGTATGGGTACGCTCT	Amplification of *β-tubulin*
HM104	GAAATGGCACCTATCACAAG	
HM89	AACCCTACGCGTCTACCAG	Screening *DsAflR* transformants
HM90	GAAGAGGACTTCCGATCTTG	
HM183	GCAACTACTGGTGGTACG	
HM184	GCGCGAGATGTCCTTTC	
HM185	CTTGCTTGGCTTTGTCG	
HM186	GTGGAACGACATACCGG	
HM211	CTGACGGCACTGAGATC	
HM15	CGAAATTGCCGTCAACCAAGCTCT	Screening *DsAflR* transformants 82 and 158
HM16	TGTTTATCGGCACTTTGCATCGGC	
HM209	GAACATCGCCTCGCTCC	
HM210	GCCGCCTCCACCATTTG	
HM187	GTATGTCGTTCCACATCTAC	Amplification of *Ds140271*
HM188	CTTCAAGATGCCTTCTCC	

HM195	CATCCTAAGAGCTGCGG	Amplification of *DsAflJ*
HM196	GATGTCGCGGATCTCTC	
HM238	CGAGACTGAGGAATCCGCTC	Amplification of geneticin cassette
HM239	TAGGCCGAATAACTTGCACAAATTG	
HM201	CCTTCCGTACAGCATCCGTG	Amplification of *Ds69328*
HM202	CCGCATTCCCAGAGCCAAC	
HM203	GCTTTCGGGAGCGAGGATC	Amplification of *DsCE3*
HM204	GCAGCACATTGGCGTAGC	
HM201	CCTTCCGTACAGCATCCGTG	Screening *Ds69328* complements
HM202	CCGCATTCCCAGAGCCAAC	
HM234	ATGCATGGGCCCCCGCACATAAGGCCAG	Sequencing *Ds69328* complements
HM235	ATGCATTCTAGAGTCACGCGTGCAAGG	
HM232	ATGCATGGGCCCGCTACACTGCGCACC	Screening and sequencing *DsCE3* complements
HM233	ATGCATTCTAGAGGCCTGGTGATCTTCG	
Amplification of probes for Southern hybridization		
HM212	GTCGACCATGTTCGCC	Amplification of probe for *DsAflR*
HM213	GCAAGACTTCCTCCGAG	
HM218	CATCTCAAGCTCGCTAGG	Amplification of probe for *Ds69328*
HM219	CAGGGTGGAGTTTGAGC	
HM220	GCGACAAGAATGCTGG	Amplification of probe for *DsCE3*
HM221	CGAGGTAGATACAAGCTG	
Gene copy number determination		
DsAflR fw	GGAAGAGTAGTGTTACCATTGT	Amplification of *DsAflR*
DsAflR rv	CATCTATTCAACGACCTCACA	
HM253	AGTGCGATCAATGTCAGTGC	Amplification of *Ds69328*
HM254	TCACACACCCGACCACTTTA	
HM249	CGTCAAAGGAAGCACGTACA	Amplification of *DsCE3*
HM250	GGGCGAACAGTCTGAAAGAG	
Fungal biomass analysis		

DsPksA fw	CTGTCTTCCTCGACCTGTT	Amplification of *DsPksA* (Chettri et al., 2012)
DsPksA rv	AGCACACCTGGAAAGAATGA	
CAD fw	CAGCAAGAGGATTTGGACCTA	Amplification of *CAD* (Chettri et al., 2012)
CAD rv	TTCAATACCCACATCTGATCAAC	

Appendix 32. Plasmids used in Chapter 5.

Plasmid name	Purpose	Antibiotic selection[1]	Reference
pCas9HygAMAccdb	Single guide RNA (sgRNA) and *Cas9* expression vector	Amp/Hyg	Rocafort et al. (2022)
pCas9HygAMAccdb-Ds69328	sgRNA targeting *Ds69328*	Amp	This study
pCas9HygAMAccdb-DsCE3	sgRNA targeting *DsCE3*	Amp	This study
pAN7-1	Backbone for donor DNA (dDNA) plasmids	Amp	Punt et al. (1990)
pII9	Used to amplify the *nptII* cassette for dDNA plasmid	Amp/Gen	Lara-Ortiz et al. (2003)
dDNA-Ds69328	*Ds69328* dDNA plasmid	Amp/Gen	This study
dDNA-DsCE3	*DsCE3* dDNA plasmid	Amp/Gen	This study
pBC-phleo	Backbone for complementation plasmids	Chl/Phleo	Silar et al. (1995)
COMP-Ds69328	*Ds69328* complementation plasmid	Chl/Phleo	This study
COMP-DsCE3	*DsCE3* complementation plasmid	Chl/Phleo	This study

1 – Antibiotic selection; Amp, ampicillin; Hyg, hygromycin; Gen, geneticin; Chl, chloramphenicol; Phleo, phleomycin.

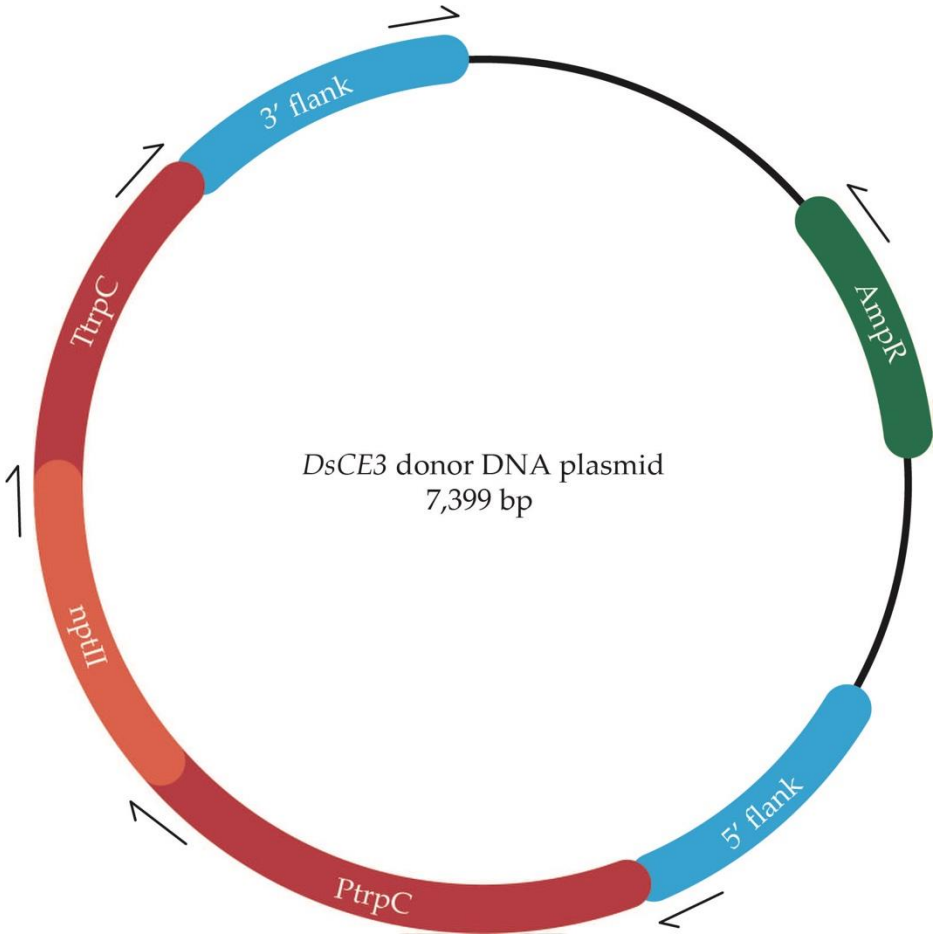

Appendix 33. Schematic of *DsCE3* donor DNA (dDNA) plasmid. Key features: *AmpR*, ampicillin resistance gene (part of the pAN7-1 backbone); *PtrpC*, *nptII* promoter; *nptII*, geneticin resistance gene; *TtrpC*, *nptII* terminator (*nptII* cassette amplified from pII99; 5' flank, *DsCE3* flank; 3' flank, *DsCE3* flank; bp, base pairs. Arrows illustrate gene orientation.

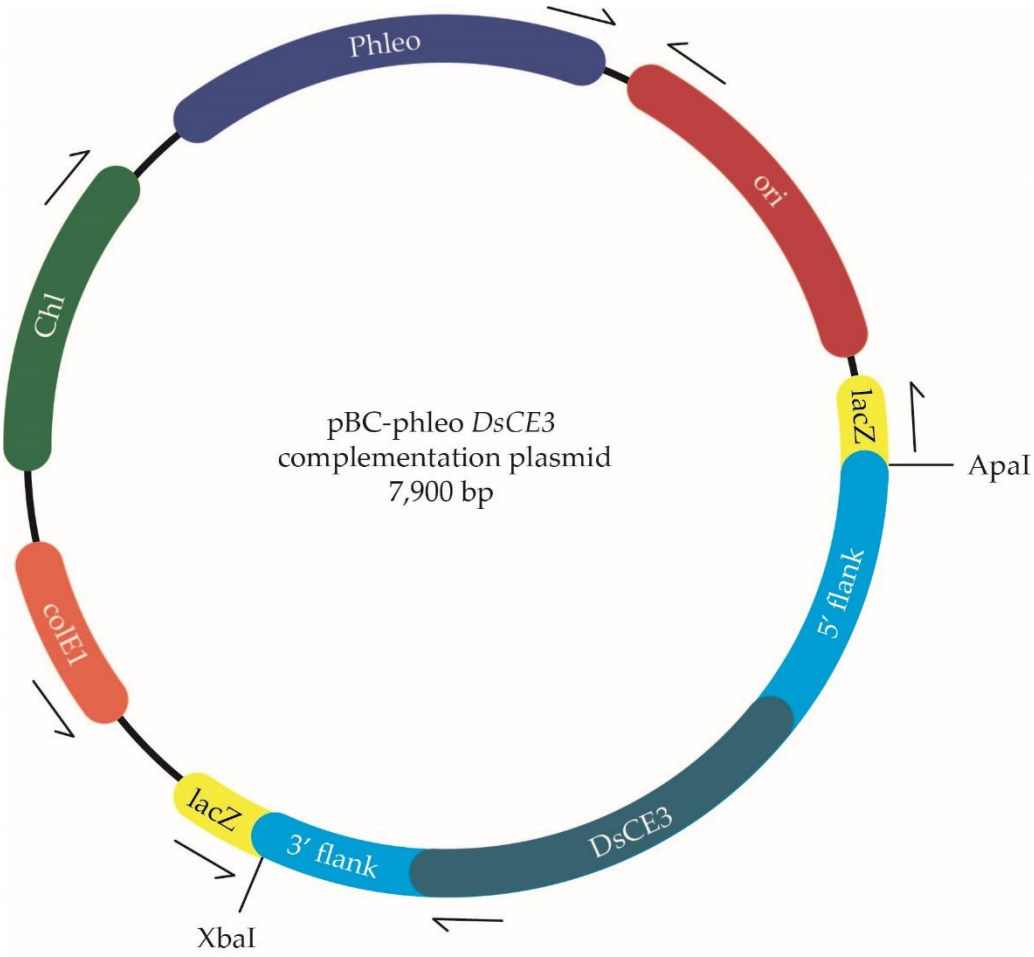

Appendix 34. Schematic of *DsCE3* complementation plasmid made using the pBC-phleo plasmid backbone. Key features: *Chl*, chloramphenicol resistance gene; *Phleo*, phleomycin resistance gen; *DsCE3*, the complemented gene copy with 5' and 3' flanks; *Apa*I and *Xba*I, restriction sites used for ligation; bp, base pairs. Arrows illustrate gene orientation.

Appendix 35. Results from virulence analysis of *Dothistroma septosporum* wild type (WT), CRISPR/Cas9 transformants, and complementation transformants on Pinus radiata seedlings. (**a**) Inoculation details. (**b**) Visual needle analysis results. (**c**) Relative biomass analysis results. (**d**) Absolute biomass analysis results.

Appendix 36. Results from the *Dothistroma septosporum* wild type (WT), CRISPR/Cas9 transformants, and complementation transformants growth characteristics. (**a**) Sporulation assay. (**b**) Radial growth assay. (**c**) Radial growth T-test.

Appendix 37. Results from the *Dothistroma septosporum* wild type (WT) and complementation transformants copy number determination analysis.

Appendices 35 to 37 can be accessed online at https://drive.google.com/drive/folders/1Yj-ODEEZSEvwmmeFGjBs8X1Ewo5AFmk0?usp=drive_link

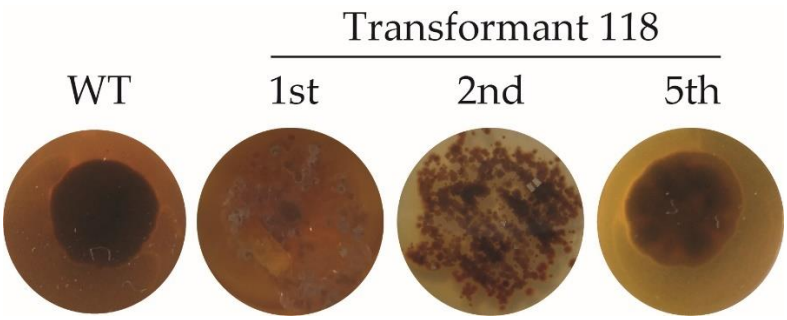

Appendix 38. Loss of the dothistromin-producing phenotype of *Dothistroma septosporum* CRISPR/Cas9 *DsAflR* transformant 118 after sub-culturing. Dothistromin production is shown by red-brown pigmentation of the media, as seen in the media supporting growth of wild type (WT) *D. septosporum*. A dothistromin-deficient phenotype is shown by absence of red-brown pigmentation of the media. CRISPR/Cas9 *DsAflR* transformants were sub-cultured multiple times during the course of this study. Transformant 118 displayed a dothistromin-producing phenotype after the 1st sub-culture, but from the 2nd sub-culture onwards, a dothistromin-deficient phenotype was observed.

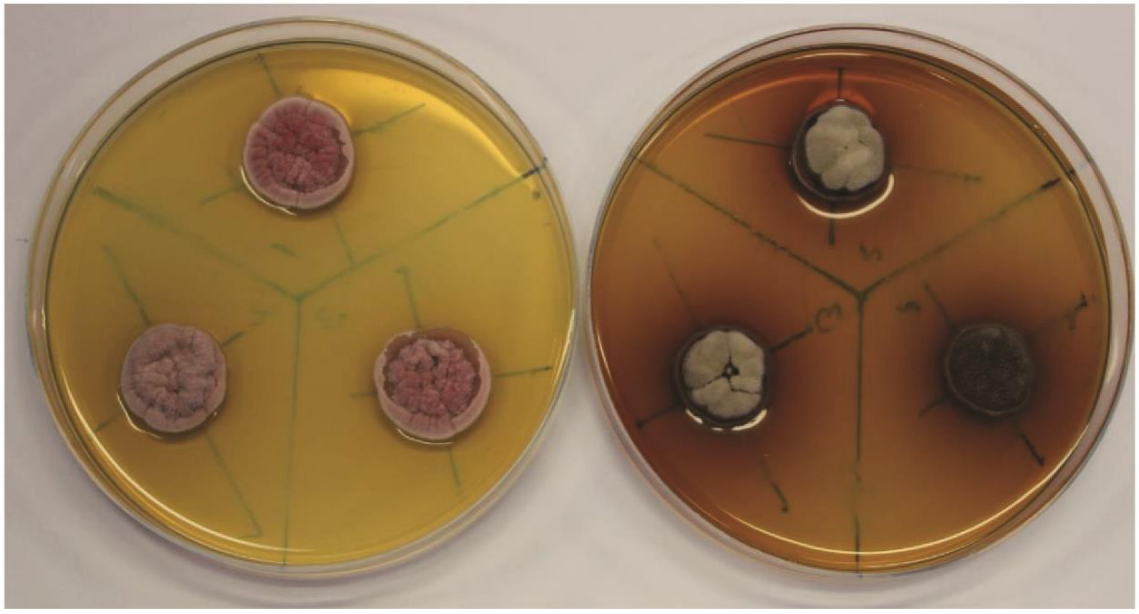

Appendix 39. Increased production of dothistromin by *Dothistroma septosporum* in the presence of 100 µg/mL $CuSO_4.5H_2O$. The plate on the left is standard Dothistroma medium (DM), while on the right is DM supplemented with 100 µg/mL $CuSO_4.5H_2O$.

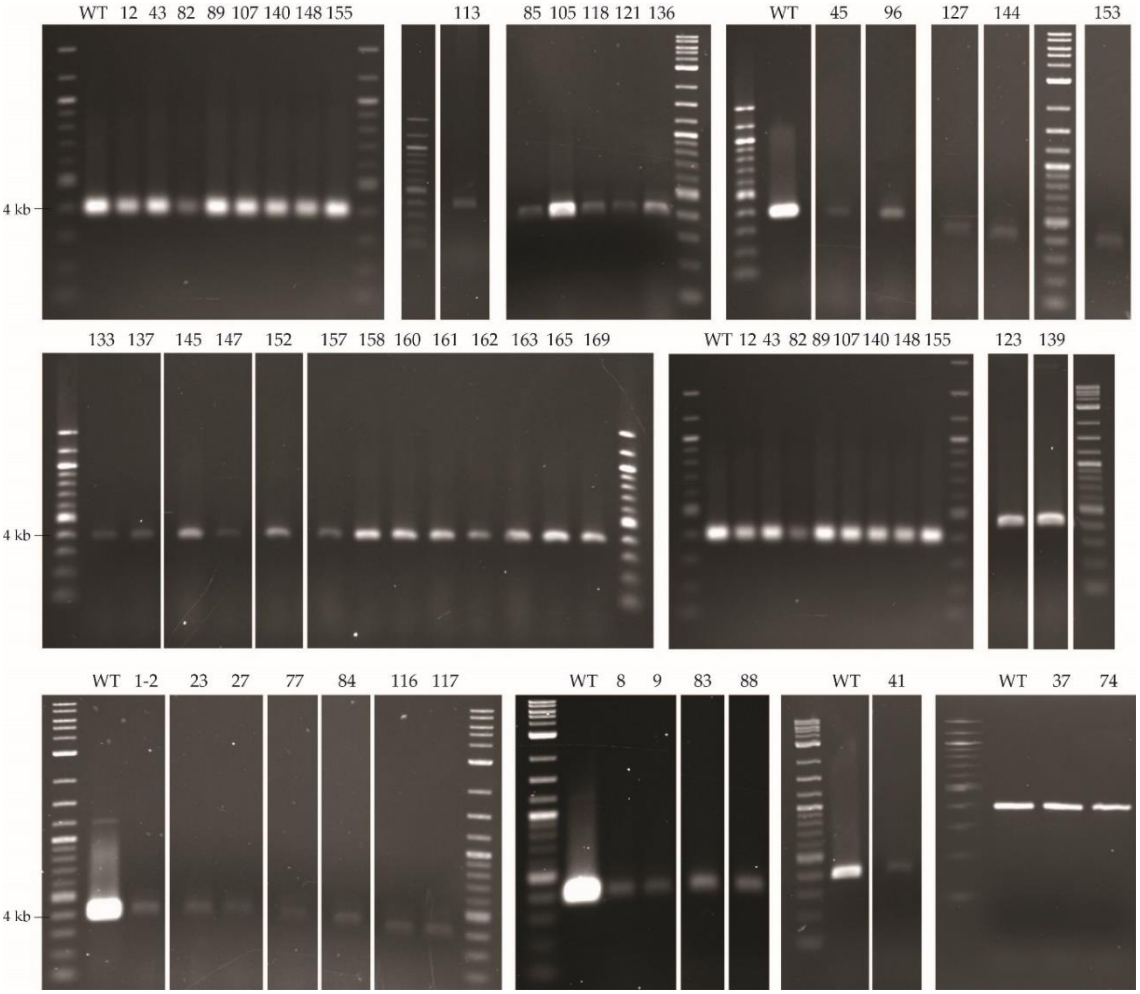

Appendix 40. PCR amplification of *β-tubulin* to test the gDNA quality of *Dothistroma septosporum* wild type (WT) and *DsAflR* CRISPR/Cas9 transformants. The *β-tubulin* gene (JGI ID: 68998) was amplified using primers listed in **Appendix 31**. The expected PCR product size of 400 bp is labelled on the left side of gel pictures. The gDNA from all transformants amplified *β-tubulin*, showing that the gDNA was of adequate quality to perform further screening.

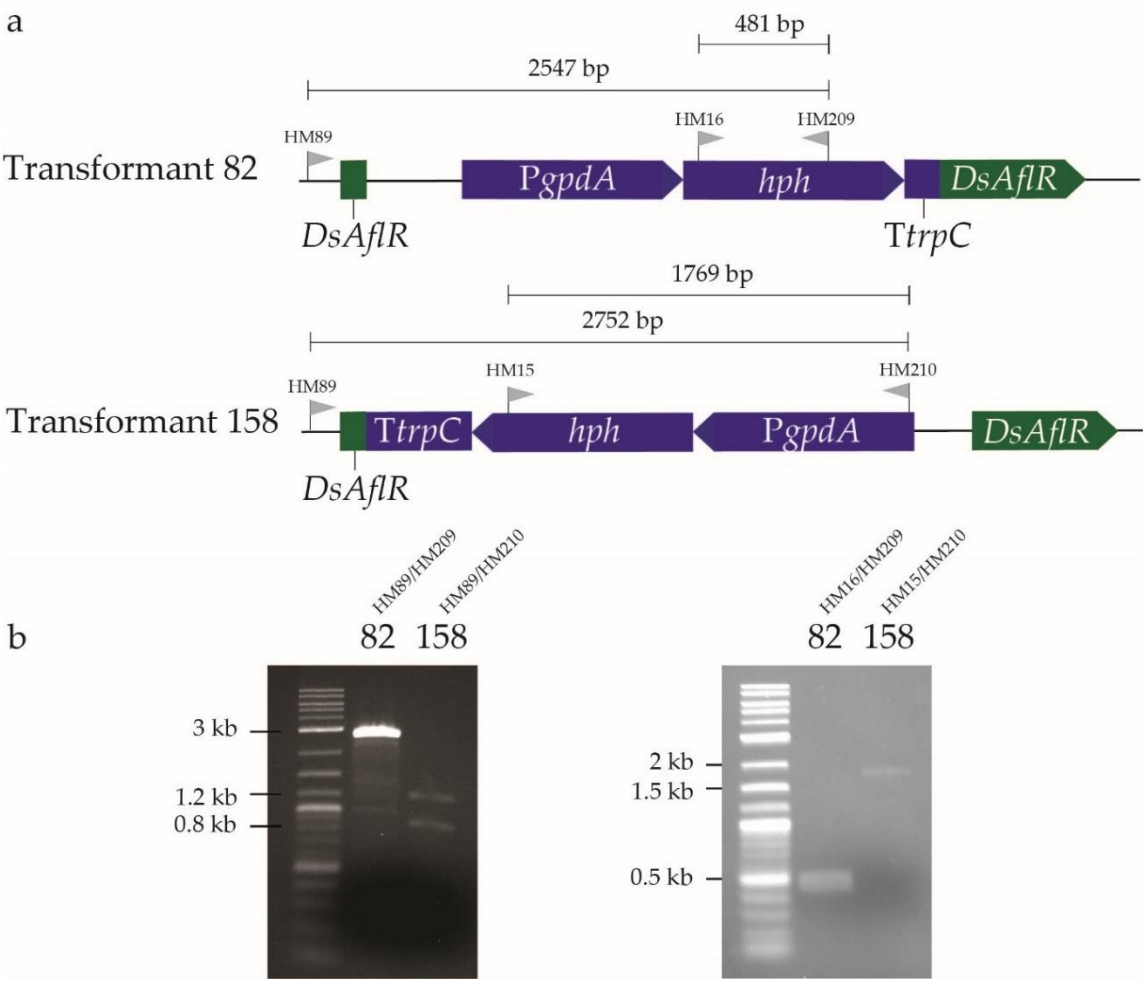

Appendix 41. PCR analysis to support estimated insertion size and content of *Dothistroma septosporum DsAflR* CRISPR/Cas9 transformants 82 and 158. (a) Schematic of transformants 82 and 158 with insertions, suggested by PCR and PCR amplicon sequencing analysis. *DsAflR* is the segmented green bar, purple bars are the *hph* (hygromycin B resistance gene) cassette, and the black bar between the separated *DsAflR* regions is part of the CRISPR/Cas9 plasmid (Cas9HygAMAccdB). Primer positions are illustrated by grey flags, with the distance between primers shown above. (b) PCRs performed on genomic DNA (gDNA) from transformants 82 and 158 using primers detailed in (a). All PCRs amplified the expected band except from gDNA of transformant 158 with primers HM89/HM210 - this was likely due to a shorter insertion than estimated from the PCR product size in earlier screens, leading to lack of a primer binding site and non-specific PCR amplification in transformant 158. Transformant number and primer pairs used are shown at the top of the gel, and relevant labels of the DNA ladder sizes are shown on the left.

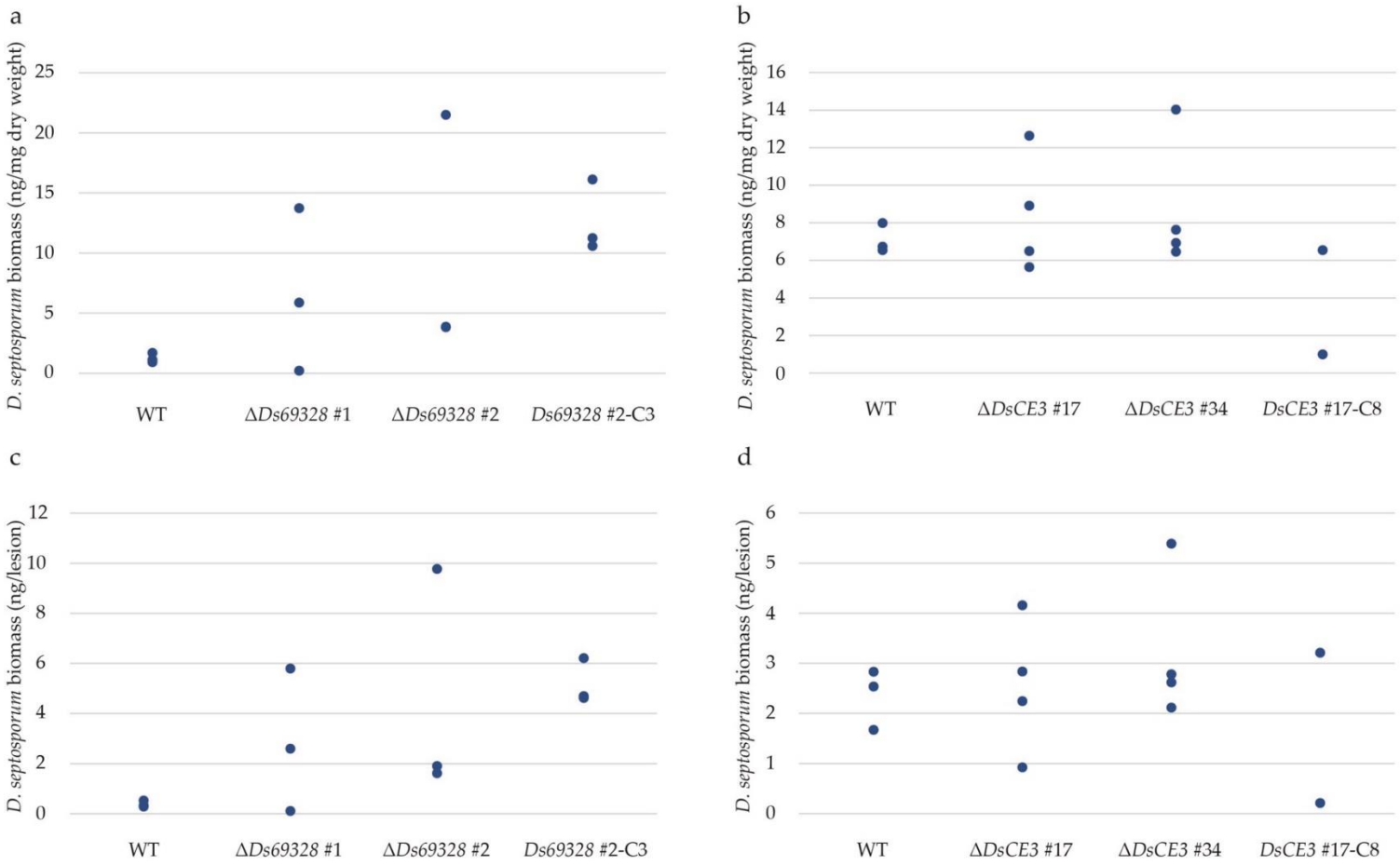

Appendix 42. Dot plot analysis of fungal biomass in wild type (WT), gene disruption, and complementation strains of *Dothistroma septosporum* in infected *Pinus radiata*, calculated by relative qPCR analysis. Results are shown for Experiment 1 (**a** and **c**), and 2 (**b** and **d**). Biomass was calculated as ng of *D. septosporum* gDNA per mg dry weight of infected needles (**a** and **b**), or per lesion (**c** and **d**). *D. septosporum* gDNA concentration was calculated from relative quantification analysis of the *D. septosporum DsPksA* target gene and the *P. radiata CAD* reference gene (**Materials and methods section 5.2.8.4**). Each dot represents one biological replicate (i.e., one *P. radiata* tree).

Appendix 43. Biomass of wild type (WT), gene disruption, and complementation strains of *Dothistroma septosporum* from infected *Pinus radiata* calculated by relative qPCR analysis.

Target gene / Strain	Fungal biomass (ng/mg)[1]	P (T-test) WT/COMP[1]	Fungal biomass (ng/ lesion)[2]	P (T-test) WT/COMP[2]
Experiment 1				
WT	1.25 ± 0.33	-	0.38 ± 0.11	-
Δ*Ds69328* #1	4.75 ± 5.54	0.24/0.23	1.97 ± 2.33	0.21/0.25
Δ*Ds69328* #2	9.74 ± 8.32	0.22/0.66	4.43 ± 3.78	0.20/0.80
Ds69328 #2-C3	12.66 ± 2.47	**0.00**/-	5.18 ± 0.73	**0.00**/-
Experiment 2				
WT	7.09 ± 0.64	-	3.48 ± 1.45	-
Δ*DsCE3* #17	8.42 ± 2.71	0.51/0.18	2.11 ± 1.23	0.83/0.58
Δ*DsCE3* #34	8.76 ± 3.07	0.47/0.19	3.23 ± 1.27	0.38/0.35
DsCE3 #17-C8	3.77 ± 2.77	0.22/-	12.42 ± 11.68	0.64/-

1 – Results are the mean ± standard deviation of fungal gDNA (ng) per dry weight of infected needles (mg).

2 – Results are the mean ± standard deviation of fungal gDNA (ng) per lesion.

T-tests were performed with the WT and with the corresponding complement. T-tests were calculated in Microsoft© Excel (T.test function), as a two-tailed test and a two sample equal variance test. A T-test value ≤0.05 indicates a significant difference (in bold).

Fungal gDNA was determined through relative quantification of *D. septosporum* target gene *DsPksA* (JGI ID: 48345), and *P. radiata* reference gene *CAD* (**Materials and methods section 5.2.8.4**).

Full data are shown in **Appendix 35d**.

References

Aglietti, C., Meinecke, C. D., Ghelardini, L., Barnes, I., van der Nest, A., & Villari, C. (2021). Rapid detection of pine pathogens *Lecanosticta acicola*, *Dothistroma pini* and *D. septosporum* on needles by probe-based LAMP assays. *Forests, 12*(4), 479.

Agrawal, G. K., Jwa, N.-S., Lebrun, M.-H., Job, D., & Rakwal, R. (2010). Plant secretome: Unlocking secrets of the secreted proteins. *PROTEOMICS, 10*(4), 799-827. 10.1002/pmic.200900514

Alves-Santos, F. M., Ramos, B., García-Sánchez, M. A., Eslava, A. P., & Díaz-Mínguez, J. M. (2002). A DNA-based procedure for *in planta* detection of *Fusarium oxysporum* f. sp. *phaseoli*. *Phytopathology, 92*(3), 237-244. 10.1094/PHYTO.2002.92.3.237

Armitage, A. D., Taylor, A., Sobczyk, M. K., Baxter, L., Greenfield, B. P. J., Bates, H. J., . . . Clarkson, J. P. (2018). Characterisation of pathogen-specific regions and novel effector candidates in *Fusarium oxysporum* f. sp. *cepae*. *Scientific Reports, 8*(1) 10.1038/s41598-018-30335-7

Asano, T., Miwa, A., Maeda, K., Kimura, M., & Nishiuchi, T. (2013). The secreted antifungal protein Thionin 2.4 in *Arabidopsis thaliana* suppresses the toxicity of a fungal fruit body lectin from *Fusarium graminearum*. *PLoS Pathogens, 9*(8), e1003581. 10.1371/journal.ppat.1003581

Barau, J., Grandis, A., Carvalho, V. M., Teixeira, G. S., Zaparoli, G. H., do Rio, M. C., . . . Pereira, G. A. (2015). Apoplastic and intracellular plant sugars regulate developmental transitions in witches' broom disease of cacao. *The Journal of Experimental Botany, 66*(5), 1325-1337. 10.1093/jxb/eru485

Barnes, I., van der Nest, A., Granados, G. M., & Wingfield, M. J. (2022). Dothistroma needle blight. In F. O. Asiegbu & A. Kovalchuk (Eds.), *Forest Microbiology* (pp. 179-199). Academic Press.

Barrangou, R., Fremaux, C., Deveau, H., Richards, M., Boyaval, P., Moineau, S., . . . Horvath, P. (2007). CRISPR provides acquired resistance against viruses in prokaryotes. *Science, 315*(5819), 1709-1712. 10.1126/science.1138140

Bhadauria, V., Banniza, S., Vandenberg, A., Selvaraj, G., & Wei, Y. (2013). Overexpression of a novel biotrophy-specific *Colletotrichum truncatum* effector, *CtNUDIX*, in hemibiotrophic fungal phytopathogens causes incompatibility with their host plants. *Eukaryotic Cell, 12*(1), 2-11. 10.1128/EC.00192-12

Blondeau, K., Blaise, F., Graille, M., Kale, S. D., Linglin, J., Ollivier, B., . . . Fudal, I. (2015). Crystal structure of the effector AvrLm4–7 of *Leptosphaeria maculans* reveals insights into its translocation into plant cells and recognition by resistance proteins. *The Plant Journal, 83*(4), 610-624. 10.1111/tpj.12913

Boller, T., & Felix, G. (2009). A renaissance of elicitors: Perception of microbe-associated molecular patterns and danger signals by pattern-recognition receptors. *Annual Review of Plant Biology, 60*(1), 379-406. 10.1146/annurev.arplant.57.032905.105346

Bolton, M. D., Van Esse, H. P., Vossen, J. H., De Jonge, R., Stergiopoulos, I., Stulemeijer, I. J. E., . . . Thomma, B. P. H. J. (2008). The novel *Cladosporium fulvum* lysin motif effector Ecp6 is a virulence factor with orthologues in other fungal species. *Molecular Microbiology, 69*(1), 119-136. https://doi.org/10.1111/j.1365-2958.2008.06270.x

Bonsch, B., Belt, V., Bartel, C., Duensing, N., Koziol, M., Lazarus, C. M., . . . Cox, R. J. (2016). Identification of genes encoding squalestatin S1 biosynthesis and *in vitro* production of new squalestatin analogues. *Chemical Communications, 52*(41), 6777-6780. 10.1039/C6CC02130A

Boontawon, T., Nakazawa, T., Inoue, C., Osakabe, K., Kawauchi, M., Sakamoto, M., & Honda, Y. (2021). Efficient genome editing with CRISPR/Cas9 in *Pleurotus ostreatus*. *AMB Express, 11*(1), 30. 10.1186/s13568-021-01193-w

Borhan, M. H., Van De Wouw, A. P., & Larkan, N. J. (2022) Molecular interactions between *Leptosphaeria maculans* and *Brassica species*. In*: Vol. 60. Annual Review of Phytopathology* (pp. 237-257).

Bradley, E. (2022). *Identification and functional characterisation of glycoside hydrolases from the kauri dieback pathogen, Phytophthora agathidicida.* (Doctor of Philosophy (PhD) in Plant Science Thesis), Massey University, Retrieved from http://hdl.handle.net/10179/17924 Available from EBSCOhost Massey Research Online database.

Bradley, E. L., Ökmen, B., Doehlemann, G., Henrissat, B., Bradshaw, R. E., & Mesarich, C. H. (2022). Secreted glycoside hydrolase proteins as effectors and invasion patterns of plant-associated fungi and oomycetes. *Frontiers in Plant Science, 13* 10.3389/fpls.2022.853106

Bradshaw, R. E., Bidlake, A., Forester, N., & Scott, D. B. (1997). Transformation of the fungal forest pathogen *Dothistroma pini* to hygromycin resistance. *Mycological Research, 101*(10), 1247-1250. https://doi.org/10.1017/S0953756297003870

Bradshaw, R. E., Guo, Y., Sim, A. D., Kabir, M. S., Chettri, P., Ozturk, I. K., . . . Cox, M. P. (2016). Genome-wide gene expression dynamics of the fungal pathogen *Dothistroma septosporum* throughout its infection cycle of the gymnosperm host *Pinus radiata*. *Molecular Plant Pathology, 17*(2), 210-224. 10.1111/mpp.12273

Bradshaw, R. E., Sim, A. D., Chettri, P., Dupont, P. Y., Guo, Y., Hunziker, L., . . . Barnes, I. (2019). Global population genomics of the forest pathogen *Dothistroma septosporum* reveal chromosome duplications in high dothistromin-producing strains. *Molecular Plant Pathology, 20*(6), 784-799. 10.1111/mpp.12791

Bradshaw, R. E., & Zhang, S. (2006). Biosynthesis of dothistromin. *Mycopathologia, 162*(3), 201-213. 10.1007/s11046-006-0054-5

Brar, S., Tabima, J. F., McDougal, R. L., Dupont, P. Y., Feau, N., Hamelin, R. C., . . . Williams, N. M. (2018). Genetic diversity of *Phytophthora pluvialis*, a pathogen of conifers, in New Zealand and the west coast of the United States of America. *Plant Pathology, 67*(5), 1131-1139. https://doi.org/10.1111/ppa.12812

Brito, N., Espino, J. J., & González, C. (2006). The endo-beta-1,4-xylanase xyn11A is required for virulence in *Botrytis cinerea*. *Molecular Plant-Microbe Interactions, 19*(1), 25-32. 10.1094/mpmi-19-0025

Brouns, S. J. J., Jore, M. M., Lundgren, M., Westra, E. R., Slijkhuis, R. J. H., Snijders, A. P. L., . . . van der Oost, J. (2008). Small CRISPR RNAs guide antiviral defense in prokaryotes. *Science, 321*, 960-963. 10.1126/science.1159689

Brown, A., & Webber, J. (2008). Red band needle blight of conifers in Britain. *Forestry commission*

Brown, D. W., Yu, J. H., Kelkar, H. S., Fernandes, M., Nesbitt, T. C., Keller, N. P., . . . Leonard, T. J. (1996). Twenty-five co-regulated transcripts define a sterigmatocystin gene cluster in *Aspergillus nidulans*. *Proceedings of the National Academy of Sciences of the United States of America, 93*, 1418-1422.

Bulman, L. S., Gadgil, P. D., Kershaw, D. J., & Ray, J. W. (2004). *Assessment and control of Dothistroma needle-blight* (Forest Research Bulletin No.229). Forest Research.

Butler, E. J., & Jones, S. G. (1949). *Tomato leaf mould, Cladosporium fulvum Cooke*. London: Macmillan.

Calmes, B., Morel-Rouhier, M., Bataillé-Simoneau, N., Gelhaye, E., Guillemette, T., & Simoneau, P. (2015). Characterization of glutathione transferases involved in the pathogenicity of *Alternaria brassicicola*. *BMC microbiology, 15*, 123. 10.1186/s12866-015-0462-0

Carnegie, A. J., & Kathuria, A. (2023). Efficacy of cuprous oxide for control of dothistroma needle blight in *Pinus radiata* plantations in Australia. *Australian Forestry*, 1-9. 10.1080/00049158.2022.2145044

Ceccaldi, R., Rondinelli, B., & D'Andrea, A. D. (2016). Repair pathway choices and consequences at the double-strand break. *Trends in Cell Biology, 26*(1), 52-64. 10.1016/j.tcb.2015.07.009

Chambers, K. R., Van de Wouw, A. P., Gardiner, D. M., Elliott, C. E., & Idnurm, A. (2021). A conserved Zn_2Cys_6 transcription factor, identified in a spontaneous mutant from *in vitro* passaging, is involved in pathogenicity of the blackleg fungus *Leptosphaeria maculans*. *Fungal Biology, 125*(7), 541-550. 10.1016/j.funbio.2021.02.002

Chang, T. C., Salvucci, A., Crous, P. W., & Stergiopoulos, I. (2016). Comparative genomics of the sigatoka disease complex on banana suggests a link between parallel evolutionary changes in *Pseudocercospora fijiensis* and *Pseudocercospora eumusae* and increased virulence on the banana host. *PLOS Genetics, 12*(8), e1005904. 10.1371/journal.pgen.1005904

Chen, H., Quintana, J., Kovalchuk, A., Ubhayasekera, W., & Asiegbu, F. O. (2015). A cerato-platanin-like protein HaCPL2 from *Heterobasidion annosum sensu stricto* induces cell death in *Nicotiana tabacum* and *Pinus sylvestris*. *Fungal Genetics and Biology, 84*, 41-51. https://doi.org/10.1016/j.fgb.2015.09.007

Chen, L., Ma, Y., Zhao, J., Geng, X., Chen, W., Ding, S., . . . Li, H. (2019). The bZIP transcription factor FpAda1 is essential for fungal growth and conidiation in *Fusarium pseudograminearum*. *Current Genetics, 66*(3), 507-515. 10.1007/s00294-019-01042-1

Chen, L. H., Kračun, S. K., Nissen, K. S., Mravec, J., Jørgensen, B., Labavitch, J., & Stergiopoulos, I. (2021). A diverse member of the fungal Avr4 effector family interacts with de-esterified pectin in plant cell walls to disrupt their integrity. *Science Advances, 7*(19), eabe0809. 10.1126/sciadv.abe0809

Chettri, P., Calvo, A. M., Cary, J. W., Dhingra, S., Guo, Y., McDougal, R. L., & Bradshaw, R. E. (2012). The *veA* gene of the pine needle pathogen *Dothistroma septosporum* regulates sporulation and secondary metabolism. *Fungal Genetics and Biology, 49*(2), 141-151. 10.1016/j.fgb.2011.11.009

Chettri, P., Dupont, P. Y., & Bradshaw, R. E. (2018). Chromatin-level regulation of the fragmented dothistromin gene cluster in the forest pathogen *Dothistroma septosporum*. *Molecular Microbiology, 107*(4), 508-522. 10.1111/mmi.13898

Chettri, P., Ehrlich, K. C., Cary, J. W., Collemare, J., Cox, M. P., Griffiths, S. A., . . . Bradshaw, R. E. (2013). Dothistromin genes at multiple separate loci are regulated by AflR. *Fungal Genetics and Biology, 51*, 12-20. 10.1016/j.fgb.2012.11.006

Cho, Y. (2015). How the necrotrophic fungus *Alternaria brassicicola* kills plant cells remains an enigma. *Eukaryotic Cell, 14*(4), 335-344. 10.1128/ec.00226-14

Cho, Y., Ohm, R. A., Grigoriev, I. V., & Srivastava, A. (2013). Fungal-specific transcription factor *AbPf2* activates pathogenicity in *Alternaria brassicicola*. *The Plant Journal, 75*(3), 498-514. 10.1111/tpj.12217

Collemare, J., Griffiths, S., Iida, Y., Karimi Jashni, M., Battaglia, E., Cox, R. J., & De Wit, P. J. G. M. (2014). Secondary metabolism and biotrophic lifestyle in the tomato pathogen *Cladosporium fulvum*. *PLoS One, 9*(1) 10.1371/journal.pone.0085877

Cook, D. E., Mesarich, C. H., & Thomma, B. P. H. J. (2015). Understanding plant immunity as a surveillance system to detect invasion. *Annual Review of Phytopathology, 53*(1), 541-563.

Cooke, I. R., Jones, D., Bowen, J. K., Deng, C., Faou, P., Hall, N. E., . . . Mathivanan, S. (2014). Proteogenomic analysis of the *Venturia pirina* (pear scab fungus) secretome reveals potential effectors. *Journal of Proteome Research, 13*(8), 3635-3644. 10.1021/pr500176c

Cooke, M. C. (1883). New american fungi. *Grevillea, 12*(61)

Darwiche, R., Mene-Saffrane, L., Gfeller, D., Asojo, O. A., & Schneiter, R. (2017). The pathogen-related yeast protein Pry1, a member of the CAP protein superfamily, is a fatty acid-binding protein. *The Journal of Biological Chemistry, 292*, 8304-8314. 10.1074/jbc.M117.781880

de Jonge, R., van Esse, H. P., Kombrink, A., Shinya, T., Desaki, Y., Bours, R., . . . Thomma, B. P. H. J. (2010). Conserved fungal LysM effector Ecp6 prevents chitin-triggered immunity in plants. *Science, 329*(5994), 953-955.

de la Rosa, S. (2022). *Identification of novel avirulence effectors in the Dothideomycete plant pathogens, Venturia inaequalis and Cladosporium fulvum.* (Doctor of Philosophy (PhD) in Plant Sciences), Massey University, Retrieved from http://hdl.handle.net/10179/17700

de Wit, P. J. G. M. (1977). A light and scanning-electron microscopic study of infection of tomato plants by virulent and avirulent races of *Cladosporium fulvum*. *Netherlands Journal of Plant Pathology, 83*(3), 109-122. 10.1007/BF01981556

de Wit, P. J. G. M. (1992). Molecular characterization of gene-for-gene systems in plant-fungus interactions and the application of avirulence genes in control of plant pathogens. *Annual Review of Phytopathology, 30*, 391-418.

de Wit, P. J. G. M. (2016). *Cladosporium fulvum* effectors: Weapons in the arms race with tomato. *The Annual Review of Phytopathology, 54*, 1-23. 10.1146/annurev-phyto-011516-040249

de Wit, P. J. G. M., Buurlage, M. B., & Hammond, K. E. (1986). The occurrence of host-, pathogen- and interaction-specific proteins in the apoplast of *Cladosporium fulvum* (syn. *Fulvia fulva*) infected tomato leaves. *Physiological and Molecular Plant Pathology, 29*(2), 159-172. 10.1016/S0048-4059(86)80018-2

de Wit, P. J. G. M., van der Burgt, A., Okmen, B., Stergiopoulos, I., Abd-Elsalam, K. A., Aerts, A. L., . . . Bradshaw, R. E. (2012). The genomes of the fungal plant pathogens *Cladosporium fulvum* and *Dothistroma septosporum* reveal adaptation to different hosts and lifestyles but also signatures of common ancestry. *PLOS Genetics, 8*(11) 10.1371/journal.pgen.1003088

Deveau, H., Barrangou, R., Garneau Josiane, E., Labonté, J., Fremaux, C., Boyaval, P., . . . Moineau, S. (2008). Phage response to CRISPR-encoded resistance in *Streptococcus thermophilus*. *The Journal of Bacteriology, 190*(4), 1390-1400. 10.1128/JB.01412-07

Dhar, J., & Chakrabarti, P. (2015). Defining the loop structures in proteins based on composite beta-turn mimics. *Protein Engineering Design & Selection, 28*(6), 153-161. 10.1093/protein/gzv017

Dixon, M. S., Golstein, C., Thomas, C. M., Van Der Biezen, E. A., & Jones, J. D. G. (2000). Genetic complexity of pathogen perception by plants: The example of *Rcr3*, a tomato gene required specifically by *Cf-2*. *Proceedings of the National Academy of Sciences of the United States of America, 97*(16), 8807-8814. 10.1073/pnas.97.16.8807

Dixon, M. S., Hatzixanthis, K., Jones, D. A., Harrison, K., & Jones, J. D. (1998). The tomato *Cf-5* disease resistance gene and six homologs show pronounced allelic variation in leucine-rich repeat copy number. *Plant Cell, 10*(11), 1915-1925. 10.1105/tpc.10.11.1915

Dixon, M. S., Jones, D. A., Keddie, J. S., Thomas, C. M., Harrison, K., & Jones, J. D. G. (1996). The tomato *Cf-2* disease resistance locus comprises two functional genes encoding leucine-rich repeat proteins. *Cell, 84*(3), 451-459. 10.1016/S0092-8674(00)81290-8

Doench, J. G., Fusi, N., Sullender, M., Hegde, M., Vaimberg, E. W., Donovan, K. F., . . . Root, D. E. (2016). Optimized sgRNA design to maximize activity and minimize off-target effects of CRISPR-Cas9. *Nature Biotechnology, 34*(2), 184-191. 10.1038/nbt.3437

Doench, J. G., Hartenian, E., Graham, D. B., Tothova, Z., Hegde, M., Smith, I., . . . Root, D. E. (2014). Rational design of highly active sgRNAs for CRISPR-Cas9-mediated gene inactivation. *Nature Biotechnology, 32*(12), 1262-1267. 10.1038/nbt.3026

Dort, E. N., Tanguay, P., & Hamelin, R. C. (2020). CRISPR/Cas9 gene editing: an unexplored frontier for forest pathology. *Frontiers in Plant Science, 11*, 1126. 10.3389/fpls.2020.01126

Doyle, J. J., & Doyle, J. L. (1987). A rapid DNA isolation procedure for small quantities of fresh leaf tissue. *Phytochemical Bullettin, 19*, 11-15.

Drenkhan, R., Tomešová-Haataja, V., Fraser, S., Bradshaw, R. E., Vahalík, P., Mullett, M. S., . . . Barnes, I. (2016). Global geographic distribution and host range of *Dothistroma* species: a comprehensive review. *Forest Pathology, 46*(5), 408-442. 10.1111/efp.12290

Dufresne, M., Perfect, S., Pellier, A., Bailey, J. A., & Langin, T. (2000). A GAL4-Like protein is involved in the switch between biotrophic and necrotrophic phases of the infection process of *Colletotrichum lindemuthianum* on common bean. *The Plant Cell, 12*(9), 1579. 10.2307/3871175

Eisenhaber, B., Schneider, G., Wildpaner, M., & Eisenhaber, F. (2004). A sensitive predictor for potential GPI lipid modification sites in fungal protein sequences and its application to genome-wide studies for *Aspergillus nidulans*, *Candida albicans*, *Neurospora crassa*, *Saccharomyces cerevisiae* and *Schizosaccharomyces pombe*. *Journal of Molecular Biology, 337*(2), 243-253. 10.1016/j.jmb.2004.01.025

El-Gebali, S., Mistry, J., Bateman, A., Eddy, S. R., Luciani, A., Potter, S. C., . . . Finn, R. D. (2018). The Pfam protein families database in 2019. *Nucleic Acids Research, 47*(D1), D427-D432. 10.1093/nar/gky995

El-Sayed, A. S. A., Abdel-Ghany, S. E., & Ali, G. S. (2017). Genome editing approaches: manipulating of lovastatin and taxol synthesis of filamentous fungi by CRISPR/Cas9 system. *Applied Microbiology and Biotechnology, 101*(10), 3953-3976. 10.1007/s00253-017-8263-z

Eranthodi, A., González-Peña Fundora, D., Montenegro Alonso, A. P., Bakkeren, G., Subramaniam, R., Ouellet, T., . . . Foroud, N. A. (2022). Cerato-platanin protein 1 is not critical for *Fusarium graminearum* growth and aggressiveness, but its overexpression provides an edge to Fusarium head blight in wheat. *Canadian Journal of Plant Pathology, 44*(4), 577-595. 10.1080/07060661.2022.2044910

Felix, G., & Boller, T. (2003). Molecular sensing of bacteria in plants: The highly conserved RNA-binding motif RNP-1 of bacterial cold shock proteins is recognized as an elicitor signal in tobacco. *Journal of Biological Chemistry, 278*(8), 6201-6208. https://doi.org/10.1074/jbc.M209880200

Felix, G., Duran, J. D., Volko, S., & Boller, T. (1999). Plants have a sensitive perception system for the most conserved domain of bacterial flagellin. *The Plant Journal, 18*(3), 265-276.

Fernando, U., Chatur, S., Joshi, M., Thomas Bonner, C., Fan, T., Hubbard, K., . . . Rampitsch, C. (2019). Redox signalling from NADPH oxidase targets metabolic enzymes and developmental proteins in *Fusarium graminearum*. *Molecular Plant Pathology, 20*(1), 92-106. https://doi.org/10.1111/mpp.12742

Finn, R. D., Attwood, T. K., Babbitt, P. C., Bateman, A., Bork, P., Bridge, A. J., . . . Mitchell, A. L. (2017). InterPro in 2017-beyond protein family and domain annotations. *Nucleic Acids Research, 45*(D1), D190-d199. 10.1093/nar/gkw1107

Flor, H. (1942). Inheritance of pathogenicity in *Melampsora lini*. *Phytopathology, 32*, 653-669.

Foster, A. J., Martin-Urdiroz, M., Yan, X., Wright, H. S., Soanes, D. M., & Talbot, N. J. (2018). CRISPR-Cas9 ribonucleoprotein-mediated co-editing and counterselection in the rice blast fungus. *Scientific Reports, 8*(1), 14355. 10.1038/s41598-018-32702-w

Franco-Orozco, B., Berepiki, A., Ruiz, O., Gamble, L., Griffe, L. L., Wang, S., . . . Avrova, A. (2017). A new proteinaceous pathogen-associated molecular pattern (PAMP) identified in Ascomycete fungi induces cell death in Solanaceae. *New Phytologist, 214*(4), 1657-1672. 10.1111/nph.14542

Friesen, T. L., & Faris, J. D. (2021). Characterization of effector-target interactions in necrotrophic pathosystems reveals trends and variation in host manipulation. *Annual Review of Phytopathology, 59*, 77-98. 10.1146/annurev-phyto-120320-012807

Fuller, K. K., Chen, S., Loros, J. J., & Dunlap, J. C. (2015). Development of the CRISPR/Cas9 system for targeted gene disruption in *Aspergillus fumigatus*. *Eukaryotic Cell, 14*(11), 1073-1080. 10.1128/EC.00107-15

Gamir, J., Darwiche, R., Van't Hof, P., Choudhary, V., Stumpe, M., Schneiter, R., & Mauch, F. (2017). The sterol-binding activity of PATHOGENESIS-RELATED PROTEIN 1 reveals the mode of action of an antimicrobial protein. *The Plant Journal, 89*(3), 502-509. 10.1111/tpj.13398

Gasiunas, G., Barrangou, R., Horvath, P., & Siksnys, V. (2012). Cas9–crRNA ribonucleoprotein complex mediates specific DNA cleavage for adaptive immunity in bacteria. *Proceedings of the National Academy of Sciences of the United States of America, 109*(39), E2579. 10.1073/pnas.1208507109

Ghanbarnia, K., Ma, L., Larkan, N. J., Haddadi, P., Borhan, M. H., & Fernando, W. G. D. (2018). *Leptosphaeria maculans* AvrLm9: a new player in the game of hide and seek with AvrLm4-7. *Molecular Plant Pathology, 19*(7), 1754-1764. 10.1111/mpp.12658

Gibson, D. G., Young, L., Chuang, R. Y., Venter, J. C., Hutchison, C. A., 3rd, & Smith, H. O. (2009). Enzymatic assembly of DNA molecules up to several hundred kilobases. *Nature Methods, 6*(5), 343-345. 10.1038/nmeth.1318

Gibson, I. A. S. (1972). Dothistroma blight of *Pinus radiata*. *The Annual Review of Phytopathology, 10*, 51-72.

Gibson, I. A. S. (1974). Impact and control of dothistroma blight of pines. *European Journal of Forest Pathology, 4*(2), 89-100. 10.1111/j.1439-0329.1974.tb00423.x

Girard, V., Dieryckx, C., Job, C., & Job, D. (2013). Secretomes: the fungal strike force. *PROTEOMICS, 13*(3-4), 597-608. 10.1002/pmic.201200282

Gold, S. E., Paz, Z., Garcia-Pedrajas, M. D., & Glenn, A. E. (2017). Rapid deletion production in fungi via *Agrobacterium* mediated transformation of OSCAR deletion constructs. *Journal of Visualized Experiments*(124) 10.3791/55239

Gómez-Pérez, D., Schmid, M., Chaudhry, V., Velic, A., Maček, B., Kemen, A., & Kemen, E. (2022). Proteins released into the plant apoplast by the obligate parasitic protist *Albugo* selectively repress phyllosphere-associated bacteria. *bioRxiv*, 2022.2005.2016.492175. 10.1101/2022.05.16.492175

González-Fernández, R., Valero-Galván, J., Gómez-Gálvez, F. J., & Jorrín-Novo, J. V. (2015). Unraveling the *in vitro* secretome of the phytopathogen *Botrytis cinerea* to understand the interaction with its hosts. *Frontiers in Plant Science, 6*(839) 10.3389/fpls.2015.00839

Gosavi, G., Yan, F., Ren, B., Kuang, Y., Yan, D., Zhou, X., & Zhou, H. (2020). Applications of CRISPR technology in studying plant-pathogen interactions: overview and perspective. *Phytopathology Research, 2*(1), 21. 10.1186/s42483-020-00060-z

Greenbaum, D., Luscombe, N. M., Jansen, R., Qian, J., & Gerstein, M. (2001). Interrelating different types of genomic data, from proteome to secretome: 'oming in on function. *Genome Research, 11*(9), 1463-1468. 10.1101/gr.207401

Griffiths, S., Mesarich, C. H., Saccomanno, B., Vaisberg, A., De Wit, P. J. G. M., Cox, R., & Collemare, J. (2016). Elucidation of cladofulvin biosynthesis reveals a cytochrome P450 monooxygenase required for anthraquinone dimerization. *Proceedings of the National Academy of Sciences, 113*(25), 6851-6856. 10.1073/pnas.1603528113

Groenewald, M., Barnes, I., Bradshaw, R. E., Brown, A. V., Dale, A., Groenewald, J. Z., . . . Crous, P. W. (2007). Characterization and distribution of mating type genes in the Dothistroma needle blight pathogens. *Phytopathology, 97*(7), 825-834. 10.1094/PHYTO-97-7-0825

Guo, X. Y., Li, Y., Fan, J., Xiong, H., Xu, F. X., Shi, J., . . . Wang, W. M. (2019). Host-induced gene silencing of *MoAP1* confers broad-spectrum resistance to *Magnaporthe oryzae*. *Frontiers in Plant Science, 10*, 433. 10.3389/fpls.2019.00433

Guo, Y. (2015). *Identification and characterization of Dothistroma septosporum effectors.* (Doctor of Philosophy (PhD) in Genetics), Massey University, Retrieved from http://hdl.handle.net/10179/7392

Guo, Y., Dupont, P. Y., Mesarich, C. H., Yang, B., McDougal, R. L., Panda, P., . . . Bradshaw, R. E. (2020). Functional analysis of RXLR effectors from the New Zealand kauri dieback pathogen *Phytophthora agathidicida*. *Molecular Plant Pathology, 21*(9), 1131-1148. 10.1111/mpp.12967

Guo, Y., Hunziker, L., Mesarich, C. H., Chettri, P., Dupont, P.-Y., Ganley, R. J., . . . Bradshaw, R. E. (2020). DsEcp2-1 is a polymorphic effector that restricts growth of *Dothistroma septosporum* in pine. *Fungal Genetics and Biology, 135*(103300), 103300. 10.1016/j.fgb.2019.103300

Gust, A. A., Pruitt, R., & Nürnberger, T. (2017). Sensing danger: Key to activating plant immunity. *Trends in Plant Science, 22*(9), 779-791. https://doi.org/10.1016/j.tplants.2017.07.005

Habig, M., Bahena-Garrido, S. M., Barkmann, F., Haueisen, J., & Stukenbrock, E. H. (2020). The transcription factor Zt107320 affects the dimorphic switch, growth and virulence of the fungal wheat pathogen *Zymoseptoria tritici*. *Molecular Plant Pathology, 21*(1), 124-138. 10.1111/mpp.12886

Hammond-Kosack, K. E., Harrison, K., & Jones, J. D. (1994). Developmentally regulated cell death on expression of the fungal avirulence gene *Avr9* in tomato seedlings carrying the disease-resistance gene *Cf-9*. *Proceedings of the National Academy of Sciences of the United States of America, 91*(22), 10445-10449. 10.1073/pnas.91.22.10445

Hammond-Kosack, K. E., Staskawicz, B. J., Jones, J. D., & Baulcombe, D. C. (1995). Functional expression of a fungal avirulence gene from a modified potato virus X genome. *Molecular Plant-Microbe Interactions, 8*(1), 181-185. 10.1094/MPMI-8-0181

Hammond, D., & Bulman, L. (2022). *The achievements of Dothistroma management in New Zealand.* Scion. Retrieved from https://www.scionresearch.com/?a=85433

Hane, J. K., Paxman, J., Jones, D. A. B., Oliver, R. P., & de Wit, P. (2019). "CATAStrophy," a genome-informed trophic classification of filamentous plant pathogens - how many different types of filamentous plant pathogens are there? *Frontiers in Microbiology, 10*(3088) 10.3389/fmicb.2019.03088

Hargreaves, C., Grace, L., Maas, S. v. d., Reeves, C., Holden, G., Menzies, M., . . . Foggo, M. (2004). Cryopreservation of *Pinus radiata* zygotic embryo cotyledons: effect of storage duration on adventitious shoot formation and plant growth after 2 years in the field. *Canadian Journal of Forest Research, 34*(3), 600-608. 10.1139/x03-226

Haridas, S., Albert, R., Binder, M., Bloem, J., LaButti, K., Salamov, A., . . . Grigoriev, I. V. (2020). 101 Dothideomycetes genomes: A test case for predicting lifestyles and emergence of pathogens. *Studies in Mycology, 96*, 141-153. 10.1016/j.simyco.2020.01.003

Harling, R., Kenyon, L., Lewis, B. G., Oliver, R. P., Turner, J. G., & Coddington, A. (1988). Conditions for efficient isolation and regeneration of protoplasts from *Fulvia fulva*. *Journal of Phytopathology, 122*(2), 143-146. https://doi.org/10.1111/j.1439-0434.1988.tb01001.x

He, Y., Zhou, X., Li, J., Li, H., Li, Y., & Nie, Y. (2021). *In vitro* secretome analysis suggests differential pathogenic mechanisms between *Fusarium oxysporum* f. sp. *cubense* Race 1 and Race 4. *Biomolecules, 11*(9) 10.3390/biom11091353

Heese, A., Hann, D. R., Gimenez-Ibanez, S., Jones, A. M. E., He, K., Li, J., . . . Rathjen, J. P. (2007). The receptor-like kinase SERK3/BAK1 is a central regulator of innate immunity in plants. *Proceedings of the National Academy of Sciences, 104*(29), 12217-12222. 10.1073/pnas.0705306104

Hellens, R., Mullineaux, P., & Klee, H. (2000). Technical Focus: a guide to *Agrobacterium* binary Ti vectors. *Trends in Plant Science, 5*(10), 446-451. 10.1016/S1360-1385(00)01740-4

Hirst, P., Richardson, T. E., Carson, S. D., & Bradshaw, R. E. (1999). *Dothistroma pini* genetic diversity is low in New Zealand. *New Zealand Journal of Forestry Science, 29*, 459-472.

Hsu, P. D., Scott, D. A., Weinstein, J. A., Ran, F. A., Konermann, S., Agarwala, V., . . . Zhang, F. (2013). DNA targeting specificity of RNA-guided Cas9 nucleases. *Nature Biotechnology, 31*(9), 827-832. 10.1038/nbt.2647

Hu, X., Wang, H., Ke, H., & Kuhlman, B. (2007). High-resolution design of a protein loop. *Proceedings of the National Academy of Sciences, 104*(45), 17668-17673. 10.1073/pnas.0707977104

Huang, W. R. H., Schol, C., Villanueva, S. L., Heidstra, R., & Joosten, M. (2021). Knocking out *SOBIR1* in *Nicotiana benthamiana* abolishes functionality of transgenic receptor-like protein Cf-4. *Plant Physiology, 185*(2), 290-294. 10.1093/plphys/kiaa047

Hudson, O., Buchholz, M., Doyle, V., & Sundue, M. A. (2019). Multilocus phylogeny of *Acrospermaceae*: New epibiotic species and placement of *Gonatophragmium, Pseudovirgaria*, and *Phaeodactylium* anamorphs. *Mycologia, 111*(6), 1041-1055. 10.1080/00275514.2019.1668905

Hunziker, L. (2018). *Effector delivery and effector characterisation in Dothistroma needle blight of pines.* (Doctor of Philosophy (Sciences) in Genetics/Molecular Plant Pathology), Massey University, Retrieved from http://hdl.handle.net/10179/14900

Hunziker, L., Tarallo, M., Gough, K., Guo, M., Hargreaves, C., Loo, T. S., . . . Bradshaw, R. E. (2021). Apoplastic effector candidates of a foliar forest pathogen trigger cell death in host and non-host plants. *Scientific Reports, 11*(1), 19958. 10.1038/s41598-021-99415-5

Hurlburt, N. K., Chen, L. H., Stergiopoulos, I., & Fisher, A. J. (2018). Structure of the *Cladosporium fulvum* Avr4 effector in complex with $(GlcNAc)_6$ reveals the ligand-binding mechanism and uncouples its intrinsic function from recognition by the Cf-4 resistance protein. *PLoS Pathogens, 14*(8) 10.1371/journal.ppat.1007263

Ibraheim, R., Tai, P. W. L., Mir, A., Javeed, N., Wang, J., Rodríguez, T. C., . . . Sontheimer, E. J. (2021). Self-inactivating, all-in-one AAV vectors for precision Cas9 genome editing via homology-directed repair *in vivo*. *Nature Communications, 12*(1), 6267. 10.1038/s41467-021-26518-y

Idnurm, A., Urquhart, A. S., Vummadi, D. R., Chang, S., Van de Wouw, A. P., & López-ruiz, F. J. (2017). Spontaneous and CRISPR/Cas9-induced mutation of the osmosensor histidine kinase of the canola pathogen *Leptosphaeria maculans*. *Fungal Biology and Biotechnology, 4*(1), 1-12. 10.1186/s40694-017-0043-0

Iida, Y., van 't Hof, P., Beenen, H., Mesarich, C., Kubota, M., Stergiopoulos, I., . . . de Wit, P. J. (2015). Novel mutations detected in avirulence genes overcoming tomato *Cf* resistance genes in isolates of a Japanese population of *Cladosporium fulvum*. *PLoS One, 10*(4), e0123271. 10.1371/journal.pone.0123271

Irieda, H., Inoue, Y., Mori, M., Yamada, K., Oshikawa, Y., Saitoh, H., . . . Takano, Y. (2019). Conserved fungal effector suppresses PAMP-triggered immunity by targeting plant immune kinases. *Proceedings of the National Academy of Sciences, 116*(2), 496-505. 10.1073/pnas.1807297116

Jashni, M. K., Mehrabi, R., Collemare, J., Mesarich, C. H., & de Wit, P. J. G. M. (2015). The battle in the apoplast: further insights into the roles of proteases and their inhibitors in plant–pathogen interactions. *Frontiers in Plant Science, 6*(584) 10.3389/fpls.2015.00584

Jenkins, J. A. (1948). The origin of the cultivated tomato. *Economic Botany, 2*(4), 379-392.

Jinek, M., Chylinski, K., Fonfara, I., Hauer, M., Doudna, J. A., & Charpentier, E. (2012). A programmable dual-RNA-guided DNA endonuclease in adaptive bacterial immunity. *Science, 337*(6096), 816-821. 10.1126/science.1225829

John, E., Singh, K. B., Oliver, R. P., & Tan, K. C. (2021). Transcription factor control of virulence in phytopathogenic fungi. *Molecular Plant Pathology, 22*(7), 858-881. 10.1111/mpp.13056

Jones, D. A., Thomas, C. M., Hammond-Kosack, K. E., Balint-Kurti, P. J., & Jones, J. D. G. (1994). Isolation of the tomato *Cf-9* gene for resistance to *Cladosporium fulvum* by transposon tagging. *Science, 266*(5186), 789-793. 10.1126/science.7973631

Jones, D. A. B., John, E., Rybak, K., Phan, H. T. T., Singh, K. B., Lin, S., . . . Tan, K. (2019). A specific fungal transcription factor controls effector gene expression and orchestrates the establishment of the necrotrophic pathogen lifestyle on wheat. *Scientific Reports, 9*(1) 10.1038/s41598-019-52444-7

Jones, J. B., Jones, J. P., Stall, R. E., & Zitter, T. A. (1997). *Compendium of tomato diseases*: St. Paul, MN: APS Press.

Jones, J. D. G., & Dangl, J. L. (2006). The plant immune system. *Nature, 444*(7117), 323-329. 10.1038/nature05286

Joosten, M. H. A. J., Cozijnsen, A. J., & De Wit, P. J. G. M. (1994). Host resistance to a fungal tomato pathogen lost by a single base-pair change in an avirulence gene. *Nature, 367*, 384-387.

Joosten, M. H. A. J., & De Wit, P. J. G. M. (1999). The tomato-*Cladosporium fulvum* interaction: A versatile experimental system to study plant-pathogen interactions. *Annual Review of Phytopathology, 37*, 335-367. 10.1146/annurev.phyto.37.1.335

Joosten, M. H. A. J., Hendrickx, L. J. M., & De Wit, P. J. G. M. (1990). Carbohydrate composition of apoplastic fluids isolated from tomato leaves inoculated with virulent or avirulent races of *Cladosporium fulvum* (syn. *Fulvia fulva*). *Netherlands Journal of Plant Pathology, 96*(2), 103-112. 10.1007/bf02005134

Juillot, S., Cott, C., Madl, J., Claudinon, J., van der Velden, N. S. J., Künzler, M., . . . Römer, W. (2016). Uptake of *Marasmius oreades* agglutinin disrupts integrin-dependent cell adhesion. *Biochimica et Biophysica Acta, 1860*(2), 392-401. https://doi.org/10.1016/j.bbagen.2015.11.002

Kabir, M. S., Ganley, R. J., & Bradshaw, R. E. (2013). An improved artificial pathogenicity assay for Dothistroma needle blight on *Pinus radiata*. *Australasian Plant Pathology, 42*(4), 503-510. 10.1007/s13313-013-0217-z

Kabir, M. S., Ganley, R. J., & Bradshaw, R. E. (2015a). Dothistromin toxin is a virulence factor in dothistroma needle blight of pines. *Plant Pathology*(1), 225-234. 10.1111/ppa.12229

Kabir, M. S., Ganley, R. J., & Bradshaw, R. E. (2015b). The hemibiotrophic lifestyle of the fungal pine pathogen *Dothistroma septosporum*. *Forest Pathology, 45*(3), 190-202. 10.1111/efp.12153

Kamoun, S. (2006). A catalogue of the effector secretome of plant pathogenic oomycetes. *Annual Review of Phytopathology, 44*, 41-60. 10.1146/annurev.phyto.44.070505.143436

Kanja, C., & Hammond-Kosack, K. E. (2020). Proteinaceous effector discovery and characterization in filamentous plant pathogens. *Molecular Plant Pathology, 21*(10), 1353-1376. https://doi.org/10.1111/mpp.12980

Kanyuka, K., & Rudd, J. J. (2019). Cell surface immune receptors: the guardians of the plant's extracellular spaces. *Current Opinion in Plant Biology, 50*, 1-8. 10.1016/j.pbi.2019.02.005

Karimi-Jashni, M., Maeda, K., Yazdanpanah, F., de Wit, P. J. G. M., & Iida, Y. (2022). An integrated omics approach uncovers the novel effector Ecp20-2 required for full virulence of *Cladosporium fulvum* on tomato. *Frontiers in Microbiology, 13*(919809) 10.3389/fmicb.2022.919809

Kariyawasam, G. K., Richards, J. K., Wyatt, N. A., Running, K. L. D., Xu, S. S., Liu, Z., . . . Friesen, T. L. (2021). The *Parastagonospora nodorum* necrotrophic effector SnTox5 targets the

wheat gene *Snn5* and facilitates entry into the leaf mesophyll. *New Phytologist, 1*, 409-426. https://doi.org/10.1111/nph.17602

Kettles, G. J., Bayon, C., Sparks, C. A., Canning, G., Kanyuka, K., & Rudd, J. J. (2018). Characterization of an antimicrobial and phytotoxic ribonuclease secreted by the fungal wheat pathogen *Zymoseptoria tritici*. *New Phytologist, 217*(1), 320-331. 10.1111/nph.14786

Kettles, G. J., & Kanyuka, K. (2016). Dissecting the molecular interactions between wheat and the fungal pathogen *Zymoseptoria tritici*. *Frontiers in Plant Science, 7*(508) 10.3389/fpls.2016.00508

Khan, H., McDonald, M. C., Williams, S. J., & Solomon, P. S. (2020). Assessing the efficacy of CRISPR/Cas9 genome editing in the wheat pathogen *Parastagonspora nodorum*. *Fungal Biology and Biotechnology, 7*(4) 10.1186/s40694-020-00094-0

Kim, H., & Kim, J.-S. (2014). A guide to genome engineering with programmable nucleases. *Nature Reviews Genetics, 15*(5), 321-334. 10.1038/nrg3686

King, R., Urban, M., Lauder, R. P., Hawkins, N., Evans, M., Plummer, A., . . . Rudd, J. J. (2017). A conserved fungal glycosyltransferase facilitates pathogenesis of plants by enabling hyphal growth on solid surfaces. *PLoS Pathogens, 13*(10), e1006672. 10.1371/journal.ppat.1006672

Kodama, S., Nishiuchi, T., & Kubo, Y. (2019). *Colletotrichum orbiculare MTF4* is a key transcription factor downstream of *MOR* essential for plant signal-dependent appressorium development and pathogenesis. *Molecular Plant-Microbe Interactions, 32*(3), 313-324. 10.1094/mpmi-05-18-0118-r

Koncz, C., & Schell, J. S. (1986). The promoter of T_L-DNA gene *5* controls the tissue-specific expression of chimaeric genes carried by a novel type of *Agrobacterium* binary vector. *Molecular Genetics and Genomics, 204*, 383-396.

Kondratev, N., Middleditch, M. J., Denton-Giles, M., Bradshaw, R. E., Cox, M. P., & Dijkwel, P. P. (2022). The secreted proteome of necrotrophic *Ciborinia camelliae* causes nonhost-specific virulence. *Plant Pathology, 71*(2), 437-445. https://doi.org/10.1111/ppa.13477

Konstantakos, V., Nentidis, A., Krithara, A., & Paliouras, G. (2022). CRISPR–Cas9 gRNA efficiency prediction: an overview of predictive tools and the role of deep learning. *Nucleic Acids Research, 50*(7), 3616-3637. 10.1093/nar/gkac192

Kooman-Gersmann, M., Honee, G., Bonnema, G., & De Wit, P. (1996). A high-affinity binding site for the AVR9 peptide elicitor of *Cladosporium fulvum* is present on plasma membranes of tomato and other Solanaceous plants. *Plant Cell, 8*(5), 929-938. 10.1105/tpc.8.5.929

Kourelis, J., Malik, S., Mattinson, O., Krauter, S., Kahlon, P. S., Paulus, J. K., & van der Hoorn, R. A. L. (2020). Evolution of a guarded decoy protease and its receptor in solanaceous plants. *Nature Communications, 11*(1) 10.1038/s41467-020-18069-5

Krogh, A., Larsson, B., von Heijne, G., & Sonnhammer, E. L. (2001). Predicting transmembrane protein topology with a hidden Markov model: application to complete genomes. *Journal of Molecular Biology, 305*(3), 567-580. 10.1006/jmbi.2000.4315

Krüger, J., Thomas, C. M., Golstein, C., Dixon, M. S., Smoker, M., Tang, S., . . . Jones, J. D. G. (2002). A tomato cysteine protease required for Cf-2-dependent disease resistance and suppression of autonecrosis. *Science, 296*(5568), 744-747. 10.1126/science.1069288

Kuscu, C., Arslan, S., Singh, R., Thorpe, J., & Adli, M. (2014). Genome-wide analysis reveals characteristics of off-target sites bound by the Cas9 endonuclease. *Nature Biotechnology, 32*(7), 677-683. 10.1038/nbt.2916

Lara-Ortíz, T., Riveros-Rosas, H., & Aguirre, J. (2003). Reactive oxygen species generated by microbial NADPH oxidase NoxA regulate sexual development in *Aspergillus nidulans*. *Molecular Microbiology, 50*(4), 1241-1255. 10.1046/j.1365-2958.2003.03800.x

Laugé, R., Goodwin, P. H., De Wit, P. J. G. M., & Joosten, M. H. A. J. (2000). Specific HR-associated recognition of secreted proteins from *Cladosporium fulvum* occurs in both host and non-host plants. *The Plant Journal, 23*(6), 735-745. https://doi.org/10.1046/j.1365-313x.2000.00843.x

Laugé, R., Joosten, M. H. A. J., Van den Ackerveken, G. F. J. M., Van den Broek, H. W. J., & De Wit, P. J. G. M. (1997). The *in planta*-produced extracellular proteins ECP1 and ECP2 of *Cladosporium fulvum* are virulence factors. *Molecular Plant-Microbe Interactions, 10*(6), 725-734. 10.1094/MPMI.1997.10.6.725

Lawrence, M., Daujat, S., & Schneider, R. (2016). Lateral thinking: How histone modifications regulate gene expression. *Trends in Genetics, 32*(1), 42-56. 10.1016/j.tig.2015.10.007

Lax, C., Tahiri, G., Patiño-Medina, J. A., Cánovas-Márquez, J. T., Pérez-Ruiz, J. A., Osorio-Concepción, M., . . . Calo, S. (2020). The evolutionary significance of RNAi in the fungal kingdom. *The International Journal of Molecular Sciences, 21*(24) 10.3390/ijms21249348

Lazar, N., Mesarich, C. H., Petit-Houdenot, Y., Talbi, N., Li de la Sierra-Gallay, I., Zélie, E., . . . Fudal, I. (2022). A new family of structurally conserved fungal effectors displays epistatic interactions with plant resistance proteins. *PLoS Pathogens, 18*(7), e1010664. 10.1371/journal.ppat.1010664

Lazo, G. R., Stein, P. A., & Ludwig, R. A. (1991). A DNA transformation-competent *Arabidopsis* genomic library in *Agrobacterium*. *Biotechnology, 9*(10), 963-967. 10.1038/nbt1091-963

Lewis, D. H., & Smith, D. C. (1967). Sugar alcohols (polyols) in fungi and green plants. II. Methods of detection and quantitative estimation in plant extracts. *The New Phytologist, 66*(2), 185-204.

Li, A., Lee, C. M., Hurley, A. E., Jarrett, K. E., De Giorgi, M., Lu, W., . . . Lagor, W. R. (2019). A self-deleting AAV-CRISPR system for *in vivo* genome editing. *Molecular Therapy – Methods & Clinical Development, 12*, 111-122. 10.1016/j.omtm.2018.11.009

Li, J., Zhang, Y., Zhang, Y., Yu, P.-L., Pan, H., Rollins Jeffrey, A., & Vidaver Anne, K. (2018). Introduction of large sequence inserts by CRISPR-Cas9 to create pathogenicity mutants in the multinucleate filamentous pathogen *Sclerotinia sclerotiorum*. *Mbio., 9*(3), e00567-00518. 10.1128/mBio.00567-18

Li, L., Chang, S. S., & Liu, Y. (2010). RNA interference pathways in filamentous fungi. *Cellular and Molecular Life Sciences, 67*(22), 3849-3863. 10.1007/s00018-010-0471-y

Li, S., Dong, Y., Li, L., Zhang, Y., Yang, X., Zeng, H., . . . Yuan, Q. (2019). The novel cerato-platanin-like protein FocCP1 from *Fusarium oxysporum* triggers an immune response in plants. *The International Journal of Molecular Sciences, 20*(11) 10.3390/ijms20112849

Liebrand, T. W. H., van den Berg, G. C. M., Zhang, Z., Smit, P., Cordewener, J. H. G., America, A. H. P., . . . Joosten, M. H. A. J. (2013). Receptor-like kinase SOBIR1/EVR interacts with receptor-like proteins in plant immunity against fungal infection. *Proceedings of the National Academy of Sciences, 110*(24), 10010-10015. 10.1073/pnas.1220015110

Lindhout, P., Korta, W., Cislik, M., Vos, I., & Gerlagh, T. (1989). Further identification of races of *Cladosporium fulvum* (*Fulvia fulva*) on tomato originating from the Netherlands France and Poland. *Netherlands Journal of Plant Pathology, 95*(3), 143-148. 10.1007/BF01999969

Liu, B., Stevens-Green, R., Johal, D., Buchanan, R., & Geddes-McAlister, J. (2022). Fungal pathogens of cereal crops: Proteomic insights into fungal pathogenesis, host defense, and resistance. *The Journal of Plant Physiology, 269*(153593) 10.1016/j.jplph.2021.153593

Liu, D., Coloe, S., Baird, R., & Pederson, J. (2000). Rapid mini-preparation of fungal DNA for PCR. *The Journal of Clinical Microbiology, 38*(1), 471-471. 10.1128/JCM.38.1.471-471.2000

Liu, R., Chen, L., Jiang, Y., Zhou, Z., & Zou, G. (2015). Efficient genome editing in filamentous fungus *Trichoderma reesei* using the CRISPR/Cas9 system. *Cell Discovery, 1*(15007) 10.1038/celldisc.2015.7

Liu, Y., Kong, D., Wu, H.-L., & Ling, H.-Q. (2021). Iron in plant–pathogen interactions. *Journal of Experimental Botany, 72*(6), 2114-2124. 10.1093/jxb/eraa516

Lu, M., Feau, N., Vidakovic, D. O., Ukrainetz, N., Wong, B., Aitken, S. N., . . . Yeaman, S. (2021). Comparative gene expression analysis reveals mechanism of *Pinus contorta* response to the fungal pathogen *Dothistroma septosporum*. *Molecular Plant-Microbe Interactions, 34*(4), 397-409. 10.1094/mpmi-10-20-0282-r

Luderer, R., Rivas, S., Nürnberger, T., Mattei, B., Van den Hooven, H. W., Van der Hoorn, R. A. L., . . . Joosten, M. H. A. J. (2001). No evidence for binding between resistance gene product Cf-9 of tomato and avirulence gene product AVR9 of *Cladosporium fulvum*. *Molecular Plant-Microbe Interactions, 14*(7), 867-876. 10.1094/MPMI.2001.14.7.867

Ma, H., Zhang, B., Gai, Y., Sun, X., Chung, K. R., & Li, H. (2019). Cell-wall-degrading enzymes required for virulence in the host selective toxin-producing necrotroph *Alternaria alternata* of citrus. *Frontiers in Microbiology, 10*(2514) 10.3389/fmicb.2019.02514

Ma, Y., Han, C., Chen, J., Li, H., He, K., Liu, A., & Li, D. (2015). Fungal cellulase is an elicitor but its enzymatic activity is not required for its elicitor activity. *Molecular Plant Pathology, 16*(1), 14-26. 10.1111/mpp.12156

Ma, Z., Huang, Y., Zhang, Z., Liu, X., Xuan, Y., Liu, B., & Gao, Z. (2022). Comparative genomic analysis reveals cellulase plays an important role in the pathogenicity of *Setosphaeria turcica* f. sp. *zeae*. *Frontiers in Microbiology, 13*(925355) 10.3389/fmicb.2022.925355

Marmeisse, R., Van Den Ackerveken, G. F. J. M., Goosen, T., De Wit, P. J. G. M., & Van Den Broek, H. W. J. (1993). Disruption of the avirulence gene *Avr9* in two races of the tomato pathogen *Cladosporium fulvum* causes virulence on tomato genotypes with the complementary resistance gene *Cf9*. *Molecular plant-microbe interactions, 6*, 412-417.

Marshall, R., Kombrink, A., Motteram, J., Loza-Reyes, E., Lucas, J., Hammond-Kosack, K. E., . . . Rudd, J. J. (2011). Analysis of two *in planta* expressed LysM effector homologs from the fungus *Mycosphaerella graminicola* reveals novel functional properties and varying contributions to virulence on wheat. *Plant Physiology, 156*(2), 756-769. 10.1104/pp.111.176347

Matzinger, P. (2002). The danger model: A renewed sense of self. *Science, 296*(5566), 301-305.

McCarthy, H. M., Tarallo, M., Mesarich, C. H., McDougal, R. L., & Bradshaw, R. E. (2022). Targeted gene mutations in the forest pathogen *Dothistroma septosporum* using CRISPR/Cas9. *Plants (Basel), 11*(8) 10.3390/plants11081016

Meinhardt, L. W., Bellato Cde, M., Rincones, J., Azevedo, R. A., Cascardo, J. C., & Pereira, G. A. (2006). *In vitro* production of biotrophic-like cultures of *Crinipellis perniciosa*, the causal agent of witches' broom disease of *Theobroma cacao*. *Current Microbiology, 52*(3), 191-196. 10.1007/s00284-005-0182-z

Melin, P., Schnürer, J., & Wagner, E. G. (2003). Characterization of *phiA*, a gene essential for phialide development in *Aspergillus nidulans*. *Fungal Genetics and Biology, 40*(3), 234-241. 10.1016/s1087-1845(03)00108-7

Mesarich, C. H., Barnes, I., Bradley, E. L., de la Rosa, S., de Wit, P. J. G. M., Guo, Y., . . . Bradshaw, R. E. (2023). Beyond the genomes of *Fulvia fulva* (syn. *Cladosporium fulvum*) and *Dothistroma septosporum*: New insights into how these fungal pathogens interact with their host plants. *Molecular Plant Pathology* https://doi.org/10.1111/mpp.13309. Epub ahead of print. PMID: 36790136.

Mesarich, C. H., Griffiths, S. A., van der Burgt, A., Okmen, B., Beenen, H. G., Etalo, D. W., . . . de Wit, P. J. (2014). Transcriptome sequencing uncovers the *Avr5* avirulence gene of the tomato leaf mold pathogen *Cladosporium fulvum*. *Molecular Plant-Microbe Interactions, 27*(8), 846-857. 10.1094/mpmi-02-14-0050-r

Mesarich, C. H., Stergiopoulos, I., Beenen, H. G., Cordovez, V., Yanan, G. U. O., Jashni, M. K., . . . De Wit, P. J. G. M. (2016). A conserved proline residue in Dothideomycete Avr4 effector proteins is required to trigger a Cf-4-dependent hypersensitive response. *Molecular Plant Pathology, 17*(1), 84-95. 10.1111/mpp.12265

Mesarich, C. H., Ökmen, B., Rovenich, H., Griffiths, S. A., Wang, C., Karimi Jashni, M., . . . de Wit, P. (2018). Specific hypersensitive response-associated recognition of new apoplastic effectors from *Cladosporium fulvum* in wild tomato. *Molecular Plant-Microbe Interactions, 31*(1), 145-162. 10.1094/mpmi-05-17-0114-fi

Mistry, J., Chuguransky, S., Williams, L., Qureshi, M., Salazar, G. A., Sonnhammer, E. L. L., . . . Bateman, A. (2021). Pfam: The protein families database in 2021. *Nucleic Acids Research, 49*(D1), D412-d419. 10.1093/nar/gkaa913

Mojica, F. J., Díez-Villaseñor, C., García-Martínez, J., & Soria, E. (2005). Intervening sequences of regularly spaced prokaryotic repeats derive from foreign genetic elements. *The Journal of Molecular Evolution, 60*(2), 174-182. 10.1007/s00239-004-0046-3

Mosen, A. M. (2022). *Development of RNA silencing as a novel disease control strategy to protect pines from Dothistroma needle blight.* (Master of Science (MSc) in Genetics), Massey University, Retrieved from http://hdl.handle.net/10179/17672 Available from EBSCOhost Massey Research Online database.

Möykkynen, T., Fraser, S., Woodward, S., Brown, A., & Pukkala, T. (2017). Modelling of the spread of *Dothistroma septosporum* in Europe. *Forest Pathology, 47*(3) 10.1111/efp.12332

Nasmith, C. G., Walkowiak, S., Wang, L., Leung, W. W., Gong, Y., Johnston, A., . . . Subramaniam, R. (2011). Tri6 is a global transcription regulator in the phytopathogen *Fusarium graminearum*. *PLoS Pathogens, 7*(9), e1002266. 10.1371/journal.ppat.1002266

Negeri, A., Wang, G. F., Benavente, L., Kibiti, C. M., Chaikam, V., Johal, G., & Balint-Kurti, P. (2013). Characterization of temperature and light effects on the defense response phenotypes associated with the maize *Rp1-D21* autoactive resistance gene. *BMC Plant Biology, 13*(106) 10.1186/1471-2229-13-106

Nie, J., Yin, Z., Li, Z., Wu, Y., & Huang, L. (2019). A small cysteine-rich protein from two kingdoms of microbes is recognized as a novel pathogen-associated molecular pattern. *New Phytologist, 222*(2), 995-1011. 10.1111/nph.15631

Nie, J., Zhou, W., Liu, J., Tan, N., Zhou, J.-M., & Huang, L. (2021). A receptor-like protein from *Nicotiana benthamiana* mediates VmE02 PAMP-triggered immunity. *New Phytologist, 229*(4), 2260-2272. https://doi.org/10.1111/nph.16995

Niño-Sánchez, J., Casado-Del Castillo, V., Tello, V., De Vega-Bartol, J. J., Ramos, B., Sukno, S. A., & Díaz Mínguez, J. M. (2016). The *FTF* gene family regulates virulence and expression of SIX effectors in *Fusarium oxysporum*. *Molecular Plant Pathology, 17*(7), 1124-1139. 10.1111/mpp.12373

Noda, J., Brito, N., & González, C. (2010). The *Botrytis cinerea* xylanase Xyn11A contributes to virulence with its necrotizing activity, not with its catalytic activity. *BMC Plant Biology, 10*(38) 10.1186/1471-2229-10-38

Ohm, R. A., Feau, N., Henrissat, B., Schoch, C. L., Horwitz, B. A., Barry, K. W., . . . Grigoriev, I. V. (2012). Diverse lifestyles and strategies of plant pathogenesis encoded in the genomes of eighteen Dothideomycetes fungi. *PLoS Pathogens, 8*(12), e1003037. 10.1371/journal.ppat.1003037

Ökmen, B., Bachmann, D., & de Wit, P. (2019). A conserved GH17 glycosyl hydrolase from plant pathogenic Dothideomycetes releases a DAMP causing cell death in tomato. *Molecular Plant Pathology, 20*(12), 1710-1721. 10.1111/mpp.12872

Ökmen, B., Etalo, D. W., Joosten, M. H. A. J., Bouwmeester, H. J., de Vos, R. C. H., Collemare, J., & de Wit, P. J. G. M. (2013). Detoxification of α-tomatine by *Cladosporium fulvum* is required for full virulence on tomato. *New Phytologist, 198*(4), 1203.

Oliver, R. P., & Solomon, P. S. (2004). Does the oxidative stress used by plants for defence provide a source of nutrients for pathogenic fungi? *Trends in plant science, 9*(10), 472-473. 10.1016/j.tplants.2004.08.006

Ortiz-Bermúdez, P., Srebotnik, E., & Hammel Kenneth, E. (2003). Chlorination and cleavage of lignin structures by fungal chloroperoxidases. *Applied and Environmental Microbiology, 69*(8), 5015-5018. 10.1128/AEM.69.8.5015-5018.2003

Ozturk, I. K., Chettri, P., Dupont, P. Y., Barnes, I., McDougal, R. L., Moore, G. G., . . . Bradshaw, R. E. (2017). Evolution of polyketide synthesis in a Dothideomycete forest pathogen. *Fungal Genetics and Biology, 106*, 42-50. 10.1016/j.fgb.2017.07.001

Ozturk, I. K., Dupont, P. Y., Chettri, P., McDougal, R., Böhl, O. J., Cox, R. J., & Bradshaw, R. E. (2019). Evolutionary relics dominate the small number of secondary metabolism genes in the hemibiotrophic fungus *Dothistroma septosporum*. *Fungal Biology, 123*(5), 397-407. 10.1016/j.funbio.2019.02.006

Pandaranayaka, E. P., Frenkel, O., Elad, Y., Prusky, D., & Harel, A. (2019). Network analysis exposes core functions in major lifestyles of fungal and oomycete plant pathogens. *BMC Genomics, 20*(1), 1020. 10.1186/s12864-019-6409-3

Paper, J. M., Scott-Craig, J. S., Adhikari, N. D., Cuomo, C. A., & Walton, J. D. (2007). Comparative proteomics of extracellular proteins *in vitro* and *in planta* from the pathogenic fungus *Fusarium graminearum*. *PROTEOMICS, 7*(17), 3171-3183. 10.1002/pmic.200700184

Parniske, M., Hammond-Kosack, K. E., Golstein, C., Thomas, C. M., Jones, D. A., Harrison, K., . . . Jones, J. D. (1997). Novel disease resistance specificities result from sequence exchange between tandemly repeated genes at the *Cf-4/9* locus of tomato. *Cell, 91*(6), 821-832. 10.1016/s0092-8674(00)80470-5

Paz, Z., García-Pedrajas, M. D., Andrews, D. L., Klosterman, S. J., Baeza-Montañez, L., & Gold, S. E. (2011). One step construction of *Agrobacterium*-recombination-ready-plasmids (OSCAR), an efficient and robust tool for ATMT based gene deletion construction in fungi. *Fungal Genetics and Biology, 48*(7), 677-684. 10.1016/j.fgb.2011.02.003

Pazzagli, L., Seidl-Seiboth, V., Barsottini, M., Vargas, W. A., Scala, A., & Mukherjee, P. K. (2014). Cerato-platanins: elicitors and effectors. *Plant Science, 228*, 79-87. 10.1016/j.plantsci.2014.02.009

Pellier, A. L., Laugé, R., Veneault-Fourrey, C., & Langin, T. (2003). *CLNR1*, the *AREA*/*NIT2*-like global nitrogen regulator of the plant fungal pathogen *Colletotrichum lindemuthianum* is required for the infection cycle. *Molecular Microbiology, 48*(3), 639-655. 10.1046/j.1365-2958.2003.03451.x

Perino, B. E. H., Glienke, C., de Oliveira Silva, A., & Deising, H. B. (2020). Molecular characterization of the purine degradation pathway genes *ALA1* and *URE1* of the maize anthracnose fungus *Colletotrichum graminicola* identified urease as a novel target for plant disease control. *Phytopathology, 110*(9), 1530-1540. 10.1094/phyto-04-20-0114-r

Petersen, T. N., Brunak, S., von Heijne, G., & Nielsen, H. (2011). SignalP 4.0: discriminating signal peptides from transmembrane regions. *Nature Methods, 8*(10), 785-786. 10.1038/nmeth.1701

Petit-Houdenot, Y., & Fudal, I. (2017). Complex interactions between fungal avirulence genes and their corresponding plant resistance genes and consequences for disease resistance management. *Frontiers in Plant Science, 8*(1072) 10.3389/fpls.2017.01072

Pierre, S., Griffith, G. W., Morphew, R. M., Mur, L. A. J., & Scott, I. M. (2017). Saprotrophic proteomes of biotypes of the witches' broom pathogen *Moniliophthora perniciosa*. *Fungal Biology, 121*(9), 743-753. https://doi.org/10.1016/j.funbio.2017.05.004

Plissonneau, Blaise, F., Ollivier, B., Leflon, M., Carpezat, J., Rouxel, T., & Balesdent, M. H. (2017). Unusual evolutionary mechanisms to escape effector-triggered immunity in the

fungal phytopathogen *Leptosphaeria maculans*. *Molecular Ecology, 26*(7), 2183-2198. 10.1111/mec.14046

Plissonneau, C., Daverdin, G., Ollivier, B., Blaise, F., Degrave, A., Fudal, I., . . . Balesdent, M.-H. (2016). A game of hide and seek between avirulence genes *AvrLm4-7* and *AvrLm3* in *Leptosphaeria maculans*. *New Phytologist, 209*, 1613-1624. 10.1111/nph.13736

Prasanth, C. N., Viswanathan, R., Malathi, P., & Sundar, A. R. (2022). Carbohydrate active enzymes (CAZy) regulate cellulolytic and pectinolytic enzymes in *Colletotrichum falcatum* causing red rot in sugarcane. *3 Biotech, 12*(2), 48. 10.1007/s13205-022-03113-6

Prokchorchik, M. (2017). *Molecular analysis of plant innate immunity triggered by secreted effectors from bacterial and fungal pathogens of apple.* (Doctor of Philosophy (PhD) in Plant Science Thesis), Massey University, Retrieved from http://hdl.handle.net/10179/13452 Available from EBSCOhost Massey Research Online database.

Punt, P. J., Dingemanse, M. A., Kuyvenhoven, A., Soede, R. D., Pouwels, P. H., & van den Hondel, C. A. (1990). Functional elements in the promoter region of the *Aspergillus nidulans gpdA* gene encoding glyceraldehyde-3-phosphate dehydrogenase. *Gene, 93*(1), 101-109. 10.1016/0378-1119(90)90142-e

Qin, W., Cho, K. F., Cavanagh, P. E., & Ting, A. Y. (2021). Deciphering molecular interactions by proximity labeling. *Nature Methods, 18*(2), 133-143. 10.1038/s41592-020-01010-5

Quoc, N. B., & Chau, N. N. B. (2017). The role of cell wall degrading enzymes in pathogenesis of *Magnaporthe oryzae*. *Current Protein and Peptide Science, 18*(2) 10.2174/1389203717666160813164955

Ramos, B., Alves-Santos, F. M., García-Sánchez, M. A., Martín-Rodrigues, N., Eslava, A. P., & Díaz-Mínguez, J. M. (2007). The gene coding for a new transcription factor (*ftf1*) of *Fusarium oxysporum* is only expressed during infection of common bean. *Fungal Genetics and Biology, 44*(9), 864-876. 10.1016/j.fgb.2007.03.003

Renko, M., Sabotič, J., & Turk, D. (2012). β-Trefoil inhibitors – from the work of Kunitz onward. *Biological Chemistry, 393*(10), 1043-1054. doi:10.1515/hsz-2012-0159

Rezende, S. J., Zivanovic, M., Costa de Novaes, M. I., & Chen, Z. Y. (2020). The AVR4 effector is involved in cercosporin biosynthesis and likely affects the virulence of *Cercospora* cf. *flagellaris* on soybean. *Molecular Plant Pathology, 21*(1), 53-65. 10.1111/mpp.12879

Rigal, A., Doyle, S. M., & Robert, S. (2015). Live cell imaging of FM4-64, a tool for tracing the endocytic pathways in *Arabidopsis* root cells. *Methods in Molecular Biology, 1242*, 93-103. 10.1007/978-1-4939-1902-4_9

Rocafort, M., Arshed, S., Hudson, D., Sidhu, J. S., Bowen, J. K., Plummer, K. M., . . . Mesarich, C. H. (2022). CRISPR-Cas9 gene editing and rapid detection of gene-edited mutants using high-resolution melting in the apple scab fungus, *Venturia inaequalis*. *Fungal Biology, 126*(1), 35-46. https://doi.org/10.1016/j.funbio.2021.10.001

Rocafort, M., Bowen, J. K., Hassing, B., Cox, M. P., McGreal, B., de la Rosa, S., . . . Mesarich, C. H. (2022). The *Venturia inaequalis* effector repertoire is expressed in waves and is dominated by expanded families with predicted structural similarity to avirulence proteins from other plant-pathogenic fungi. *bioRxiv*, 2022.2003.2022.482717. 10.1101/2022.03.22.482717

Rooney, H. C. E., Van't Klooster, J. W., Van Der Hoorn, R. A. L., Joosten, M. H. A. J., Jones, J. D. G., & De Wit, P. J. G. M. (2005). *Cladosporium* Avr2 inhibits tomato Rcr3 protease required for Cf-2-dependent disease resistance. *Science, 308*(5729), 1783-1786. 10.1126/science.1111404

Ruibal, C., Gueidan, C., Selbmann, L., Gorbushina, A. A., Crous, P. W., Groenewald, J. Z., . . . de Hoog, G. S. (2009). Phylogeny of rock-inhabiting fungi related to Dothideomycetes. *Studies in Mycology, 64*, 123-133. 10.3114/sim.2009.64.06

Rybak, K., See, P. T., Phan, H. T. T., Syme, R. A., Moffat, C. S., Oliver, R. P., & Tan, K. C. (2017). A functionally conserved Zn2Cys6 binuclear cluster transcription factor class regulates necrotrophic effector gene expression and host-specific virulence of two major Pleosporales fungal pathogens of wheat. *Molecular Plant Pathology, 18*(3), 420-434. 10.1111/mpp.12511

Sabotič, J., Bleuler-Martinez, S., Renko, M., Avanzo Caglič, P., Kallert, S., Štrukelj, B., . . . Künzler, M. (2012). Structural basis of trypsin inhibition and entomotoxicity of cospin, serine protease inhibitor involved in defense of *Coprinopsis cinerea* fruiting bodies. *The Journal of Biological Chemistry, 287*(6), 3898-3907. 10.1074/jbc.M111.285304

Sabotič, J., Renko, M., & Kos, J. (2019). β -Trefoil protease inhibitors unique to higher fungi. *Acta Chimica Slovenica, 66*(1), 28-36.

Sánchez-Vallet, A., Saleem-Batcha, R., Kombrink, A., Hansen, G., Valkenburg, D.-J., Thomma, B. P. H. J., & Mesters, J. R. (2013). Fungal effector Ecp6 outcompetes host immune receptor for chitin binding through intrachain LysM dimerization. *Elife, 2*, e00790. 10.7554/eLife.00790

Sang, H., & Kim, J.-I. (2020). Advanced strategies to control plant pathogenic fungi by host-induced gene silencing (HIGS) and spray-induced gene silencing (SIGS). *Plant Biotechnology Reports, 14*(1), 1-8. 10.1007/s11816-019-00588-3

Scherm, B., Orrù, M., Balmas, V., Spanu, F., Azara, E., Delogu, G., . . . Migheli, Q. (2011). Altered trichothecene biosynthesis in *TRI6*-silenced transformants of *Fusarium culmorum* influences the severity of crown and foot rot on durum wheat seedlings. *Molecular Plant Pathology, 12*(8), 759-771. 10.1111/j.1364-3703.2011.00709.x

Schubert, M., Bleuler-Martinez, S., Butschi, A., Wälti, M. A., Egloff, P., Stutz, K., . . . Künzler, M. (2012). Plasticity of the β-Trefoil protein fold in the recognition and control of invertebrate predators and parasites by a fungal defence system. *PLoS Pathogens, 8*(5), e1002706. 10.1371/journal.ppat.1002706

Schuster, M., & Kahmann, R. (2019). CRISPR-Cas9 genome editing approaches in filamentous fungi and oomycetes. *Fungal Genetics and Biology, 130*, 43-53. https://doi.org/10.1016/j.fgb.2019.04.016

Schwelm, A., Barron, N. J., Baker, J., Dick, M., Long, P. G., Zhang, S., & Bradshaw, R. E. (2009). Dothistromin toxin is not required for dothistroma needle blight in *Pinus radiata*. *Plant Pathology, 58*(2), 293-304. 10.1111/j.1365-3059.2008.01948.x

Schwelm, A., Barron, N. J., Zhang, S., & Bradshaw, R. E. (2008). Early expression of aflatoxin-like dothistromin genes in the forest pathogen *Dothistroma septosporum*. *Mycological Research, 112*(2), 138-146. 10.1016/j.mycres.2007.03.018

Scott, P., & Williams, N. (2014). Phytophthora diseases in New Zealand forests. *New Zealand Journal of Forestry, 59*(2), 14-21.

Seong, K., & Krasileva, K. V. (2023). Prediction of effector protein structures from fungal phytopathogens enables evolutionary analyses. *Nature Microbiology, 8*(1), 174-187. 10.1038/s41564-022-01287-6

Seong, K. Y., Pasquali, M., Zhou, X., Song, J., Hilburn, K., McCormick, S., . . . Kistler, H. C. (2009). Global gene regulation by *Fusarium* transcription factors *Tri6* and *Tri10* reveals adaptations for toxin biosynthesis. *Molecular Microbiology, 72*(2), 354-367. 10.1111/j.1365-2958.2009.06649.x

Shao, D., Smith, D. L., Kabbage, M., & Roth, M. G. (2021). Effectors of plant necrotrophic fungi. *Frontiers in Plant Science, 12*(687713) 10.3389/fpls.2021.687713

Shaw, G. J., Chick, M., & Hodges, R. A. (1978). A 13C-NMR study of the biosynthesis of the anthraquinone dothistromin by *Dothistromin pini*. *Phytochemistry, 17*, 1743-1745.

Shi, T. Q., Liu, G. N., Ji, R. Y., Shi, K., Song, P., Ren, L. J., . . . Ji, X. J. (2017). CRISPR/Cas9-based genome editing of the filamentous fungi: the state of the art. *Applied Microbiology and Biotechnology, 101*(20), 7435-7443. 10.1007/s00253-017-8497-9

Shostak, K., Bonner, C., Sproule, A., Thapa, I., Shields, S. W. J., Blackwell, B., . . . Subramaniam, R. (2020). Activation of biosynthetic gene clusters by the global transcriptional regulator TRI6 in *Fusarium graminearum*. *Molecular Microbiology, 114*(4), 664-680. 10.1111/mmi.14575

Silar, P. (1995). Two new easy to use vectors for transformations. *Fungal Genetics Reports, 42*(1) 10.4148/1941-4765.1353

Snelders, N. C., Rovenich, H., Petti, G. C., Rocafort, M., van den Berg, G. C. M., Vorholt, J. A., . . . Thomma, B. (2020). Microbiome manipulation by a soil-borne fungal plant pathogen using effector proteins. *Nature Plants, 6*(11), 1365-1374. 10.1038/s41477-020-00799-5

Soares, M. A., Nogueira, G. B., Bazzolli, D. M. S., de Araújo, E. F., Langin, T., & de Queiroz, M. V. (2014). *PacCl*, a pH-responsive transcriptional regulator, is essential in the pathogenicity of *Colletotrichum lindemuthianum*, a causal agent of anthracnose in bean plants. *European Journal of Plant Pathology, 140*(4), 769-785. 10.1007/s10658-014-0508-4

Solomon, P. S., & Oliver, R. P. (2002). Evidence that γ-aminobutyric acid is a major nitrogen source during *Cladosporium fulvum* infection of tomato. *Planta, 214*(3), 414-420.

Song, Y., & Thomma, B. (2018). Host-induced gene silencing compromises *Verticillium wilt* in tomato and Arabidopsis. *Molecular Plant Pathology, 19*(1), 77-89. 10.1111/mpp.12500

Southern, E. M. (1975). Detection of specific sequences among DNA fragments separated by gel electrophoresis. *The Journal of Molecular Biology, 98*(3), 503-517. 10.1016/s0022-2836(75)80083-0

Sperschneider, J., & Dodds, P. N. (2021). EffectorP 3.0: Prediction of apoplastic and cytoplasmic effectors in fungi and oomycetes. *Molecular Plant-Microbe Interactions, 35*(2), 146-156. 10.1094/MPMI-08-21-0201-R

Stergiopoulos, I., De Kock, M. J. D., Lindhout, P., & De Wit, P. J. G. M. (2007). Allelic variation in the effector genes of the tomato pathogen *Cladosporium fulvum* reveals different modes of adaptive evolution. *Molecular Plant-Microbe Interactions, 20*(10), 1271-1283. 10.1094/MPMI-20-10-1271

Stergiopoulos, I., van den Burg, H. A., Ökmen, B., Beenen, H. G., van Liere, S., Kema, G. H. J., & de Wit, P. J. G. M. (2010). Tomato Cf resistance proteins mediate recognition of cognate homologous effectors from fungi pathogenic on dicots and monocots. *Proceedings of the National Academy of Sciences of the United States of America, 107*(16), 7610.

Stukenbrock, E. H., Bataillon, T., Dutheil, J. Y., Hansen, T. T., Li, R., Zala, M., . . . Schierup, M. H. (2011). The making of a new pathogen: insights from comparative population genomics of the domesticated wheat pathogen *Mycosphaerella graminicola* and its wild sister species. *Genome Research, 21*(12), 2157-2166. 10.1101/gr.118851.110

Takken, F. L., Luderer, R., Gabriëls, S. H. E. J., Westerink, N., Lu, R., De Wit, P. J. G. M., & Joosten, M. H. A. J. (2000). A functional cloning strategy, based on a binary PVX-expression vector, to isolate HR-inducing cDNAs of plant pathogens. *The Plant Journal, 24*(2), 275-283. https://doi.org/10.1046/j.1365-313x.2000.00866.x

Takken, F. L., Thomas, C. M., Joosten, M. H., Golstein, C., Westerink, N., Hille, J., . . . Jones, J. D. (1999). A second gene at the tomato *Cf-4* locus confers resistance to *Cladosporium fulvum* through recognition of a novel avirulence determinant. *The Plant Journal, 20*(3), 279-288. 10.1046/j.1365-313x.1999.t01-1-00601.x

Tarallo, M. (2022). *Identification and characterization of effector proteins from pine needle pathogens.* (Doctor of Philosophy (Sciences) in Genetics), Massey University, Retrieved from https://search.ebscohost.com/login.aspx?direct=true&AuthType=sso&db=ir00033a&AN=massnz.10179.18304&site=eds-live&scope=site.

Tarallo, M., McDougal, R. L., Chen, Z., Wang, Y., Bradshaw, R. E., & Mesarich, C. H. (2022). Characterization of two conserved cell death elicitor families from the

Dothideomycete fungal pathogens *Dothistroma septosporum* and *Fulvia fulva* (syn. *Cladosporium fulvum*). *Frontiers in Microbiology, 13*(964851) 10.3389/fmicb.2022.964851

Taylor, A., Armitage, A. D., Handy, C., Jackson, A. C., Hulin, M. T., Harrison, R. J., & Clarkson, J. P. (2019). Basal rot of *Narcissus*: Understanding pathogenicity in *Fusarium oxysporum* f. sp. *narcissi*. *Frontiers in Microbiology, 10*(2905) 10.3389/fmicb.2019.02905

Taylor, R. G., Walker, D. C., & McInnes, R. R. (1993). *E. coli* host strains significantly affect the quality of small scale plasmid DNA preparations used for sequencing. *Nucleic Acids Research, 21*(7), 1677-1678. 10.1093/nar/21.7.1677

Thomazella, D. P., Teixeira, P. J., Oliveira, H. C., Saviani, E. E., Rincones, J., Toni, I. M., . . . Pereira, G. A. (2012). The hemibiotrophic cacao pathogen *Moniliophthora perniciosa* depends on a mitochondrial alternative oxidase for biotrophic development. *New Phytologist, 194*(4), 1025-1034. 10.1111/j.1469-8137.2012.04119.x

Thomma, B. P. H. J., van Esse, H. P., Crous, P. W., & de Wit, P. J. G. M. (2005). *Cladosporium fulvum* (syn. *Passalora fulva*), a highly specialized plant pathogen as a model for functional studies on plant pathogenic Mycosphaerellaceae. *Molecular Plant Pathology, 6*(4), 379-393. 10.1111/j.1364-3703.2005.00292.x

Thordal-Christensen, H. (2020). A holistic view on plant effector-triggered immunity presented as an iceberg model. *Cellular and Molecular Life Sciences, 77*(20), 3963-3976. 10.1007/s00018-020-03515-w

Tjalsma, H., Bolhuis, A., Jongbloed, J. D., Bron, S., & van Dijl, J. M. (2000). Signal peptide-dependent protein transport in *Bacillus subtilis*: a genome-based survey of the secretome. *Microbiology and Molecular Biology Reviews, 64*(3), 515-547. 10.1128/mmbr.64.3.515-547.2000

Trakunyingcharoen, T., Lombard, L., Groenewald, J. Z., Cheewangkoon, R., To-Anun, C., Alfenas, A. C., & Crous, P. W. (2014). Mycoparasitic species of *Sphaerellopsis*, and allied lichenicolous and other genera. *IMA Fungus, 5*(2), 391-414. 10.5598/imafungus.2014.05.02.05

Urban, M., Cuzick, A., Seager, J., Wood, V., Rutherford, K., Venkatesh, S. Y., . . . Hammond-Kosack, K. E. (2020). PHI-base: the pathogen–host interactions database. *Nucleic Acids Research, 48*(D1), 613-620. 10.1093/nar/gkz904

Urquhart, A. S., & Idnurm, A. (2019). Limitations of transcriptome-based prediction of pathogenicity genes in the plant pathogen *Leptosphaeria maculans*. *FEMS Microbiology Letters, 366*(7) 10.1093/femsle/fnz080

Van den Ackerveken, G., Vossen, P., & De Wit, J. (1993). The AVR9 race-specific elicitor of *Cladosporium fulvum* is processed by endogenous and plant proteases. *Plant Physiology, 103*(1), 91-96. 10.1104/pp.103.1.91

Van den Ackerveken, G. F. J. M., Dunn, R. M., Cozijnsen, A. J., Vossen, J. P. M. J., De Wit, P. J. G. M., & Van den Broek, H. W. J. (1994). Nitrogen limitation induces expression of the avirulence gene *avr9* in the tomato pathogen *Cladosporium fulvum*. *MGG Molecular & General Genetics, 243*(3), 277-285-285. 10.1007/BF00301063

van den Burg, H. A., Harrison, S. J., Joosten, M. H., Vervoort, J., & de Wit, P. J. (2006). *Cladosporium fulvum* Avr4 protects fungal cell walls against hydrolysis by plant chitinases accumulating during infection. *Molecular Plant-Microbe Interactions, 19*(12), 1420-1430. 10.1094/mpmi-19-1420

Van Der Biezen, E. A., & Jones, J. D. G. (1998). Plant disease-resistance proteins and the gene-for-gene concept. *Trends in Biochemical Sciences, 23*(12), 454-456. 10.1016/S0968-0004(98)01311-5

van der Burgh, A. M., & Joosten, M. (2019). Plant immunity: Thinking outside and inside the Box. *Trends in Plant Science, 24*(7), 587-601. 10.1016/j.tplants.2019.04.009

van Esse, H. P., Bolton, M. D., Stergiopoulos, I., de Wit, P. J., & Thomma, B. P. (2007). The chitin-binding *Cladosporium fulvum* effector protein Avr4 is a virulence factor. *Molecular Plant-Microbe Interactions, 20*(9), 1092-1101. 10.1094/mpmi-20-9-1092

van Esse, H. P., Van't Klooster, J. W., Bolton, M. D., Yadeta, K. A., van Baarlen, P., Boeren, S., . . . Thomma, B. P. (2008). The *Cladosporium fulvum* virulence protein Avr2 inhibits host proteases required for basal defense. *The Plant Cell, 20*(7), 1948-1963. 10.1105/tpc.108.059394

van Kan, J. A., van den Ackerveken, G. F., & de Wit, P. J. (1991). Cloning and characterization of cDNA of avirulence gene *avr9* of the fungal pathogen *Cladosporium fulvum*, causal agent of tomato leaf mold. *Molecular Plant-Microbe Interactions, 4*(1), 52-59. 10.1094/MPMI-4-052

Varrot, A., Basheer, S. M., & Imberty, A. (2013). Fungal lectins: structure, function and potential applications. *Current Opinion in Structural Biology, 23*(5), 678-685. https://doi.org/10.1016/j.sbi.2013.07.007

Verbon, E. H., Trapet, P. L., Stringlis, I. A., Kruijs, S., Bakker, P. A. H. M., & Pieterse, C. M. J. (2017). Iron and immunity. *Annual Review of Phytopathology, 55*(1), 355-375. 10.1146/annurev-phyto-080516-035537

Vincent, D., & Bedon, F. (2014). Secretomics of plant-fungus associations: More secrets to unravel. *Journal of Plant Biochemistry and Physiology, 1*(5) 10.4172/2329-9029.1000e117

Vincent, D., Rafiqi, M., & Job, D. (2020). The multiple facets of plant–fungal interactions revealed through plant and fungal secretomics. *Frontiers in Plant Science, 10*(1626) 10.3389/fpls.2019.01626

Vleeshouwers, V. G. A. A., & Oliver, R. P. (2014). Effectors as tools in disease resistance breeding against biotrophic, hemibiotrophic, and necrotrophic plant pathogens. *Molecular Plant-Microbe Interactions, 27*(3), 196-206. 10.1094/MPMI-10-13-0313-IA

Wang, A., Meng, F., Xu, X., Wang, Y., & Li, J. (2007). Development of molecular markers linked to *Cladosporium fulvum* resistant gene *Cf-6* in tomato by RAPD and SSR methods. *HortScience, 42*, 11-15.

Wang, C., Cai, X., & Zheng, Z. (2005). High humidity represses Cf-4/Avr4- and Cf-9/Avr9-dependent hypersensitive cell death and defense gene expression. *Planta, 222*(6), 947-956. 10.1007/s00425-005-0036-8

Wang, C., & Rollins, J. A. (2021). Efficient genome editing using endogenous U6 snRNA promoter-driven CRISPR/Cas9 sgRNA in *Sclerotinia sclerotiorum*. *Fungal Genetics and Biology, 154*(103598) https://doi.org/10.1016/j.fgb.2021.103598

Wang, D., Zhang, D. D., Song, J., Li, J. J., Wang, J., Li, R., . . . Chen, J. Y. (2022). *Verticillium dahliae* CFEM proteins manipulate host immunity and differentially contribute to virulence. *BMC Biology, 20*(1), 55. 10.1186/s12915-022-01254-x

Wang, F., Lu, Y. Y., Liu, M. M., Xiao, S. Q., Gao, Y. B., Yuan, M. Y., & Xue, C. S. (2020). Effects of iron on the asexual reproduction and major virulence factors of *Curvularia lunata*. *European Journal of Plant Pathology, 157*(3), 497-507. 10.1007/s10658-020-02009-6

Wang, S., Boevink, P. C., Welsh, L., Zhang, R., Whisson, S. C., & Birch, P. R. J. (2017). Delivery of cytoplasmic and apoplastic effectors from *Phytophthora infestans* haustoria by distinct secretion pathways. *New Phytologist, 216*, 205-215. 10.1111/nph.14696

Wang, Y., Deng, C., Tian, L., Xiong, D., Tian, C., & Klosterman, S. J. (2018). The transcription factor *VdHapX* controls iron homeostasis and is crucial for virulence in the vascular pathogen *Verticillium dahliae*. *mSphere, 3*(5) 10.1128/mSphere.00400-18

Watanabe, H., Horinouchi, H., Muramoto, Y., & Ishii, H. (2017). Occurrence of azoxystrobin-resistant isolates in *Passalora fulva*, the pathogen of tomato leaf mould disease. *Plant Pathology, 66*(9), 1472-1479. 10.1111/ppa.12701

Wenderoth, M., Pinecker, C., Voß, B., & Fischer, R. (2017). Establishment of CRISPR/Cas9 in *Alternaria alternata*. *Fungal Genetics and Biology, 101*, 55-60. https://doi.org/10.1016/j.fgb.2017.03.001

Westerink, N., Brandwagt, B. F., De Wit, P. J. G. M., & Joosten, M. H. A. J. (2004). *Cladosporium fulvum* circumvents the second functional resistance gene homologue at the *Cf-4* locus (*Hcr9-4E*) by secretion of a stable avr4E isoform. *Molecular Microbiology, 54*(2), 533-545. https://doi.org/10.1111/j.1365-2958.2004.04288.x

Wilson, F. M., Harrison, K., Armitage, A. D., Simkin, A. J., & Harrison, R. J. (2019). CRISPR/Cas9-mediated mutagenesis of phytoene desaturase in diploid and octoploid strawberry. *Plant Methods, 15*(45) 10.1186/s13007-019-0428-6

Wohlschlager, T., Butschi, A., Zurfluh, K., Vonesch, S. C., auf dem Keller, U., Gehrig, P., . . . Künzler, M. (2011). Nematotoxicity of *Marasmius oreades* agglutinin (MOA) depends on glycolipid binding and cysteine protease activity. *Journal of Biological Chemistry, 286*(35), 30337-30343. 10.1074/jbc.M111.258202

Wolpert, T. J., & Lorang, J. M. (2016). Victoria blight, defense turned upside down. *Physiological and Molecular Plant Pathology, 95*, 8-13. 10.1016/j.pmpp.2016.03.006

Woods, A. (2003). Species diversity and forest health in northwest British Columbia. *The Forestry Chronicle, 79*(5), 892-897. https://doi.org/10.5558/tfc79892-5

Woods, A., Coates, K. D., & Hamann, A. (2005). Is an unprecedented Dothistroma needle blight epidemic related to climate change? *BioScience, 55*(9), 761-769. 10.1641/0006-3568(2005)055[0761:IAUDNB]2.0.CO;2

Woods, A. J., Martín-García, J., Bulman, L., Vasconcelos, M. W., Boberg, J., La Porta, N., . . . Diez, J. J. (2016). Dothistroma needle blight, weather and possible climatic triggers for the disease's recent emergence. *Forest Pathology, 46*(5), 443-452. 10.1111/efp.12248

Wu, X., Scott, D. A., Kriz, A. J., Chiu, A. C., Hsu, P. D., Dadon, D. B., . . . Sharp, P. A. (2014). Genome-wide binding of the CRISPR endonuclease Cas9 in mammalian cells. *Nature Biotechnology, 32*(7), 670-676. 10.1038/nbt.2889

Wubben, J. P., Joosten, M. H., & De Wit, P. J. (1994). Expression and localization of two *in planta* induced extracellular proteins of the fungal tomato pathogen *Cladosporium fulvum*. *Molecular Plant-Microbe Interactions, 7*(4), 516-524. 10.1094/mpmi-7-0516

Wulff, B. B. H., Thomas, C. M., Smoker, M., Grant, M., & Jones, J. D. G. (2001). Domain swapping and gene shuffling identify sequences required for induction of an Avr-dependent hypersensitive response by the tomato Cf-4 and Cf-9 proteins. *The Plant Cell, 13*(2), 255-272. 10.1105/tpc.13.2.255

Xu, C., Zhang, X., Qian, Y., Chen, X., Liu, R., Zeng, G., . . . Fang, W. (2014). A high-throughput gene disruption methodology for the entomopathogenic fungus *Metarhizium robertsii*. *PLoS One, 9*(9), e107657. 10.1371/journal.pone.0107657

Yan, L., Chen, J., Zhang, C., & Ma, Z. (2008). Molecular characterization of benzimidazole-resistant isolates of *Cladosporium fulvum*. *FEMS Microbiology Letters, 278*(2), 242-248. 10.1111/j.1574-6968.2007.00999.x

Yang, X., McMahon, M. B., Ramachandran, S. R., Garrett, W. M., LeBlanc, N., Crouch, J. A., . . . Luster, D. G. (2021). Comparative analysis of extracellular proteomes reveals putative effectors of the boxwood blight pathogens, *Calonectria henricotiae* and *C. pseudonaviculata*. *Bioscience Reports, 41*(3) 10.1042/bsr20203544

Yang, Y., Zhu, K., Li, H., Han, S., Meng, Q., Khan, S. U., . . . Zhou, Y. (2018). Precise editing of CLAVATA genes in *Brassica napus* L. regulates multilocular silique development. *Plant Biotechnology Journal, 16*(7), 1322-1335. https://doi.org/10.1111/pbi.12872

Yarrington, R., Verma, S., Schwartz, S., Trautman, J., & Carroll, D. (2018). Nucleosomes inhibit target cleavage by CRISPR-Cas9 *in vivo*. *Proceedings of the National Academy of Sciences, 115*(38), 9351-9358. 10.1073/pnas.1810062115

Yelton, M. M., Hamer, J. E., & Timberlake, W. E. (1984). Transformation of *Aspergillus nidulans* by using a trpC plasmid. *Proceedings of the National Academy of Sciences of the United States of America, 81*(5), 1470-1474. 10.1073/pnas.81.5.1470

Yokoyama, A., Izumitsu, K., Irie, T., & Suzuki, K. (2019). The homeobox transcription factor *CoHox1* is required for the morphogenesis of infection hyphae in host plants and pathogenicity in *Colletotrichum orbiculare*. *Mycoscience, 60*(2), 110-115. 10.1016/j.myc.2018.11.001

Yoshino, K., Irieda, H., Sugimoto, F., Yoshioka, H., Okuno, T., & Takano, Y. (2012). Cell death of *Nicotiana benthamiana* is induced by secreted protein NIS1 of *Colletotrichum orbiculare* and is suppressed by a homologue of CgDN3. *Molecular Plant-Microbe Interactions, 25*(5), 625-636. 10.1094/mpmi-12-11-0316

Zaccaron, A. Z., Chen, L.-H., Samaras, A., & Stergiopoulos, I. (2022). A chromosome-scale genome assembly of the tomato pathogen *Cladosporium fulvum* reveals a compartmentalized genome architecture and the presence of a dispensable chromosome. *Microbial Genomics, 8*(4) https://doi.org/10.1099/mgen.0.000819

Zhai, Y., Yu, K., Cai, S., Hu, L., Amoo, O., Xu, L., . . . Zhou, Y. (2020). Targeted mutagenesis of *BnTT8* homologs controls yellow seed coat development for effective oil production in *Brassica napus* L. *Plant Biotechnology Journal, 18*(5), 1153-1168. https://doi.org/10.1111/pbi.13281

Zhang, C., Meng, X., Wei, X., & Lu, L. (2016). Highly efficient CRISPR mutagenesis by microhomology-mediated end joining in *Aspergillus fumigatus*. *Fungal Genetics and Biology, 86*, 47-57. 10.1016/j.fgb.2015.12.007

Zhang, H., Kim, M. S., Huang, J., Yan, H., Yang, T., Song, L., . . . Shim, W. B. (2022). Transcriptome analysis of maize pathogen *Fusarium verticillioides* revealed FvLcp1, a secreted protein with type-D fungal LysM and chitin-binding domains, that plays important roles in pathogenesis and mycotoxin production. *Microbiological Research, 265*(127195) https://doi.org/10.1016/j.micres.2022.127195

Zhang, H., Yohe, T., Huang, L., Entwistle, S., Wu, P., Yang, Z., . . . Yin, Y. (2018). dbCAN2: a meta server for automated carbohydrate-active enzyme annotation. *Nucleic Acids Research, 46*(W1), W95-W101. 10.1093/nar/gky418

Zhang, S., Schwelm, A., Jin, H., Collins, L. J., & Bradshaw, R. E. (2007). A fragmented aflatoxin-like gene cluster in the forest pathogen *Dothistroma septosporum*. *Fungal Genetics and Biology, 44*(12), 1342-1354. 10.1016/j.fgb.2007.06.005

Zhang, W. Q., Gui, Y. J., Short, D. P. G., Li, T. G., Zhang, D. D., Zhou, L., . . . Dai, X. F. (2018). *Verticillium dahliae* transcription factor VdFTF1 regulates the expression of multiple secreted virulence factors and is required for full virulence in cotton. *Molecular Plant Pathology, 19*(4), 841-857. 10.1111/mpp.12569

Zhang, X., Dodds, P. N., & Bernoux, M. (2017). What do we know about NOD-like receptors in plant immunity? *Annual Review of Phytopathology, 55*(1), 205-229. 10.1146/annurev-phyto-080516-035250

Zheng, Y. M., Lin, F. L., Gao, H., Zou, G., Zhang, J. W., Wang, G. Q., . . . Hu, D. (2017). Development of a versatile and conventional technique for gene disruption in filamentous fungi based on CRISPR-Cas9 technology. *Scientific Reports, 7*(1), 9250. 10.1038/s41598-017-10052-3

Zhu, X., Liu, W., Chu, X., Sun, Q., Tan, C., Yang, Q., . . . Kang, Z. (2018). The transcription factor PstSTE12 is required for virulence of *Puccinia striiformis* f. sp. *tritici*. *Molecular Plant Pathology, 19*(4), 961-974. 10.1111/mpp.12582

Zipfel, C., & Oldroyd, G. E. D. (2017). Plant signalling in symbiosis and immunity. *Nature, 543*(7645), 328-336. 10.1038/nature22009